



**SURVIVABILITY • SUSTAINABILITY • MOBILITY  
SCIENCE AND TECHNOLOGY  
SOLDIER SYSTEM INTEGRATION**

TECHNICAL REPORT  
NATICK/TR-94/035

AD \_\_\_\_\_

# **VISCOELASTIC PROPERTIES OF ADVANCED POLYMER COMPOSITES FOR BALLISTIC PROTECTIVE APPLICATIONS**

by

**Frank K. Ko, Charles Lei, Anisur Rahman, Manal Shaker,  
Antonios Zavaliangos, Jenny Z. Yu,  
and John Song\***

DREXEL UNIVERSITY  
Philadelphia, PA 19107

September 1994



Final Report

September 1992 - August 1993

Approved for Public Release, Distribution Unlimited

Prepared for

**UNITED STATES ARMY NATICK  
RESEARCH, DEVELOPMENT AND ENGINEERING CENTER  
NATICK, MASSACHUSETTS 01760-5000**

**\*SCIENCE AND TECHNOLOGY DIRECTORATE**

**19950530 004**

DTIC QUALITY INSPECTED 1

### DISCLAIMERS

The findings contained in this report are not to be construed as an official Department of the Army position unless so designated by other authorized documents.

Citation of trade names in this report does not constitute an official endorsement or approval of the use of such items.

### DESTRUCTION NOTICE

#### For Classified Documents:

Follow the procedures in DoD 5200.22-M, Industrial Security Manual, Section II-19 or DoD 5200.1-R, Information Security Program Regulation, Chapter IX.

#### For Unclassified/Limited Distribution Documents:

Destroy by any method that prevents disclosure of contents or reconstruction of the document.

# REPORT DOCUMENTATION PAGE

Form Approved  
OMB No. 0704-0188

Public reporting burden for this collection of information is estimated to average 1 hour per response, including the time for reviewing instructions, searching existing data sources, gathering and maintaining the data needed, and completing and reviewing the collection of information. Send comments regarding this burden estimate or any other aspect of this collection of information, including suggestions for reducing this burden, to Washington Headquarters Services, Directorate for Information Operations and Reports, 1215 Jefferson Davis Highway, Suite 1204, Arlington, VA 22202-4302, and to the Office of Management and Budget, Paperwork Reduction Project (0704-0188), Washington, DC 20503.

1. AGENCY USE ONLY (Leave blank)		2. REPORT DATE Sept 1994	3. REPORT TYPE AND DATES COVERED Final Sept 1992 - Aug 1993	
4. TITLE AND SUBTITLE VISCOELASTIC PROPERTIES OF ADVANCED POLYMER COMPOSITES FOR BALLISTIC PROTECTIVE APPLICATIONS			5. FUNDING NUMBERS DAAK - 60-92-K-0004	
6. AUTHOR(S) Frank K. Ko, Charles Lei, Anisur Rahman, Manal Shaker, Antonios Zavaliangos, Jenny Z. Yu, John Song				
7. PERFORMING ORGANIZATION NAME(S) AND ADDRESS(ES) Drexel University 31st and Market Sts., Philadelphia, PA 19107			8. PERFORMING ORGANIZATION REPORT NUMBER	
9. SPONSORING/MONITORING AGENCY NAME(S) AND ADDRESS(ES) U.S. Army Natick RD&E Center Attn: SATNC-YSM (John Song) Kansas St. Natick, MA 01760-5015			10. SPONSORING/MONITORING AGENCY REPORT NUMBER NATICK/TR-94/030	
11. SUPPLEMENTARY NOTES  The professional affiliation of John Song is U.S. Army Natick RD&E Center				
12a. DISTRIBUTION/AVAILABILITY STATEMENT  Approved for public release, distribution unlimited			12b. DISTRIBUTION CODE	
13. ABSTRACT (Maximum 200 words) The aim of the program on ballistically resistant structures is to develop a fundamental understanding of damage resistance characteristics of protective composite materials of interest of the Army, carried out by a systematic characterization of composite viscoelastic behavior. In the first year of the program, the experimental setup and tooling was organized. DMA testing of Kevlar™ 29 and KM2 was initiated to determine long-term mechanical properties for this material system. R-F Plasma of allylamine onto Kevlar 29 fiber was carried out to optimize the interfacial surface. The gradient design concept was developed and demonstrated. High and low velocity impact tests were carried out. Post-failure damage assessment was done using optical microscopy and SEM. The objective of modeling of viscoelastic armor was to complement the experimental component of this study so as to obtain a thorough understanding of deformation, energy absorption mechanisms and failure of viscoelastic armors. Initial work was directed towards identifying the specifics to develop a realistic model and to perform simplified computer simulations based on assumed data.				
14. SUBJECT TERMS viscoelastic materials viscoelastic properties advanced polymers			15. NUMBER OF PAGES 286	
ballistic protection polymer composites polyamide plastics			16. PRICE CODE	
17. SECURITY CLASSIFICATION OF REPORT UNCLASSIFIED	18. SECURITY CLASSIFICATION OF THIS PAGE UNCLASSIFIED	19. SECURITY CLASSIFICATION OF ABSTRACT UNCLASSIFIED	20. LIMITATION OF ABSTRACT	

## TABLE OF CONTENTS

List of Figures .....	iv
List of Tables .....	vii
Preface .....	viii
Executive Summary .....	1
1. Introduction .....	4
1.1 Background and Objectives .....	4
2. Material Characterization.....	6
2.1 Introduction.....	6
2.1.1 Material Systems Used.....	6
2.1.2 Viscoelastic Behavior.....	6
2.2 Dynamic Mechanical Analysis .....	7
2.2.1 Sample Preparation .....	9
2.2.2 Experimental Approach and Testing Procedure.....	10
2.3 Test Results and Discussion.....	13
2.4 Plan for the Second Year of the Project .....	25
2.4.1 Material Characterization.....	25
3. Surface Modification of Kevlar 29 and Kevlar KM2 Using R-F Plasma .....	26
3.1 Introduction.....	26
3.1.1 Objectives.....	26
3.2 Technical Approach .....	26
3.3 Experimental Procedures.....	29
3.5 Results and Discussion .....	36
3.6 Conclusions.....	49
3.7 Future Work.....	49
4. Gradient Design Concept for Composite Armor.....	50
4.1 Introduction.....	50
4.2 Gradient Design Concept.....	50
4.2.1 Design of Experiment.....	51
4.2.2 Composite Formation.....	53
4.3 Low Velocity Impact Behavior.....	55
4.3.1 Drop Weight Impact Testing Conditions.....	55
4.3.2 Impact Result and Discussion.....	56
4.3.3 Damage Characterization .....	64
4.4 High Velocity Impact Behavior.....	80
4.4.1 Ballistic Test Conditions .....	81
4.4.2 Test Results.....	82
5.1 Introduction.....	87
5.2 Objectives and General Approach.....	88
5.2.1 Material Characterization.....	89
5.2.2 Modeling.....	90
5.2.3 Impact Simulation.....	92
5.3 Representative Results .....	94
5.3.1 Low Velocity Impact .....	94
5.3.2 High Velocity Impact.....	104
5.4 Future Efforts.....	119
References .....	121
Appendix A. Definition Of Complex Modulus.....	124
Appendix B. Literature Review on Impact Response of Composites .....	126
Appendix C. Sample Input and Output Files of DYNA3D Analysis of High Velocity Impact of a Steel Ball on a Composite Target.....	182



## LIST OF FIGURES

Integration of Research Components .....	5
Figure 1. Compression Molding.....	9
Figure 2. Specimen Undergoes a Flexural Deformation in DMA Testing [5].....	10
Figure 3. The Defined "Length" of the Specimen [3].....	12
Figure 4. LogE', LogE " and $\tan\delta$ vs.T and Frequency for Pure Matrix .....	13
Figure 5. LogE', LogE" and $\tan\delta$ vs.T and Frequency for Composite 1.....	14
Figure 6. LogE', LogE " and $\tan\delta$ vs.T and Frequency for Composite 2 .....	14
Figure 7. Raw Data of Log E' vs.Frequency for Pure Matrix.....	15
Figure 8. Raw Data of Log E' vs.Frequency for Composite 1 .....	15
Figure 9. Raw Data of Log E' vs.Frequency for Composite 2 .....	16
Figure 10. Raw Data of Log E " vs.Frequency for Pure Matrix.....	16
Figure 11. Raw Data of Log E " vs.Frequency for Composite 1.....	17
Figure 12. Raw Data of Log E "vs.Frequency for Composite 2 .....	17
Figure 13. LogE' vs.Log(Frequency) for Pure Matrix.....	19
Figure 14. LogE' vs.Log(Frequency) for Composite 1 .....	19
Figure 15. LogE' vs.Log(Frequency) for Composite 2 .....	20
Figure 16. LogE " vs.Log(Frequency) for Pure Matrix.....	20
Figure 17. LogE " vs.Log(Frequency) for Composite 1.....	21
Figure 18. LogE " vs.Log(Frequency) for Composite 2.....	21
Figure 19. Log(a) vs.Temperature for E' and E " of Pure Matrix.....	22
Figure 20. Log(a) vs.Temperature for E' and E " of Composite 1 .....	22
Figure 21. Log(a) vs.Temperature for E' and E " of Composite 2 .....	23
Figure 22. Mechanism of Plasma Polymerization .....	30
Figure 23. Single Filament Pull-out Test.....	31
Figure 24. Three Geometries That May Be Employed for Single Fiber Pull-out Test..	32
Figure 25. Plot of Applied Load Pm vs.Embedded Length L .....	32
Figure 26. Schematic of Single Filament Pull-Out Test .....	33
Figure 27. Typical Pull Out Load vs.Displacement .....	34
Figure 28. Schematic Drawing Of The Sequence Of Events .....	34
Figure 29. Schematic Representation of Single Fiber Pull-Out Test .....	35
Figure 30. Schematic of Single Filament Pull-Out Test .....	36
Figure 31. Untreated Kevlar KM2.....	41
Figure 32. Kevlar KM2 After 7 Minutes of Trichloroethane Treatment.....	41
Figure 33. Kevlar KM2 After 30 Minutes of Trichloroethane Treatment .....	42
Figure 34. Kevlar KM2 After Argon Treatment (5 minutes at 70W).....	42
Figure 35. Kevlar KM2 After Allylamine Treatment (15 minutes at 50W).....	43
Figure 36. Kevlar KM2 After Allylamine Treatment (30 minutes at 50W).....	43
Figure 37. Kevlar KM2 After Allylamine Treatment (45 minutes at 50W).....	44
Figure 38. Untreated Kevlar 29.....	44
Figure 39. Kevlar 29 After 30 Minutes of Trichloroethane Treatment.....	45
Figure 40. Kevlar 29 After Argon Treatment (5 minutes at 70W).....	45

Figure 41.	Kevlar 29 After Allylamine Treatment (15 minutes at 50W).....	46
Figure 42.	Kevlar 29 After Allylamine Treatment (30 minutes at 50W).....	46
Figure 43.	Artificially Cracked Kevlar 29 After Allylamine Treatment.....	47
Figure 44.	Kevlar 29 After Allylamine Treatment (45 minutes at 50W).....	47
Figure 45.	Gradient Design Concept For Multifunctional Ballistic Composites.....	50
Figure 46.	Components of GDC Composites.....	51
Figure 47.	Design of Experiments .....	52
Figure 48.	Schematic Diagram of Resin Transfer Molding .....	54
Figure 49.	Testing Equipment and Conditions.....	55
Figure 50.	General Impact Response of Composites.....	57
Figure 51.	Impact Load and Energy vs.Time, Category I Composites.....	58
Figure 52.	Impact Load and Energy vs.Time, Category II Composites.....	60
Figure 53.	Impact Load and Energy vs.Time, Category III Composites.....	61
Figure 54.	Impact Load and Energy vs.Time, Category IV Composites.....	62
Figure 55.	Impact Load and Energy vs.Time, Category V Composites.....	63
Figure 56.	Total Specific Energy Absorption Comparison.....	64
Figure 57.	Samples Penetrated by Impactor.....	65
Figure 57.	Samples Penetrated by Impactor (cont'd).....	66
Figure 58.	Photos of Post-Damaged Composites.....	67
Figure 59.	Photos of Post-Damaged Composites.....	69
Figure 60.	Photos of Post-Damaged Composites.....	70
Figure 61.	Photos of Post-Damaged Composites.....	71
Figure 62.	Schematic Diagram of The Sectioning for Microscopic Graphs.....	72
Figure 63.	Schematic diagram of the Locations Examined Using Optical and SEM Microscopic Techniques.....	73
Figure 64.	Side Views of Fracture Surface of the 3-D Braided Composite.....	74
Figure 65.	Matrix Cracks Near the Entrance of the Penetration .....	75
Figure 66.	Optical Photo of the Sample From the Top.....	76
Figure 67.	SEM Micrographs of Fracture Surface.....	77
Figure 68.	SEM Fractograph of the Damaged Sample .....	78
Figure 69.	Fracture Surface of Damage Area Near the Point of Penetration .....	79
Figure 70.	Closer View of the Damaged Area Introduced by the Impact Tup .....	80
Figure 71.	Schematic of Ballistic Test Setup.....	81
Figure 72.	Kinetic Energy Absorbed During Ballistic Impact.....	83
Figure 73.	Ballistic Limit of Each Type of Composite.....	84
Figure 74.	V50 Of Each Type Of Composite.....	85
Figure 75.	Comparison Of The Specific Energy Absorption .....	86
Figure 76.	Mises Stress (MPa) Contours in the Elastic-Plastic Target.....	97
Figure 77.	Principal Stress (MPa) Contours in the Elastic-Plastic Target .....	98
Figure 78.	Shear Stress (MPa) Contours in the Elastic-Plastic Target.....	99
Figure 79.	Mises Stress (MPa) Contours in the Elastic-Plastic Target.....	100
Figure 80.	Mises Stress (MPa) Contours in the Elastic-Plastic Target.....	101

By _____	
Distribution / _____	
Availability Codes	
Dist	Avail and/or Special
A-1	

Figure 81.	Mises Stress (MPa) Contours in the Elastic-Plastic Target.....	102
Figure 82.	Displaced Mesh at 3.819 ms After Impact.....	103
Figure 83.	Effective Stress Contours (GPa) on an Elastic Composite Target.....	105
Figure 84.	Effective Stress Contours (GPa) on an Elastic Composite Target.....	106
Figure 85.	Effective Stress Contours (GPa) on an Elastic Composite Target.....	107
Figure 86.	Effective Stress Contours (GPa) on a Visco-Elastic Composite Target 2 $\mu$ S After Impact With a Steel FSP.....	108
Figure 87.	Effective Stress Contours (GPa) on a Visco-Elastic Composite Target 4 $\mu$ S After Impact With a Steel FSP.....	109
Figure 89.	Effective Stress Contours (GPa) on a Visco-Elastic Composite Target 6 $\mu$ S After Impact With a Steel FSP.....	110
Figure 89.	Effective Stress Contours (GPa) on an Elastic Plastic Composite With A Pressure Cutoff Failure, 10 $\mu$ S After Impact With a Steel FSP.....	112
Figure 90.	Effective Stress Contours (GPa) on an Elastic Plastic Composite With A Pressure Cutoff Failure, 15 $\mu$ S After Impact With a Steel FSP.....	113
Figure 91.	Effective Stress Contours (GPa) on an Elastic Plastic Composite With A Pressure Cutoff Failure, 20 $\mu$ S After Impact With a Steel FSP.....	114
Figure 92.	Displacement of a Composite Target Upon Impact With a Spherical Steel Ball at Different Time Intervals.....	115
Figure 93.	Effective Stress Contours (Pa) on a Viscoelastic Composite 50 ms After Impact with a Spherical Steel Ball.....	116
Figure 94.	Hydrostatic Stress Contours (Pa) on a Viscoelastic Composite 50 ms After Impact with a Spherical Steel Ball.....	117
Figure 95.	Shear Stress Contours (Pa) on a Viscoelastic Composite 50 ms After Impact with a Spherical Steel Ball.....	118
Figure 96.	Flow Chart of Future Experimental/Modeling Work.....	120

## LIST OF TABLES

Table 1.	Basic Mechanical Properties of the Materials .....	6
Table 2.	Initial DMA Test Results.....	23
Table 3.	Flexural Three Point Bend Test Results.....	24
Table 4.	Measured Tenacity, Load, Breaking Elongation and Modulus of Coated vs Uncoated Kevlar.....	39
Table 5.	Measured Tenacity , Load, Breaking Elongation and Modulus vs. Allylamine Coating for Kevlar KM2 and K29 After Removing the Sizing.	40
Table 6.	Interfacial Shear Strength (t).....	48
Table 7.	Interfacial Shear Strength (t).....	48
Table 8.	Proposed Treatment, Kevlar 29 and KM2 .....	49
Table 9.	Impact Properties of GDC Composites.....	58
Table 10.	Impact Properties of GDC Composites.....	60
Table 11.	Impact Properties of GDC Composites.....	61
Table 12.	Impact Properties of GDC Composites.....	62
Table 13.	Impact Properties of GDC Composites.....	63
Table 14.	Kinetic Energy Absorbed Upon Ballistic Impact .....	82
Table 15.	Ballistic Limit of Each Type of Composite.....	84
Table 16.	V50 Of Each Type Of Composite.....	85
Table 17.	Outline of Material Response.....	88
Table 18.	Material Properties Used for Impact Simulation .....	96

## **PREFACE**

This report describes work on viscoelastic properties of advanced polymer composites for ballistic protective applications that was undertaken by the authors at Drexel University's Fibrous Materials Research Laboratory. The U.S. Army Natick Research, Development and Engineering Center's Project Officer was John Song and the work was under Contract Number DAAK60-92-K-0004. This phase of the project began in 9/92 and ended in 8/93.

The citation of trade names in this report does not constitute an official endorsement or approval of the use of a product or item.

Revised: April, 1994

# **VISCOELASTIC PROPERTIES OF ADVANCED POLYMER COMPOSITES FOR BALLISTIC PROTECTIVE APPLICATIONS**

## **Executive Summary**

The specific aim of the program on ballistically resistant structures is to develop a fundamental understanding of the damage resistance characteristics of protective composite materials of interest to the Army. This aim is carried out by a systematic characterization of the viscoelastic behavior of the structural components of the composites.

The Viscoelastic Composites Program is structured as a multiple year effort. The first year is dedicated to instrumentation, tooling, establishment of protocols for the characterization of the component materials, exploration of the gradient design concept and the establishment of a framework for modeling the viscoelastic response of composite structures under impact. A close working relationship has been established with Natick technical personnel. Two joint papers have been published on the viscoelastic properties of polymeric composites. A workshop on the engineering properties of fibrous materials was also offered in conjunction with faculty members of the Textile Technology Center through the support of Natick and the State of Pennsylvania. Technical accomplishments in the first year of the program are summarized below:

### **Study of the Fundamental Properties**

In the first year of the program, the experimental setup and tooling has been organized for testing the fiber. Experiments with Kevlar 29 fiber and KM2 have been initiated. To determine the long term mechanical properties for this material system, the time-temperature superposition principle has been employed to generate dynamic flexural storage and loss modulus master curves over a wide frequency range of 0 to 100,000 HZ for pure matrix and unidirectional fiber reinforced composite using the TA Dynamic Mechanical Analyzer (DMA-983). Three point bend testing was conducted using an Instron 1127 Universal Tester to verify the DMA test method and specimen clamping configuration.

### **Interfacial Surface Modification**

The interface between the fiber and matrix has a significant effect on the overall performance of a composite. In the first year of the project, the focus was on optimizing the R-F Plasma polymerization of allylamine onto the Kevlar 29 fibers. The

treatment was carried out in two steps, first the fiber is treated with Argon and in the second step with allylamine. It was found that, under the optimum treatment conditions, the plasma treatment does not adversely affect the tensile properties of the fibers. This allows flexibility in the tailoring of interfacial properties to optimize the energy absorption capability of the composites. It was also found that interfacial adhesion between PPTA fiber (Kevlar) filament and matrix increases as the plasma allylamine coating increases.

### Gradient Design Concepts

The gradient design concept was developed and demonstrated in order to address the need for multifunctional composites to defeat the threats a composite would encounter in defense roles. The gradient design concept makes use of a hybrid method combining appropriate architecture and/or material to address a particular type of threat.

Fourteen samples of different design concepts were fabricated by resin transfer molding. They include putting various sizes of hard aluminum oxide spherical particles or filaments into the resin, introducing multiaxial linear systems and a 3-D integrated system. The fiber architectures used in the gradient design composites included woven fabrics, multiaxial warp knits and 3-D braids.

### Impact Testing and Damage Characterization

Drop weight impact testing was performed on panels made of neat matrix and composite panels made of single layer and the gradient designed composites. The impact load vs. time and impact energy vs. time response were characterized for each sample. It was found that fiber architecture plays a significant role in the impact resistance of composite structures. Three dimensional, fully integrated structures such as 3-D braids promise to improve the lower velocity impact resistance of composites. At low velocity, the impact response of the composite is global, while at high speeds, the behavior of the composite is localized due to the shock wave effect.

In order to study the effect of fiber volume fraction on impact behavior, 3-D braided composites with a high fiber volume fraction of 75% were fabricated for future impact testing. In order to characterize the damage modes and failure mechanism involved in impacted composite structures, a series of damage assessments have been carried out on post-impact samples at the macroscopic as well as microscopic level. In order to gain some insight into the damage behavior

of the composites, the failure mechanisms and crack propagation behavior of 3-D braided composite samples were studied by means of photographs, optical microscopy and SEM.

It was found that 3-D braided composites experience a complex path of crack propagation, acting as a network of crack arrestors. Failure processes include matrix microcracking, fiber/matrix debonding and fiber pull-out.

### Modeling of Impact Behavior

The objective of the computational modeling of viscoelastic armor is to complement the experimental component of this study so as to obtain a thorough understanding of deformation, energy absorption mechanisms and failure of viscoelastic armors. The long-term objective of the research is to develop a model that relates the viscoelastic properties of the composite and the processing parameters to the energy absorption and damage mechanisms of the composite armor.

Based on our review of the literature in the field, it was decided to use finite element method to simulate the impact phenomenon. ABAQUS was used to investigate low velocity impact and DYNA2D and DYNA3D was used for high velocity impact. The DYNA2D and DYNA3D software was obtained by a collaborative agreement with the Lawrence Livermore National Laboratories in Livermore, CA. A National Science Foundation award was obtained for supercomputing time on CRAY-C90 at the Pittsburgh Supercomputer Center. The modeling team also has access to a Sun/670, a Sun 3/160 and Macintosh workstations. All these resources are interconnected to the local campus Ethernet and INTERNET.

Initial work was directed towards identifying the need to develop a realistic model and to perform simplified computer simulations based on assumed data. The simulations are necessary in order to assess the computer requirements and to converge the mesh. The needs that have been identified for immediate attention are in material characterization in the dynamic range based on the dynamic test data and in incorporating an anisotropic viscoelastic constitutive model in the finite element program.



## **1. Introduction**

### **1.1 Background and Objectives**

This program is funded by the U.S. Army Natick Research, Development and Engineering Center through the Textile Technology Center which consists of three institutions- Drexel University, Philadelphia College of Textiles and Science and Temple University. The general objective of the Textile Technology Center is to develop the science and technology base for multifunctional fibrous materials which addresses the needs of Army personnel protective systems. The current focus of the program is on the fundamental issues of ballistically resistant structures. The program is structured in such a way that the areas of focus will be modified or expanded to reflect the changing needs of the Army.

The specific aim of the program on ballistically resistant structures is to develop a fundamental understanding of the damage resistance characteristics of protective composite materials of interest to the Army. This aim is carried out by a systematic characterization of the viscoelastic behavior of the structural components of the composites.

It is expected that, through microscopic evaluation and macroscopic observation at various structural levels, a solid foundation will be established for the modeling of the impact behavior of the composites. Coupled with innovative materials concepts, this mechanism-based modeling will enhance our capability to design and tailor composite structures for ballistic protection.

Accordingly, the overall objective of this program is to establish an integrated design framework for the development of ballistic-protective composites through a thorough understanding of the mechanisms fundamental to the response of viscoelastic armor.

The specific tasks for this multiple year program include:

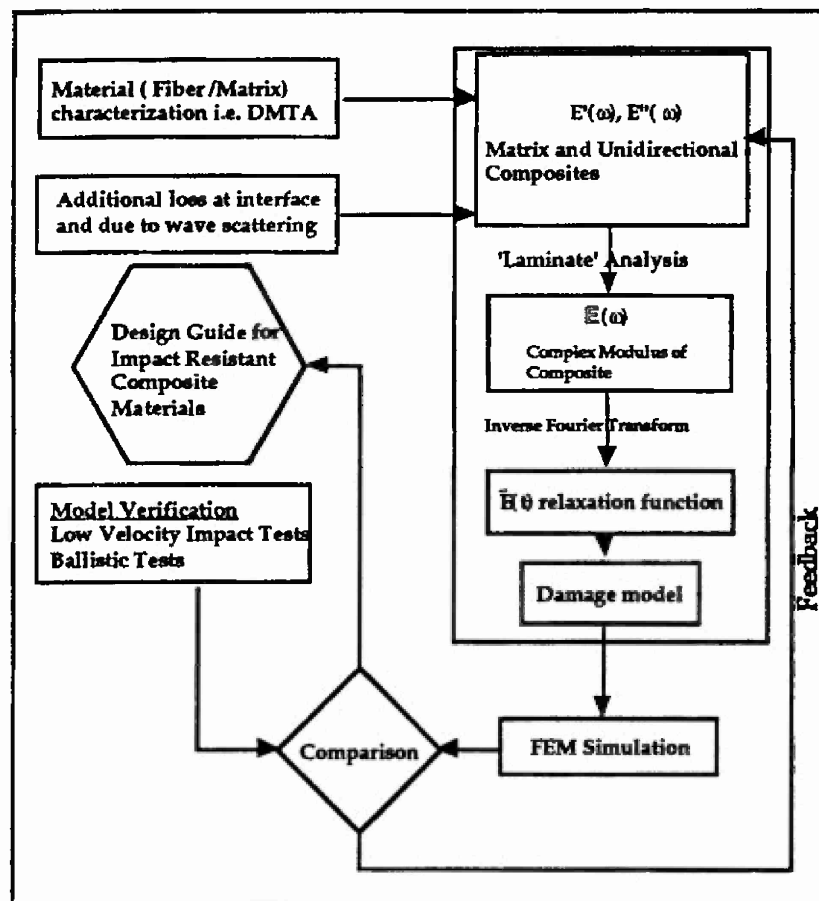
- Establishment of experimental facilities for the characterization and processing of the material components of the viscoelastic composites;
- generation of the fundamental viscoelastic materials data;
- characterization and understanding of the ballistic behavior of the composite structure;
- establishment of a viscoelastic model for ballistic protective composites;
- demonstration of innovative design concepts for ballistic protective composites.

This first year program is organized into four areas of study aiming at exploratory investigations, establishment of experimental procedures and analytical frameworks as well as developing a better definition of the problem in

ballistic composites. The following four interrelated topics of study were carried out by one graduate student and four post doctorate and research associates under the direction of the principal investigator:

- Material Characterization
- Surface Modification of Kevlar® 29 and Kevlar KM2
- Gradient Design Concept for Composite Armor
- Computational Modeling of Impact Behavior of Textile Composites

The integration of the research components in this study can best be illustrated in the following flow diagram:



**Integration of Research Components**

By establishing a quantitative relationship of energy absorption of the composites to the processing parameters, fiber architecture and material properties, this study will provide guidance for the design and manufacture of multifunctional fibrous systems for ballistic protection.

## 2. Material Characterization

### 2.1 Introduction

Excellent mechanical properties and low density make Kevlar® reinforced polymeric composites the current ballistic protective materials in the Army. Because of the viscoelastic nature of the fiber and matrix, the behavior of the composite is viscoelastic. An understanding of the viscoelastic behavior upon ballistic impact is necessary in order to predict and optimize the durability of the composite system.

In order to characterize the viscoelastic behavior of the fiber and matrix within the composite and to elucidate their contribution to the viscoelastic behavior of composites under impact loading, creep, stress relaxation, the dynamic and thermal-mechanical properties of the fiber, yarn, fabrics, matrix and composite must be thoroughly examined.

#### 2.1.1 Material Systems Used

Kevlar 29 1500 denier yarns used in this study was obtained from DuPont. The matrix material was Epon® resin 8132/curing agent U obtained from the Shell Chemical Company. The basic mechanical properties provided by the manufactures for both fiber and matrix are shown in Table 1.

**Table 1. Basic Mechanical Properties of the Materials**

	Kevlar 29	Epoxy
Strength (Ksi)	425	7.5
Modulus (Msi)	10.6	0.45
Density (g/cc)	1.44	1.21

#### 2.1.2 Viscoelastic Behavior

Viscoelastic effects in solid polymers are traditionally observed under four experimental situations: creep, stress relaxation, energy dissipation, and dynamic loading. The viscoelastic effects are manifested in creep as the polymer deforms under constant load. In stress relaxation, the stress required to maintain constant deformation decreases. Strain energy dissipates when a polymer experiences loading. This dissipation is confirmed by the hysteresis loop in the stress-strain behavior [1]. Finally, under cyclic dynamic loading, the stress is out of phase with the applied strain as a result of viscoelastic effects.

The viscoelastic properties of the fiber, matrix and composite such as: tensile, creep, stress relaxation will be characterized in the second year. The dynamic mechanical behavior of the matrix and composite material were studied in the first year and will be discussed in the following section.

Note that the total energy dissipation reflects the combined effect of:

- Material properties of the polymeric matrix and fiber.
- Loading mode (i.e. in-plane tension or shear, bending or torsion): Because of the anisotropic character of the stiffness of the composite, different loading modes result in different energy absorption levels.
- The state and geometry of interfaces. (This has been experimentally observed in the damping behavior of uniaxial composites, i.e. the matrix and fiber behavior were found not to be enough to justify for the total energy dissipation provided by the composite. It has been postulated that the matrix/fiber interfaces offer an additional contribution to energy dissipation.)
- The macro and micro geometry of the structure.

Because of the time-dependent character of the material properties of the composites, it is necessary to completely characterize the behavior of the composites over a large range of frequencies (or equivalent time). High frequency behavior (or its short-time equivalent) is crucial for impact problems since the event of impact is completed in a short time ( milliseconds for low velocity impacts and microseconds for high velocity impacts). Both the moduli and the ability to dissipate energy must be characterized.

Simple creep/relaxation tests are not adequate, since short-time behavior is masked by transients due to machine limitations. Dynamic mechanical testing analysis (DMTA) will be employed to characterize the behavior of the composites at frequencies from 0.1Hz to above 1000Hz.

## 2.2 Dynamic Mechanical Analysis

When a polymeric material is subjected to cyclic loading at high frequency, the viscoelastic characteristics of the material can be determined by measuring the strain response of the material. The energy dissipation in the specimen causes the corresponding strain to be out of phase with respect to the applied stress.

In the study of the response of a viscoelastic material to a cyclic loading, the important parameters are stress, strain and frequency. Two types of dynamic responses appear in the viscoelastic material: linear or nonlinear behavior. For example, if the applied stress varies sinusoidally with time at a given frequency, and its amplitude is small enough, the corresponding strain will also vary sinusoidally with time and be proportional to the applied stress amplitude. This is the linear behavior. However, if the amplitude of the stress is large and beyond a certain limit, then the strain will still vary with a same frequency but will not be sinusoidal, meaning nonlinear viscoelastic behavior[2]. In this annual report the linear viscoelastic behavior of Kevlar fiber reinforced composite was studied.

The dynamic mechanical properties of viscoelastic materials can be expressed using a complex notation<sup>1</sup>. The stress and strain are given as:

$$\varepsilon(t) = \varepsilon_0 \exp i\omega t$$

$$\text{and } \sigma(t) = \sigma_0 \exp i(\omega t + \delta)$$

$$\text{where } i = (-1)^{1/2}$$

The overall complex modulus  $E^*$  is then given as

$$E^* = \sigma(t)/\varepsilon(t) = (\sigma_0/\varepsilon_0) (\cos\delta + i\sin\delta) = E' + iE''$$

where

$E'$ : the storage modulus, which related to the storage of energy as potential energy during the cyclic deformation.

$E''$ : the loss modulus, which associated with the dissipation of energy as heat when the material is deformed.

$\tan\delta = E''/E'$ : the loss tangent, which is also called internal friction or mechanical damping. The loss tangent is the ratio of energy dissipated per cycle to the maximum potential energy stored during a cycle [2].

The storage modulus describes the stiffness of composite under dynamic stress and strain conditions. It is essentially equal to Young's modulus of the composites and depends upon the testing temperature and frequency [3]. When a viscoelastic material is subjected to high frequency or high strain rates, such as high velocity impact event, the stiffness of the material increases dramatically, which resembles the behavior of viscoelastic material at low temperature. Therefore the storage modulus and the damping properties of Kevlar fiber reinforced composites are very important parameters to the understanding of the energy absorption mechanism upon ballistic impact, since both directly affect penetration resistance as well as deformation upon ballistic impact. An investigation of their viscoelastic behavior over a wide range of frequencies is essential.

The measurement principle of Dynamic Mechanical Analysis involves the application of oscillating strain over a designated temperature span at a number of pre-selected frequencies. In fact, most of the tests are performed at rather low frequencies. High frequency behavior (up to several kHz) is obtained by extrapolation based on the principle of time-temperature superposition.

---

<sup>1</sup>For a formal and precise definition of the complex modulus for composites see Appendix A.

In order to clarify the individual contributions of matrix, fibers, interface, and to optimize the geometry of the composite it is important to characterize the matrix material, the fibers and the composite. Initial efforts have focused on the viscoelastic behavior of the matrix, and unidirectional composites at different levels of fiber reinforcement.

### 2.2.1 Sample Preparation

- Molding of Unidirectional Composite

Unidirectional Kevlar 29 composite samples were fabricated by a compression molding technique as shown in Figure 1. The unidirectional lay-up Kevlar 29 yarns were placed into the bottom tools with surplus of resin. The assembly was then placed into a vacuum to degas and remove the trapped air between the fibers and resin. The top portion of the tool was sealed into the bottom and pressed together, forcing the resin to flow through the fibrous structure. The extra resin was squeezed out of the mold through the gap between the top tool and the bottom tool. The dimension of the mold is 7 x 1.3 x 0.4 cm as shown in Figure 1.

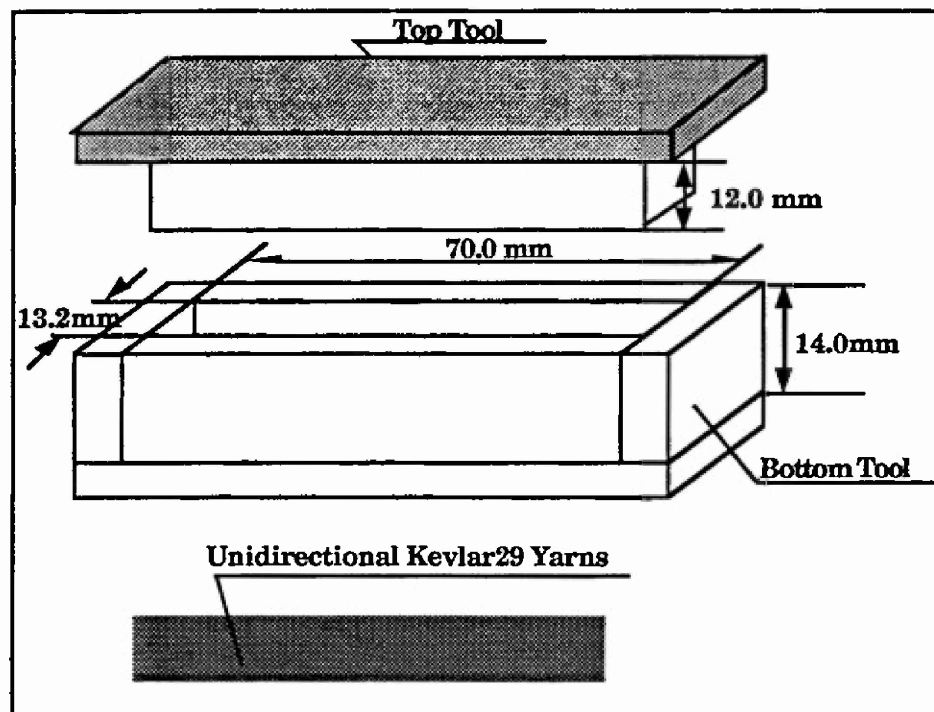


Figure 1. Compression Molding

Initially, the dynamic mechanical properties of pure matrix, unidirectional Kevlar 29 composites with 70% fiber volume fraction were studied in order to understand the composite failure and energy absorption mechanisms demonstrated upon impact and investigate the contribution of matrix and fiber to the viscoelastic behavior of the composite.

### 2.2.2 Experimental Approach and Testing Procedure

A DuPont Dynamic Mechanical Analyzer (DMA-983) was used for the testing of dynamic properties. All samples were measured by using fixed frequency multiplexing method (MULTZ). This method is generally used for [4]:

- Frequency dependent transitions
- Time-temperature superpositioning
- Extrapolating the sample's damping characteristics to extremely low or high frequencies.

This last application is of particular interest. The dynamic mechanical properties of the composite materials over a wide frequency range of 0.1 HZ to 100,000 are our focus in this study.

Figure 2 is the schematic diagram of the operation mechanism. The test specimen is clamped between two parallel arms which are mounted on low-friction pivots. This configuration limits the movements of arms on a single horizontal plane. One of the arms is fixed onto the electromagnetic drive and attached to the LVDT measuring the samples' response (strain and frequency) to the applied stress. The other arm is free to move as shown in Figure 2. The distance between the arms can be adjusted to accommodate various specimen lengths (from 6-65mm) [5]. The electromagnetic motor drives the motor arm to a selected strain (or amplitude). When the motor arm is displaced, the same specimen will 'drag' the free arm to rotate around the pivot toward the same direction. The deformation of the specimen with vertical clamps can be illustrated as follows: the test specimen is clamped between the two arms. Assuming that the original perpendicular distance between the arms is  $B$ , as shown in Figure 2, when the arms rotate an angle  $\phi$ , this distance becomes  $B \cos \theta$  which is shorter than  $B$ . Since the specimen is restrained by the clamps, the specimen has to undergo a flexural (bending) deformation as shown in Figure 2.

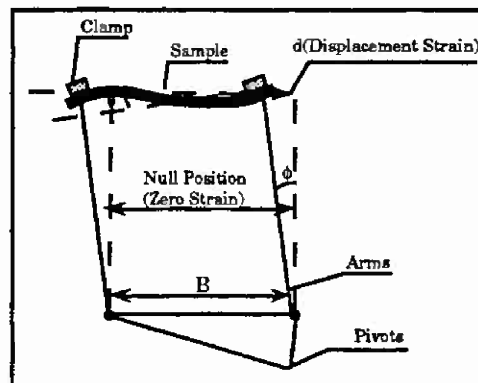


**Figure 2. Specimen Undergoes a Flexural Deformation in DMA Testing [5]**

Because the loading mode is not purely uniaxial as it would be in a tension/compression or four points bending configuration, it is possible to have both

bending and shear in the specimen. Separation of uniaxial deformation from shear deformation is even more important in composite materials where the uniaxial response is characterized by the very high modulus of fibers while the through thickness shear mostly reflects the matrix behavior.

For these reasons a high length/thickness ratio is necessary to minimize shear contribution and obtain information about the flexural modulus. A low length/thickness ratio can provide data for the through thickness shear modulus.

Modulus Equation[4]: when  $L/T > 8$

$$E' = \left[ \frac{4\pi^2 J f^2 - K}{(L/2 + D)^2} \cdot \frac{L^3}{24k^2 A} \right] \cdot \beta(f)$$

where:

$E'$  = Elastic Modulus

$J$  = Moment of Inertia

$f$  = Frequency

$D$  = Clamping Distance

$L$  = Sample Length

$A$  = Sample Cross-Sectional Area

$T$  = Sample Thickness

$R$  = Sample Radius

$K$  = Pivot Spring Constant

$\beta(f)$  = Instrument Compliance Correction

$k$  = Sample Cross-section, Radius of Gyration

=  $T/\sqrt{12}$  for Flat Samples

=  $R/2$  for Cylindrical Samples

Modulus Equation[4]: when  $L/T < 1$

$$G' = \left[ \frac{4\pi^2 J f^2 - K}{2(L/2 + D)^2} \cdot \frac{L}{A} \right] \cdot \alpha \cdot \beta(f)$$

Where:



$G'$  = Shear Modulus

$J$  = Moment of Inertia

$f$  = Frequency

$K$  = Pivot Spring Constant

$L$  = Sample Length

$A$  = Sample Cross-Sectional Area

$D$  = Clamping Distance

$\alpha$  = Shear Distortion Factor

$\beta(f)$  = Instrument Compliance Correction

Lost Energy--Stored Energy Ratio

$$\tan \delta = \frac{E''}{E'} = \frac{\text{Loss Modulus}}{\text{Elastic Modulus}}$$

The defined "length" to the test is shown in Figure 3. The actual size of the test specimens for obtaining  $E'$  and  $E''$  is 62X13.15X1.93mm, and for  $G'$  and  $G''$  is 70 x 2.02 x 10.88 mm.

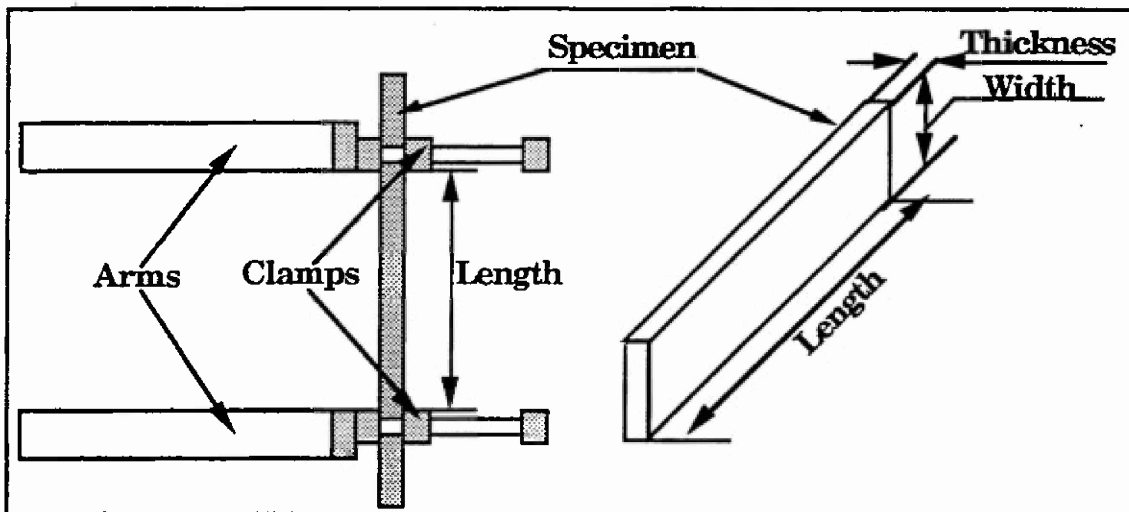


Figure 3. The Defined "Length" of the Specimen [3]

In order to accommodate the dimension requirement for obtaining  $E'$  and  $E''$ ,  $G'$  and  $G''$ , different specimen clamping methods were used. To get  $E'$  and  $E''$ , a vertical configuration of clamping was used as shown in Figure 3. A horizontal

configuration of clamping was employed for  $G'$  and  $G''$ , that is, the thickness became the width and the width became the thickness.

### 2.3 Test Results and Discussion

The focus of this initial study was the dynamic mechanical properties of the composite materials over a wide frequency range of 0.1 to 100,000 Hz. A time-temperature superposition method was employed in order to obtain the dynamic mechanical properties over this frequency range. Modulus data over a temperature range of 0° C to 27.5° C with a 2.5° C increment within a frequency range of 0.1, 0.32, 1.0, 3.2 Hz were collected. Figure 4 to Figure 21 are the testing results, which will be discussed in detail in the following pages. In order to examine the linear viscoelasticity of the composite system, two different strain levels (oscillation amplitude) of 0.1 mm and 0.2 mm were used in the experiment. The title of "Composite 1" in the corresponding figures stands for the unidirectional composite under a strain level of 0.1 mm and "composite 2" for the unidirectional composite under a strain level of 0.2 mm.

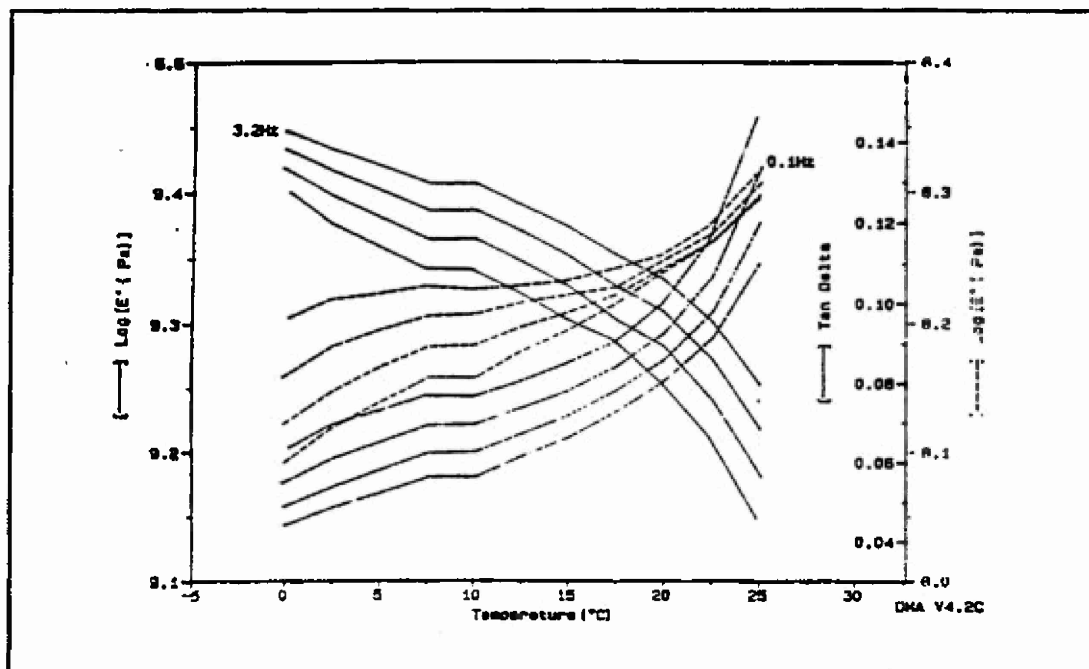


Figure 4.  $\text{Log} E'$ ,  $\text{Log} E''$  and  $\tan \delta$  vs.  $T$  and Frequency for Pure Matrix

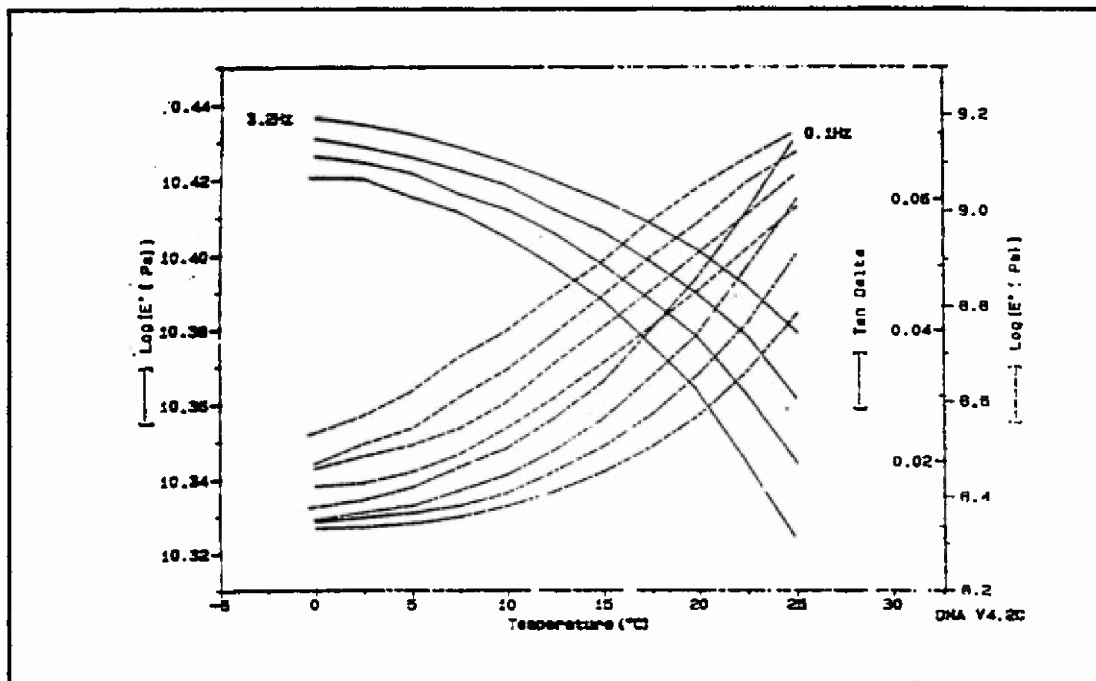


Figure 5.  $\text{Log} E'$ ,  $\text{Log} E''$  and  $\tan \delta$  vs.  $T$  and Frequency for Composite 1

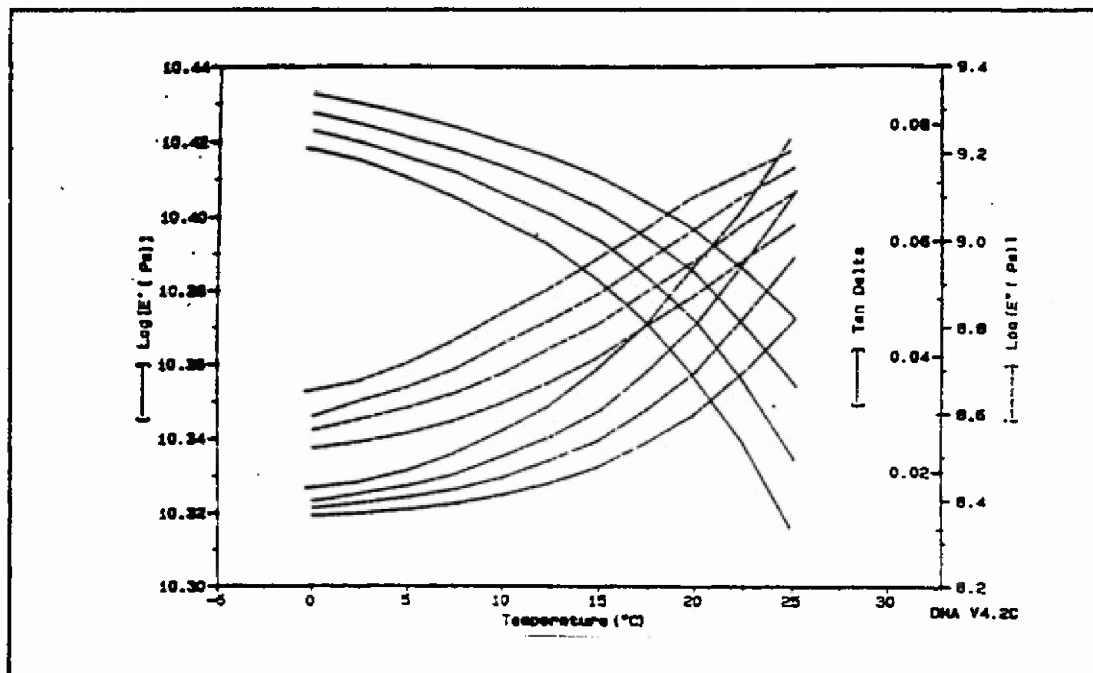


Figure 6.  $\text{Log} E'$ ,  $\text{Log} E''$  and  $\tan \delta$  vs.  $T$  and Frequency for Composite 2

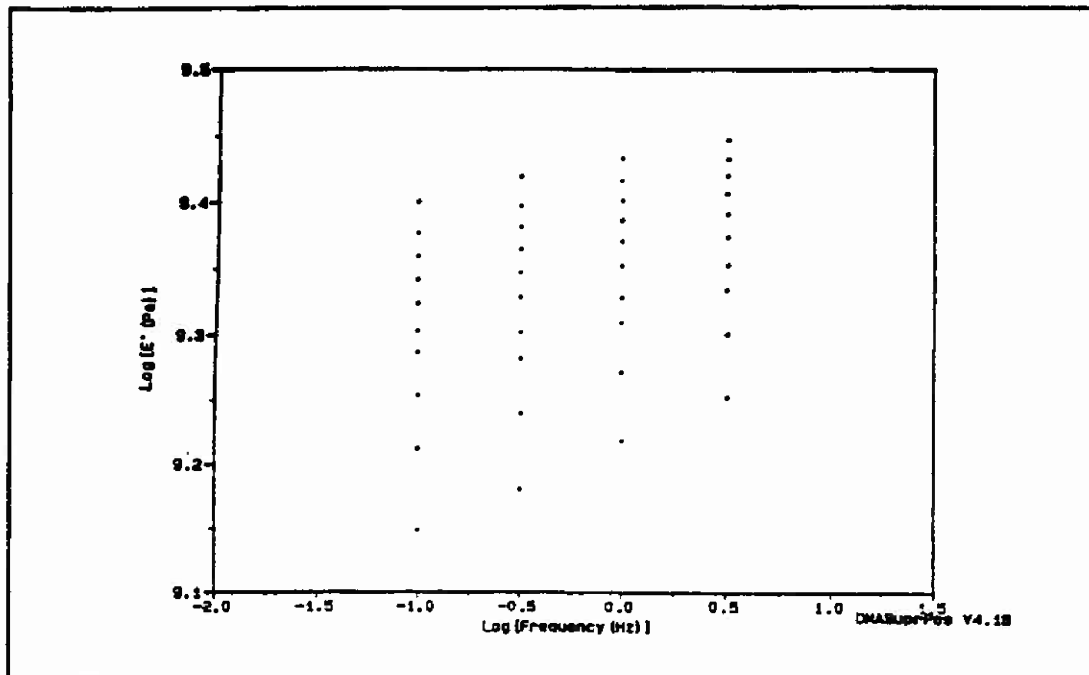


Figure 7. Raw Data of  $\text{Log } E'$  vs. Frequency for Pure Matrix

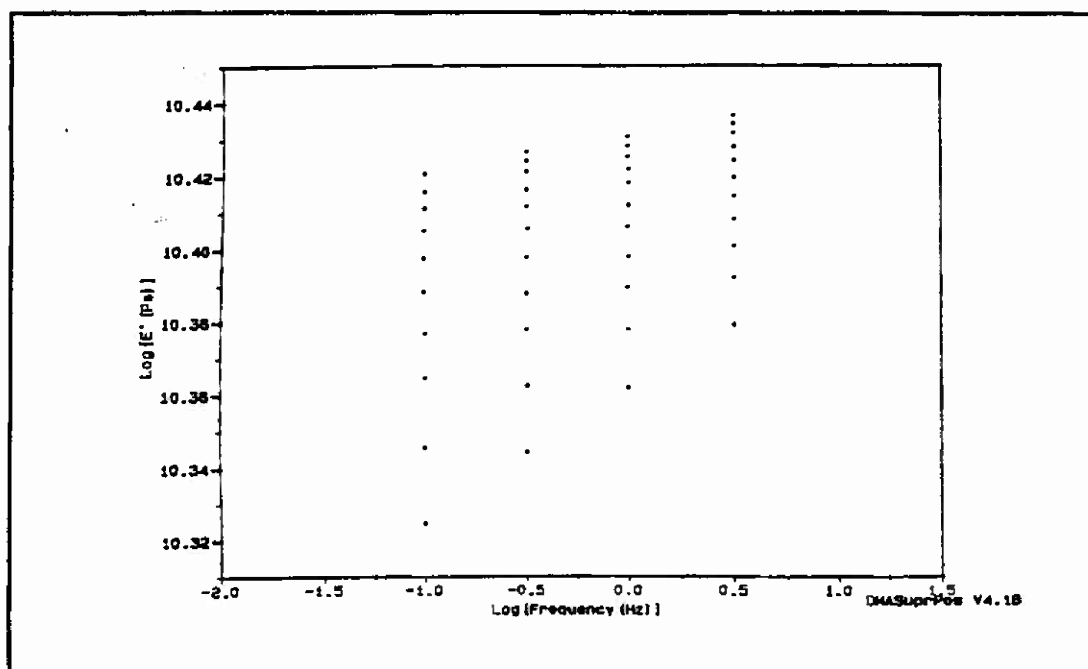


Figure 8. Raw Data of  $\text{Log } E'$  vs. Frequency for Composite 1

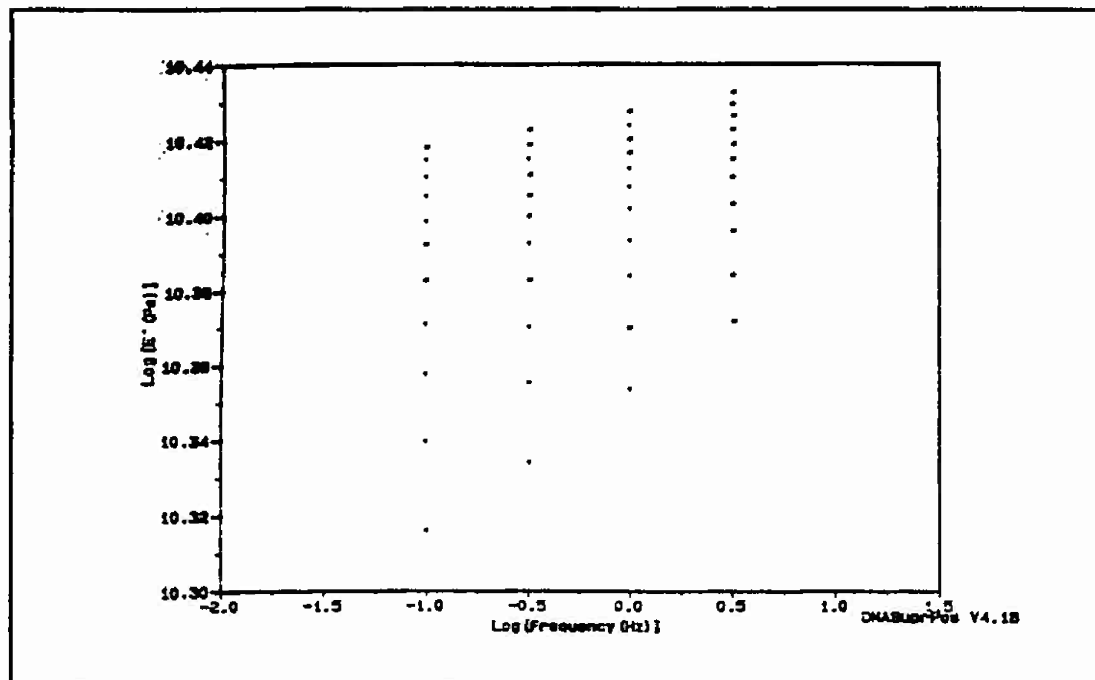


Figure 9. Raw Data of  $\text{Log } E'$  vs. Frequency for Composite 2

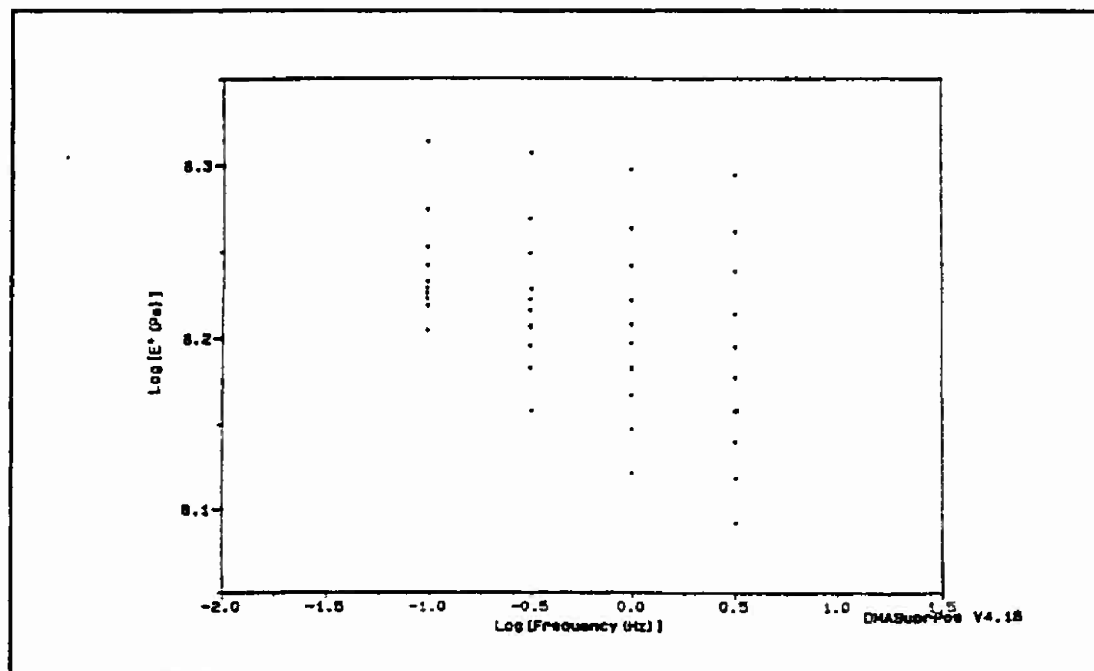


Figure 10. Raw Data of  $\text{Log } E''$  vs. Frequency for Pure Matrix

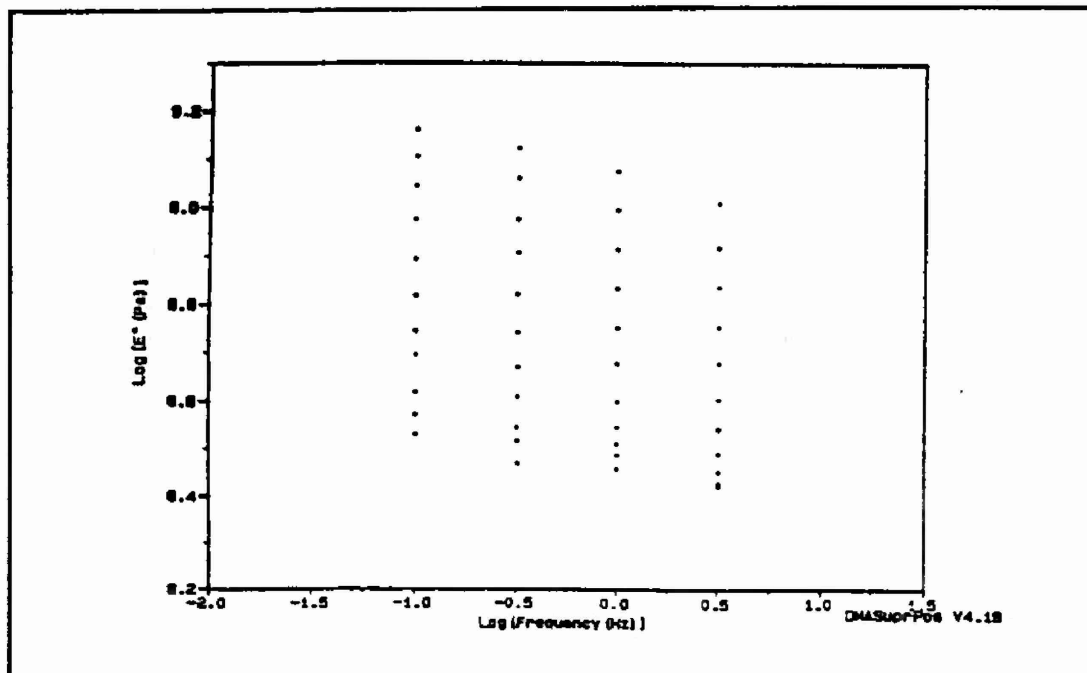


Figure 11. Raw Data of  $\text{Log } E''$  vs. Frequency for Composite 1

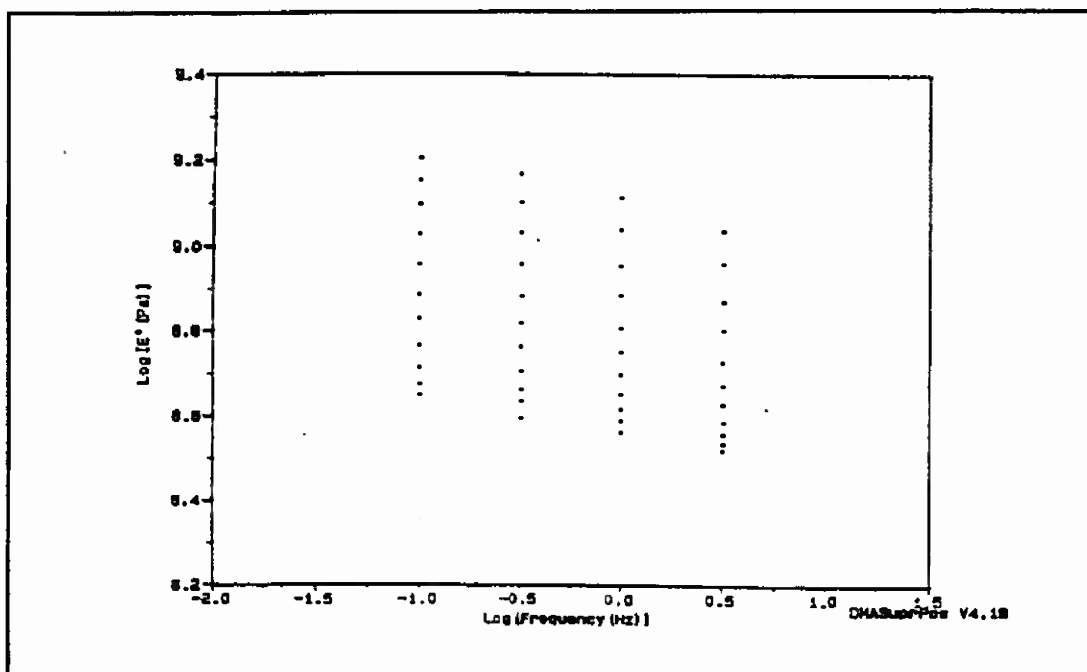


Figure 12. Raw Data of  $\text{Log } E''$  vs. Frequency for Composite 2

Figures 4 to 6 show the raw data for pure matrix unidirectional composites having a fiber volume fraction of 70% under 0.1 mm and 0.2 mm strain levels. All data are plotted modulus versus temperature under different frequencies. Figures 7 to 12 show that the raw data of  $E'$  and  $E''$  were plotted on a modulus versus frequency plot for the above three tests. In order to yield the relevant master curves, a time-temperature shift needed to be performed on the data in Figures 7 to 12. A reference temperature of 23°C (room temperature) was chosen for the master curves. WLF equation was used for finding the dependence of the shift factor on temperature.

Since the behavior of viscoelastic material at high frequency (high strain rate) is similar to the behavior at very low temperature[6], all the  $E'$  data in Figure 7 to Figure 9 above the reference temperature were shifted horizontally and sequentially in a decreasing temperature order towards the high frequency values and all the data below the reference temperature were shifted horizontally in a increasing temperature order towards the lower frequency values so that a smooth master curve was created. The same reference temperature of 23° C and the WLF equation were applied to the  $E''$  data in Figure 10 to Figure 12 as well. When performing the temperature shift, the data above the reference temperature are shifted towards lower frequency direction and the data below the reference temperature are shifted towards higher frequency direction, since damping behavior decreases as frequency increases.

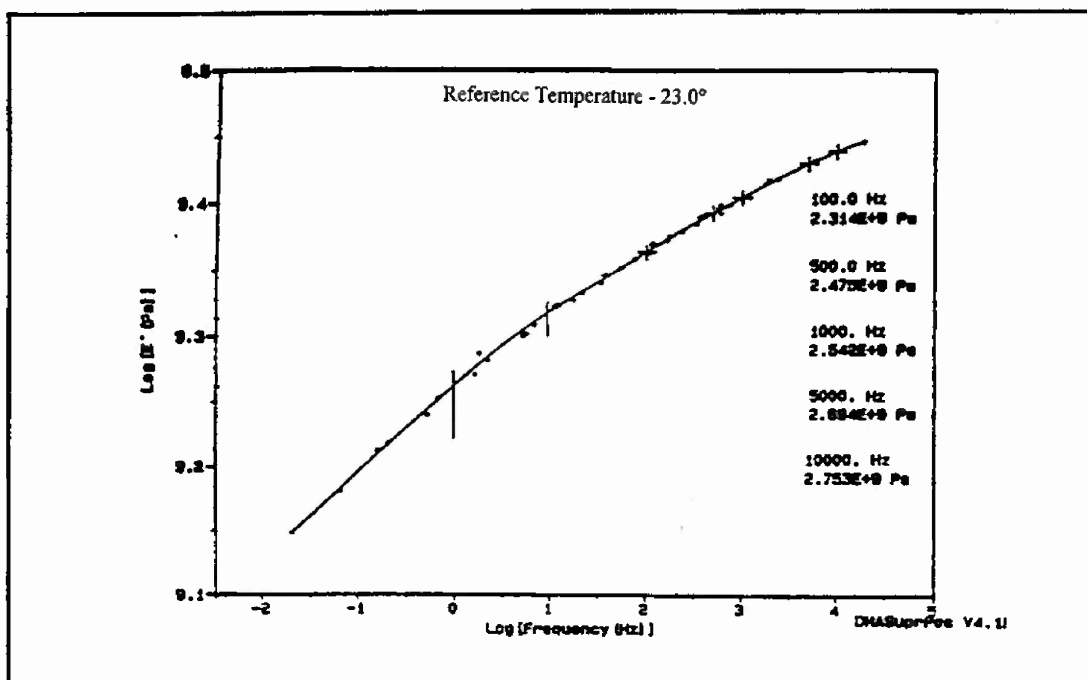


Figure 13. LogE' vs. Log(Frequency) for Pure Matrix

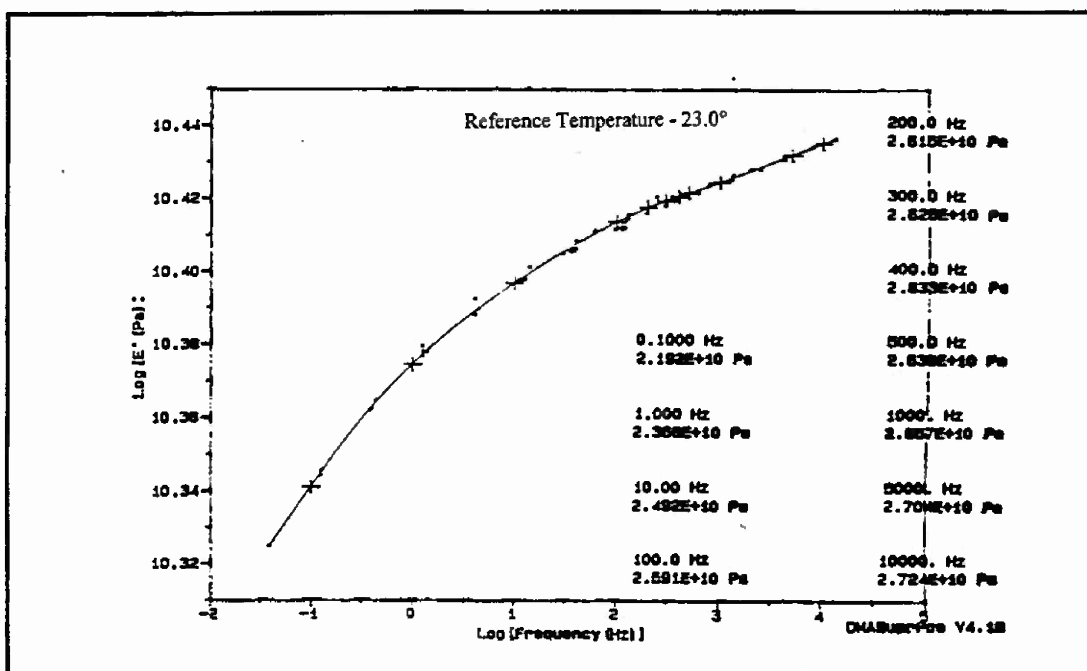


Figure 14. LogE' vs. Log(Frequency) for Composite 1



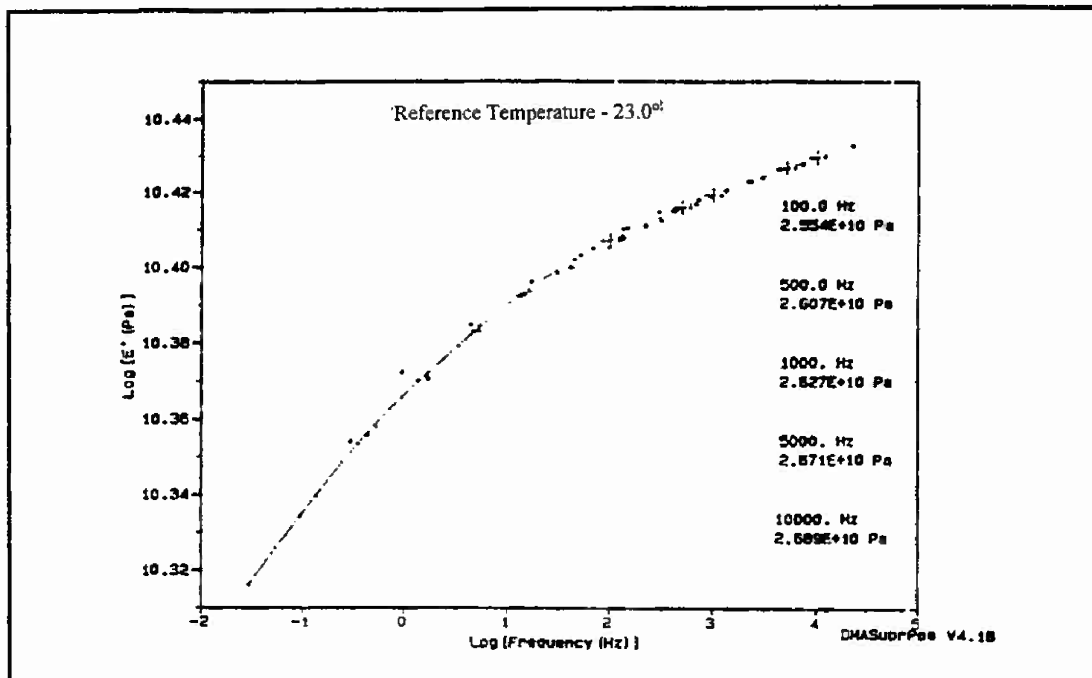


Figure 15. LogE' vs. Log(Frequency) for Composite 2

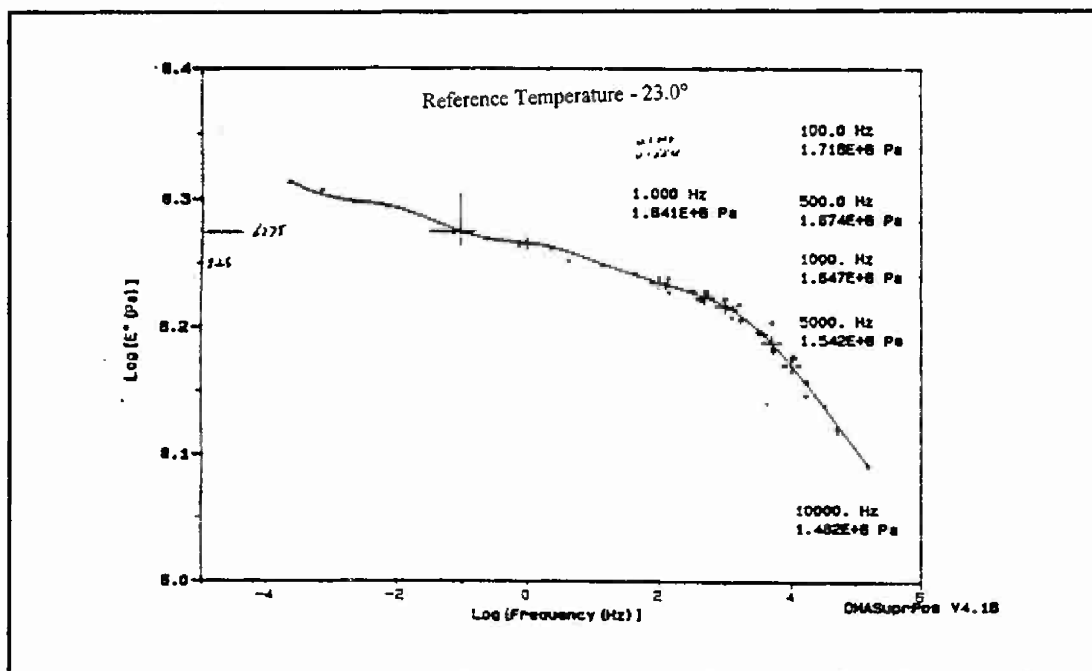


Figure 16. LogE'' vs. Log(Frequency) for Pure Matrix

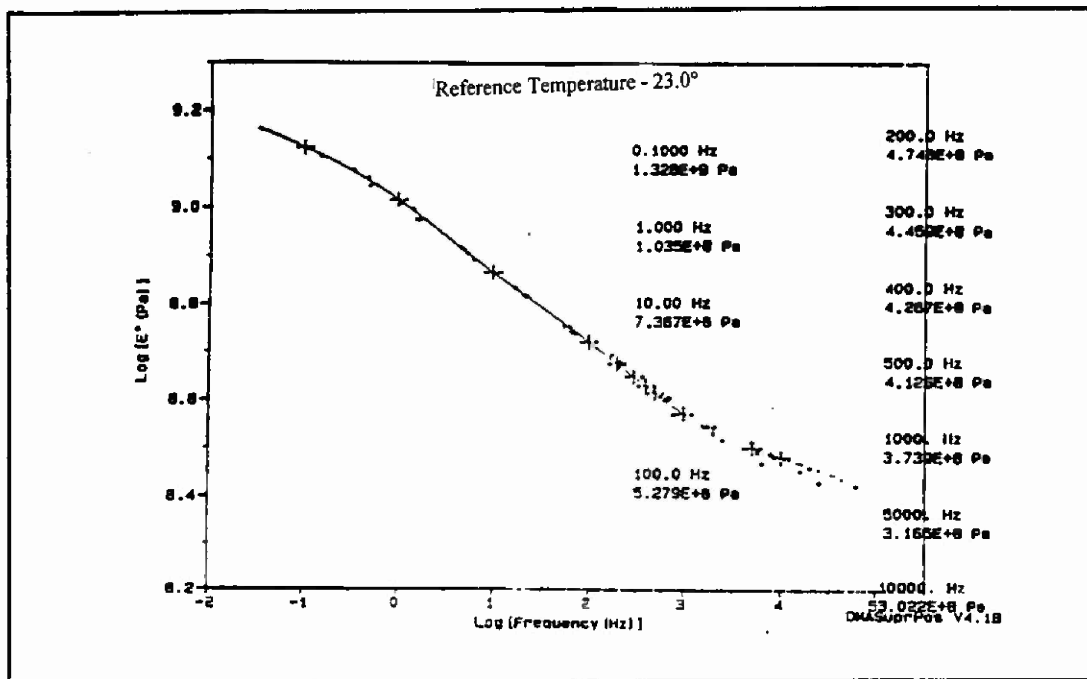


Figure 17. LogE'' vs. Log(Frequency) for Composite 1

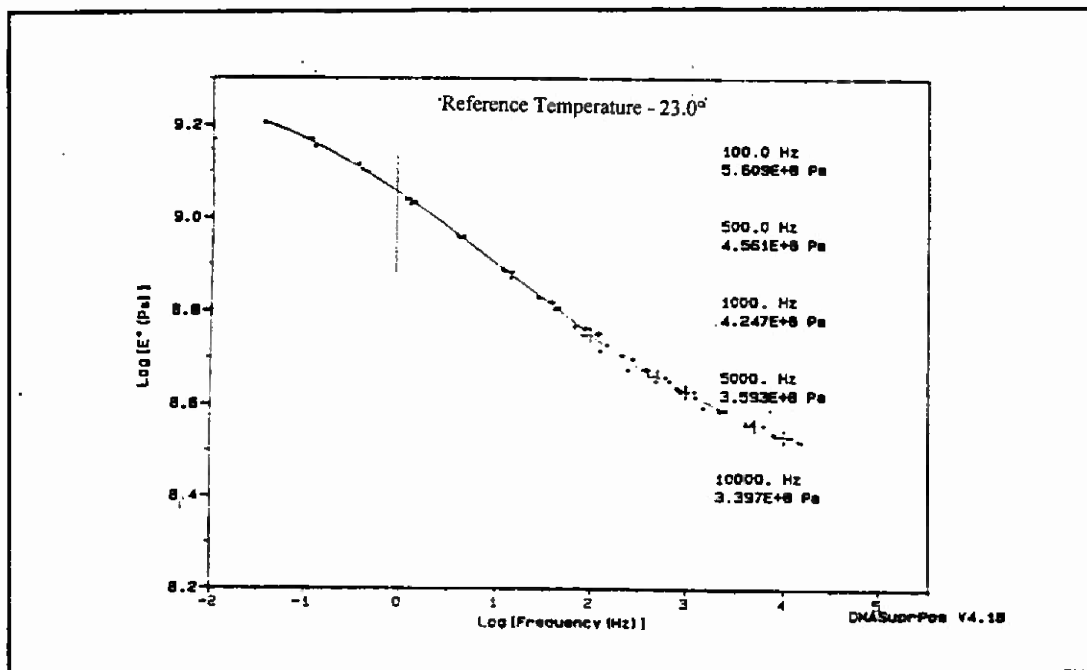


Figure 18. LogE'' vs. Log(Frequency) for Composite 2

Figures 13 to 15 show the variation of the logarithm storage modulus with frequency, Figures 16 to 18 show the variation of the logarithm loss modulus with frequency. The logarithm shift factor as a function of frequency is given in Figures 19 to 21.

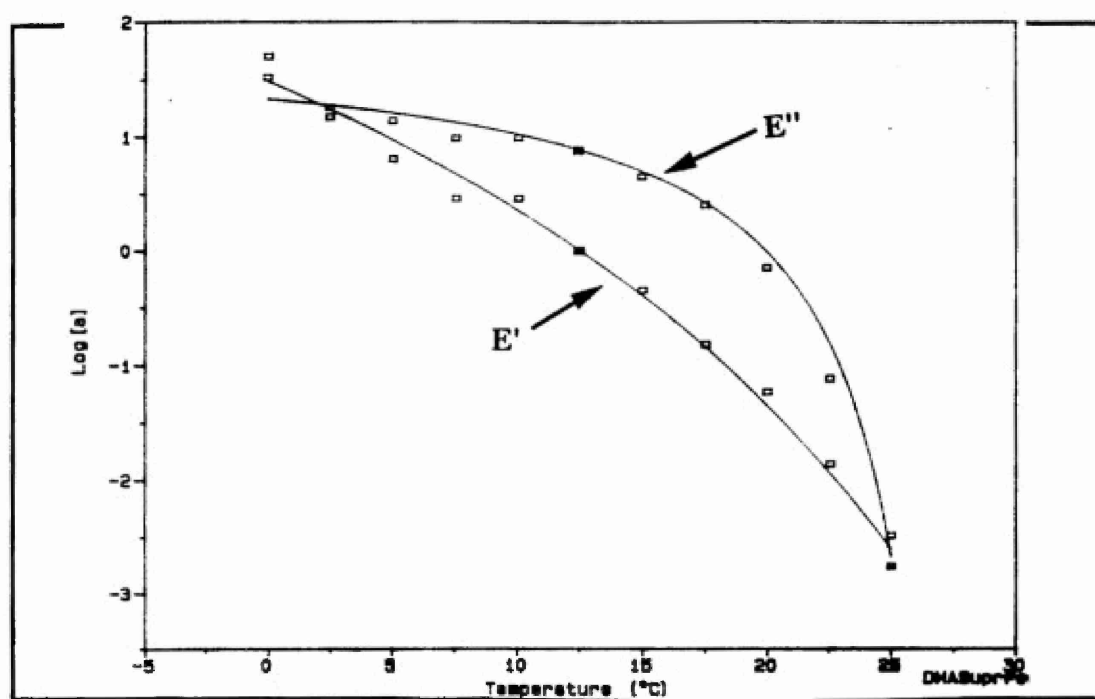


Figure 19.  $\text{Log}(a)$  vs. Temperature for  $E'$  and  $E''$  of Pure Matrix

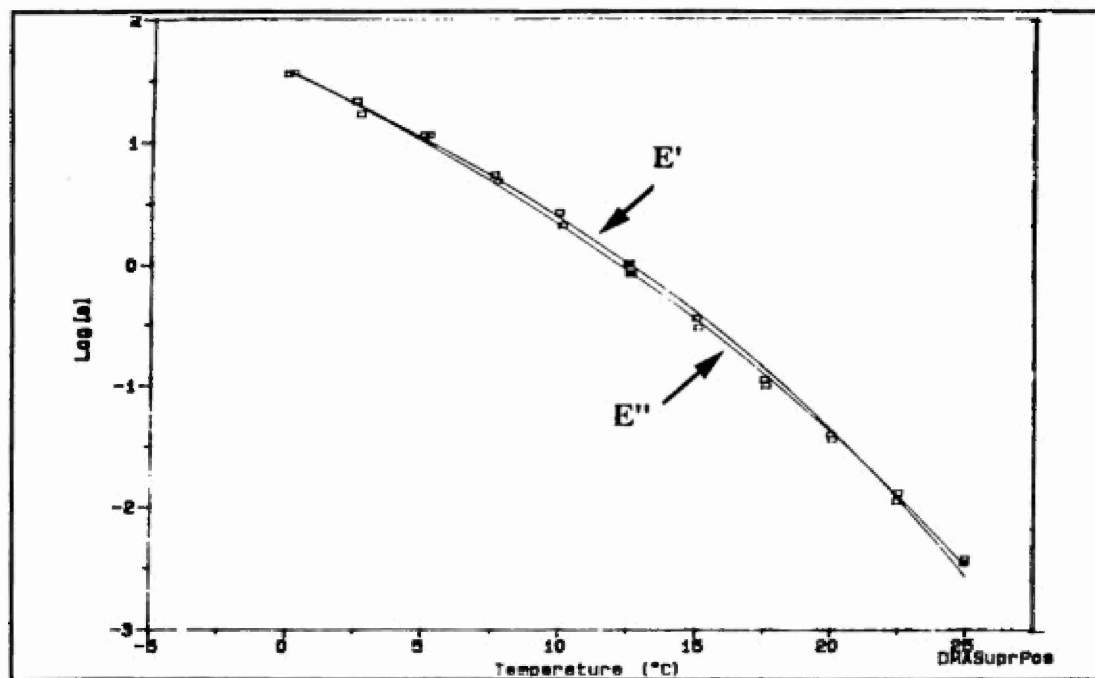


Figure 20.  $\text{Log}(a)$  vs. Temperature for  $E'$  and  $E''$  of Composite 1

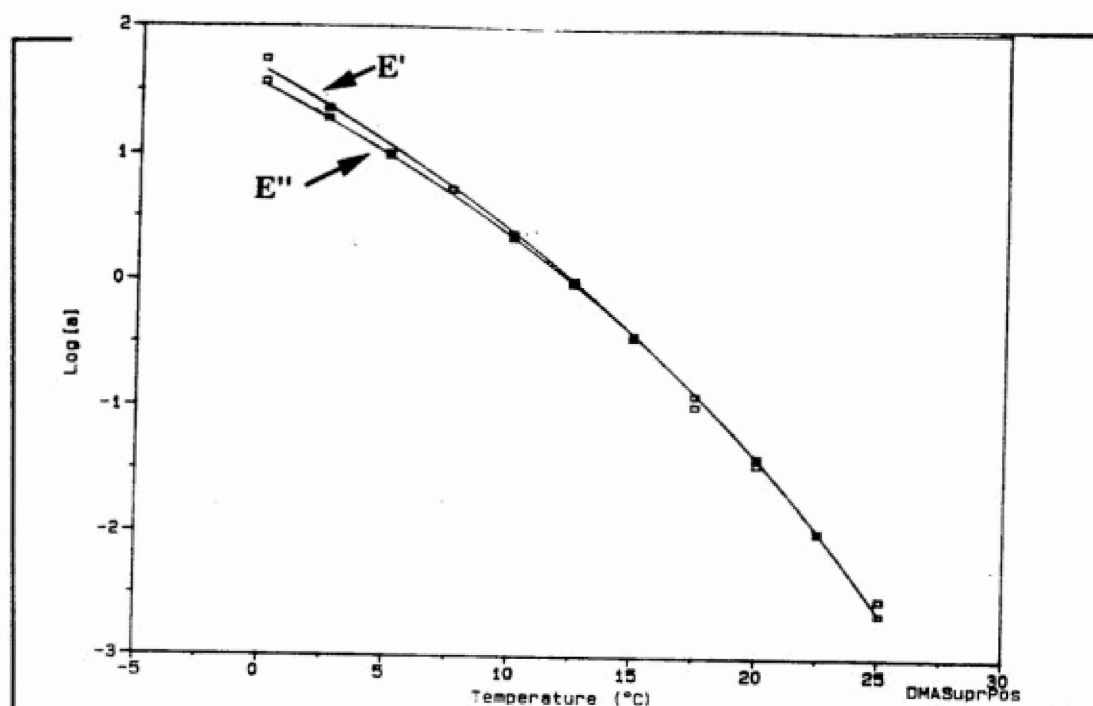


Figure 21. Log(a) vs. Temperature for E' and E'' of Composite 2

Table 2. INITIAL DMA TEST RESULTS

	E' GPa			E '' GPa			tan δ		
	Pure	Composite		Pure	Composite		Pure	Composite	
w/HZ	resin	70%1	70%2	resin	70%1	70%2	resin	70%1	70%2
0.1	1.809	21.92	21.63	0.188	1.328	1.479	0.104	0.061	0.068
1.0	2.065	23.66	23.23	0.184	1.035	1.135	0.089	0.044	0.049
100	2.314	25.91	25.54	0.172	0.528	0.561	0.074	0.020	0.022
500	2.475	26.39	26.07	0.167	0.413	0.456	0.068	0.016	0.017
1000	2.542	26.57	26.27	0.165	0.374	0.425	0.065	0.014	0.016
5000	2.694	27.04	26.71	0.154	0.317	0.359	0.057	0.012	0.012
10000	2.753	27.24	26.89	0.148	0.302	0.339	0.054	0.011	0.012

Note:

70%<sup>1</sup>: Composite with 70% fiber volume fraction was tested at a oscillation amplitude (strain ) of 0.1 mm.

70%<sup>2</sup>: Composite with 70% fiber volume fraction was tested at a oscillation amplitude (strain ) of 0.2 mm.

Within the test-covered temperature range of 0°C--27.5°C and the frequency range of 0.1 - 100,000 Hz, no apparent transitions were found for both pure matrix and composite. The test results indicate that the contribution of fiber is very significant. The storage modulus  $E'$  of a unidirectional composite having a 70% fiber volume fraction is more than 10 times higher than that of the pure matrix. Since the specimen composites were reinforced by unidirectional Kevlar fiber, the dynamic mechanical properties of the specimen are test direction dependent. In this study, only testing along the fiber direction was done. In phase II of the project, angular dependence of the dynamic properties of the material system such as the transverse, bias and other angular directions will be studied.

In order to verify if the test method and specimen clamping configuration were appropriate for obtaining  $E'$  and  $E''$ , three point bend tests were conducted using an Instron 1127 Universal Tester according to ASTM Standard D 790-71. The test results and the specimen directions are summarized in Table 3.

The DMA test results of  $E'$  shown in Table 2 and the three points bend test results of  $E$  in Table 3 for the unidirectional composite are not very close. A three point bending test gives a flexural modulus of 35.7 GPa, while DMA gives  $E'$  of 21.8 GPa. The lower  $E'$  obtained from the DMA test is mostly due to some of the inhomogeneous distribution of the aligned Kevlar yarns in the composite. In order to achieve 70% fiber volume fraction during sample preparation, the fiber has to be compressed very hard and packed very densely. This causes the aligned fibers to distort and eventually lower the modulus of the composite. Another possible factor in lower  $E'$  is inappropriate sample clamping configuration; this will be investigated further in the phase II of the project.

The data shown in Table 2 also demonstrate that the viscoelastic behavior of the composite system is linear for the levels of amplitude applied in our experiment. Unfortunately it is not possible to increase the amplitude of oscillation arbitrarily in order to prove the limit of linear behavior because of the load limit for the safe operation of the DMA.

**Table 3. Flexural Three Point Bend Test Results**

	Modulus(GPa)	Dimension of Specimen(mm) (LxWxT)	Crosshead Speed(mm/min)
Neat Matrix-1	1.44	51.39x11.32x2.58	1.0
Neat Matrix-2	1.49	51.39X10.50X2.60	1.0
Uni-composite-1	35.35	51.39X13.15X1.93	1.0
Uni-composite-2	35.97	51.39X10.88X2.02	1.0

## 2.4 Plan for the Second Year of the Project

### 2.4.1 Material Characterization

In the first year of the program, experimental setup and tooling has been organized. Initial dynamic mechanical testing and three points bend test have been conducted using the DuPont DMA and an Instron machine. Based on the results from the initial study and the experience obtained in the earlier work with PEEK/Graphite composite, the following material characterization experimental work will be conducted in the second year of the project:

- Further investigation of the dynamic mechanical behavior of Kevlar/Epoxy composite systems, including the characterizations of the dynamic mechanical properties of the matrix, fiber and composite materials over a wide frequency range of 0--10<sup>6</sup> HZ using time and temperature superposition technique.
- The viscoelastic behavior of the material system under simple tension at various strain rate, creep and stress relaxation will be conducted using Kawabata evaluation system, an Instron machine and DMA, respectively.

### **3. Surface Modification of Kevlar 29 and Kevlar KM2 Using R-F Plasma**

#### **3.1 Introduction**

Plasma polymerization of a monomer onto the fiber surface is a powerful technique, which produces a linked interface. The plasma-produced film layer is pin-hole free, highly crosslinked and is well grafted to the fiber substrate. Functional groups on the surface of the grafted film will act as a coupling agent. A further advantage of this technique is fine control over coating thickness. For example, the thickness of the grafted polymer layer produced can be made very small compared to the fiber diameter.

The plasma polymerization technique has several advantages over conventional coating methods. The strong interfacial bonding between treated fibers and the matrix will provide for effective load transfer and protect the interface from aggressive environmental attacks. Monomer selection for polymerization is based on the functional groups desired and their compatibility with the matrix material.

The current study deals with the modification of Kevlar 29 and KM2 fibers by RF plasma. The objective of this approach is to optimize the bonding between Kevlar 29 and Kevlar KM2 fibers and epoxy resin matrix. The gas media utilized in the chamber was argon followed by three kind of monomer. The effect of plasma treatment on the interface between fiber and matrix materials will be tested by: a) Single fiber pull-out and b) Tensile test of Kevlar fibers yarn.

##### **3.1.1 Objectives**

###### **General Objectives**

Optimization of the bonding between Kevlar 29 and Kevlar KM2 and the epoxy resin matrix by RF-Plasma polymerization of the following monomers were investigated onto:

- a) Allylamine
- b) Ethylene diamine
- c) Styrene

#### **3.2 Technical Approach**

##### **Argon Plasma Treatment**

Argon plasma etching at 5 minutes and 50 W for Kevlar 29 KM2 was used. At 30 W, the etching was very slow and lacked uniformity along the fiber length; above 50 W, the plasma power reduced the tensile strength of the fiber.

##### **Plasma Polymerization and Coating of Allylamine**

The Kevlar fibers were first treated with argon plasma for 5 minutes at 50 W before the vapor of allylamine monomer was introduced into the reactor chamber at the same plasma power level. The monomer flow rate was kept constant at 0.02 g/min, which resulted in a 0.5 Torr reactor pressure. The desired plasma power of 50 W was selected. Treatment time varied from 15 to 45 minutes. Plasma power was terminated at the end of the treatment.

### SEM Examination

The surface morphology of the treated fibers was examined under the SEM (JOEL model JSM-35CF). Fibers were coated with a vapor-deposited thin layer of gold to induce conductivity before examination under the SEM.

### The Use of RF Plasma

A plasma is partially ionized gas composed of ions, electrons and neutral species. It is a state of matter that can be created by such diverse techniques as flames, electrical discharge, electron beams, lasers or nuclear fusion. Plasma created in a reactor chamber is used to modify the surface of materials. In this technique, free electrons acquire energy from the imposed electric field and lose it through collisions with neutral gas molecules. These collisions produce metastable atoms, free radicals, ions, etc. which act as precursors to unique and novel chemical reactions. The plasma created is characterized by electron energies in the range of 1-10 eV and by electron densities in the range of  $10^9$ - $10^{12}$  cm<sup>-3</sup>. It is also characterized by a lack of thermal equilibrium. While the bulk temperature is near ambient temperature (300-600 K), the temperature of free electrons in the ionized gas can be 10-100 times higher. This type of plasma is referred to as "cold plasma".

### Mechanism of Polymerization

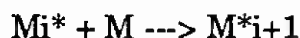
Many of the common polymers such as polyethylene and polyester are formed by addition and condensation polymerization. Monomers are linked to form polymers by various kinds of initiation, followed by propagation and finally termination. In plasma polymerization, the initiation of the polymer can be characterized as atomic or elemental. In this class of polymerization there is no specific site for energy absorption of the monomers. Thus the resulting polymer is highly complex, and the molecular structure of the monomers is not retained. Plasma polymer structures are strongly dependent upon the plasma reaction parameter under which they are formed.

Plasma polymerization mechanisms may be categorized into two groups: plasma-induced polymerization and plasma polymerization. In plasma-induced polymerization, reactive species induced by the plasma initiate the polymerization. The structure of the starting monomer must contain polymerizable sites, such as olefinic double bonds. The chain propagation mechanism of plasma-induced polymerization can be shown as follows:

propagation







termination

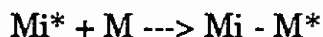


The plasma polymerization mechanism involves large rearrangement and fragmentation of the atoms in the original organic compound in the plasma state. Repeated step-wise reaction is one of the proposed mechanisms of plasma polymerization.

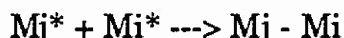
initiation or reinitiation



propagation



termination



where

$M^*$  monofunctional reactive species such as free radical  $i$  and  $j$  are the differences in the size of species involved,  $i = j = 1$  represents the original monomer

### Surface Modification by Plasma Treatment

Plasma treatment of materials may be classified into three major groups. This classification is based on the consumption and mode of gas used to produce the plasma. The three groups are: 1) chemically nonreactive plasma, 2) chemically reactive plasma, and 3) polymer layer grafting plasma. Single atomic inert gases such as argon gas are used to produce chemically nonreactive plasma. Argon plasma is not consumed in the plasma chamber while it ionizes other molecules or etches the surface. Inorganic and organic gases such as  $O_2$ ,  $CF_4$  and  $N_2$  chemically react with the substrate, but do not form a polymeric layer. Vapors of organic compounds such as allylamine and acrylic acid form a polymeric solid layer by themselves on the substrate.

Ablation of material would occur in all three forms of plasma treatment; however, the mechanism of this ablation is specific to the plasma type. In chemically nonreactive plasma processing, ablation occurs by momentum exchange; in chemically reactive plasma processing, ablation can occur by both chemical and physical etching. In the plasma forming process, ablation and deposition occur at the same time; however, the deposition rate is greater than the ablation rate.

In the work done by Krishnamuthy [7] and Kamel, the surface of the glass fiber was modified by means of plasma treatment. In this technique the fiber surface was first treated with chemically nonreactive plasma (argon gas), then a vapor of organic monomer (allylamine) was introduced to form a thin layer of highly crosslinking polymer film on the fiber surface. Most of the organic compound vapors tended to form a film on the surface subject to the glow discharge depositing covalently bonded polymer surface on the substrate. Deposition of these films on the surface of the glass fiber resulted in surface modification and

improved the compatibility between fibers and the matrix material. The biggest advantage of this technique is the fact that plasma polymerization only changes the surface properties without affecting the bulk properties of the substrate. This is due to the very low penetration range of plasma polymerization.

In general the surface treatment utilizes four major chemical effects (a) to (d) of plasma treatment on the substrate:

(a) Ablation or Microetching

In this process, materials are removed by the etching action of the inert gas. Low molecular weight fractions are formed by means of plasma-induced degradation reaction.

(b) Cleaning

All materials in contact with the environment absorb oils and other organic material that are not easily detectable. When exposed to an oxidative plasma, these contaminants are broken into smaller parts having a low molecular weight and are eventually flushed out of the chamber.

(c) Crosslinking

This is a chemical process in which primary covalent bonds along the main chain of polymer are broken by introduction of inert gases, such as helium or argon. Active sites are produced by introduction of inert gases which react with free radicals of adjacent chains or monomers introduced into the chamber to form crosslinking.

(d) Surface Activation

Various activities such as ion impact, and free radical interaction result in the creation of active sites on the substrate surface. Introducing functional groups as a result of the direct reaction of the active gas with the activated polymer surface is very effective in increasing the surface energy. Plasma reactions, such as graft polymerization, are also obtained due to surface activation.

The above four processes happen simultaneously. The new surface chemistry depends on substrate chemistry, gas chemistry, and the parameters of the reactor chamber. This process is called Competitive Ablation and Polymerization (CAP). Figure 22 shows the overall mechanism of the glow discharge polymerization.

### 3.3 Experimental Procedures

#### Materials

The Kevlar 29 and Kevlar KM2 fibers were obtained from Du Pont. The individual filaments had an average diameter of 11 mm. Laboratory grade Argon gas Airco company was used for the plasma treatment. Epon resin and curing agent was obtained from Shell Chemical Company and polyvinyl butyral modified phenolic

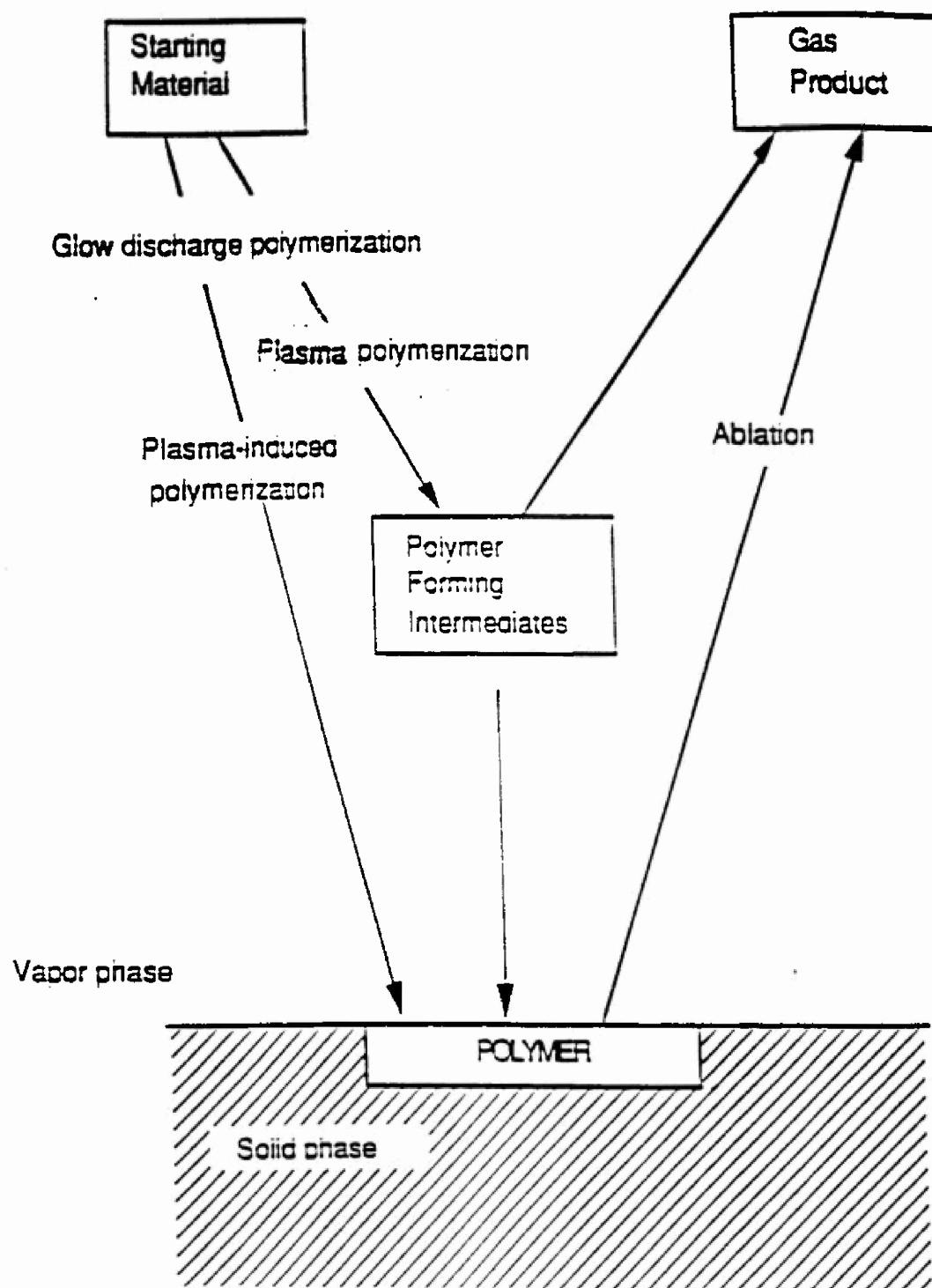


**Figure 22. Mechanism of Plasma Polymerization**

resin from Lewcote Corporation. Allylamine with 98% purity and ethylenediamine with 99% purity were procured from Aldrich Chemical Company, Inc. Styrene from Polysciences, Inc. was the selected monomer for the plasma coating.

#### Tensile Tests at Room Temperature

Yarns were tested at a gage length of 25 cm. Ten specimens of gage length were tested for different treatment of yarns. The test specimen preparation included mounting the yarn on a cut board frame with no twist added. The mounted yarns were sandwiched at the end tab parts with another piece of cardboard and glued together with a structural adhesive (EA 9303, manufactured by the Dexter Corporation, Hoysol Division). The end tabs of the specimens were dried under pressure for 24 hours. The neck part of the paper frame was cut after the specimen was mounted in the grips and before testing.

Room temperature tensile tests were carried out on a model 1127 Instron tester. Tests were performed under standard testing conditions at 70°F, 65% relative humidity. Wedge-section friction grips were used for all the tests. Test specifications for gage length are as follows:

Gage Length (mm)	Full Scale Load (Kg)	Cross Head Speed (mm/min)	Linear Density (den)
250	50	100	1500

#### Fiber Handling

This process was developed to handle the fibers during plasma treatment and the molding of end tabs in preparation for testing. The spectra fibers were stretched on a 10 cm x 4 cm vinyl frame with a centered 7 cm x 3 cm cut out section. The fibers were glued to the frame using vinyl end tabs and cyanoacrylate glue as shown in Figure 23

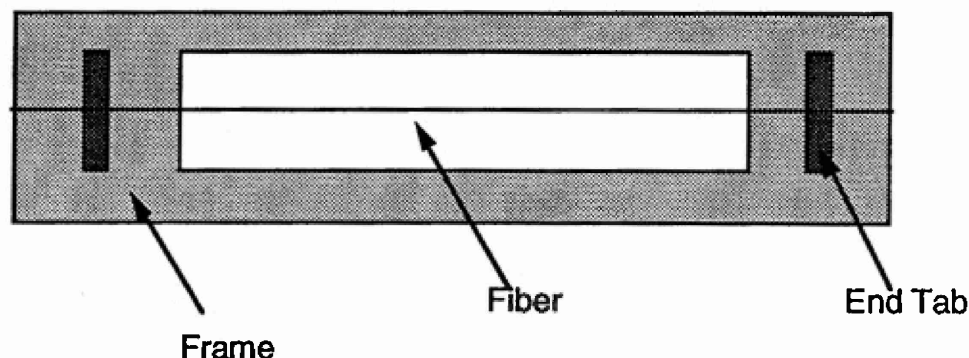


**Figure 23. Single Filament Pull-out Test**

Single filament pull out tests were performed for the direct measurement of fiber-matrix interfacial bond strength. In this method a portion of the fiber length is

surrounded by a small volume of cured matrix. The interfacial strength is measured by pulling the fiber out of the surrounding matrix. Some of the single fiber pull-out geometries are shown in Figure 24.

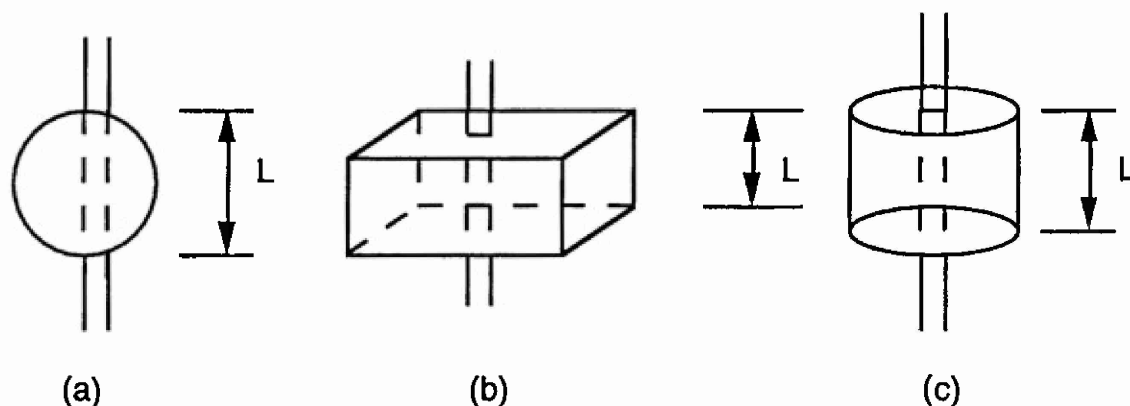


**Figure 24. Three Geometries That May Be Employed for Single Fiber Pull-Out Test**

In order to fully understand the results obtained from the pull out test, the interfacial strength is measured. Some of the single fiber pull-out geometries are shown in Figure 25. This illustrates the effect of maximum load ( $P_m$ ) as a function of the embedded length ( $L$ ). The curve of maximum load vs. embedded length consists of two zones.

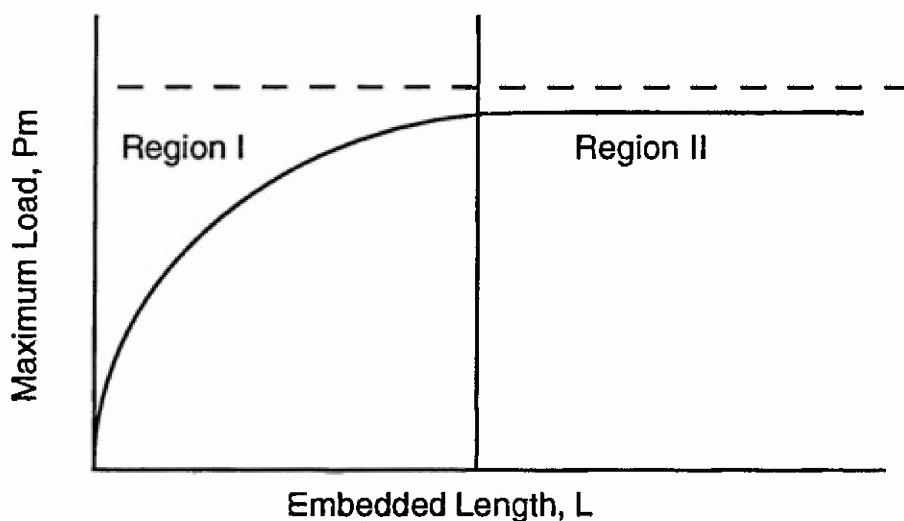


**Figure 25. Plot of Applied Load  $P_m$  vs. Embedded Length  $L$**

Region I is the zone of increasing  $P_m$  while Region II is a zone of constant  $P_m$ . In Region I, proportionality between  $P_m$  and  $L$  is indicative of a simultaneous, uniform interfacial yielding along the entire embedded interface. From this uniform distribution, shear strength value can be calculated using the quotient of the maximum applied load and interfacial area  $P_m/A$ . However, the possibility of

uniform stress distribution at the interface is very unlikely due to a complex state stress which exists on the matrix during the test.

In addition, crack development and propagation were observed under SEM which contradict the assumption of simultaneous yielding. In Region II,  $P_m$  reaches a constant value. In this zone the value of  $P_m$  is not related

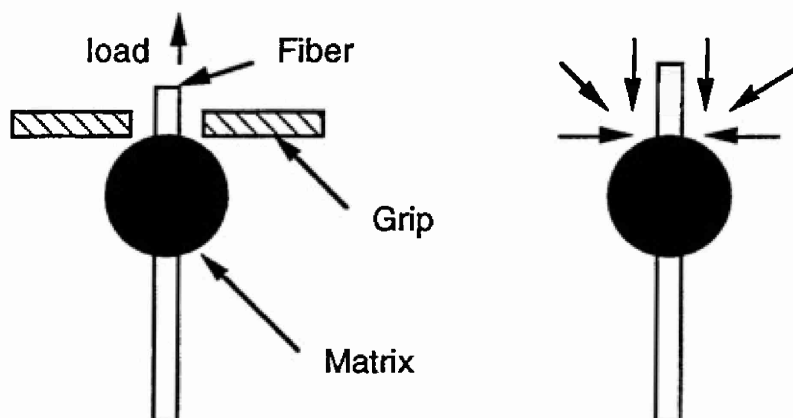


**Figure 26. Schematic of Single Filament Pull-Out Test**

to the interfacial area ( $A$ ), which contradicts the initial assumption of uniform interfacial yielding. Thus, this region is to be avoided in order to produce experimental data sensitive to the size of the interface. This experimental limitation represents difficulties when the fiber diameter is very small. For example for carbon fibers (7 mm diameter) maximum embedded length should not exceed 350 mm in order for the data to be limited to Region I (Figure 25). This length is indeed difficult to work with. Each point in Figure 25 represents the maximum load obtained from a load displacement curve. A schematic of a single filament pull out test is shown in Figure 26.

A typical pull-out load vs. displacement curve (Figure 27) is shown below. The peak in this figure is associated with fiber / matrix debonding. The irregular trace following debonding corresponds to the friction generated as the fiber is pulled out of the matrix. Frictional forces are attributed to resin shrinkage during curing and Poisson expansion as the load drops, which results in an increase in fiber diameter.

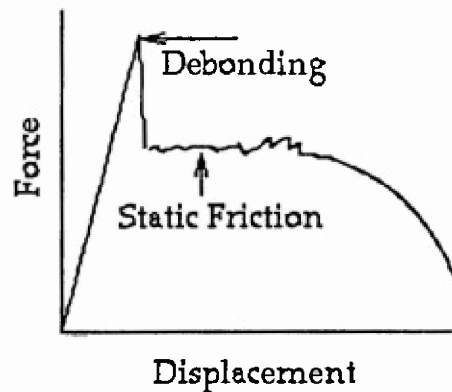


**Figure 27. Typical Pull Out Load vs. Displacement for a Single Fiber Pull-Out Test**

Penn, et al,[8,9] examined the fiber/matrix interface during single fiber pull-out under the SEM. They reported that: a) at the beginning of the loading the unembedded length of the fiber became taut and the fiber diameter reduced slightly, b) as the loading continued a circumferential crack developed at the fiber matrix interface, and c) as the crack propagation stopped, the fiber starts to pull-out of the matrix. Figure 28 illustrates sequence of events during the single fiber pull-out test.

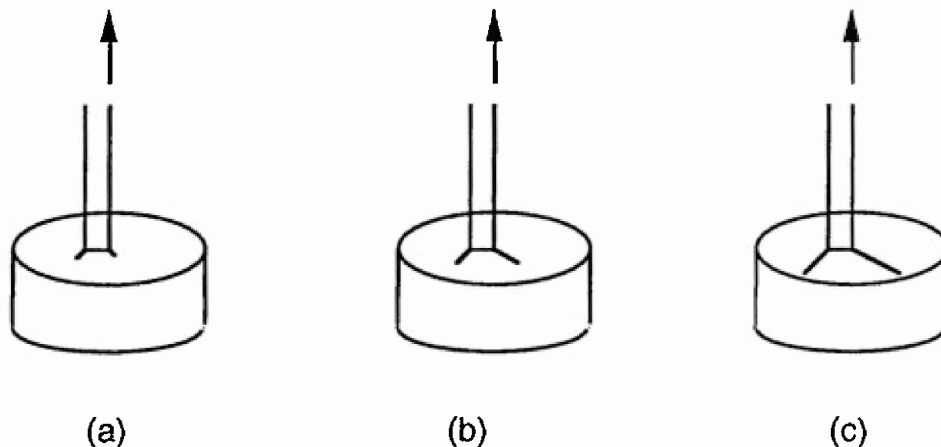


**Figure 28. Schematic Drawing Of The Sequence Of Events During The Single Fiber Pull-Out Test**

Comparing the load-displacement curve to graphical representation of pull-out test, the following observations were made: a) Maximum load is reached at the end of the debonding process and b) the sudden drop in load is associated with the start of fiber pull-out. Therefore, it appears that failure occurs due to crack initiation and propagation at the interface.

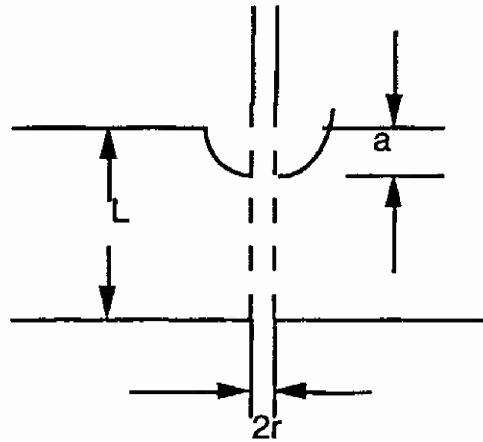


**Figure 29. Schematic Representation of Single Fiber Pull-Out Test With Part of its Length Embedded in the Matrix. Crack Length "A" and the Original Embedded Length L are Illustrated**

Figure 29 illustrates the above observation, with a fiber cured in matrix having a crack of length "a" (which is difficult to measure experimentally, and varies from sample to sample). Based on this model, the effective embedded length is the measured embedded length minus the crack length,  $L_{eff} = L - a$ . As the application of the load continues, the crack length "a" increases, until total debonding occurs. At this stage the load drops and the fiber starts to pull out of the matrix.

Fracture mechanical analysis was used to explain the dependence of  $P_m$  on  $L$ . This model predicted both the rising and the plateau regions of the  $P_m$  vs.  $L$  plots. According to this analysis,  $P_m$  is a function of  $L$  for small values of  $L$ , while it is independent of  $L$  for large values of  $L$ . Other parameters that influence  $P_m$  are fiber elastic properties, fracture surface energy and size. Based on the above discussion, the problem with single fiber pull-out is large scatter in the results, which does not provide unique characteristics for interfacial shear strength. These, however, may be minimized by increasing the size of the matrix section to prevent distortion during fiber pull-out. If that assumption is valid, the interfacial strength can be calculated assuming uniform yielding where the pull-out load is directly balanced by the shear stress ( $\tau$ ) along the embedded length ( $L_e$ ), as follows: from single fiber pull-out, tensile stress, which is required to produce bond breakage, must be equated with interfacial shear strength

$$P_m = \pi s r^2 = 2\pi r L_e \tau$$

$$\tau = s r / 2 L_e$$

where  $r$  is the fiber's radius.



## Sample Preparation and Testing

In order to measure the interfacial shear strength between the Kevlar and the epoxy matrix, a fiber pull-out test was used [11]. In this test, the fiber end of the test sample was placed into a 1 mm-deep silicone rubber cavity, which was filled with epoxy resin. At the other fiber end, extra fiber length was packed into a 35 x 20 mm silicone rubber mold; the fiber ends were 2 cm apart. Epoxy resin was poured into the mold cavities and allowed to cure for 36 hours at room temperature. After removal of the cured epoxy from the molds an aluminum piece of 15 x 15 mm was attached to the 2 mm-thick end using a cyanoacrylate adhesive. The sample was gripped during testing from this aluminum part, to prevent distortion of the thin epoxy test section and pulled at the rate of 1 mm/min. Figure 30 shows the overall shape of the test sample.

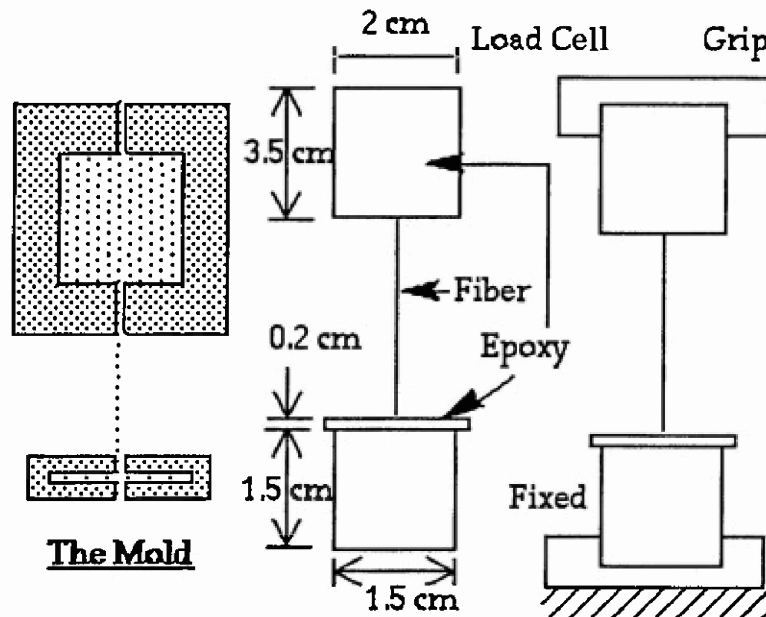


**Figure 30. Schematic of Single Filament Pull-Out Test**

## 3.5 Results and Discussion

### Plasma Treatment

Plasma treatment of Kevlar 29 and Kevlar KM2 is classified into two steps as follows:

#### a- Argon Plasma Treatment

Plasma etching of the fiber surface was found to be sensitive to the presence of oxygen. Therefore, care was taken in purging the reaction chamber three times with argon before starting the plasma etching process. The plasma power selected for the treatment was chosen to be 50 W. At 30 W the etching was very

slow and lacked uniformity along the fiber length. Above 50 W, the tensile strength of the fiber was reduced; for example, at 70 W power and 5 minutes exposure time, the tenacity of Kevlar 29 fibers dropped by 30% of the as-received values shown in Table 4. At higher power, the degradation in strength could be due to rapid etching at higher temperature that may result from a faster rate of bombardment by ions and electrons of the fiber surface. Changes in the fiber surface morphology as a result of argon plasma etching are shown in Figures 40 (Kevlar 29) and 34 (Kevlar KM2).

The argon plasma treatment decreased the Kevlar fibers' apparent diameter.

#### b- Allylamine Plasma Treatment

SEM micrographs of allylamine plasma coated fibers showed an increase in the fiber diameter change in the surface texture. It can be seen from Figures 41 (Kevlar 29) and 35 (Kevlar KM2) that after 15 minutes of allylamine plasma coating, the overall diameter increases by 10%. This coating can be increased by increasing the monomer polymerization time to a maximum of up to 50 % of original diameter after 45 minutes of coating (as shown in picture 37 and 44 for Kevlar KM2 and K29 respectively). The appearance of surface microstructures was changed after 15 minutes of plasma treatment. However after 30 to 45 minutes of treatment, a very smooth thick coating covered the original morphology, causing drawing marks of etched surface defects to disappear from the surface.

Table 4 shows measured tenacity, load, breaking elongation and modulus of coated vs. uncoated Kevlar. The tenacity of allylamine-coated Kevlar 29 and Kevlar KM2 at 15 minutes and 50 W increased slightly over the untreated fiber, due to the chemical bond between the allylamine-plasma and the sizing agent. It is also interesting to observe that, after 30 and 45 minutes of plasma treatment, the tenacity drops from 17.29 g/den to 15.36 g/den- approximately the same tenacity as the sizing. During tenacity measuring, the thick layer of plasma treatment (30-45 minutes) cracked and separated from the fiber surface. This means that the bond between the fiber and the sizing agent was not as strong as the bond between the sizing agent and the allylamine.

Table 5 shows measured tenacity, load, breaking elongation and modulus vs. the allylamine coating for Kevlar KM2 and K29 after removing the sizing. The tenacity decreased after the sizing was removed by soaking the fiber as received in 1:1:1 trichloroethane, and the diameter for single fiber decrease as in Figures 33 and 39 for Kevlar KM2 and Kevlar 29. Yarn sizing aids in load transfer and lowers inter-fiber frictional stress. When the sizing is removed, the filaments in the yarn are no longer bound together. When loaded, instead of acting as a monofilament, the filaments break individually. Once a filament breaks, it ceases to contribute to yarn tension. In Table 4, it is shown that tenacity increases rapidly with up to 15 minutes of plasma treatment, while the tenacity of Kevlar 29 and KM2 with 30-45 minutes plasma treatment remains unchanged with values very similar to the original fiber.

At higher reaction times, a multilayer coating is formed, as the bond between layers of allylamine is not as strong as that between allylamine and fiber. Overall tenacity may decrease or remain the same. This behavior may reflect that the bonding between Kevlar and allylamine is stronger than the bonding between two molecules of allylamine in a multilayer plasma treatment. The allylamine chains, in this case, are able to slip under the localized stress over neighboring chains, which will break and produce molecular flaws, further enhancing stress inhomogeneity and leading progressively to catastrophic rupture. When measuring tenacity, the thick layer of plasma cracked and the multilayer coating separated from the yarn. This means that the role played by bonding between fiber and monomer is more detectable.

Table 4. Measured Tenacity, Load, Breaking Elongation and Modulus of Coated vs. Uncoated Kevlar

Type	Tenacity (g/Den)	Deviation	Load (Kg)	Deviation	Breaking Elongation%	Deviation	Modulus(gm/den)	Deviation
K29 Original Fiber	16.47	0.881	24.71	1.322	2.68	0.111	630.1	2.13
K29 remove Sizing	15.35	2.075	23.03	3.11	2.64	0.133	604.6	8.2
K29 After Treat Original (1)	17.29	0.95	25.95	1.43	2.75	0.168	644.6	1.64
K29 After Treat Original (2)	15.36	0.72	23.01	1.08	2.58	0.22	603.2	2.24
K29 After Treat Original (3)	14.09	0.93	21.13	1.4	2.58	0.34	567.5	2.9

Type	Tenacity (g/den)	Deviation	Load (Kg)	Deviation	Breaking Elongation%	Deviation	Modulus(gm/den)	Deviation
KM2 Original Fiber	19.2	1.42	28.8	2.13	3.132	0.231	621.7	1.43
KM2 remove Sizing	18.32	1.15	27.48	1.73	3.035	0.1996	609.3	2.53
KM2 After treat remove	20.12	1.07	30.19	1.6	3.126	0.1901	636.9	2.19
KM2 After treat original (1)	19.28	1.05	28.91	1.58	3.129	0.162	634.2	2.81
KM2 After treat original (2)	17.2	1.11	25.8	1.17	3.04	0.28	573	2.337
KM2 After treat original (3)	17.85	1.64	26.78	2.46	3.27	0.55	559.7	3.88

(1) Treatment with argon at 5 min 50 w and Allylamine 15 min 50 w power

(2) Treatment with argon at 5 min 50 w and Allylamine 30 min 50 w power

(3) Treatment with argon at 5 min 50 w and Allylamine 45 min 50 w power

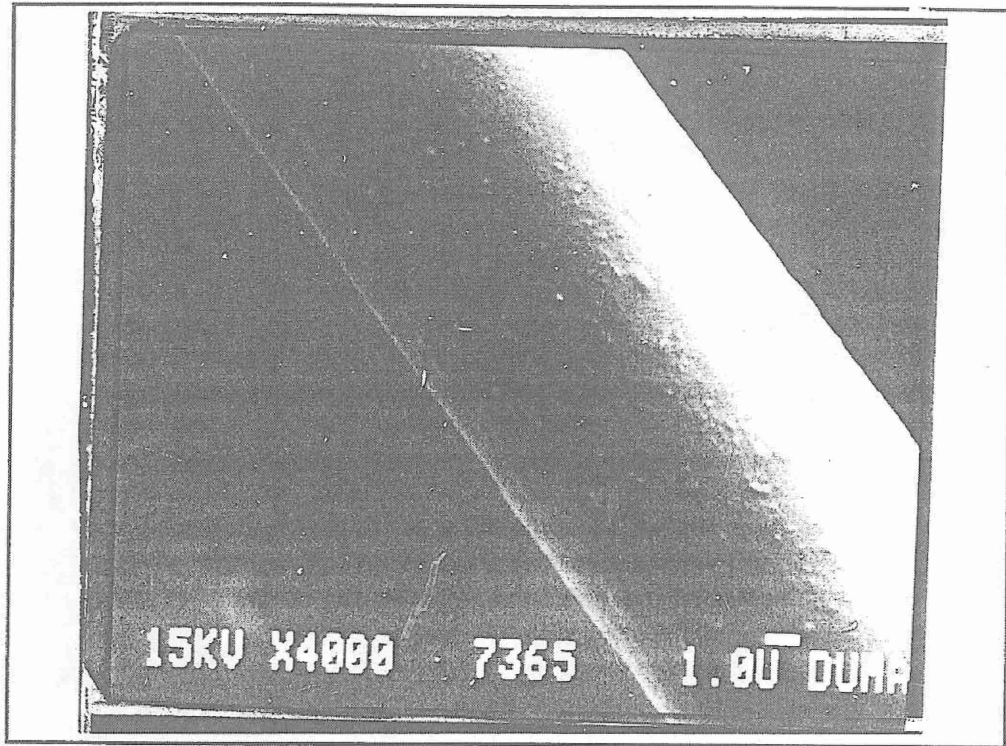
(4) Number of observations = 20

Table 5. Measured Tenacity, Load, Breaking Elongation and Modulus vs. the Allylamine Coating for Kevlar KM2 and K29 After Removing the Sizing

Type	Tenacity (g/den)	Deviation	Load (Kg)	Deviation	Breaking Elongation%	Deviation	Modulus(gm/den)	Deviation
K29 Original Fiber	16.47	0.881	24.71	1.322	2.68	0.111	630.1	2.13
K29 remove Sizing	15.35	2.075	23.03	3.11	2.64	0.133	604.6	8.2
K29 After Treat remove (1)	14.79	1.88	22.19	2.84	2.16	0.204	578.6	4.66
K29 After Treat remove (2)	17.62	0.887	26.42	1.3	2.82	0.164	648.5	2.56
K29 After Treat remove (3)	16.14	2.89	24.2	4.33	2.49	0.601	667.5	11.46
K29 After Treat remove (4)	16.95	1.71	25.43	2.57	2.69	0.723	644.4	2.03

Type	Tenacity (g/den)	Deviation	Load (Kg)	Deviation	Breaking Elongation%	Deviation	Modulus(gm/den)	Deviation
KM2 Original Fiber	19.2	1.42	28.8	2.13	3.132	0.231	621.7	1.43
KM2 remove Sizing	18.32	1.15	27.48	1.73	3.035	0.1996	609.3	2.53
KM2 After treat remove (2)	20.12	1.07	30.19	1.6	3.126	0.1904	636.9	2.19
KM2 After treat remove (3)	19.18	0.63	28.77	0.94	3.06	0.208	632.4	1.35
KM2 After treat remove (4)	18.34	1.26	27.851	1.89	3.11	0.321	597.5	3.55

- (1) Treatment with argon at 5 min 70 w and Allylamine 15 min 50 w power  
(2) Treatment with argon at 5 min 50 w and Allylamine 15 min 50 w power  
(3) Treatment with argon at 5 min 50 w and Allylamine 30 min 50 w power  
(4) Treatment with argon at 5 min 50 w and Allylamine 45 min 50 w power  
(5) Number of observation = 20



**Figure 31. Untreated Kevlar KM2**

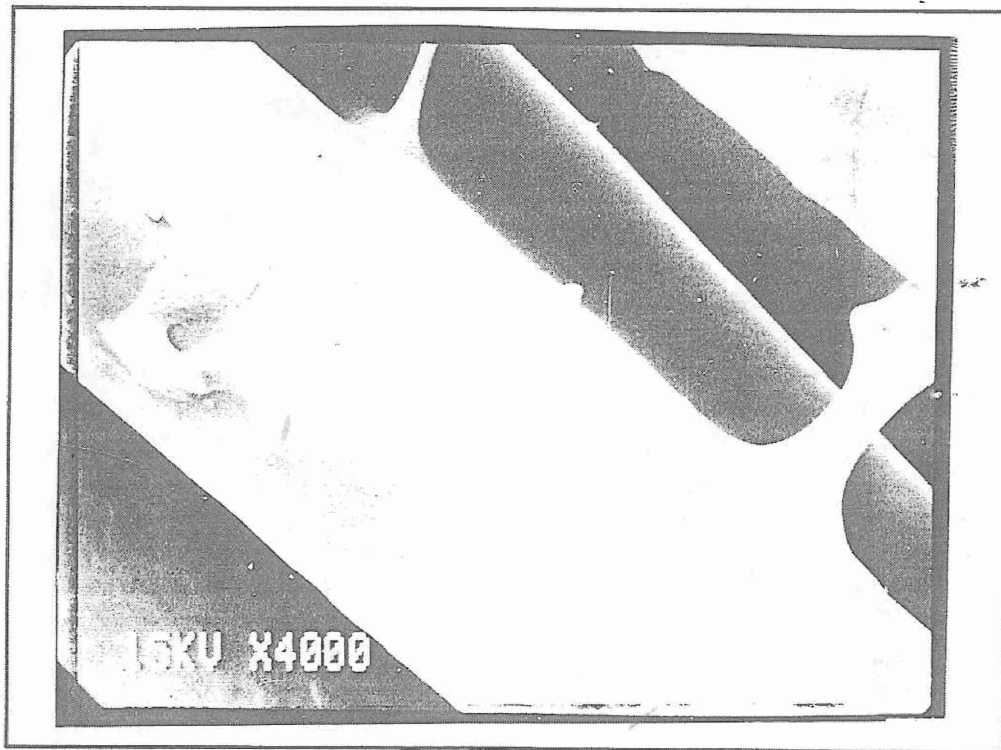


**Figure 32. Kevlar KM2 After 7 Minutes of Trichloroethane Treatment to Remove Sizing**

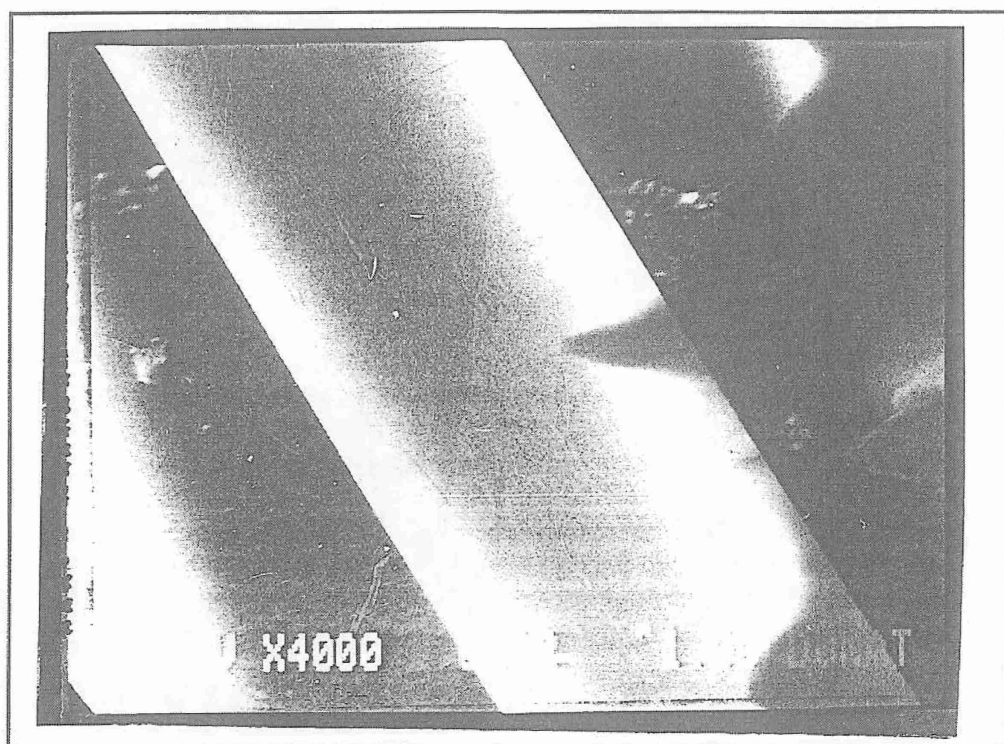


**Figure 33. Kevlar KM2 After 30 Minutes of Trichloroethane Treatment**

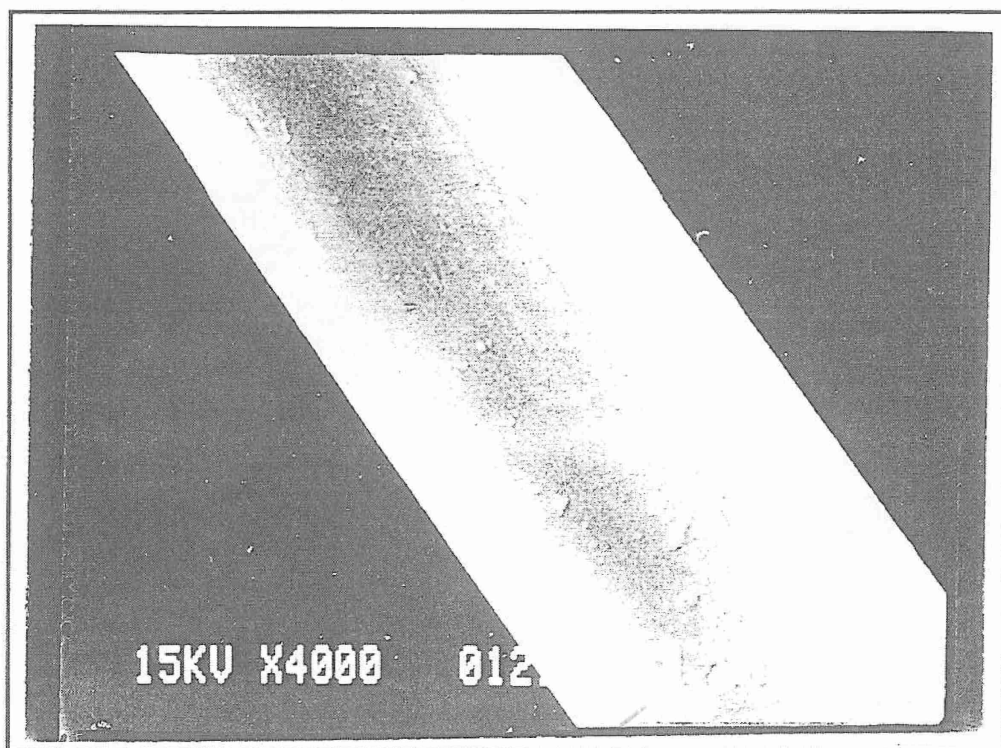


**Figure 34. Kevlar KM2 After Argon Treatment (5 minutes at 70W)**



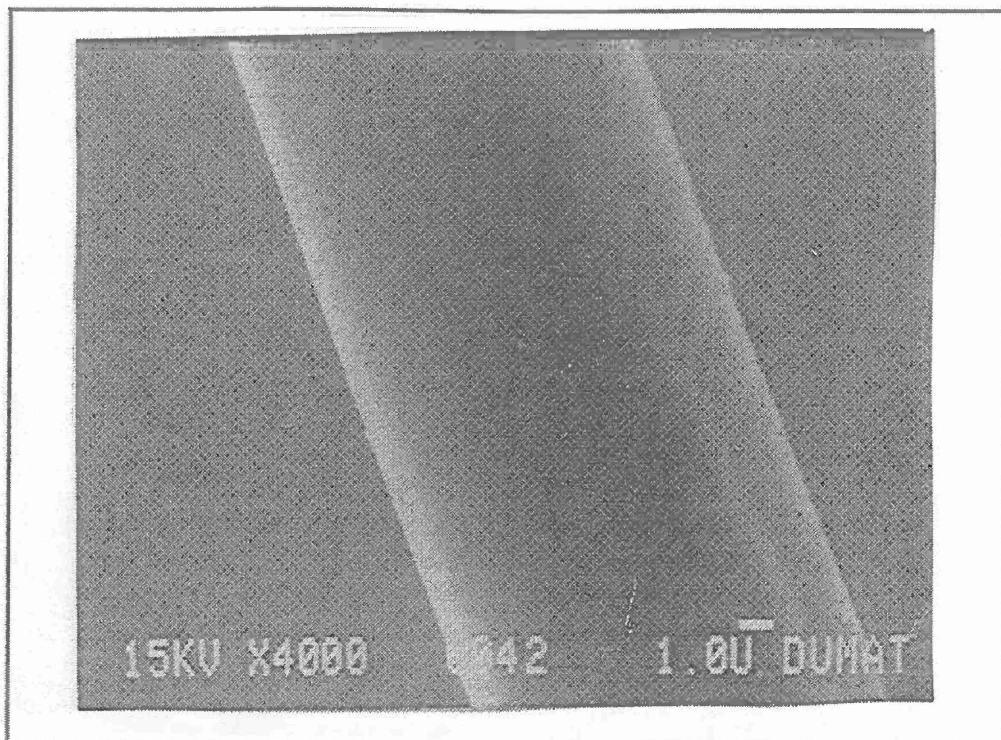


**Figure 35. Kevlar KM2 After Allylamine Treatment (15 minutes at 50W)**

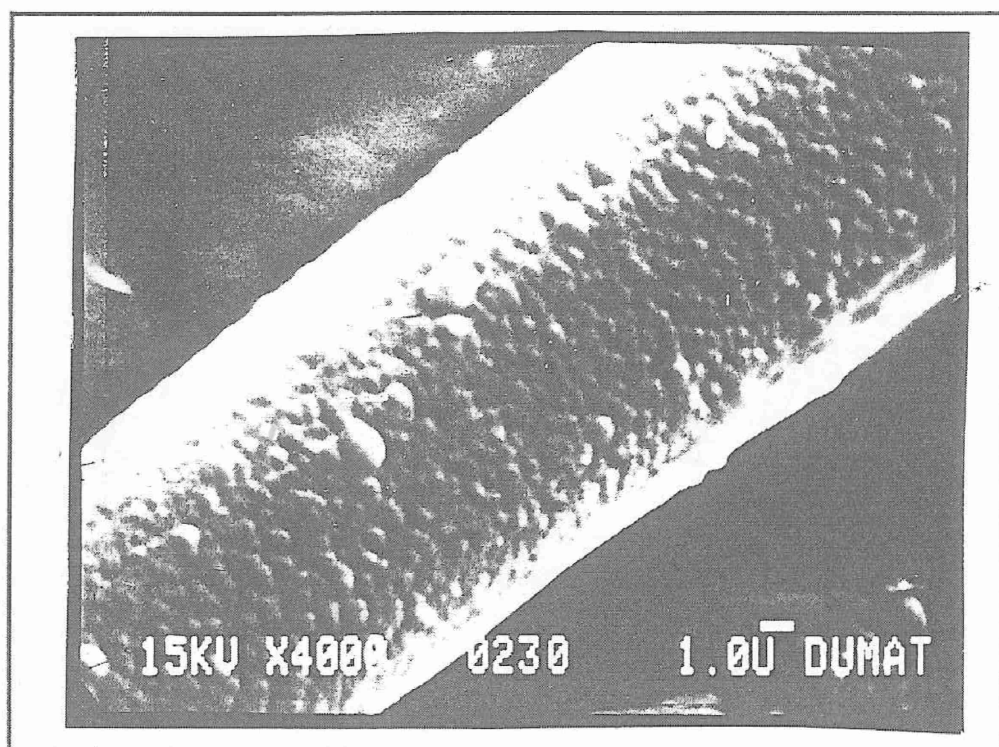


**Figure 36. Kevlar KM2 After Allylamine Treatment (30 minutes at 50W)**



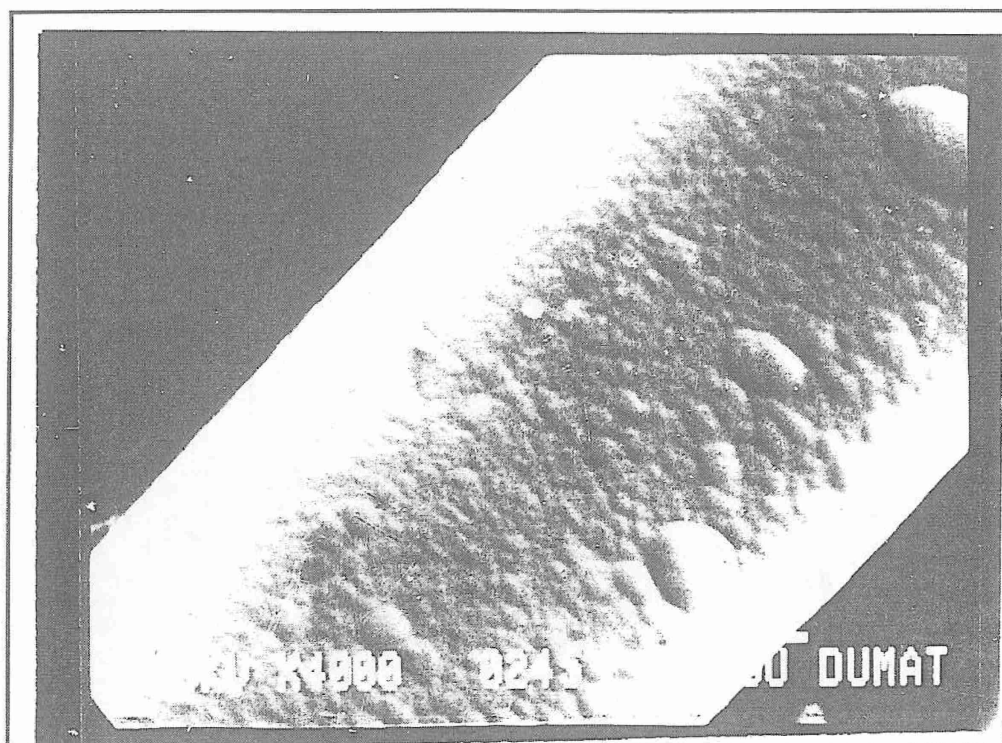


**Figure 37. Kevlar KM2 After Allylamine Treatment (45 minutes at 50W)**

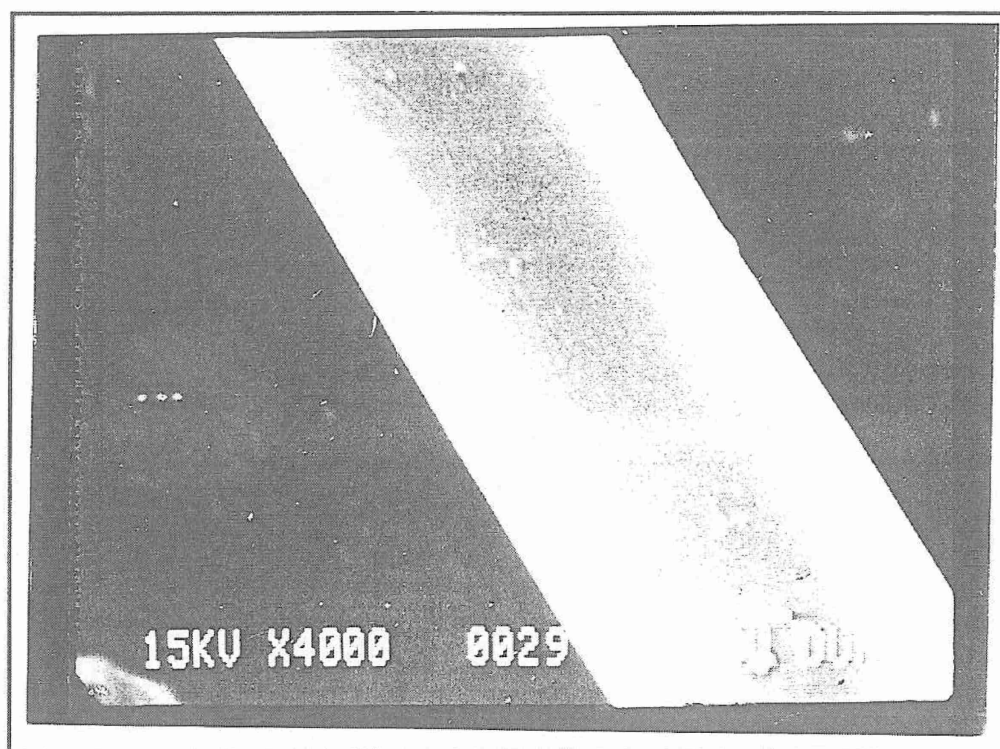


**Figure 38. Untreated Kevlar 29**

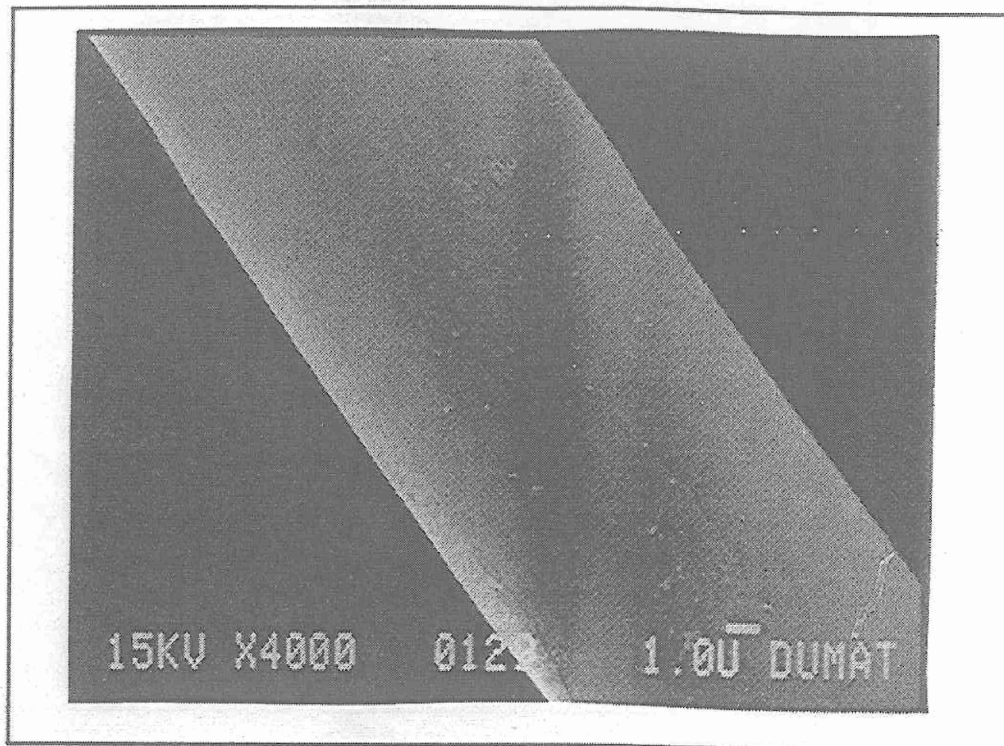


**Figure 39. Kevlar 29 After 30 Minutes of Trichloroethane Treatment to Remove Sizing**

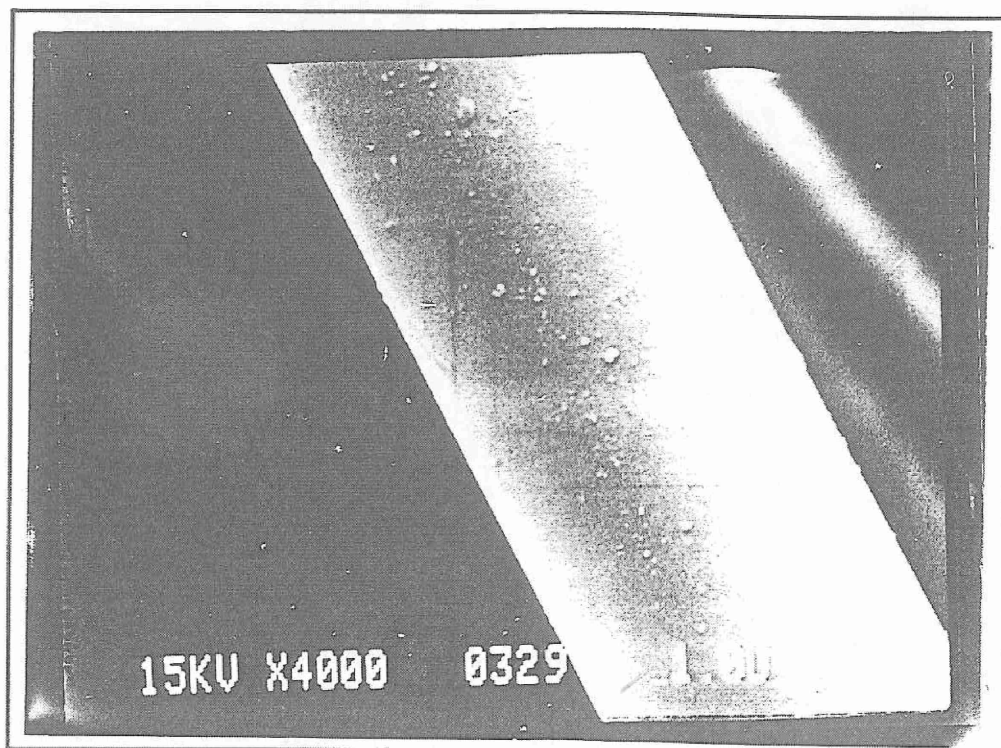


**Figure 40. Kevlar 29 After Argon Treatment (5 minutes at 70W)**

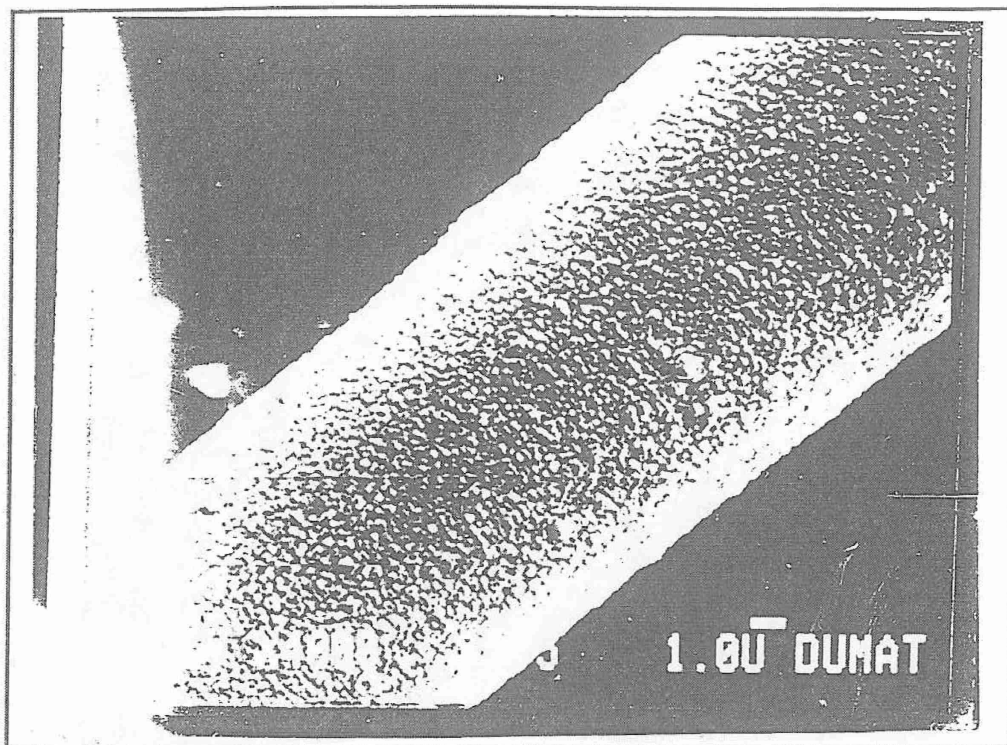


**Figure 41. Kevlar 29 After Allylamine Treatment (15 minutes at 50W)**

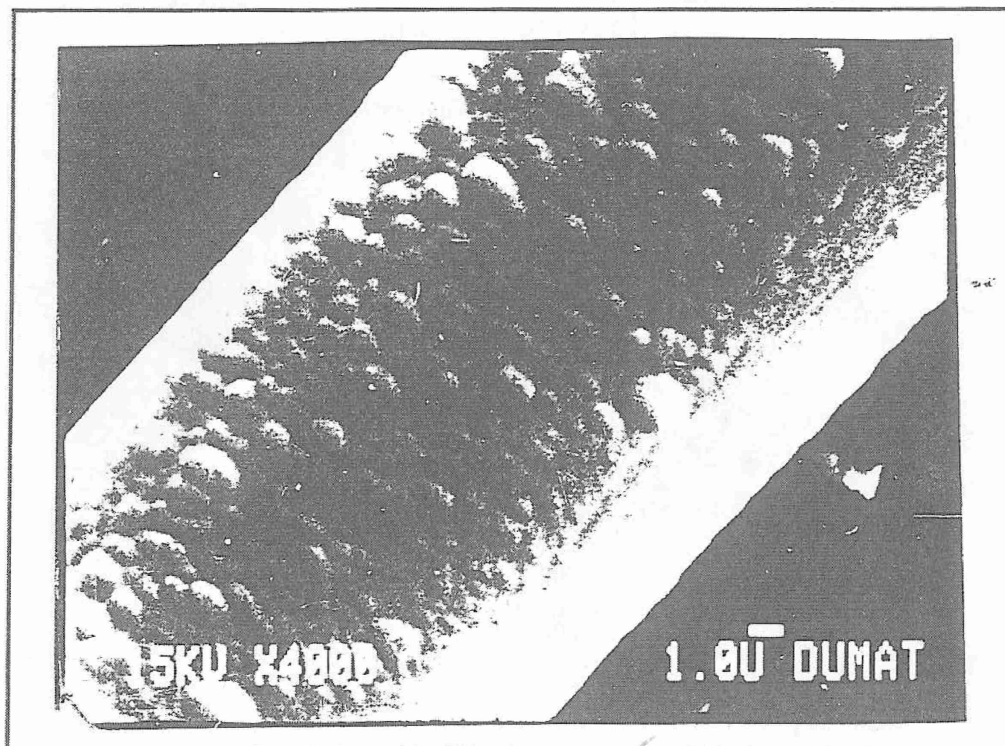


**Figure 42. Kevlar 29 After Allylamine Treatment (30 minutes at 50W)**

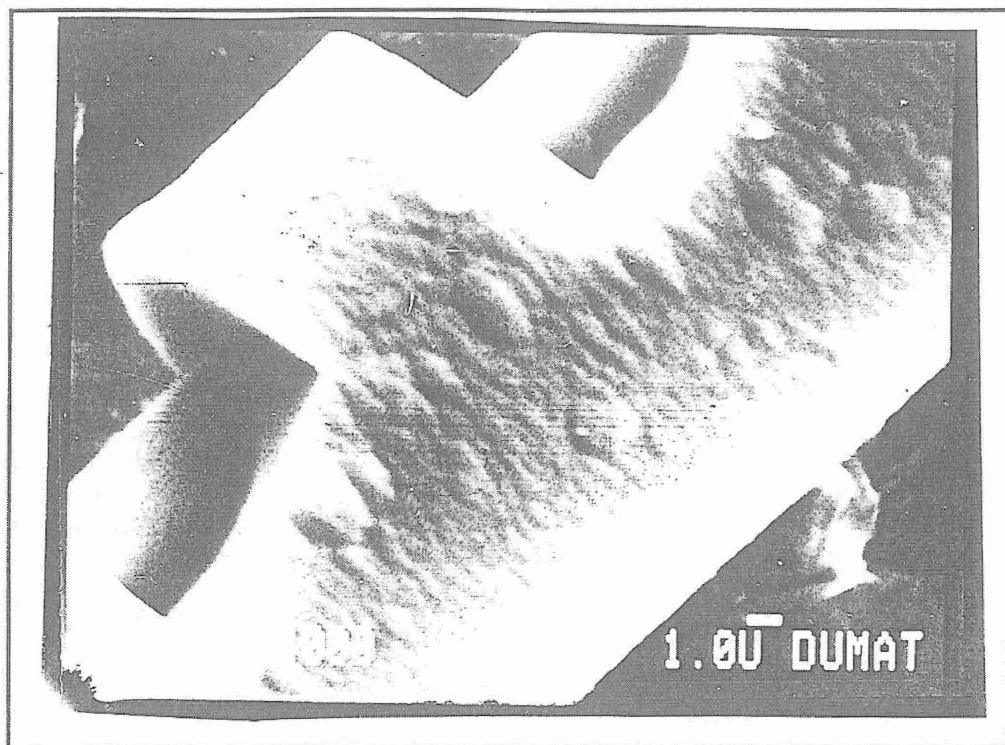


**Figure 43. Artificially Cracked Kevlar 29 After Allylamine Treatment (30 minutes at 50W)**

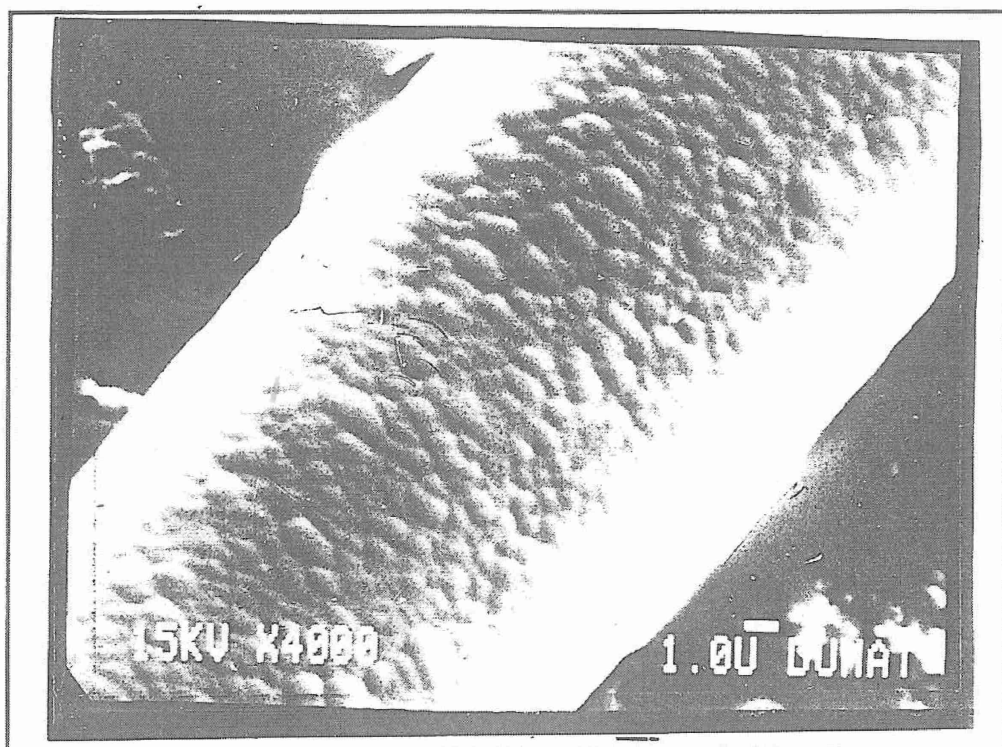


**Figure 44. Kevlar 29 After Allylamine Treatment (45 minutes at 50W)**



## Interfacial Testing

A trial was made to modify the surface of a PPTA fiber. Tables 6 and 7 show the pull-out load when one end of the Kevlar fiber (PPTA) was embedded in an epoxy matrix. From the pull-out load, the average shear (at the interface between the fiber and matrix) was calculated.

As shown in these tables, the untreated Kevlar fibers have a very low level of adhesion to epoxy resin (0.24- 0.28 MPa). The allylamine plasma treatment of Kevlar fiber increased the adhesion up to 0.49-0.54 MPa after 45 minutes treatment, which is an increase of 90-92 % over the untreated fibers. It was found that as adhesion increased, plasma coating time increased. This gives evidence that plasma treatment of fiber is a very good tool for enhancing the interfacial adhesion between PPTA fiber and matrix. The role played by fiber in creating plasma treatment and/or adhesion between PPTA fiber and matrix is marked at higher treatment times.

**Table 6. Interfacial Shear Strength ( $\tau$ )  
vs. Polymer Plasma Treatment Time for Kevlar KM2**

Treatment Time (min)	Diameter (mm)	Pull-out Load (N)	Avg. $\tau$ (MPa)	( $\tau/\tau_0$ )
0	0.010	0.284	4.522	1
15	0.011	0.323	4.675	1.033
30	0.012	0.480	6.369	1.408
45	0.0152	0.549	5.751	1.271

**Table 7. Interfacial Shear Strength ( $\tau$ )  
vs. Polymer Plasma Treatment Time for Kevlar 29**

Treatment Time (min)	Diameter (mm)	Pull-out Load (N)	Avg. $\tau$ (MPa)	( $\tau/\tau_0$ )
0	0.010	0.245	3.901	1
15	0.011	0.313	4.530	1.61
30	0.015	0.392	4.161	1.066
45	0.015	0.480	5.095	1.306

### 3.6 Conclusions

The results of this study are summarized below:

- RF-plasma was effective in enhancing the fiber-matrix interfacial adhesion when allylamine was coated to fiber surface. The interfacial shear strength between allylamine plasma coated Kevlar 29 and Kevlar KM2 fibers and matrix material showed five-fold increase over untreated fibers.
- The tenacity of argon/allylamine treated fibers yarn is optimum at 5 minutes and 50 W argon plasma etching followed by 15 minutes and 50 W of allylamine plasma coating.
- Interfacial adhesion between PPTA fiber (Kevlar) filament and matrix increases with increasing plasma coating. This holds great promise that the impact resistance of the composite structure will be improved, which is the main goal of the present study.

### 3.7 Future Work

In the next phase, parametric studies of fiber treatment will be carried out in the following manner:

- 1) Treatment with argon at 5 minutes and 50 W.
- 2) Treatment with different kinds of monomers.

**Table 8. Proposed Treatment, Kevlar 29 and KM2**

Type of Monomer	Ethylene Diamine			Styrene		
Treatment Time (min)	15	30	45	15	30	45
Original Fiber	x*	x*	x*	x*	x*	x*
Fiber After Removing Sizing	x*	x*	x*	x*	x*	x*

\* Ten specimens of each will be measured for tensile and interfacial shear strength.

## 4. Gradient Design Concept for Composite Armor

### 4.1 Introduction

Recognizing the fact that ballistic composite structures can be subjected to different types of threats, gradient design concepts (GDC) will be employed in the design and optimization of the performance of ballistic composites. The concept of GDC for high damage resistant fibrous textile structures can be demonstrated using a 3-D braided fiber network as a base structure to accommodate the selective placement of longitudinal components of varying stiffness, strength, and density.

The 3-D fiber network provides shear resistance and damage constraint; the longitudinal component promotes stress wave dissipation and resists penetration. Based on an understanding of the effect of the placement of the longitudinal components and frequency of interlacing (a geometric hybrid), the concept of material hybrids will be investigated using the fibers selected in this program. The composites fabricated by GDC will be tested and investigated under low velocity (drop weight) and high velocity impact (ballistic) conditions. The tested samples will be examined using optical and scanning electronic microscopes in order to study the failure mechanism under impact load.

### 4.2 Gradient Design Concept

The GDC strategically integrates the hardened, high energy absorption and damage containment layers into a ballistic protective assembly, such as helmet. Depending on the nature of the threat, the location and proportion of the layers will be tailored according to the models developed in this program. Figure 45 illustrates the GDC for a multifunctional ballistic composite.

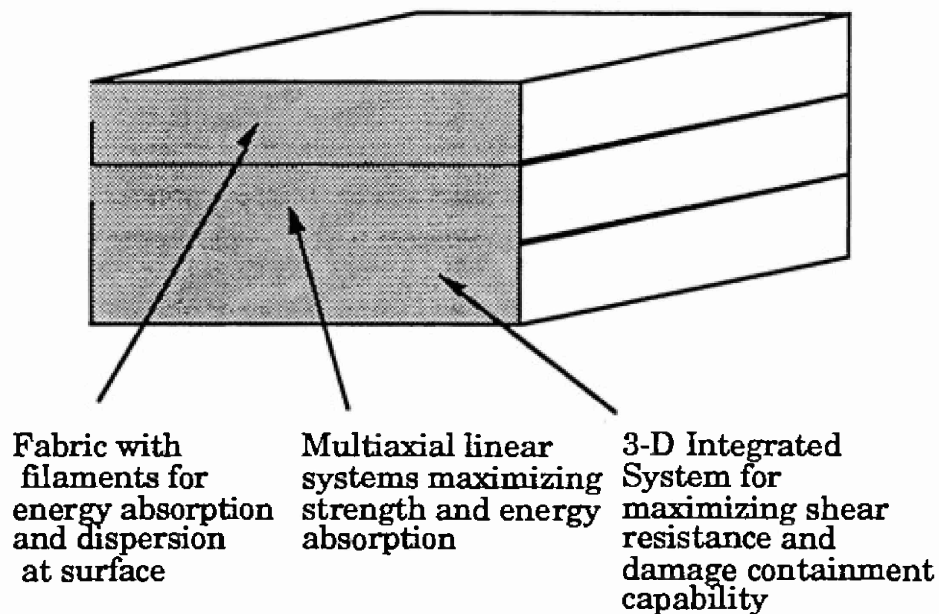


**Figure 45. Gradient Design Concept For Multifunctional Ballistic Composites**

Therefore, the main objective of impact testing is to examine the gradient design concept for impact resistance of composites and optimize the performance of ballistic composites. To this goal, a series of samples were designed and fabricated. They include putting various sizes of hard aluminum oxide spherical particles into the resin, introducing multiaxial linear systems, and 3-D integrated system. Both low velocity impact and high velocity impact were performed for each type of samples in order to study the response of GDC composites under various impact velocities.

The viability of GDC has been investigated in the first year of the program. The studies will be extended to identify the gradients best suited for different material systems and different kinds of ballistic threats.

#### 4.2.1 Design of Experiment

The fabric preforms selected for this study include basket weave, triaxial weave, multiaxial warp knitted fabric and 3-D braid structures. Employed are: 20nm  $\text{Al}_2\text{O}_3$  and 2.5mm  $\text{Al}_2\text{O}_3$  particles for the hardened layers, 20 $\mu\text{m}$   $\text{Al}_2\text{O}_3$  filament and 100 $\mu\text{m}$  Boron filament for the multiaxial linear systems, and Kevlar yarns and graphite yarns for through-thickness stitching. The resin system are bisphenal-A epichlor-hydrin based epoxy (Epon 828), and Epon Curing agent U, a eutectic aromatic amine. Figure 46 is the schematic diagram of the GDC composites and Figure 47 shows the design of the experimental work.

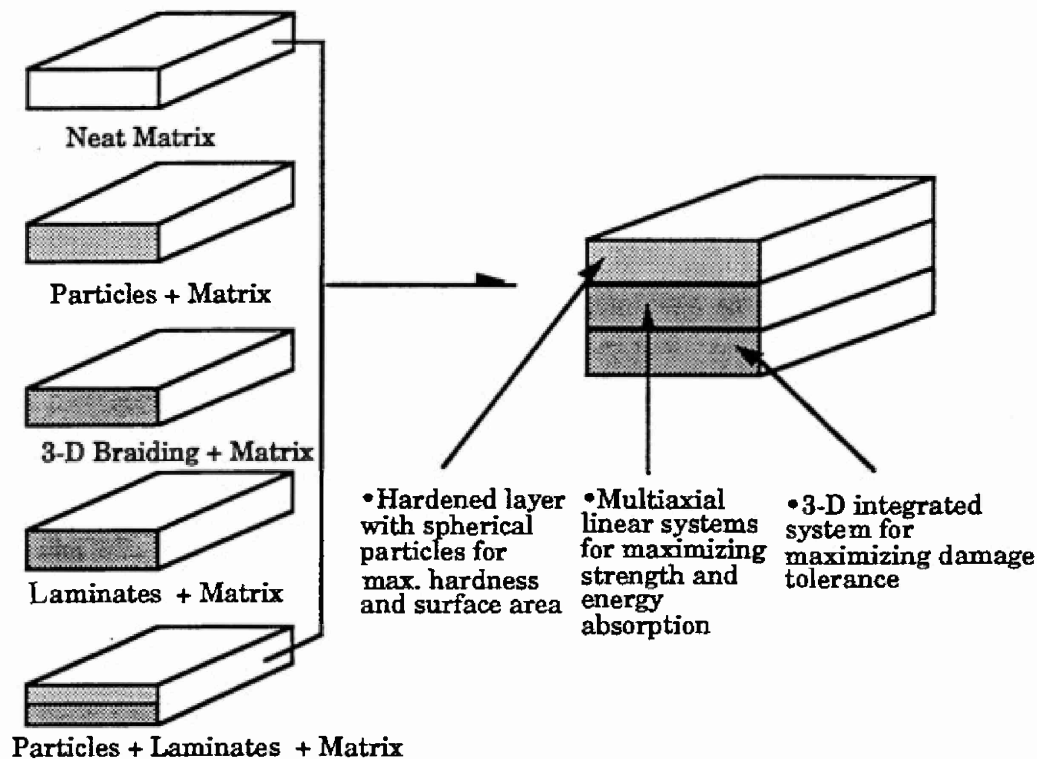







Figure 46. Components of GDC Composites



VARIABLES	LEVEL		
• Reinforcement Sphere Size	20nm---2.5mm	Al2O3	• ●
• Reinforcement Filament Diameter	20μm---100μm		
• Filament Materials	Al2O3 Filament---Boron Filament		
• Fiber Architecture	Basket Weave 	Triaxial Weave 	Multiaxial Warp Knitted Fabric 
• Through Thickness Reinforcement Geometry	Orthogonal Stitching 	3-D Braid 	
• Stitching Materials	Graphite Yarn	Kevlar Yarn	

**Figure 47. Design of Experiments**

In order to examine the impact resistance of different structures, the design utilized a similar fiber type (Kevlar 29), the same composite manufacturing method (resin transfer molding) and the same specimen size. Fourteen types of composites selected in terms of reinforcing filament, balls and fiber architecture, are listed below. The density of balls, fibers and matrix, fiber volume fraction of each type of composite and areal density of each composite are listed. In order to study the effect of each ingredient on the behavior of the composites, fourteen types of GDC composites are classified into five categories. Within each category, the composites have similar Kevlar fiber volume fraction. The classification is as following:

**Category I: The effect of spherical size on matrix:**

Epoxy Neat Matrix,

20nm Al<sub>2</sub>O<sub>3</sub>+Matrix,

2.5mm Al<sub>2</sub>O<sub>3</sub>+Matrix

**Category II:** The effect of spherical size on the triaxial weave composites:

Triaxial-Weave,

20nm  $\text{Al}_2\text{O}_3$ +Triaxial-Weave,

2.5mm  $\text{Al}_2\text{O}_3$ +Triaxial-Weave,

20 $\mu\text{m}$   $\text{Al}_2\text{O}_3$ +Triaxial-Weave,

100 $\mu\text{m}$  Boron Filament + Triaxial-Weave

**Category III:** The effect of Kevlar fiber volume fraction and through thickness reinforcement on:

Triaxial-Weave  $V_f=33\%$ ,

Triaxial-Weave  $V_f=50\%$ ,

Triaxial-Weave + Kevlar Stitching,

3-D Braiding

**Category IV:** The effect of fiber architecture:

MWK Fabric,

Triaxial-Weave,

Basket Weave,

3-D Braiding

**Category V:** The effect of the reinforcement in through the thickness direction:

Triaxial-Weave,

Triaxial-Weave + Kevlar Stitching,

3-D Braiding

#### 4.2.2 Composite Formation

In order to change the preforms from their flexible and conforming dry state into a rigid structure, a matrix has to be introduced into the fibers. Resin transfer molding (RTM) is an impregnation technique employed for composites manufacturing. In RTM, the preforms is placed into a closed die mold and is penetrated by pre-catalyzed resin through pressurized injection. The diagram of the RTM system used in this study is shown in Figure 48. On the left is a vacuum source and resin trap used to evacuate the entire system before the resin is injected. the center is the molding tool with inlet and outlet ports. On the right is

a compressed air source and the pressured vessel in which the catalyzed resin is placed after it is degassed. The RTM operational procedure is as follows:

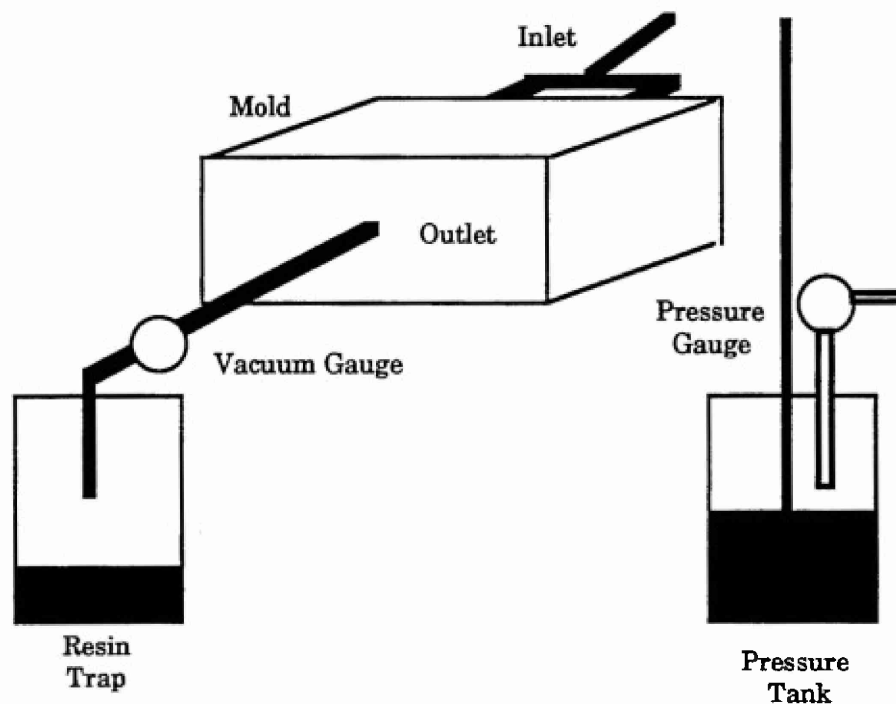


**Figure 48. Schematic Diagram of Resin Transfer Molding**

**Operation procedures:**

- Preform materials are placed into the tool at room temperature.
- The resin is mixed with catalyst and placed into a vacuum tank to degas for 10 minutes. After degas the resin is placed in the resin tank. The tool is connected to the vacuum source and resin tank. A vacuum is applied to the entire system in order to remove all the air from the preforms.
- Resin flow is initiated by gradually applying pressure to the resin tank while vacuum remains at the exit ports. The pressure is increased to 10 psi and held until flow is seen at the exit ports.
- Once resin flow reaches the exit ports, the vacuum is halted and the port is closed. Pressure is then increased to 60 psi.
- The exit port is opened slightly to allow a moderate flow of resin through the tool. Flow is continued till the flow of air bubbles ceases to exit the tool.
- The exit port is closed and the injection pressure is maintained for one and half hours to allow for shrinkage during cure. After curing, all lines are disconnected, and the tool is placed at room temperature for four hours before opening the mold.

## 4.3 Low Velocity Impact Behavior

### 4.3.1 Drop Weight Impact Testing Conditions

Drop-weight impact testing was performed on each sample. The impact load vs. time and impact energy vs. time responses were characterized for each sample. All the impact tests were performed on a Dynatup model 8140 instrumented impact tester in conjunction with a Dynatup model 730-1 data acquisition system driven by an IBM PC-30. The specimen size is 6 inches by 6 inches, with a normal thickness of 0.5 inches and a test area of 4.5 inches in diameter. Figure 49 shows the schematic diagram for the impact tester.

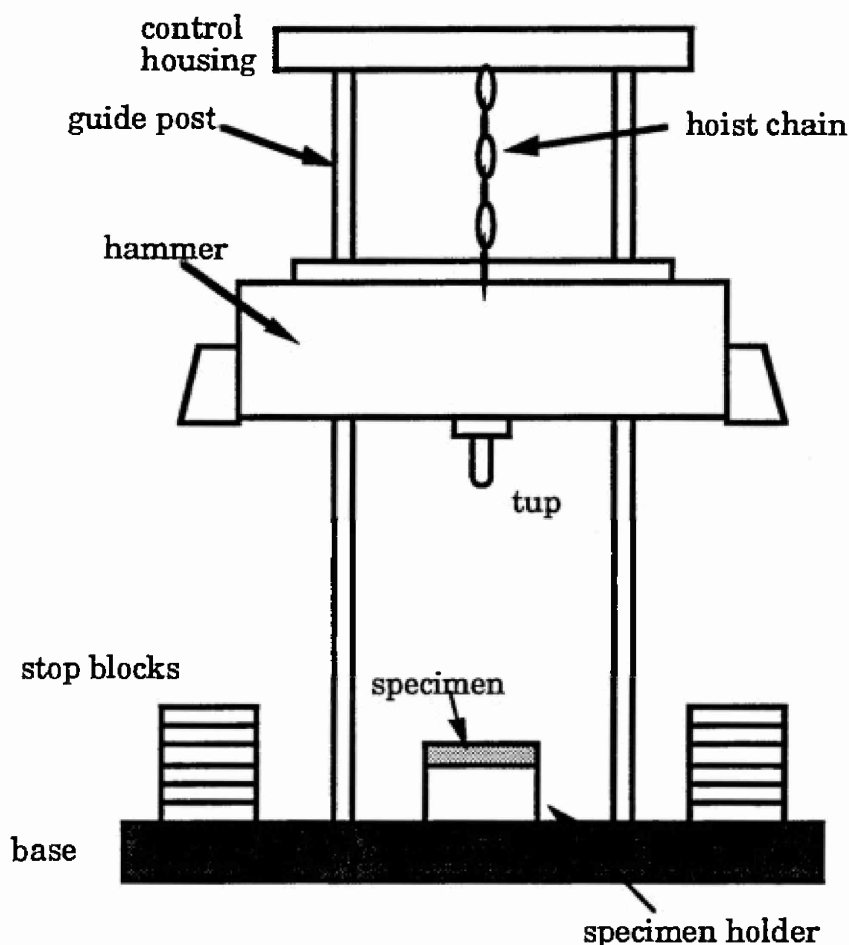


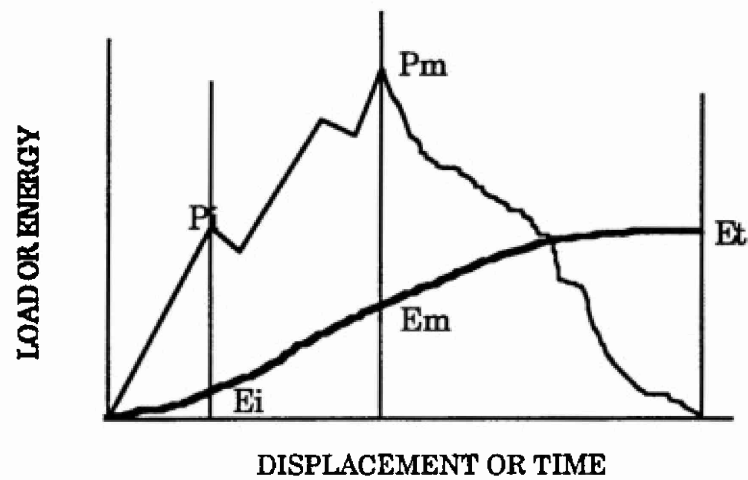
**Figure 49. Testing Equipment and Conditions**

For the testing conditions, the striking energy should be greater than needed to penetrate the toughest of the samples while not exceeding load cell capabilities. Through testing, it was found that the following conditions are a suitable combination for the samples in this study:

- Drop Weight: 605 lb
- Tup Diameter: 0.5 inch
- Velocity: 10.18 ft/s
- Impact Energy: 982.36 ft-lb (1332.92 Joules)
- Time range: 25 ms
- Full-Scale Load: 25,000 lb

#### 4.3.2 Impact Result and Discussion

The data acquisition system records a complete history of load and energy versus time or deflection in each of the impact events. Figure 50 shows a general impact response of composites.



#### MAJOR POINTS OF INTEREST

$P_i, E_i$  ----- LOAD, ENERGY (INCIPIENT DAMAGE POINT,  
BACK FACE CRACKING)

$P_m, E_m$  ----- LOAD, ENERGY AT MAXIMUM OR FAILURE  
POINT (THROUGH CRACK)

$E_t$  ----- TOTAL ENERGY (FULL PENETRATION)

**Figure 50. General Impact Response of Composites**

## Effect of Spherical Size on the Matrix

In order to see the effect of spherical size on the impact behavior of the neat matrix, the composite panels in Category I were fabricated by introducing 20 nm  $\text{Al}_2\text{O}_3$  or 2.5 mm  $\text{Al}_2\text{O}_3$  spheres into the neat matrix. Figure 51 shows the impact load and energy versus time curves of the composites in Category I. Because there is no fiber reinforcement in the composites at all, the samples are very brittle. After the impact, the neat matrix and 20 nm  $\text{Al}_2\text{O}_3$  reinforced matrix fragmented into several pieces. The 2.5 mm  $\text{Al}_2\text{O}_3$  reinforced composites still held together although there were some cracks, which indicate larger spheres have better damage containment. Since the composites in this category have different areal density, to fairly compare the impact behavior of the composite, the specific energy absorption is used for comparison, which is defined as the total energy absorbed by the system divided by the areal density of the system. Based on Table 9 and the bar chart in Figure 51, 2.5 mm  $\text{Al}_2\text{O}_3$  reinforced matrix had the highest specific energy absorption and propagation energy ( $E_{\text{total}} - E_{\text{Max. load}}$ ).

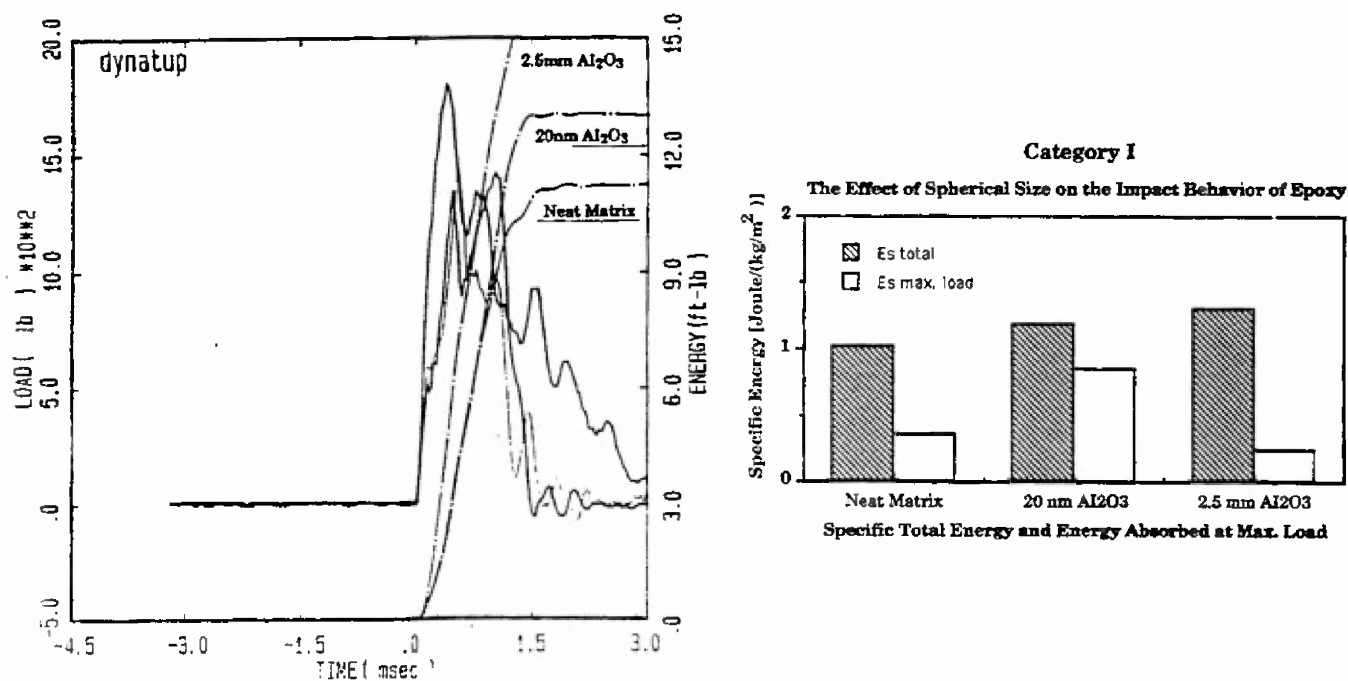


Figure 51. Impact Load and Energy vs. Time, Category I Composites

Table 9. Impact Properties of GDC Composites

Samples	Energy(Joule) E total	Energy(Joule) E max. load	Areal Density (kg/m <sup>2</sup> )	Specific Energy(Joule) Es total	Specific Energy J/(kg/m <sup>2</sup> ) Es max. load
Neat Matrix	15.19	5.32	14.86	1.02	0.35
20 nm $\text{Al}_2\text{O}_3$	17.66	12.67	14.98	1.18	0.84
2.5mm $\text{Al}_2\text{O}_3$	34.85	6.10	26.78	1.30	0.23

## Effect of Reinforcement Geometry on the Triaxial Weave Composites

To study the effect of reinforcement shape(form)--spherical particles and multi-axial filament, six types of composites were included and compared in Category II, in which hardened layers of spherical particles or filaments combined with multi-axial linear systems of maximizing strength and energy absorption (such as triaxial weave fabric) were strategically integrated together into an assembly. No. 2 and No. 3 composites have hardened layers of 20 nm and 2.5 mm  $\text{Al}_2\text{O}_3$  spherical particles respectively besides the triaxial weave fabrics. No. 4 and No. 5 composites have  $0^\circ/90^\circ$  20  $\mu\text{m}$  filament and 100 $\mu\text{m}$  Boron filament reinforced as the hardened layer accordingly besides the triaxial weave fabric as the laminated reinforcement. No. 1 composite only has triaxial weave reinforcement without a hardened layer, which can be used as a comparison basis. No. 6 composite consists of a fully integrated non-linear 3-D braid system, which also can be used as a comparison basis to see how three dimensional reinforcement structure is different from 2 dimensional reinforcement structure in low velocity impact test.

Figure 52 and Table 10 show that when comparing the energy absorption data directly without dividing by the areal density of the system,  $0^\circ/90^\circ$  20  $\mu\text{m}$   $\text{Al}_2\text{O}_3$  filament or 100  $\mu\text{m}$  Boron filament plus 2-D laminate structure exhibit higher energy absorption level; but, once the energy data is normalized by the areal density of the system, another picture is given. The advantages of filament reinforcement plus 2-D laminate composite systems were counterbalanced by the higher density of  $\text{Al}_2\text{O}_3$  (density = 3.5g/cc) or Boron (density = 2.57 g/cc). The 20 nm  $\text{Al}_2\text{O}_3$  reinforced triaxial weave composite system shows higher specific energy absorption than filament reinforcement forms. The 3-D braided system shows a significant highest specific absorption energy among this category.



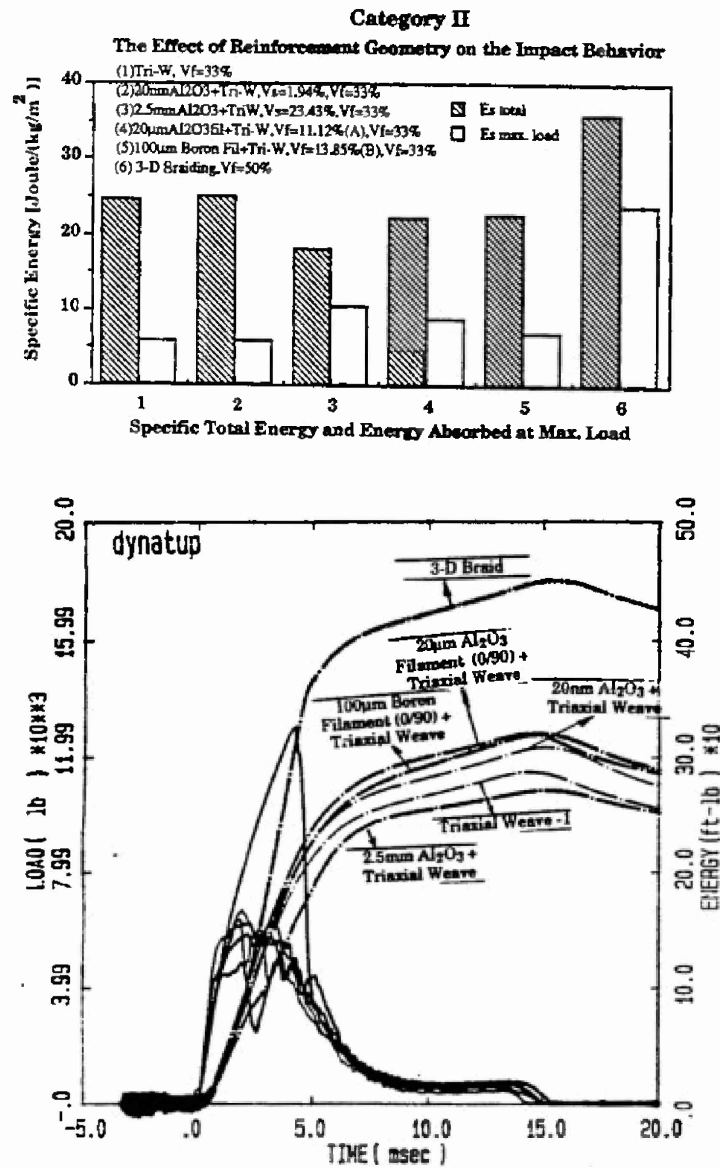


Figure 52. Impact Load and Energy vs. Time, Category II Composites

Table 10. Impact Properties of GDC Composites

Samples	Energy(Joule) E total	Energy(Joule) E max. load	Areal Density (kg/m <sup>2</sup> )	Specific Energy(Joule) Es total	Specific Energy J/(kg·m <sup>2</sup> ) Es max. load
Tri-Weave-1	389.54	90.28	15.87	24.55	5.69
20nmAl <sub>2</sub> O <sub>3</sub> + Tri-Weave	417.82	96.60	16.77	24.92	5.76
2.5mmAl <sub>2</sub> O <sub>3</sub> +Tri-Weave	367.45	209.26	20.25	18.15	10.33
20 $\mu$ mAl <sub>2</sub> O <sub>3</sub> Filament (0/90)+Tri- Weave	433.65	173.51	19.58	22.15	8.86
100 $\mu$ mAl <sub>2</sub> O <sub>3</sub> Filament (0/90)+Tri- Weave	433.61	132.83	19.21	22.57	6.92
3-D Braid	609.70	405.02	17.02	35.82	23.80

### Effect of Fiber Volume Fraction

Figure 53 shows impact load and energy versus time curves of the composites in Category III. It is obvious that higher fiber volume fraction helps to increase the specific energy absorption levels from 24.55 J/(kg/m<sup>2</sup>) of  $V_f = 33\%$  to 27.14 J/(kg/m<sup>2</sup>) of  $V_f = 50\%$ . The through thickness stitching further increases energy absorption from 27.14 J/(kg/m<sup>2</sup>) to 30.15 J/(kg/m<sup>2</sup>). The 3-D braid structure still holds the highest among them all.

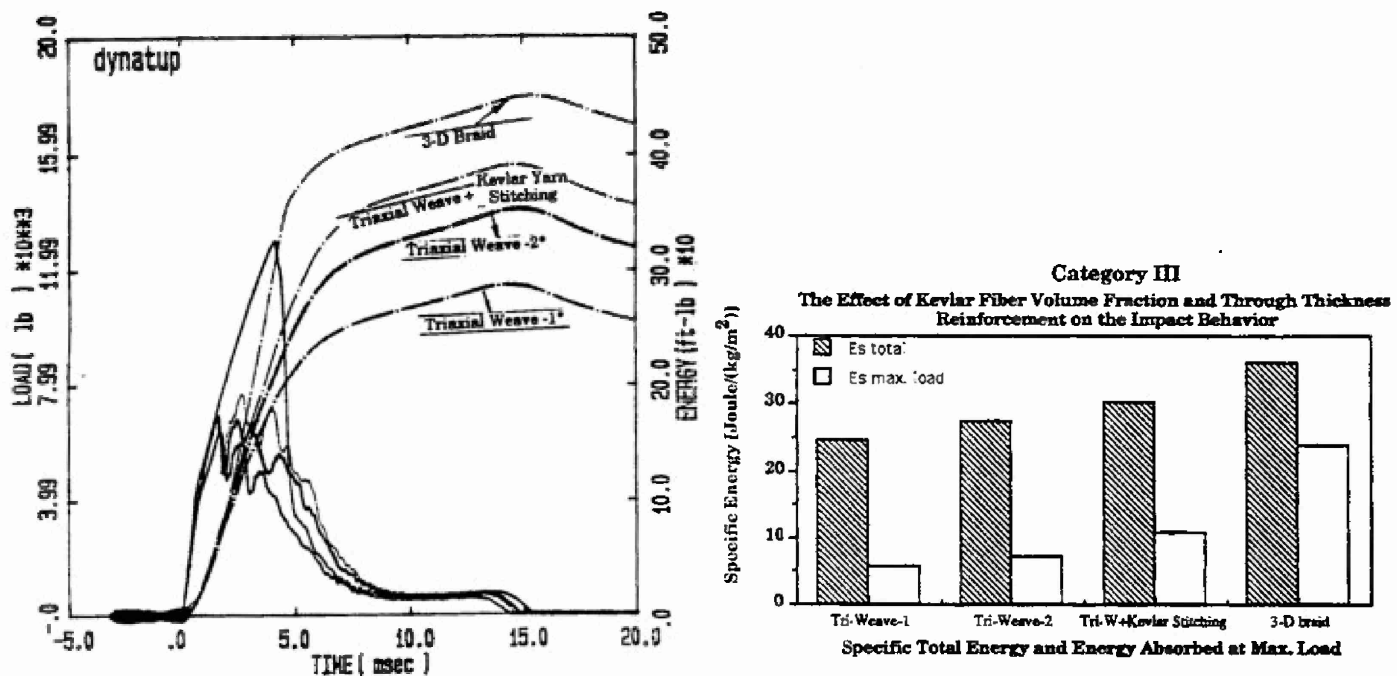


Figure 53. Impact Load and Energy vs. Time, Category III Composites

Table 11. Impact Properties of GDC Composites

Samples	Energy(Joule) E total	Energy(Joule) E max. load	Areal Density (kg/m <sup>2</sup> )	Specific Energy(Joule) Es total	Specific Energy J/ (kg/m <sup>2</sup> ) Es max. load
Tri-Weave-1	389.54	90.28	15.87	24.55	5.69
Tri-Weave-2	457.13	123.41	17.21	27.14	7.17
Tri-W+Kevlar Yarn stitching	530.94	188.88	17.61	30.15	10.73
3-D Braid	609.69	405.02	17.02	35.82	23.80

## Effect of Fiber Architecture

Figure 54 shows that fiber architecture plays a role in impact energy absorption. Among MWK, basket weave and triaxial-weave structures, basket weave has the highest specific absorbed energy. One of the reasons which causes the basket weave showing the highest specific absorbed energy among the three probably is due to its higher fiber interlacing density. Further investigation of the role of the fiber architecture will be carried on in the second year of the program.

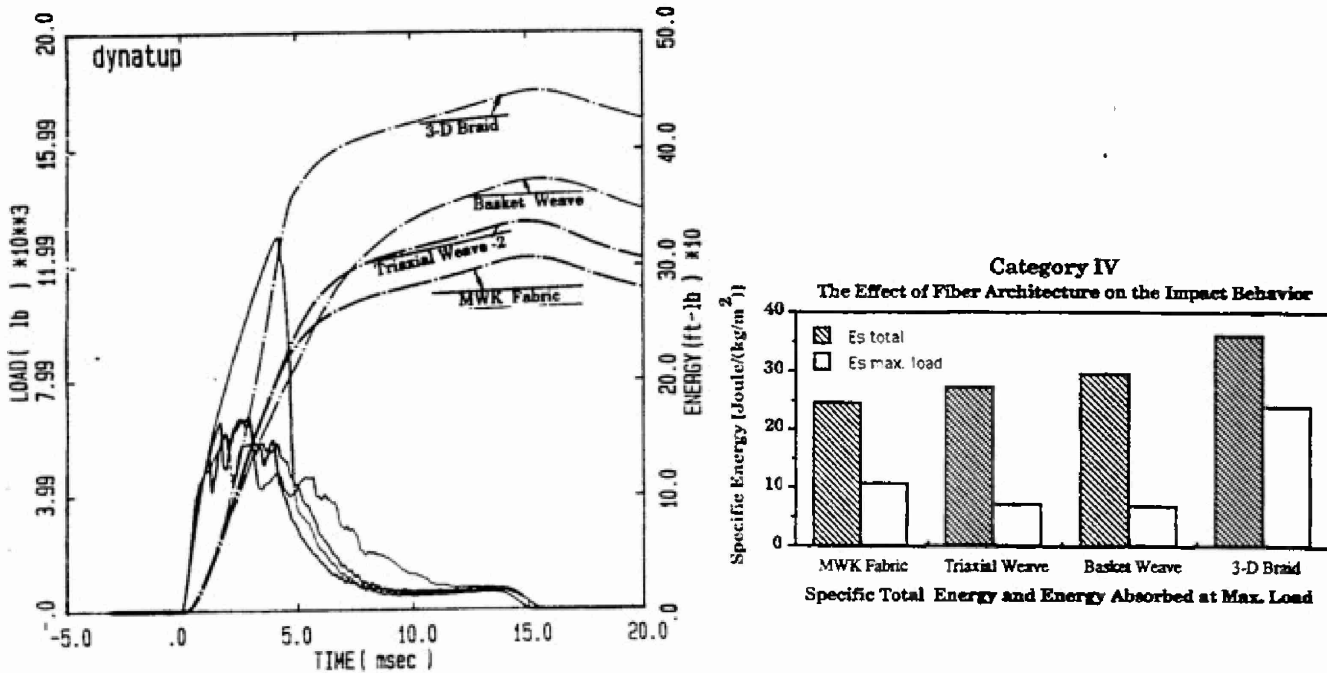


Figure 54. Impact Load and Energy vs. Time, Category IV Composites

Table 12. Impact Properties of GDC Composites

Samples	Energy(Joule) E total	Energy(Joule) E max. load	Areal Density (kg/m²)	Specific Energy(Joule) Es total	Specific Energy J/ (kg/m²) Es max. load
MWK *	416.35	178.40	17.01	24.48	10.49
Triaxial Weave	467.13	123.41	17.21	27.14	7.17
Basket Weave	502.37	117.15	17.03	29.50	6.88
3-D Braid	609.70	405.02	17.02	35.82	23.80

\* MWK: Multi-axial Warp Knit

## Effect of Reinforcement in the Through-Thickness Direction

Figure 55 depicts Category V specimens. The stitch yarns absorb the impact energy in the through thickness direction and prevent the delamination propagating between layers. The complex paths of crack propagation in 3-D braided composites have made them absorb the highest amount of energy. The energy absorption mechanism of 3-D braided composite will be explored more in the following section.

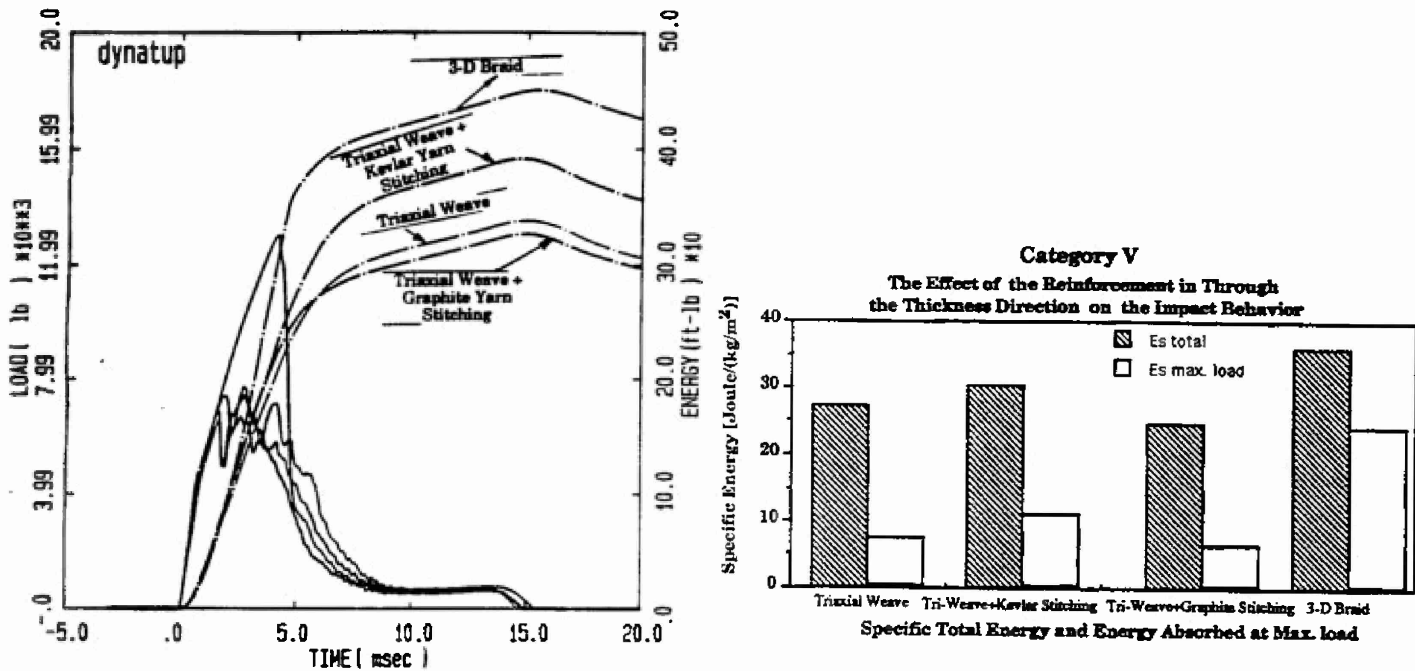


Figure 55. Impact Load and Energy vs. Time, Category V Composites

Table 13. Impact Properties of GDC Composites

Samples	Energy(Joule) E total	Energy(Joule) E max. load	Areal Density (kg/m <sup>2</sup> )	Specific Energy(Joule) Es total	Specific Energy J/(kg/m <sup>2</sup> ) Es max. load
Triaxial Weave	344.49	123.41	17.21	27.14	7.17
Tri-Weave+ Kevlar Stitching	391.55	188.88	17.61	30.15	10.73
Tri-Weave+ Graphite Stitching	306.33	104.21	16.80	24.73	6.20
3-D Braid	449.63	405.02	17.02	35.82	23.80

Figure 56 compares specific impact energy absorption for the 14 types of GDC composites tested. It is evident that a fully integrated nonlinear 3-D braid system renders the highest impact damage resistance.

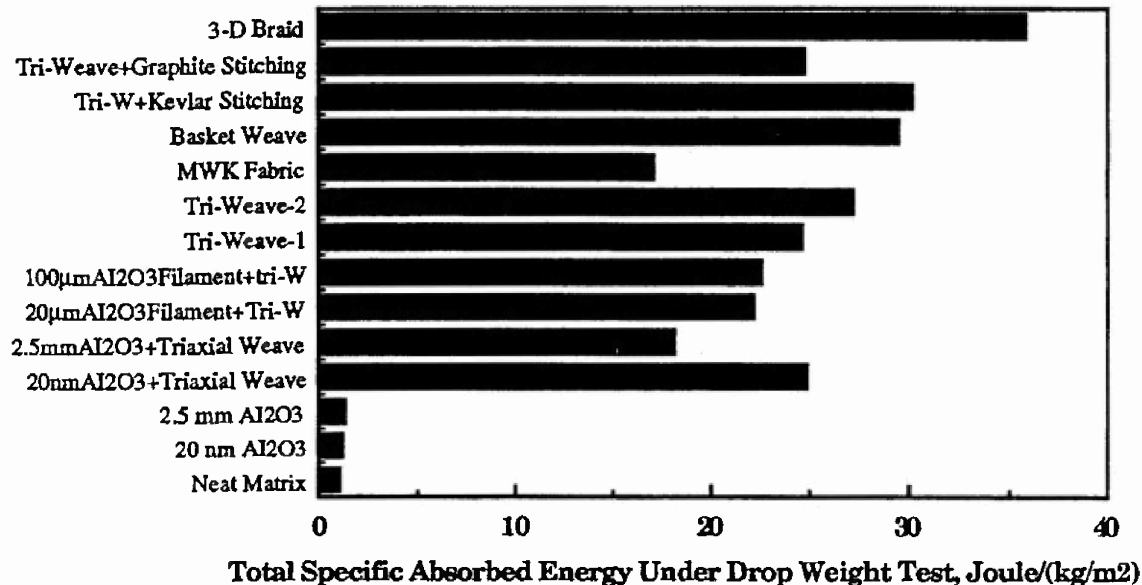


Figure 56. Total Specific Energy Absorption Comparison

It was found that fiber architecture plays a significant role in the impact resistance of composite structures. Three dimensional, fully integrated structures such as 3-D braid are promising to improve the impact resistance of composites. Future work will concentrate on understanding the energy absorption mechanism of 3-D integrated composites.

#### 4.3.3 Damage Characterization

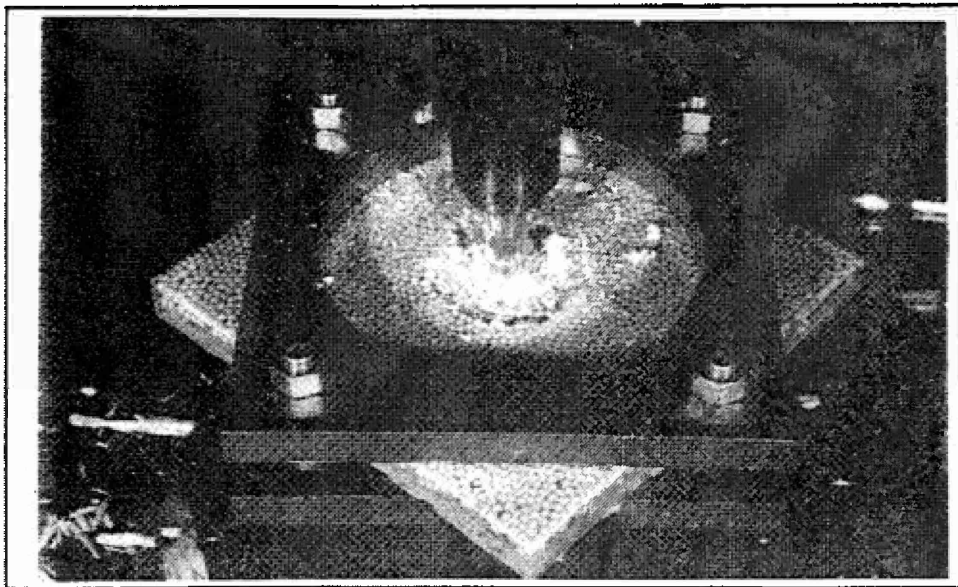
In order to characterize damage modes and failure mechanisms involved in ballistically impacted composite structures, a series of damage assessments must be carried out on post-impact samples at the macroscopic as well as microscopic level. Prior to microscopic examination, the impacted structure was photographed. These photographs provide a record of visually observable surface damage, while SEM pictures reveal microcracking on the surface as well as damage within the structure. By using optical and electron microscopy, micro-damage (e.g., fibrillation, rupture, fiber pull-out, fiber/matrix debonding, and delamination, etc.) can be examined and identified.

Microscopic studies of damage from samples of a series of controlled-depth penetration tests will yield information about damage initiation and failure evolution. This information should provide a better understanding of the failure mechanisms in impacted composites as well as provide guidance in the design of a system that resists ballistic impact more efficiently.

In order to gain some insight into the damage behavior of the composites, the failure mechanisms and crack propagation behavior of 3-D braided composite sample were studied as an example first by means of photographs, optical microscopy and SEM. The microscopic examination of the rest of the GDC composite samples will be conducted in the second year of the project.

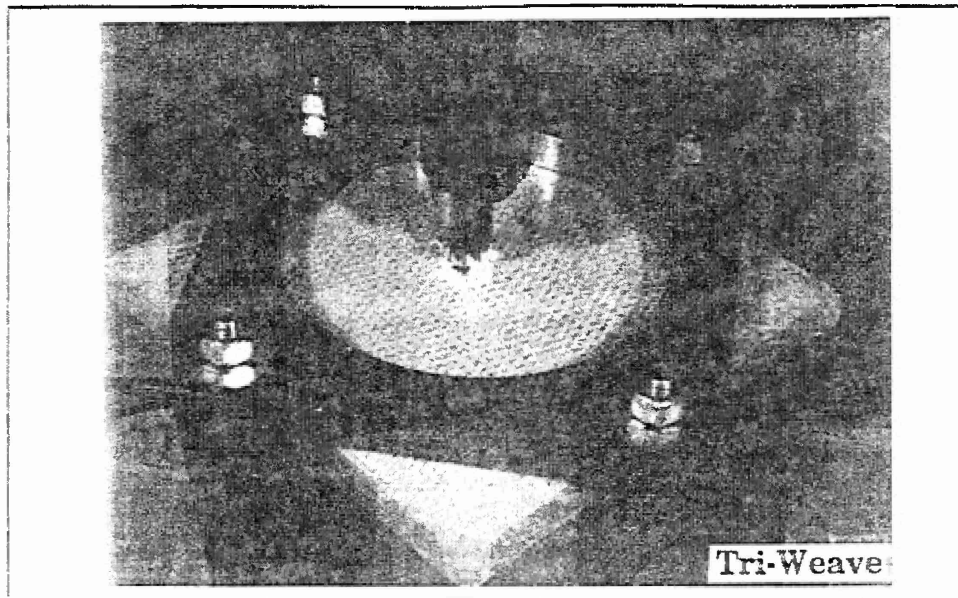
#### Photographic Observations

Figure 57 shows that the impactor is penetrating the samples. Each sample is rigidly mounted in a holder. The impactor is attached to the Dynatup impact machine. The samples in Figure 4.13 are .125"  $\text{Al}_2\text{O}_3$  particles embedded in the resin, tri-axial woven and 3-D braided composites. After each sample was tested, photos were taken to study surface failure at a macroscale level.

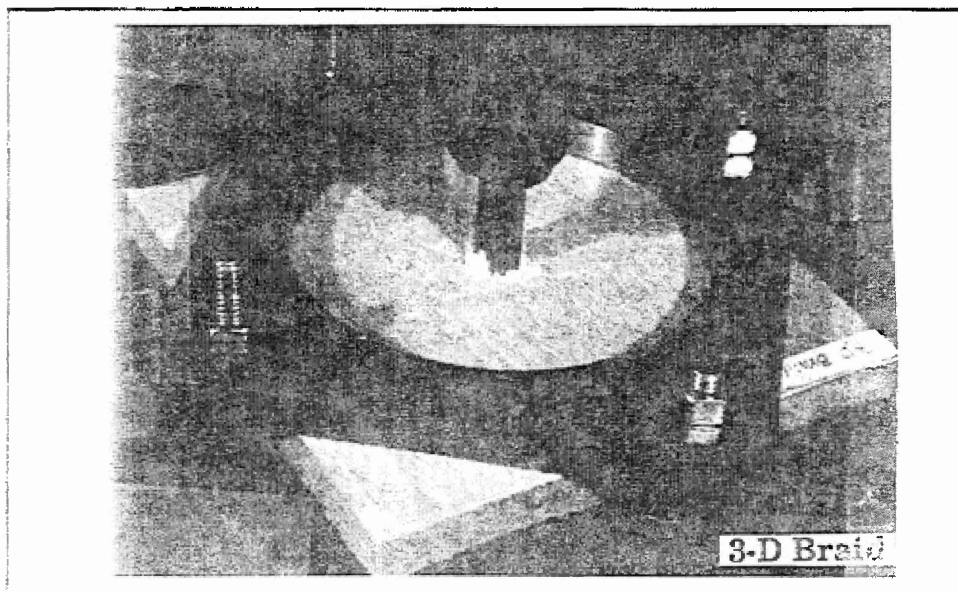


(a) 0.125"  $\text{Al}_2\text{O}_3$  Particles Embedded in the Resin

Figure 57. Samples Penetrated by Impactor



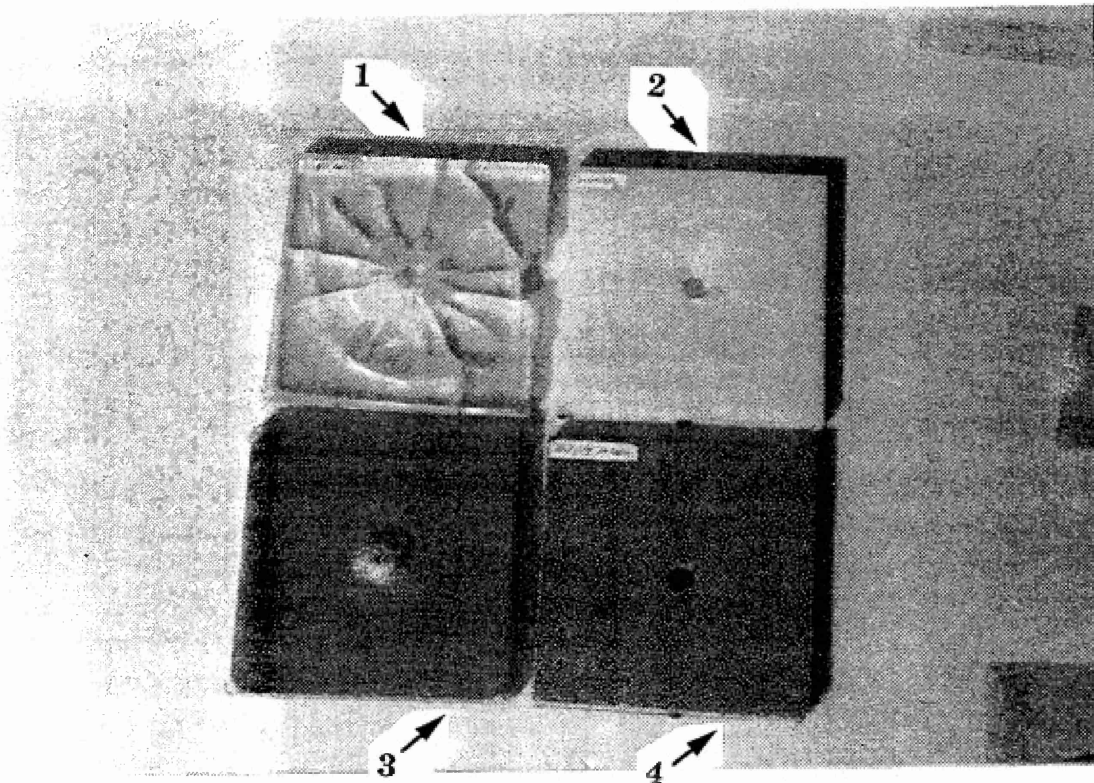
(b) Tri-axial Woven Composite



(c) 3-D Braided Composite

Figure 57. Samples Penetrated by Impactor (cont'd)

Figure 58 shows the photographs of post-damaged composites. The neat matrix and 20 nm  $\text{Al}_2\text{O}_3$  particle reinforced composites were shattered, while the larger particle (0.125" inch)  $\text{Al}_2\text{O}_3$  reinforced composite suffered only a small area of chipping. The triaxial fiber architecture tended to confine damage propagation and fiber push-out can be seen only around the penetration hole. Observations indicate that the delamination area is around the penetration hole, unlike the conventional laminated composite having a large area of delamination.



1. Neat Matrix,
2. 20 nm $\text{Al}_2\text{O}_3$  Particles Reinforced Composite,
3. 20nm $\text{Al}_2\text{O}_3$ +Triaxial Woven Fabric Reinforced Composite,
4. 0.125"  $\text{Al}_2\text{O}_3$  Particles Reinforced Composite

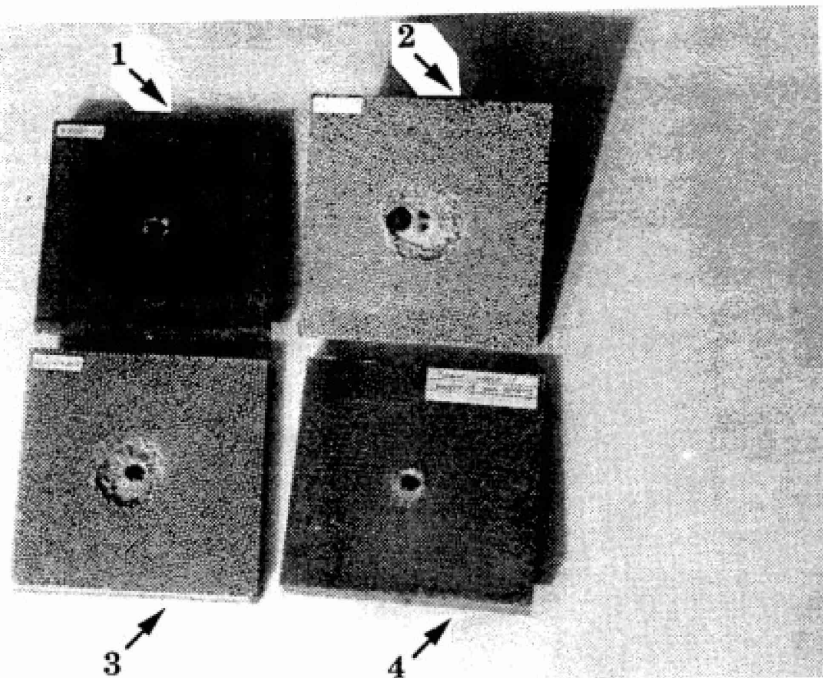
Figure 58. Photos of Post-Damaged Composites



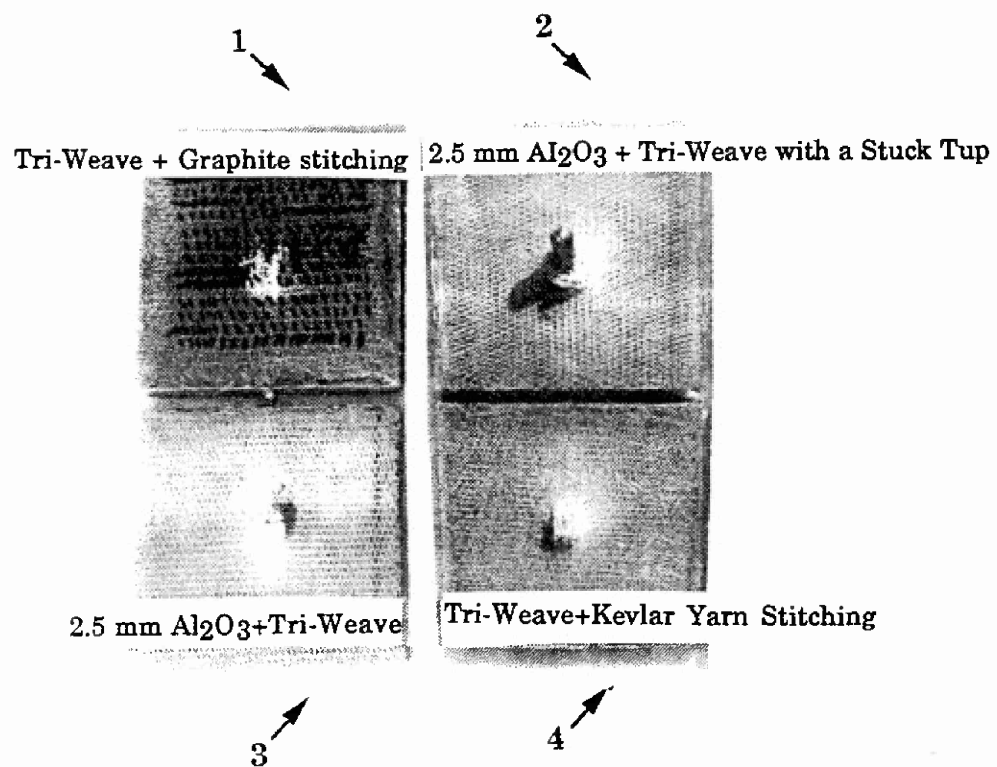
Figure 59 shows the photographs of the post-damaged composites from both top and bottom sides. Specimens in the figure are reinforced by Triaxial-weave + Kevlar yarn stitching, 2.5 mm  $\text{Al}_2\text{O}_3$  + Triaxial-weave, 2.5 mm  $\text{Al}_2\text{O}_3$  + Triaxial-weave with a stuck tip and Triaxial-weave + graphite stitching, respectively. As it can be seen, the damage area is small and delamination is confined around penetration hole. The stitch yarn in the stitched composites plays a role in resisting delamination propagation. Therefore, the stitched composites, triaxial weave with graphite yarn stitch and triaxial weave with Kevlar yarn stitch, exhibit smaller delamination area.

Figure 60 shows the photographs of the post-damaged composites from both top and bottom sides. Specimens in the figure are composite samples reinforced by 3-D braided structure (with multiple hits), plain weave, 100um Boron filament + triaxial-weave and  $\text{Al}_2\text{O}_3$  20 $\mu\text{m}$  filament + Triaxial-weave, respectively. A small area of damage and delamination for each sample can be observed. The 3-D braided composite suffers multiple impact; however, it does not exhibit any delamination. Therefore, the highest energy is needed to penetrate the fully integrated 3-D braided composite.

Figure 61 shows the photographs of the post-damaged composites under ballistic impact from both top and bottom sides. From observation, only the 3-D braided composite shows no delamination at all. Among the delaminated composites, the stitched (Triaxial weave with graphite yarn stitch) composite exhibits little delamination area around the penetration hole. The stitch yarns absorb the impact energy in the through thickness direction and prevent delamination propagation between layers.

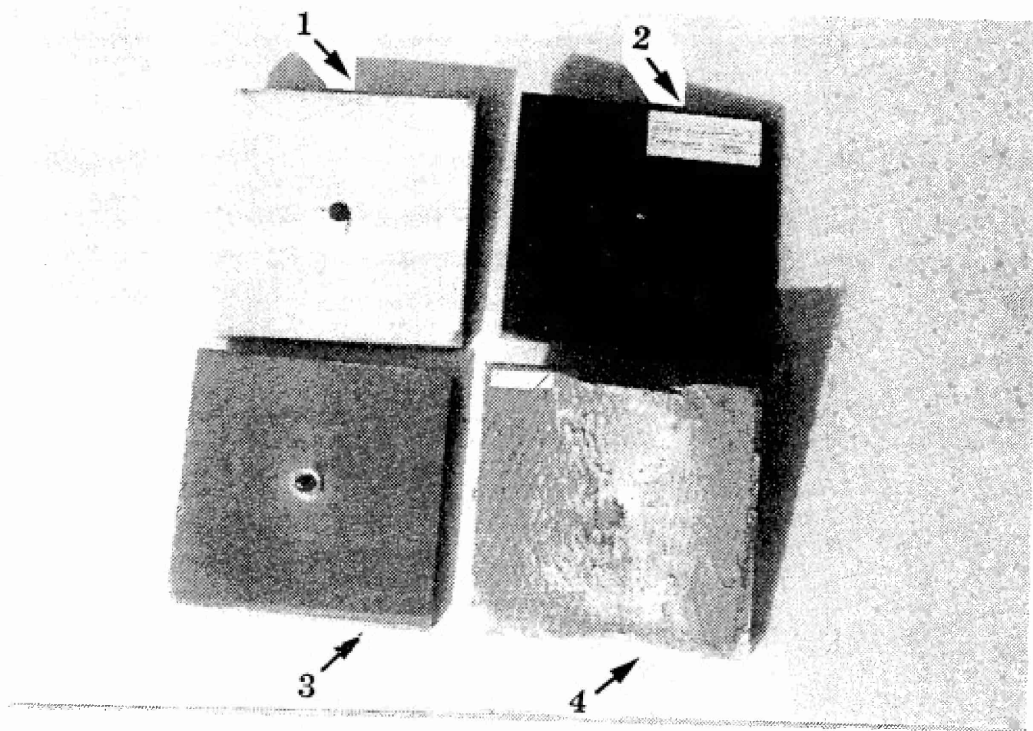


(a) Top View

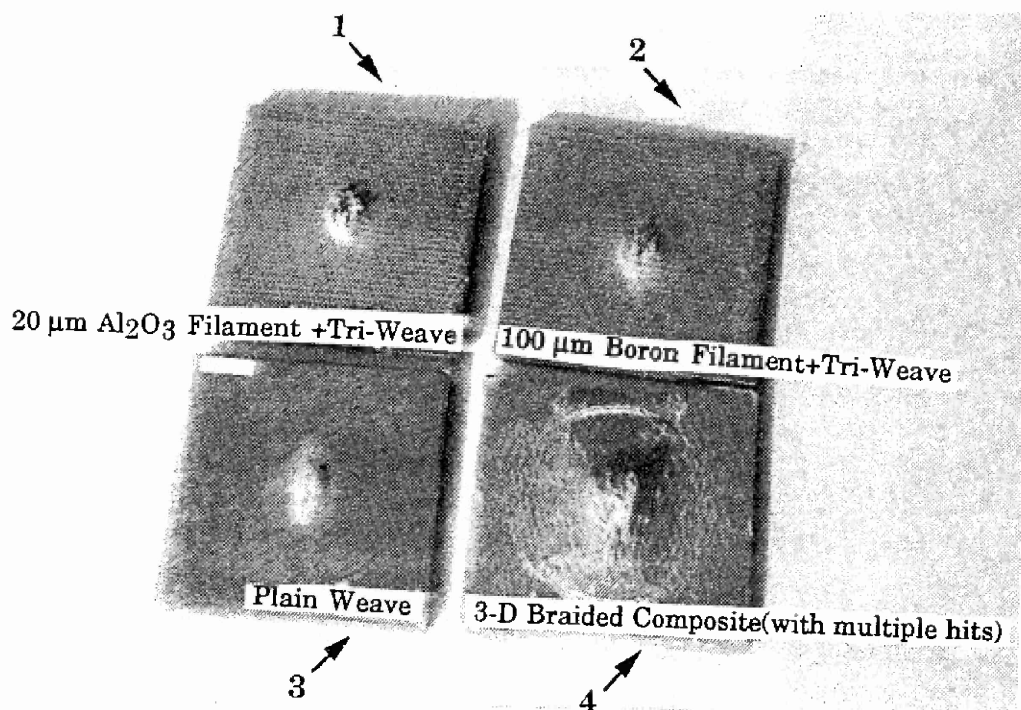


(b) Bottom View

Figure 59. Photos of Post-Damaged Composites

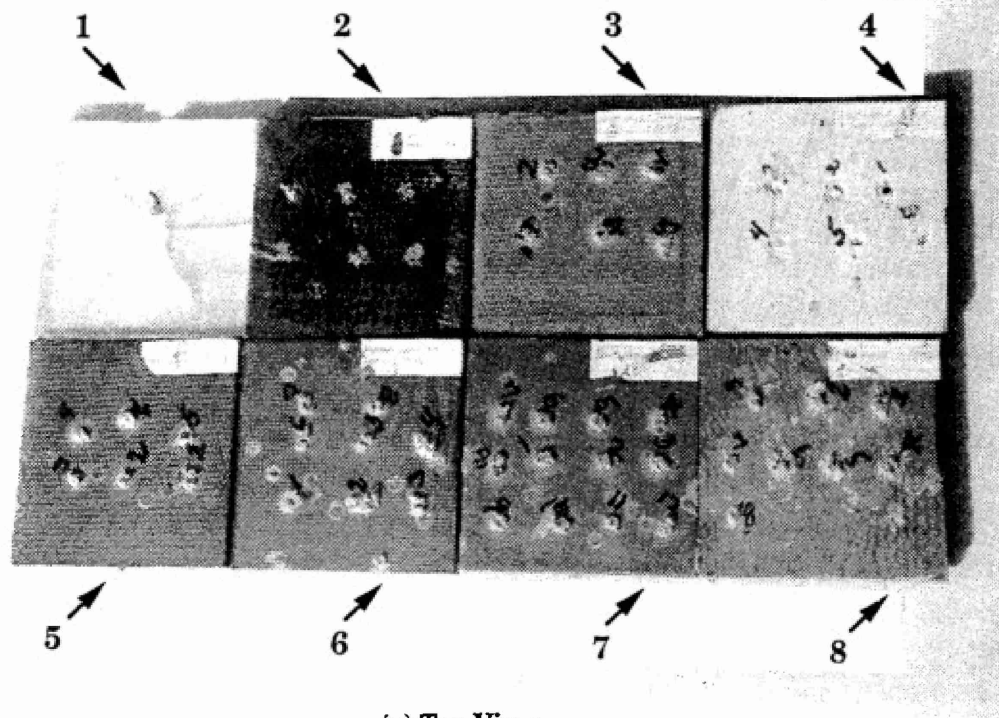


(a) Top View

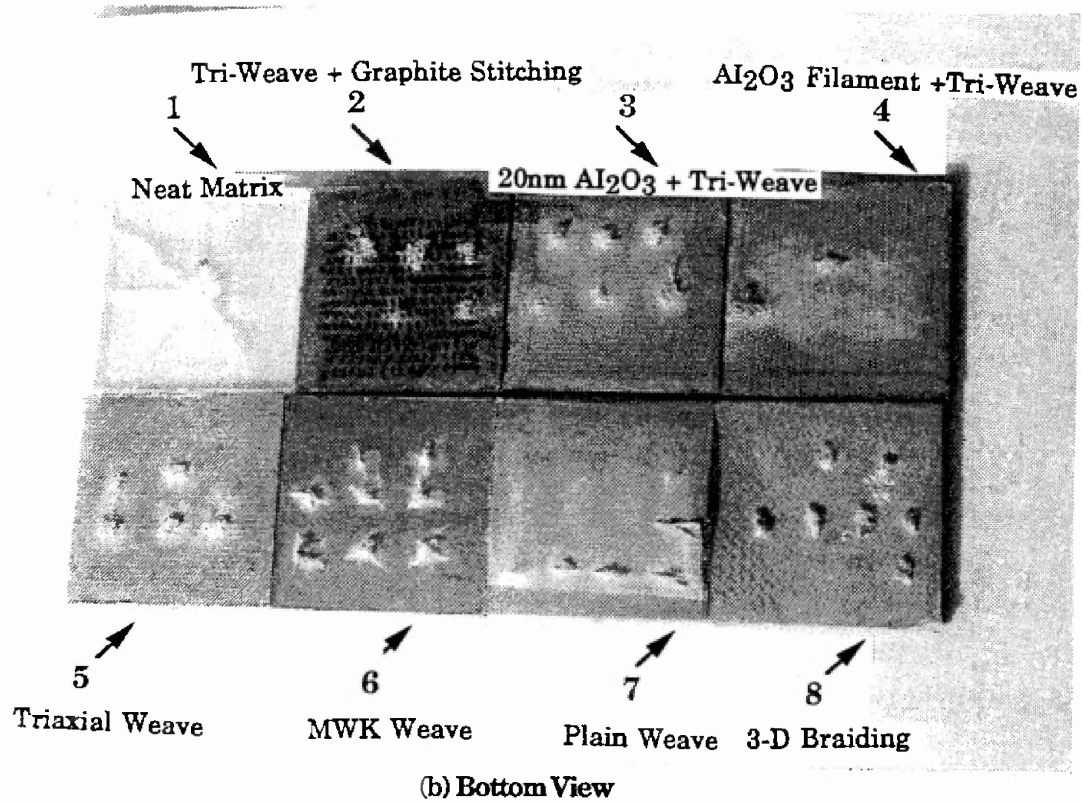


(b) Bottom View

Figure 60. Photos of Post-Damaged Composites



(a) Top View



(b) Bottom View

Figure 61. Photos of Post-Damaged Composites

## SEM And Optical Micrograph Observations

A 3-D braided composite was sectioned by diamond razor saw as shown in Figure 62 in order to study the cracks propagation and failure phenomena of the composite. The sections were cut in such a manner as to provide damage information in both the longitudinal and transverse directions.

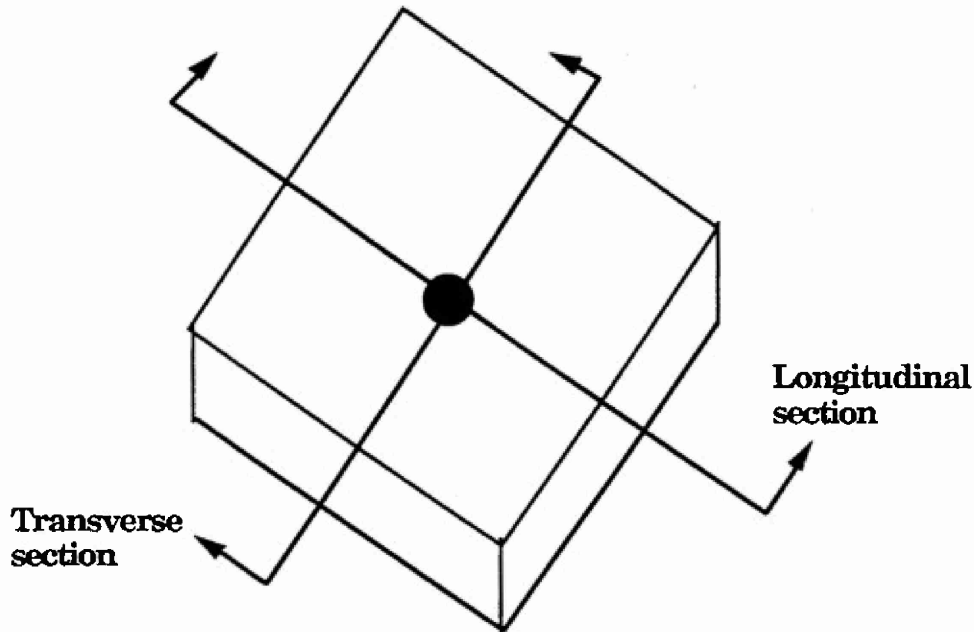


**Figure 62. Schematic Diagram of The Sectioning for Microscopic Graphs**

Figure 63 is a schematic diagram of one quarter of the sectioned 3-D sample, which indicates all the examined locations. Two quarters of the sectioned sample were used: one was polished for optical microscope and the other one was coated with a vapor-deposited thin layer of gold to introduce conductivity before examination under SEM (JOEL Model JSM-35CF).

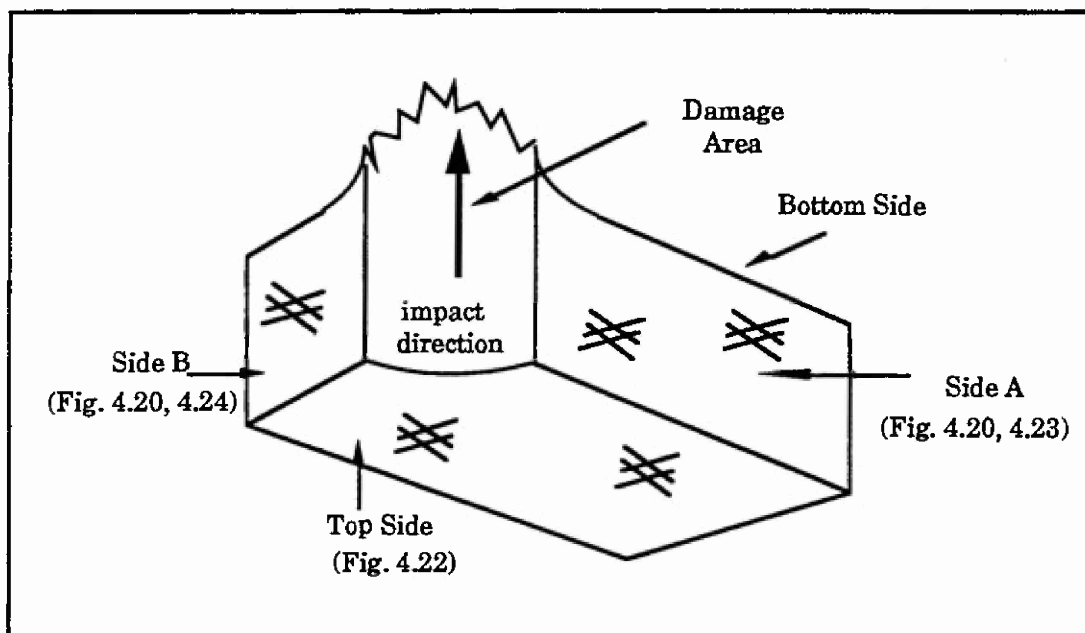
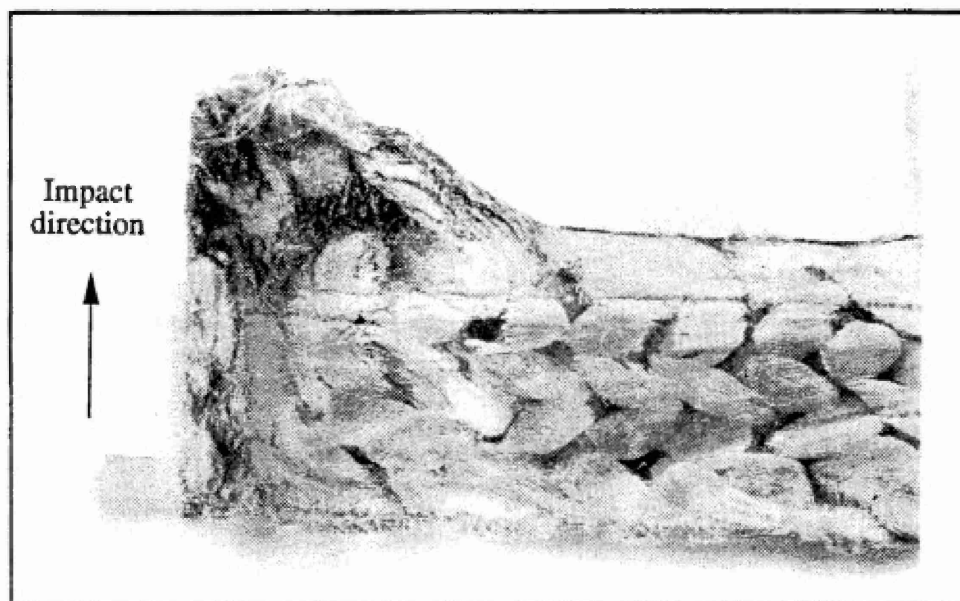


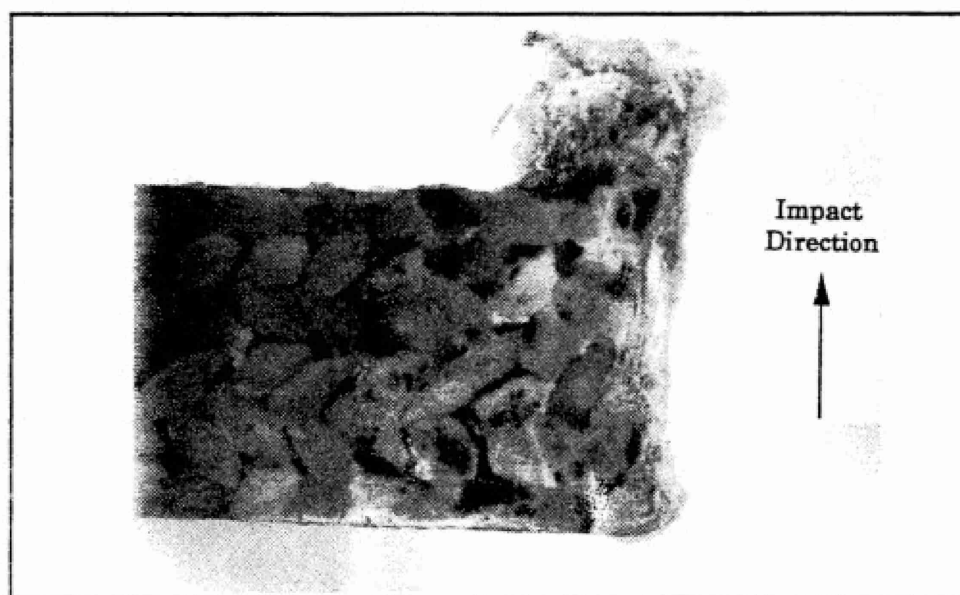
**Figure 63. Schematic diagram of the Locations Examined Using Optical and SEM Microscopic Techniques**

Composite failure is the result of a combination of different mechanisms, such as shear or fiber cutting, tension or fiber breakage, fiber debonding, fiber pull out, delamination and matrix failure. Visual examination of the impacted composite panels suggests a variety of failure mechanisms occurred.

Figure 64 shows that, upon impact, the tup pushes a strip of composite toward the rear of the panel. The deformation occurs in two directions: one is in the radial direction, which is perpendicular to the direction of impact; the other direction is along the impact axis. However, as the picture shows, the braid pattern does not change (due to the deformation) in a short distance from the impact hole. The deformed region only shows the pattern change, and no delamination is observed. Because the high impact energy creates stress waves in 3-D directions, there is evidence of matrix cracking in the braided composites.



(a) Side(side A) View of Fracture Surface



(b) Side(side B) View of Fracture Surface

**Figure 64. Side Views of Fracture Surface of the 3-D Braided Composite**

From these observations, it can be seen that matrix cracking occurs on the top surface, around the penetration hole in the composite. The direction of matrix cracking propagates radially from the penetration hole along the braiding yarn path, and is stopped at three or four yarn diameters from the penetration hole. In general, matrix cracking does not propagate through the braiding yarn bundles. As the distance from the top surface increases, the matrix cracking area becomes smaller. On the bottom surface, no matrix cracking can be found. Figure 65 shows the matrix cracking along the braiding yarn path near the penetration entrance. Figure 66 shows that the matrix cracks propagate radially from the center of the damage area and are stopped by the interlacing yarns.

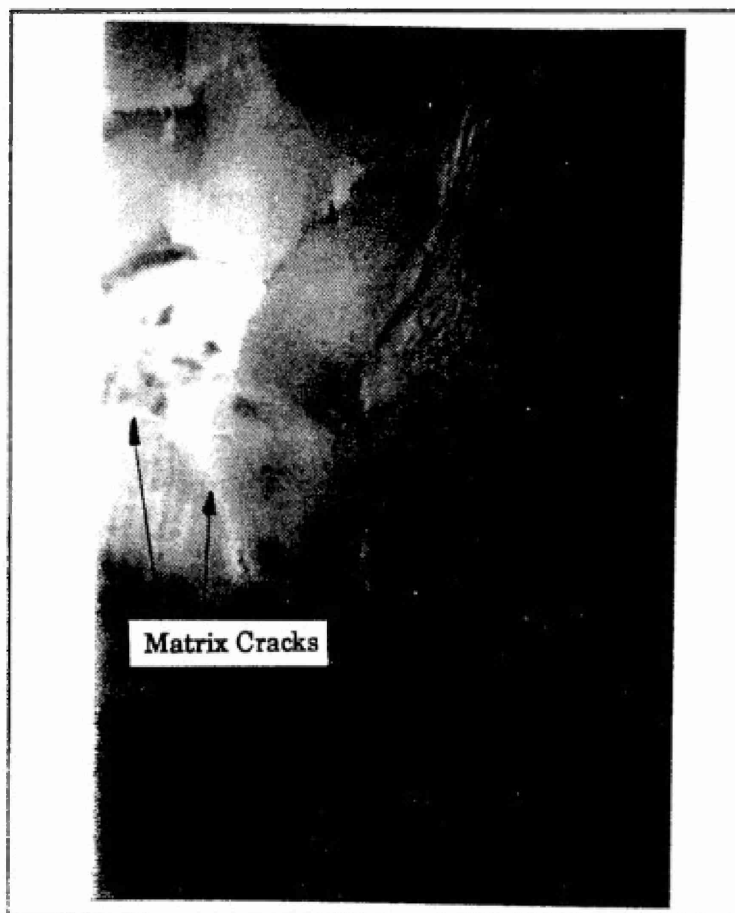
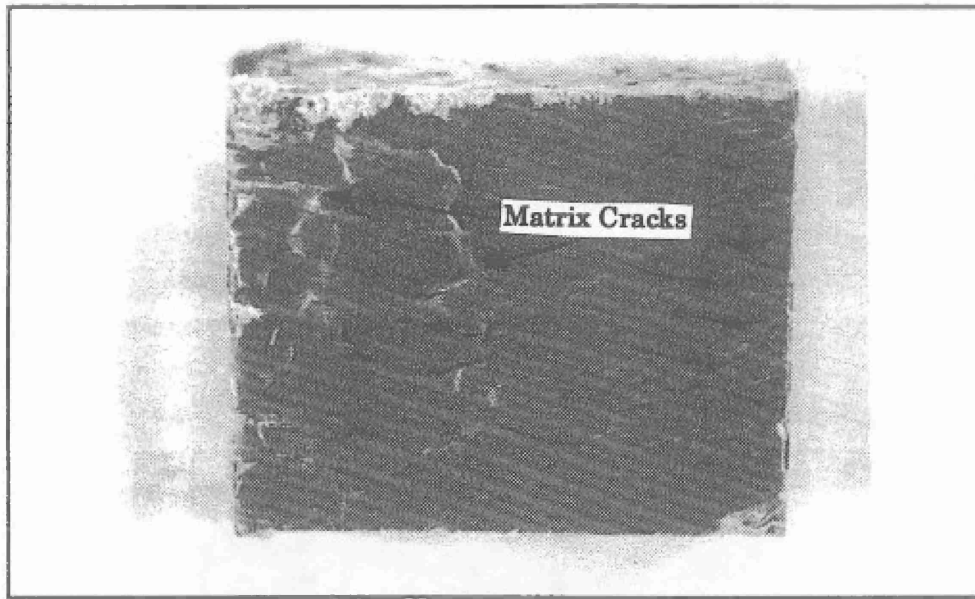
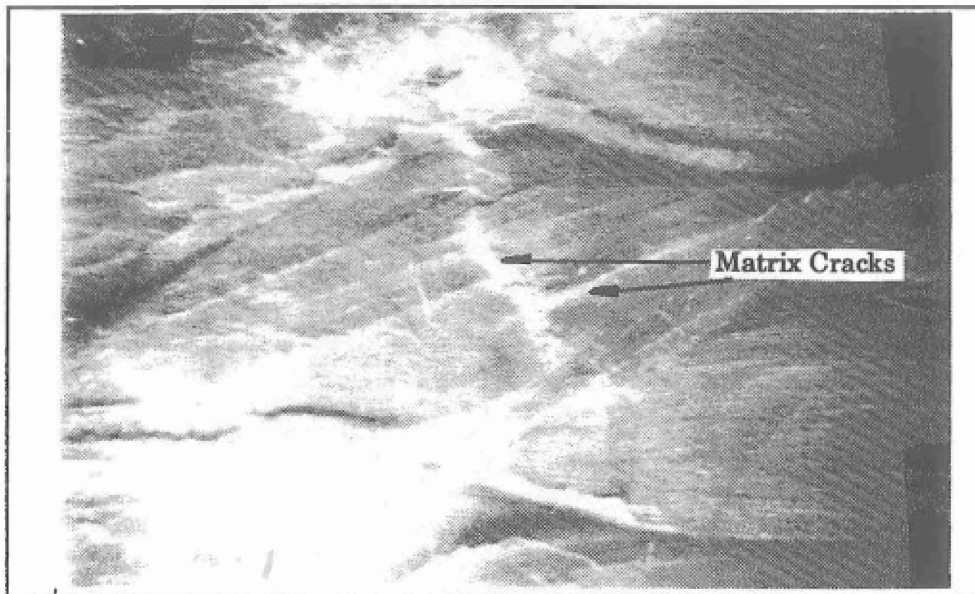


**Figure 65. Matrix Cracks Near the Entrance of the Penetration**





(a) X1



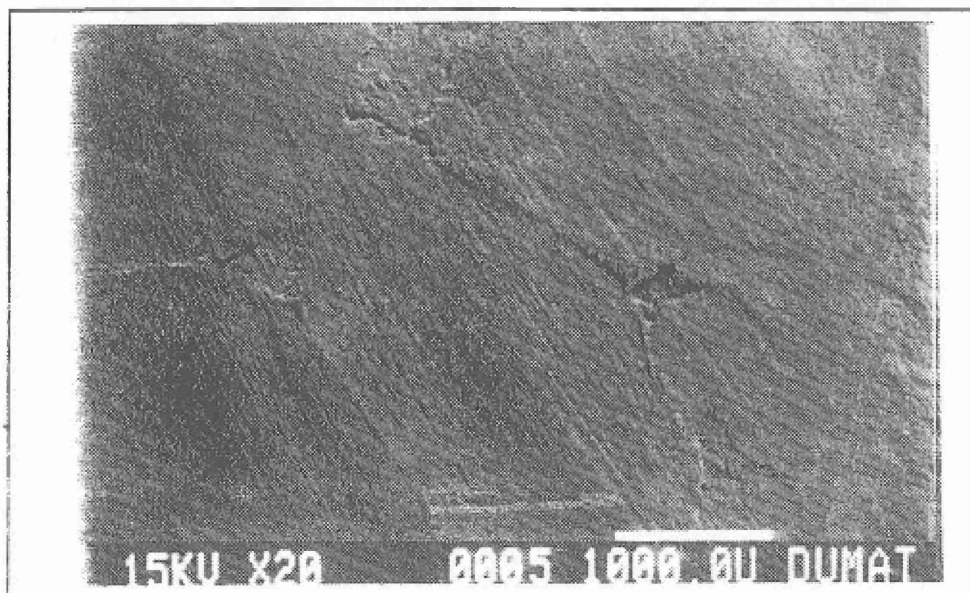
(b) X10

Figure 66. Optical Photo of the Sample From the Top

The SEM picture of the sectioned sample in Figure 67 illustrates how the cracks grow along the matrix fiber interfaces (near the circumference of each fiber bundle) and are retarded by the fibers. However, at this juncture, crack growth might continue directly through the whole bundle of fibers, as shown in Figure 68.



(a) SEM Micrographs of Fracture Surface at 10X Magnification



(b) SEM Micrographs of Fracture Surface at 20X Magnification

Figure 67. SEM Micrographs of Fracture Surface

A close observation of Figure 68 shows that, at point A, the crack propagates not only along the interfaces but also directly through the whole bundle of the fibers, breaking the fibers and causing fiber debonding. Because this is the only evidence of yarn bundle breakage, it is not conclusive that the breakage is due only to impact stress waves. Breakage may be induced during the sectioning process. Further study on this subject is needed.

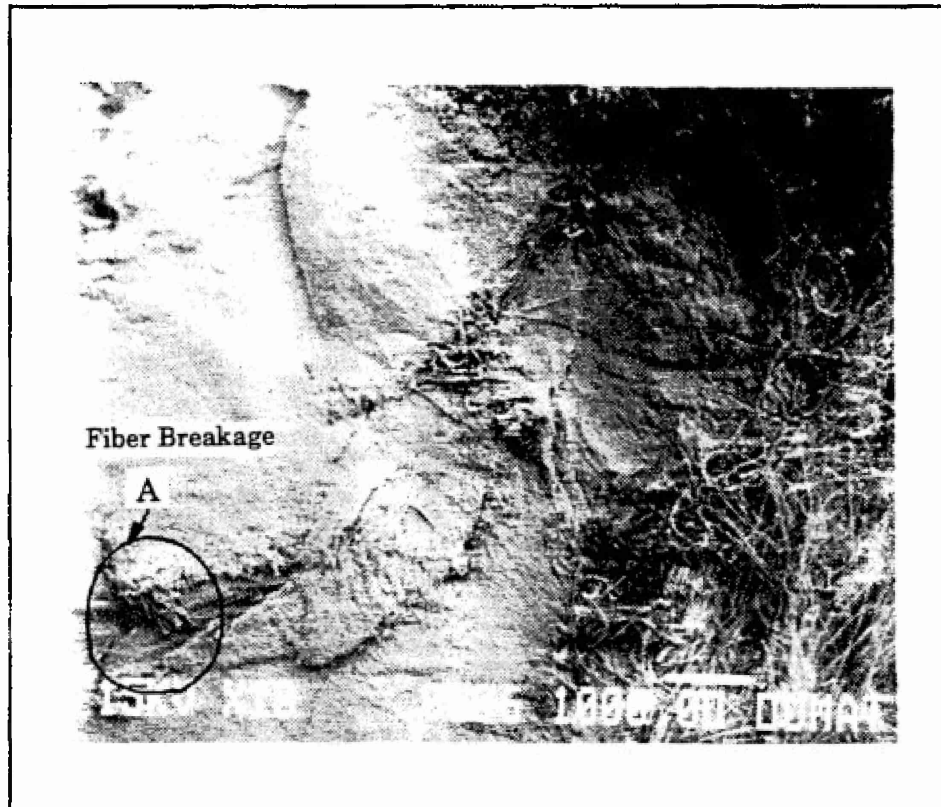
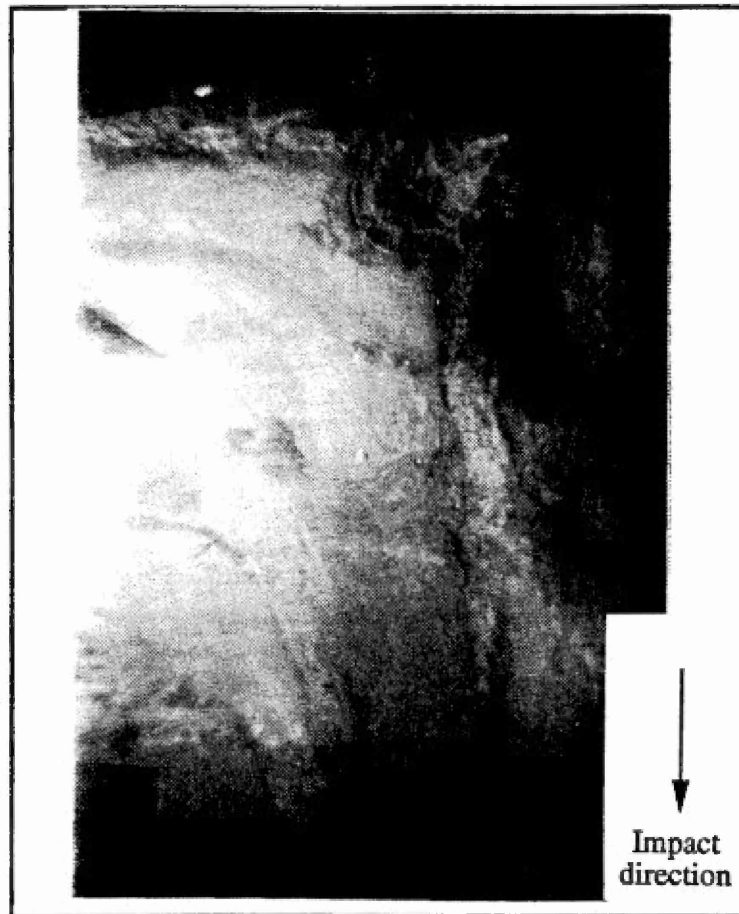


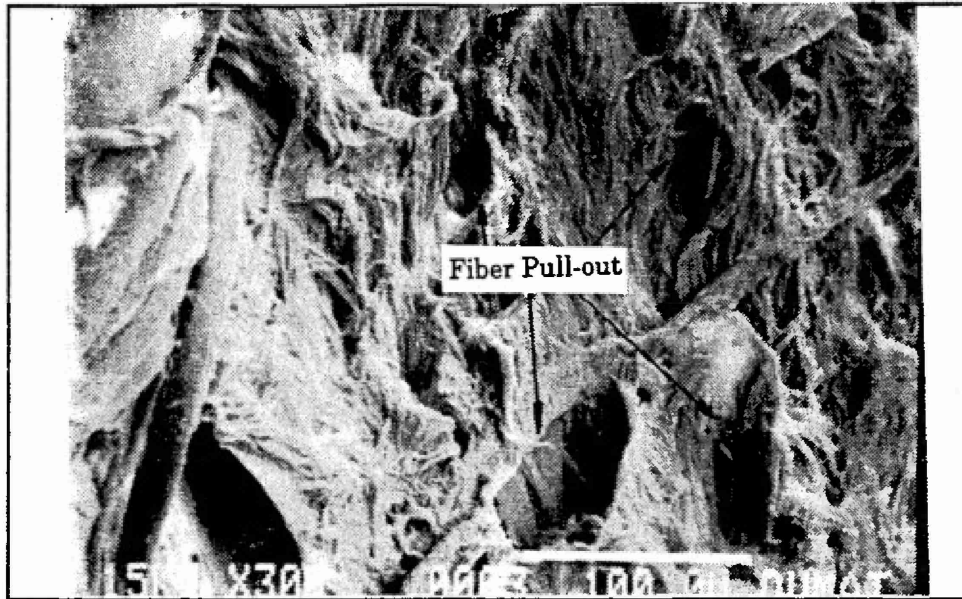
Figure 68. SEM Fractograph of the Damaged Sample

Figure 69 shows a closer look at the entrance of the pushed strip, depicting fiber breakage, fiber/matrix debonding and fiber fibrillation. The high impact energy created high compressive stress in front of the impactor and shear stress along the path of push-out. The high stresses caused fiber breakage, and the enormous transverse compression in the fiber bundles not only deformed the fiber bundles, but also caused fibrillation of the individual fibers.



**Figure 69. Fracture Surface of Damage Area Near the Point of Penetration**

Figure 70 shows a close view of the damage area introduced by the impact tup. As expected, the matrix is crumpled and exhibits dark pores, indicating fiber pull-out as a result of poor fiber/matrix interfacial bonding.



**Figure 70. Closer View of the Damaged Area Introduced by the Impact Tup**

In summary, the cracks were initiated at the site of impact and primarily followed the braiding yarn path. 3-D braided composites experience a complex path of crack propagation, acting as a network of crack arrestors. The failure processes include matrix microcracking, fiber/matrix debonding and fiber pull-out. Detailed microscopic examination of the samples damaged by ballistic impact will be conducted in the second year of the project through the use of optical and scanning electronic microscopy.

#### **4.4 High Velocity Impact Behavior**

At low velocity, the response of the composites is global; impactor parameters such as impactor mass and nose shape are important factors affecting the extent of damage and damage mode on the composite. At high speeds, the behavior of composites due to effects of shock waves is significant and normally the damage is very localized.

As projectile speed increases, effects due to shock waves will dominate since contact time is shorter than the time it takes for mechanical waves to reflect from the boundary of the target. Therefore, the damage mode and extent of each individual damage mode in the composites will not be the same as that in the low velocity impact. The impact-resistant characteristics of composites during high speed impact are different from those at low velocity impact conditions. Results from this study will be useful in identifying a material system that can defeat ballistic impact. High velocity testing will be performed at Natick using projectiles from a rifle or light gas gun.

#### 4.4.1 Ballistic Test Conditions

Kinetic energy absorption during the ballistic penetration was measured using the high speed impact apparatus located at the Army Research Laboratory. Ballistic resistance tests were conducted in accordance with Military Standard MIL-STD-662E, V50 Ballistic Test For Armor. The fragment simulating projectile was the .22 caliber type 2 conforming to MIL-P-46593, weighing 17 grains. The composites were stored in the ballistic test chamber for 24 hours prior to testing. The impact points were a minimum distance of 1 1/2 inches from each other. The samples were rigidly mounted with the area of impact normal to the lines of fire. The schematic of the test setup is shown in Figure 71.

In Figure 71, the barrel is a .30 caliber rifled barrel with a one-in-sixteen twist. The barrel length is 28 inches. The silver gridded papers were placed directly in front of and behind the test sample with the emulsion side facing the sample. The gridded papers were used to determine the degree of the yaw. The composites were 12.5 feet forward of the rifle muzzle and perpendicular to the trajectory of the projectile.

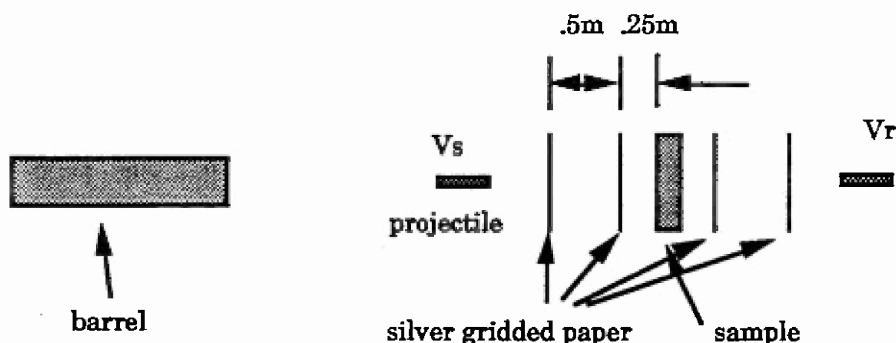


Figure 71. Schematic of Ballistic Test Setup

The testing conditions are summarized as follows:

- Type of Bullet: Fragment simulator projectile
- Weight of FSP: 17 grains (1.1 g)
- Shape of FSP: Cylinder with flat head or chiseled head
- Diameter of FSP: 5.59 mm
- L/D of FSP: 1.0
- FSP Material: Steel
- Modulus of FSP: 200GPa
- V50 of Actual Helmet: 2150 ft/s. (656 m/s)
- Density of Steel: 7.8 g/cm<sup>3</sup>

Assuming that the projectile mass was constant during the penetration of the target, the kinetic energy (KE) absorbed by the target is:

$$KE = \frac{1}{2} m(V_s^2 - V_r^2)$$

where  $m$  is the projectile mass (Kg),  $V_s$  and  $V_r$  are striking and residual velocities (m/s), respectively.

In this study, the ballistic limit (BL) is considered to be the single highest striking velocity where the residual velocity,  $V_s$ , equals zero, and can be estimated with:

$$BL = \left( \frac{2KE}{m} \right)^{1/2}$$

$V_{50}$  is determined by averaging the three lowest complete penetration velocities and the three highest partial penetration velocities.

#### 4.4.2 Test Results

Ballistic tests were carried out at US Army Natick R.D.&E. Center. Multiple shots were fired at each sample according to the requirements suggested by military standard. For each sample, the striking velocities and residual velocities (if complete penetration occurs) were recorded, and thus the  $V_{50}$  of each sample was determined. The kinetic energy absorption and ballistic limit for each sample were calculated according to the formulas given above. The kinetic energies and specific kinetic energies absorbed by each kind of composite during ballistic impact are listed in Table 14 and plotted in Figure 72.

**Table 14. Kinetic Energy Absorbed Upon Ballistic Impact**

Sample	Areal Density (kg/m <sup>2</sup> )	Specific KET J/(kg/m <sup>2</sup> )	Kinetic Energy	
			(ft-lb.)	(J)
Neat Resin	14.86	8.22	90.036	122
20 nm Al <sub>2</sub> O <sub>3</sub>	14.98	8.72	96.309	130.5
2.5 mm Al <sub>2</sub> O <sub>3</sub>	26.78	N/A	N/A	N/A
20 nm Al <sub>2</sub> O <sub>3</sub> + Triaxial Weave	16.77	7.99	98.892	134
2.5 mm Al <sub>2</sub> O <sub>3</sub> + Triaxial Weave	20.25	N/A	N/A	N/A
20 μm Al <sub>2</sub> O <sub>3</sub> filament (0/90) + Triaxial Weave	19.58	10.05	145.09	196.6
Triaxial Weave	17.21	10.92	138.6	187.8
Multiaxial Warp Knit (MWK)	17.01	9.46	118.67	160.8
Plain (Basket) Weave	17.03	13.28	166.78	226.15
3-D Braid	17.02	10.82	135.86	184.1
Triaxial + Graphite Stitch	16.80	11.57	143.32	194.2
Helmet Laminate*	8.79	20.05	130.00	176.28

\* Note: Data was obtained from DuPont "Preliminary Information Bulletin".

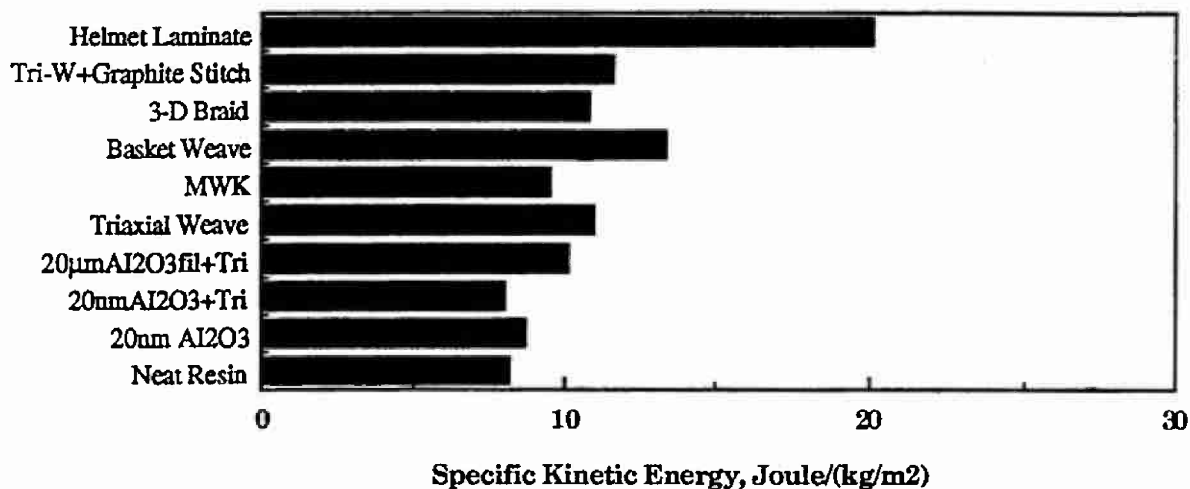


**Figure 72. Kinetic Energy Absorbed During Ballistic Impact**

Based on the results shown in the table, fiber reinforcements appear to dissipate more energy than sphere reinforcements. The reinforcing fibers create friction between impactor and fibers during the penetration process. This causes the impactor to slow down and dissipates the kinetic energy. For example, the MWK composite, which contains no yarn interlacing, absorbs less energy in comparison to interlaced fiber-reinforced composites. Fiber interlacing plays an important role in preventing separation of the individual fibers. And how interlacing density affects energy absorption requires further studies.

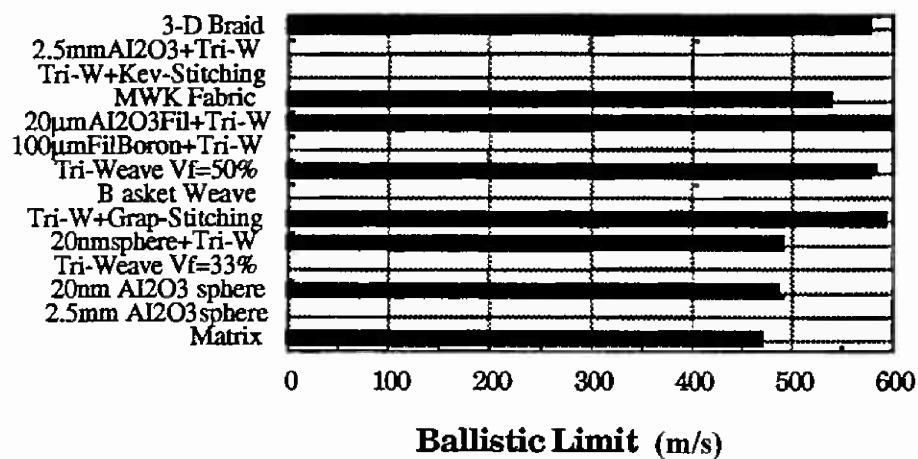
Table 15 lists the ballistic impact limit for each type of composites. The same results are shown graphically in Figure 73. As can be seen, the same trend is found: the reinforcing fibers increase the ballistic limit, and the MWK composites exhibit lower ballistic limits, indicating that yarn interlacing increases the threshold of penetration.

Table 16 and Figure 74 show the  $V_{50}$  of fiber-reinforced composites. As can be seen, the MWK composite has the lowest value of all. For the same interpretation, the linear arrangement of fibers renders less resistance to penetration.



**Table 15. Ballistic Limit of Each Type of Composite**

Sample	Ballistic Limit	
	(ft/s)	(m/s)
Neat Resin	1547.244	471.6
20 nm Al <sub>2</sub> O <sub>3</sub>	1598.425	487.2
2.5 mm Al <sub>2</sub> O <sub>3</sub>	N/A	N/A
20 nm Al <sub>2</sub> O <sub>3</sub> + Triaxial	1618.766	493.4
2.5 mm Al <sub>2</sub> O <sub>3</sub> + Triaxial	N/A	N/A
20 $\mu$ m Al <sub>2</sub> O <sub>3</sub> filament (0/90) + triaxial	1960.63	597.6
Triaxial	1917.323	584.4
Multiaxial Warp Knit (MWK)	1773.622	540.6
Plain (Basket) Weave	N/A	N/A
3D Braid	1897.966	578.5
Triaxial + Graphite Stitch	1948.163	593.8



**Figure 73. Ballistic Limit of Each Type of Composite**

**Table 16. V<sub>50</sub> Of Each Type Of Composite**

Sample	V <sub>50</sub>	
	(ft/sec)	(m/sec)
Neat Resin	N/A	N/A
20 nm Al <sub>2</sub> O <sub>3</sub>	N/A	N/A
2.5 mm Al <sub>2</sub> O <sub>3</sub>	N/A	N/A
20 nm Al <sub>2</sub> O <sub>3</sub> + Triaxial	1887.47	575.3
2.5 mm Al <sub>2</sub> O <sub>3</sub> + Triaxial	N/A	N/A
20 μm Al <sub>2</sub> O <sub>3</sub> filament (0/90) + triaxial	2048.88	624.5
Triaxial	1917.323	584.4
Multiaxial Warp Knit (MWK)	1773.622	540.6
Plain (Basket) Weave	N/A	N/A
3D Braid	N/A	N/A
Triaxial + Graphite Stitch	N/A	593.8

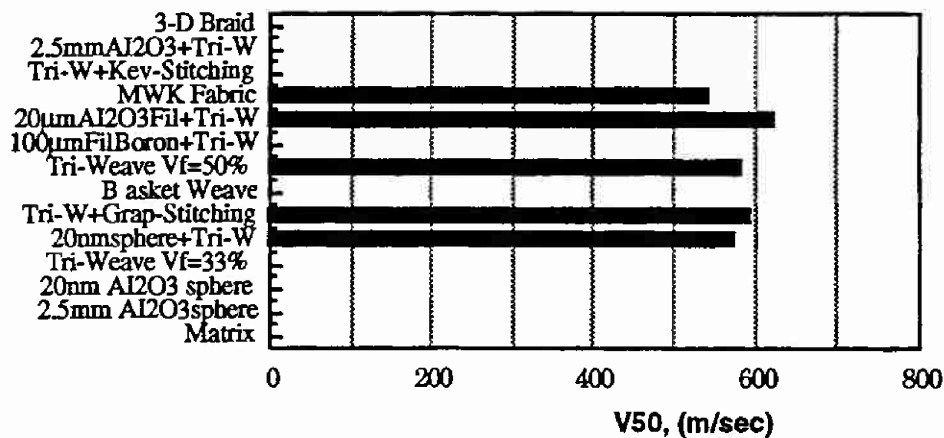


**Figure 74. V<sub>50</sub> Of Each Type Of Composite**

It is of interest to compare the total energy absorbed during low velocity and high velocity impacts. Figure 75 shows the energy absorption for each type of composite under high and low velocity impact conditions.

Owing to the global response which the composites (targets) render upon impact, more energy is absorbed during low velocity impact. Another factor may be that time duration is longer in low velocity impacts, giving more time for the composite to resist the impactor.

Among the composites, fully integrated 3-D braided composites absorb the most energy under low velocity impact. Under ballistic impact, 3-D braided composites behave similarly to composites reinforced by other fibrous structures. Composite response due to the effects of high speed shock waves induced from ballistic impact is localized, and only reinforcing fibers play an important role in controlling damage.

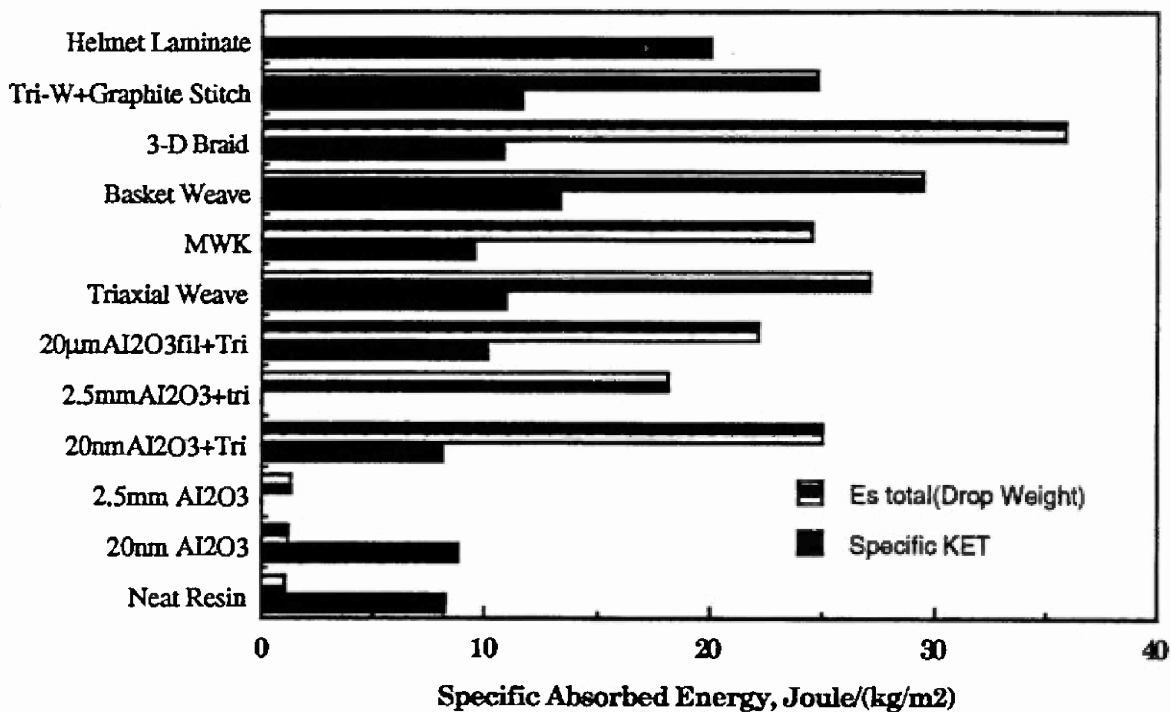


**Figure 75. Comparison Of The Specific Energy Absorption Between Ballistic Impact And Low Velocity Impact**

## **5. Computational Modeling of Impact Behavior of Textile Composites**

### **5.1 Introduction**

The anisotropic response and the plethora of damage/energy absorption mechanisms in composite armors make modeling impact behavior extremely complex and challenging. It is, however, the same complexity, that enables us to afford to tailor the properties of the armor to specific threats, since several parameters can be manipulated during material/geometry selection and design.

The objective of the computational modeling of viscoelastic armor is to complement the experimental component of this study so as to obtain a thorough understanding of deformation, energy absorption mechanisms and failure of viscoelastic armors.

The most deleterious threats to armor are dynamic and impulsive in nature. Such short duration phenomena are difficult to observe experimentally. Under optimum conditions impact experiments can provide us with a) macroscopic measurements such as deflections, velocities and accelerations, and b) postmortem data on damage and failure. In other words, experiments alone can not yield a complete picture of impact response of armors. Moreover, the textile composites can have almost infinite variation in fiber architecture and material selection, which makes it impossible to entirely rely on experimental efforts. Modeling on the other hand, can shed light to the complex stress-strain histories and damage development and evolution at every point of the target and projectile during impact. Successful modeling, however, is possible only when it is based on an accurate and complete description of the material behavior of the target and projectile under conditions similar to those occurring during impact.

The response of the armor material to impact loading depends strongly on impact velocity and the associated strain rates. The nature of the involved phenomena and the corresponding material behavior vary dramatically with strain rate. Table 17 below gives a broad outline of material response at different velocities, strain rates and methods of loading.

**Table 17. Outline of Material Response**

	Low velocity impact	High velocity impact
Important mechanism	Inertia	Wave propagation
Projectile velocity	5 m/s	500 m/s
Typical strain rate	$10^3/s$	$10^5-10^6/s$
Characteristic time	10 ms	1 ms <sup>(2)</sup>
Characteristic frequency	100 Hz	100 kHz
Experimental Characterization	DMTA	High strain rate tests e.g. Hopkinson bar
Modeling	Viscoelastic FGM type with appropriate modifications for loss of energy at interfaces.  Damage.	Viscoelastic FGM type with appropriate modifications for energy loss due to interfaces and geometric attenuation due to wave scattering by the fibers.  Damage.
Computational platform	ABAQUS	DYNA3D

## 5.2 Objectives and General Approach

Approximate numerical solutions that shed light on the impact behavior of thin woven fabric body armor systems have been successfully carried out [12].

Optimization of the ballistic performance of thick armor plates necessitates a more detailed effort. The objectives of this research are:

- (a) to identify the parameters that are significant to impact response of fibrous armor to ballistic threats.
- (b) to develop and implement an efficient finite element model that will include the viscoelastic character of the response, together with a realistic failure criteria of the armor.
- (c) to understand the propagation of stress waves and shock fronts in the armor to gain insight to the energy absorption mechanisms.

---

<sup>2</sup> In this case, the characteristic time depends on the wave propagation velocity

(d) to verify model predictions by using the experimental results obtained by the experimental mechanics team.

(e) to incorporate the gradient design concept in the finite element modeling and provide input for improving the gradient design.

(f) Animation of damage progression based on the finite element results

In this part of the study, exploratory steps were carried out to identify the needs. Initial, simplified analysis was performed. Our efforts have focused on two directions:

- experimental characterization of the composites in the dynamic range;
- preliminary computer simulations based on assumed data.

#### 5.2.1 Material Characterization

The energy absorption mechanisms in composite armors are:

- strain energy absorption, a large amount of the energy is absorbed as recoverable strain energy due to viscoelastic deformation of the armor
- energy dissipation, due to the viscoelastic character of both matrix and fibers. Additional dissipation is also expected to occur due to relative slipping at the matrix-fiber interface.
- geometric attenuation, due to wave scattering by the inhomogeneous microstructure of the composite (at high frequencies).
- damage development and accumulation, which depend in a complicated manner on material properties, macrogeometry and microstructure of the target and the penetrator.

Experimental work focusing on the explanation and quantification of these mechanisms, is given in Chapter 2.

The total energy dissipation also reflects the combined effect of:

- loading mode (i.e., in-plane tension or shear, bending or torsion),
- the macro and micro geometry of the structure,
- the state and geometry of interfaces,
- material properties of the polymeric matrix and fiber.

Because of the time dependent character of the material properties of the composites, it is necessary to completely characterize the behavior of the composites over a large range of frequencies (or, equivalently, time). High frequency behavior (or its short-time equivalent) is crucial for impact problems

since the event of impact is completed in a short time (milliseconds for low velocity impacts and microseconds for high velocity impacts). Both moduli and ability to dissipate energy must be characterized.

Simple creep/relaxation tests are not adequate, since short-time behavior is masked by transients due to machine limitations. The dynamic mechanical testing analysis (DMTA) is employed to characterize the behavior of the composites at frequencies from 0.1Hz to above 1000Hz. The measurement principle involves the application of oscillating strain over a designated temperature span at a number of pre-selected frequencies. In fact, most of the tests are performed at rather low frequencies. High frequency behavior (up to several kHz) is obtained by extrapolation based on the principle of time-temperature superposition. The range of 0.1-10,000Hz is sufficient for typical frequencies for low velocity impact.

In order to clarify the individual contributions of matrix, fibers and interface, and to optimize the geometry of the composite, it is important to characterize the matrix material, the fibers and the composite. Initial efforts have focused on the viscoelastic behavior of the matrix and unidirectional composites at different levels of fiber reinforcement.

### 5.2.2 Modeling

#### Viscoelastic Behavior of the Composite

Because of the complexity of the interaction between material properties and fiber architecture it is practically impossible to find a detailed solution of the dynamic equations in textile composites. Approximate solutions will be obtained at two different levels of approximation:

a) Approximation based on effective physical properties: The utilization of effective physical properties is the less complex method (e.g., [13]). The composite is considered as a homogeneous body with properties given by an appropriately weighted statistical average of the properties of the matrix and the fibers. Experience with such models has shown that they are accurate enough to predict at least macroscopic deformations and energy based quantities. The justification for the success of this method is based on the following argument. An inhomogeneous body, such as composites, can be imagined that consists of a collection of representative volume elements. Effective physical properties are useful if the average values of stress and strain vary slowly over a multiple of the characteristic size of the representative element. It is expected that there is an upper bound of frequency (or a lower bound in time, respectively) above which the accuracy of the effective properties method deteriorates. The lever of these bounds depend on the properties of the composite, such as density, Young's modulus, and the size of the representative characteristic length.

b) Approximation based on varying stress/strain fields: More complicated methods have been proposed that try to take into account the effects of rapidly varying strain/stress fields in fiber reinforced composites [14, 15, 16]. At this point

it practically impossible to obtain full numerical solutions using these methodologies for complex geometry problems on textile composites.

In this part of our work we have focused on the effective properties method. Due to the complex geometry of textile composites, it is very difficult to predict the macroscopic properties from the properties of the matrix and fibers, even under static conditions. The fabric geometry model [17] is an approximate method, which has been successful in estimating elastic moduli of the composite from the moduli of the matrix and fibers and the geometry of the reinforcement. A brief description of the method follows.

The first step in the geometric modeling of fabric reinforced composites is the identification of the orientation of the yarns in the composite. Once the fiber geometry is quantified, the results can be used together with the fiber and matrix properties to predict the mechanical properties of the composite system through a modified lamination theory. The assumption is made that each system of yarn can be represented by a comparable unidirectional lamina with an elastic stiffness matrix,  $[C]$ . Then the elastic stiffness matrix,  $[C']$ , of this fiber system in the structural system of the panel can be expressed as

$$[C'] = [T_e]^T [C] [T_e]$$

in which  $[T_e]$  is the transformation matrix, a function of fiber orientation.

It is noted that the static material properties of a unidirectional lamina,  $E_{11}$ ,  $E_{22}$ ,  $G_{12}$ , etc., can be easily obtained using the well established micromechanics relationships.

With the elastic stiffness matrix of each yarn system determined, the total elastic stiffness matrix,  $[C_c]$ , of the composite can be obtained by the equation

$$[C_c] = \sum K_i [C']_i$$

where  $k_i$  is the fractional volume of the  $i^{\text{th}}$  yarn system.

Current efforts in our laboratory include extending the FGM to viscoelastic materials. The key concept is that the averaging procedure must be now carried out in the frequency domain, in particular on the complex moduli of fibers and matrices<sup>3</sup>. The most difficult step is the inversion procedure, since it is frequently necessary to perform it numerically.

The extension of FGM to viscoelastic material is not trivial, because additional energy is dissipated on the matrix/fiber interfaces. Therefore, additional corrections to the theoretical solution maybe necessary. This phenomenon has

---

<sup>3</sup>A rigorous definition of the complex modulus for composites is given in the Appendix.



been observed in the literature in the context of damping properties of composites [18] but has not been quantified yet. This is an area we begin to address in our research. Also the contribution of the dispersive character of the wave propagation must be taken into account for the high velocity impact.

## Damage

Prediction of damage evolution in the modeling of impact is very important since damage evolution occurs in the same time scale with impact. Therefore, it is an integral part of the response of the composite.

The damage due to impact on composite materials is significantly different and more complex than in monolithic materials. The limited ability of the composites to undergo large deformations due to the brittleness of the fibers and a number of different types of failure, such as matrix cracking, delamination and fiber breakage are characteristic of the problem. The importance of the damage caused by impact on an armor plate is two-fold a) it can be viewed as an energy absorption mechanism (and therefore it should be somehow promoted if the main purpose of the armor is to stop the penetration), b) the residual properties of the armor depend on the extent of the damage (which should be minimized if the residual properties are important for the specific application).

Once failure occurs, material properties in the damaged area degenerate. The level of property loss is strongly related to the failure mechanisms. Different types of failure, such as matrix cracking, delamination and fiber breakage may appear, which influence the subsequent response of the structure [19]. There is need for:

- (anisotropic) failure criteria for the different damage mechanisms:
- a model for property degradation.

The knowledge of the property degradation is necessary for the prediction of the residual strength properties of the structure. The knowledge of residual properties is also important to predict the impact performance of the material that has been subjected to prior impact. This is crucial for body armor applications.

Unfortunately, little useful experimental data documenting damage due to impact on textile composite exists. Our future efforts will be guided from conclusions drawn from the experimental results of our study.

### 5.2.3 Impact Simulation

The continuum approach to model any energy transport phenomenon is based on the differential form of balance laws. The linear momentum and energy balance law in the local form can be represented by

$$\nabla \cdot \sigma + b = \rho a \quad (1)$$

$$\sigma \cdot \nabla \mathbf{v} + \nabla \cdot \mathbf{q} + r = \dot{E} \quad (2)$$

where  $\mathbf{v}$  is particle velocity,  $\mathbf{a}$  is particle acceleration,  $\sigma$  is the Cauchy stress tensor,  $\mathbf{q}$  the heat flux vector per current area,  $\rho$  the current density,  $E$  the internal energy and  $r$  the internal heat generation rate apart from stress power.

Since this research is focused on impact, stress waves and high frequency response, at this time scale heat conduction is not important and the second term of the equation drops out, thus becoming a point equation. This reduction does not impose any restrictions on our ability to examine heat generation due to plastic deformation, which may be important in some high velocity impact situations. Internal energy can then be regarded as an internal variable of the constitutive model and the energy balance equation as its rate equation.

The analytical solution of Equations (1) and (2) is intractable except for very simple material constitutive laws and geometry. Numerical or semi-empirical approaches are the usual course of action. In this project Finite Element Method is used to obtain the solution.

Based on our survey of the last 20 years of research on developing armor computational tool for high velocity impact analysis (see Appendix), DYNA3D was chosen as the software of choice<sup>4</sup>. DYNA3D is actually one of a package of software developed at Lawrence Livermore Laboratories in Livermore, CA (LLL). The initiative started in 1976 under Hallquist [9] and was geared towards weapons research. LLL is continually working to develop the code and the code has obtained wide acceptance in the industry as the state of art for analyzing Nonlinear Dynamic Solid Mechanics problems.

For a nonlinear dynamic situation, such as impact, the spatial discretization is carried out by variational principles and the temporal discretization by the finite difference formulation. The spatial discretization is performed by a global orthogonalization of the error in the differential equation with respect to an assumed basis:

$$\int \phi^T (\nabla \cdot \sigma + \mathbf{b} - \rho \mathbf{a}) dV = 0$$

which leads to the matrix form [5-1] given below:

$$\mathbf{M} \mathbf{a} + \mathbf{F}(\mathbf{x}, t) = \mathbf{P}(\mathbf{x}, t) \quad (3)$$

where  $\mathbf{M}$  is the lumped mass matrix,  $\mathbf{F}$  is the nodal force vector and  $\mathbf{P}$  is the body force vector. For path dependent material  $\mathbf{F}(\mathbf{x}, t)$  can be expressed by  $\mathbf{F}(\sigma, \mathbf{x})$ .

---

<sup>4</sup>We are also extensively using ABAQUS for low and medium velocity impact problems.

Implicit dissipative terms can be introduced by appropriate constitutive equations for:

$$\dot{\sigma} = \dot{\sigma}(\sigma, \nabla \mathbf{v}) \quad (4)$$

### 5.3 Representative Results

Application of FEM to dynamic cases requires special attention in two areas. The first aspect of the problem is to describe as faithfully as possible the essential features of the involved physical phenomena during impact. The other aspect of the problem relates to the selection and performance of the numerical tools and parameters, such as the mesh size, the solution method used, the constraints posed by computational platform, etc. The setup of the problem and selection of computational platform are essential to the success of the program. We have assembled a wide range of computational tools to attack the problem. For the low velocity impact problem, we employ ABAQUS running on an IBM/RISC6000 engineering workstation. To handle the high velocity impact problems, we have established DYNA and NIKE on a SUN/670 engineering workstation and on a CRAY-C90 supercomputer.

#### 5.3.1 Low Velocity Impact

Initial simulations have been focused on mesh geometry and solution tolerance optimization. Finite element calculations are based on the discretization of the geometry to finite size cells. It is desirable to increase the resolution of the discretization (e.g., the number of elements) as well as to decrease the time incrementation, in order to improve the accuracy of the solution and provide adequate information for transient effects. The computational size of the problem increases nonlinearly with resolution (i.e. approximately proportional to the third power of the number of elements) and is inverse proportional to the time step. Tolerances on convergence and step size have been appropriately selected.

Two sample calculations are included herein. First, we performed a comparison of low velocity impact response of both elastic and viscoelastic targets (with the same instantaneous modulus) in the absence of damage. A simple Prony series model was assumed for the viscoelastic response (see Appendix). Under the selected conditions the spherical projectile (here, it is assumed to be rigid), partially penetrates the plate and bounces back under the impulse produced by the springback of the plate. The amount of energy that remains in the plate (an elastic energy that causes the plate to vibrate) is negligible compared to the initial kinetic energy of the projectile. The penetration in the viscoelastic plate is slightly higher (+10%) and the maximum force on the projectile is lower (-10%), than in the purely elastic case. Also the time of contact is longer for the viscoelastic plate. When the penetrator bounces back, it has a kinetic energy approximately 20% lower than its initial value (before impact). The distributions of effective stress, shear stress and maximum principal stress are shown in Figures 76 to 78. The maximum effective stress at the time of impact is maximum below the surface under the penetrator; a typical result in computational simulations of impact. The maximum stress in the viscoelastic case is 10% less than the elastic one. The

amount of energy dissipated by the viscoelastic model depends strongly on the parameters of the model. Mainly, the characteristic relaxation times must be of the order of the time of contact in order to dissipate a significant portion of the kinetic energy of the projectile. In this sample calculation a relaxation time of 1 ms was used while the duration of impact was of the order of 5 seconds.

Attention was then focused on initial estimates of failure criteria. There are no experimentally verified failure criteria for composites under dynamic situations due to the anisotropic behavior and the plethora of damage and failure mechanisms in composites. A very crude approximation of a failure criterion can be an energy based one, and it has been used to observe the penetration process. A sequence of the deformed armor plate in time is shown in Figures 79 to 82.

The material properties used for the simulations are tabulated in Table 18.

**Table 18. Material Properties Used for Impact Simulation**

**Low Velocity Impact**

**Elastic Analysis**

**Projectile**

Rigid Mass

**Target**

$E=50 \text{ GPa}$ ,  $\nu=0.3$

$\rho=2 \times 10^{-9} \text{ kg/mm}^3$

**High Velocity Impact**

**Projectile**

$E=200 \text{ GPa}$

$\nu=0.3$

$\rho=8000 \text{ kg/m}^3$

**Elastic Analysis**

**Target**

$E=55 \text{ GPa}$

$\nu=0.25$

$\rho=1300 \text{ kg/m}^3$

**Elastic Plastic -Hydrodynamic Analysis**

$\rho=1300 \text{ kg/m}^3$

$\sigma_y=68.95 \text{ MPa}$

$G=22 \text{ GPa}$

$E_h=1 \times 10^5$  (hardening modulus)

$p_c=1 \times 10^3$  (cutoff pressure)

$K=36.7 \text{ GPa}$

Equation of State  $P=K\mu^2$

where  $\mu = \frac{\rho}{\rho_0} - 1$

**Viscoelastic Analysis**

**Projectile**

Rigid Mass

**Target**

$E=50 \text{ GPa}$ ,  $\nu=0.3$

$\rho=2 \times 10^{-9} \text{ kg/mm}^3$

Characteristic time 1 ms

$\frac{G_0}{G_\infty} = \frac{K_0}{K_\infty} = 0.8$

**Viscoelastic Analysis**

$\rho=1300 \text{ kg/m}^3$

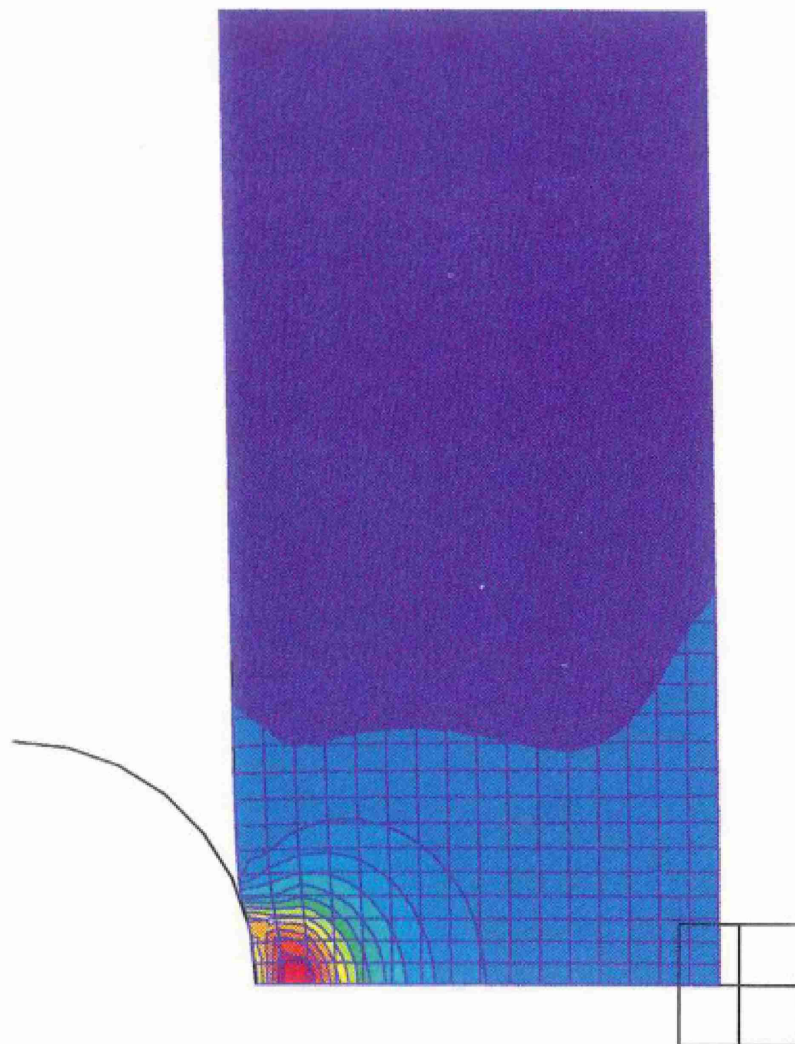
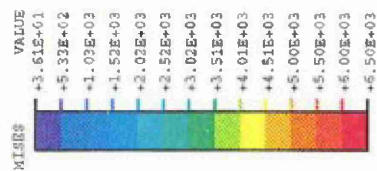
$K=36.67 \text{ GPa}$

$G_0=22 \text{ GPa}$

$G_\infty=17.6 \text{ GPa}$

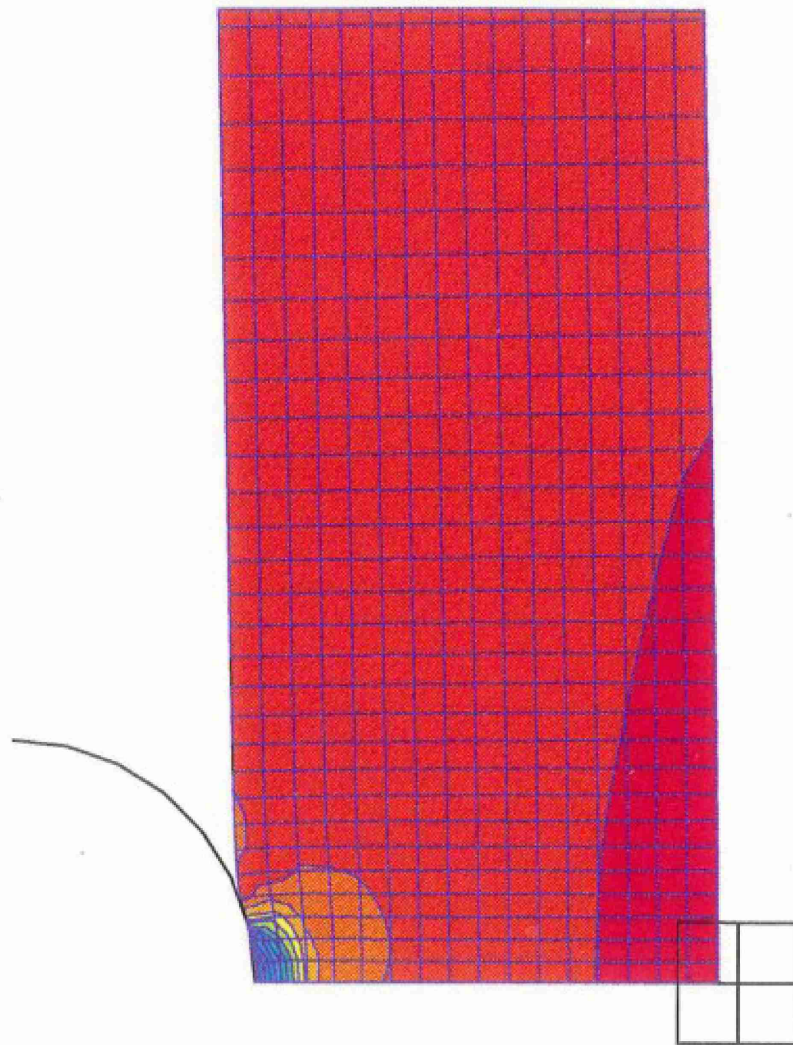
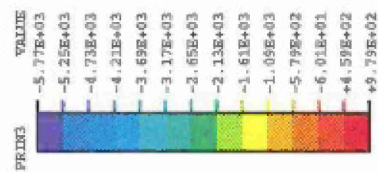
$\beta=100$

$G(t)=G_\infty+(G_0-G_\infty) e^{-\beta t}$



DISPLACEMENT MAGNIFICATION FACTOR = 1.00  
 TIME COMPLETED IN THIS STEP 5.074E-04 TOTAL ACCUMULATED TIME 5.074E-04  
 ABAQUS VERSION: 5.2-7 DATE: 10-JUN-93 TIME: 15:53:04 STEP 1 INCREMENT 100

Figure 76. Mises Stress (Mpa) Contours in the Elastic-Plastic Target at 0.5074 ms after Impact.



2  
 3  
 1  
 DISPLACEMENT MAGNIFICATION FACTOR = 1.00  
 TIME COMPLETED IN THIS STEP 5.074E-04 TOTAL ACCUMULATED TIME 5.074E-04  
 ABAQUS VERSION: 5.2-7 DATE: 10-JUN-93 TIME: 15:53:04 STEP 1 INCREMENT 100

Figure 77. Principal Stress (Mpa) Contours in the Elastic-Plastic Target at 0.5074 ms after Impact.



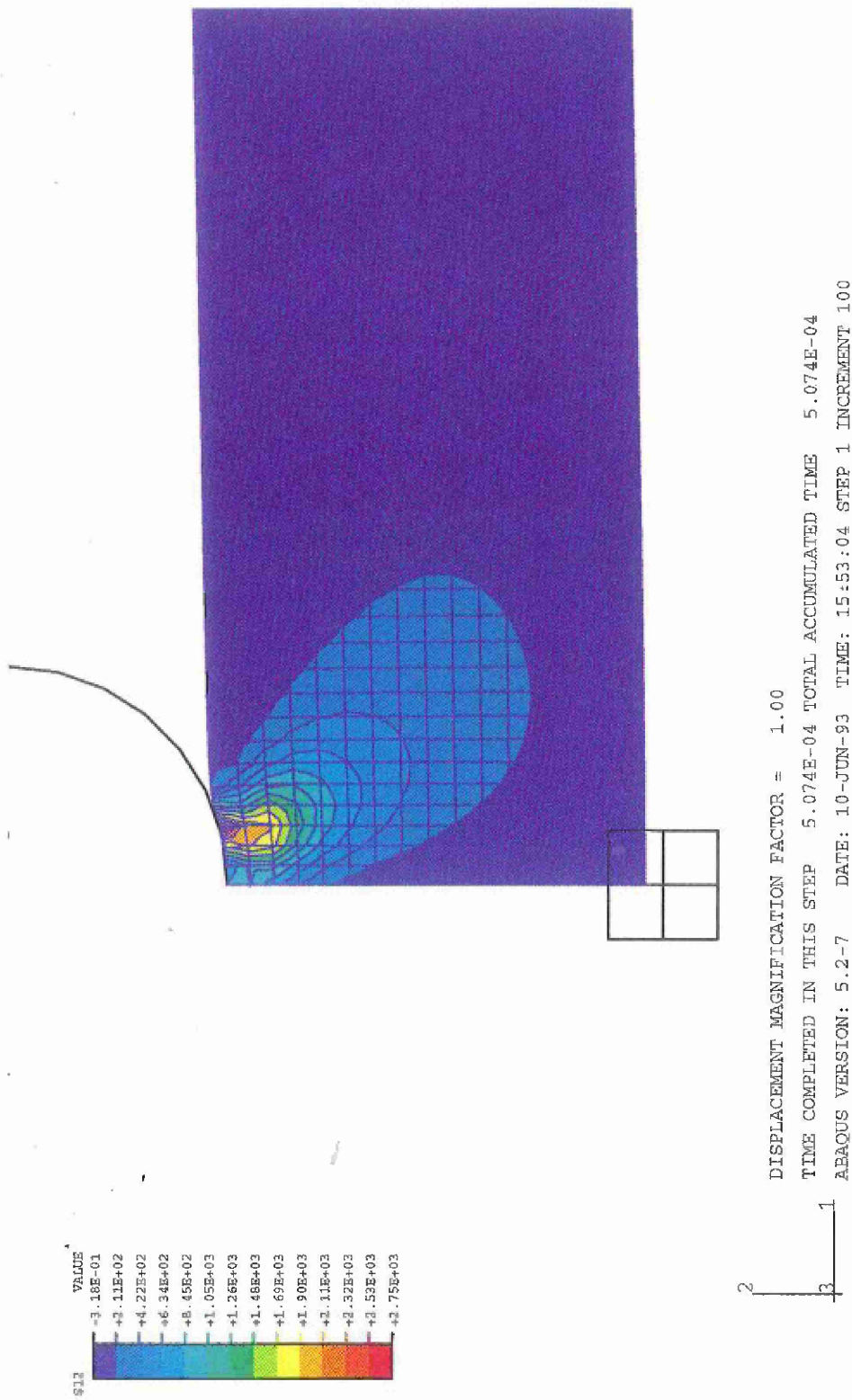


Figure 78. Shear Stress (MPa) Contours in the Elastic-Plastic Target at 0.5074 ms after Impact.



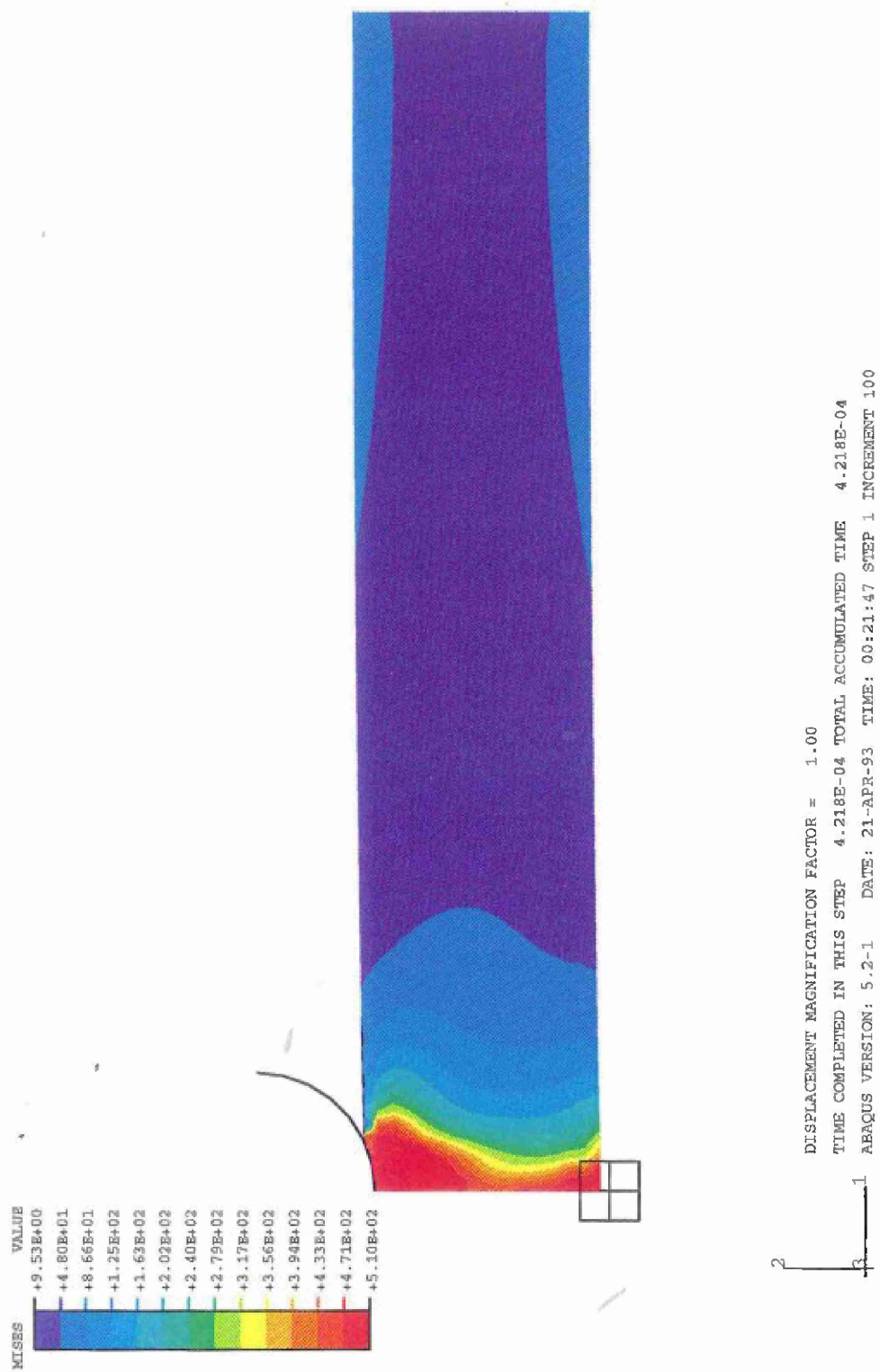


Figure 79. Mises Stress (MPa) Contours in the Elastic-Plastic Target at 0.4218 ms After Impact

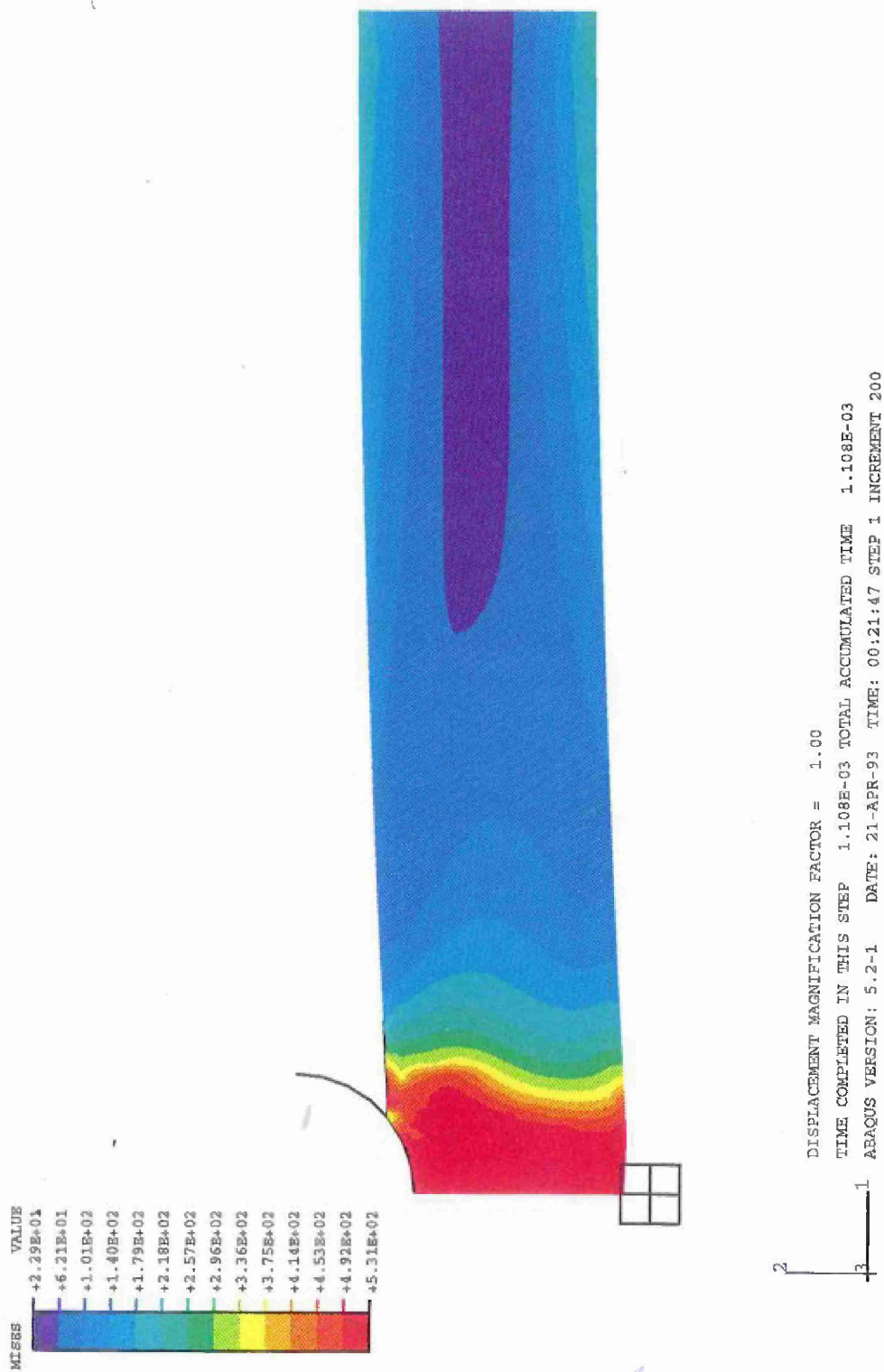


Figure 80. Mises Stress (MPa) Contours in the Elastic-Plastic Target at 1.108 ms after Impact

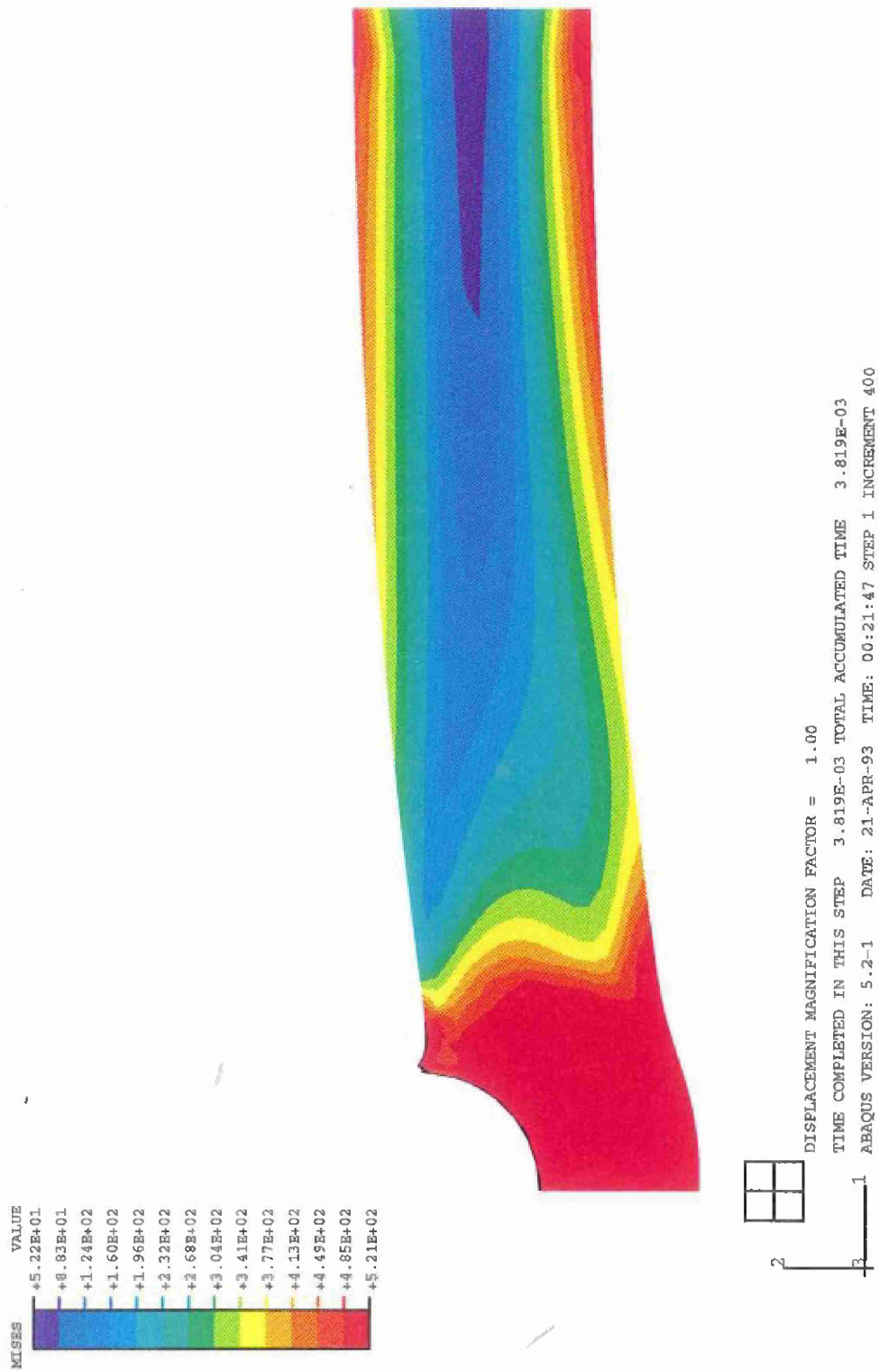


Figure 81. Mises Stress (MPa) Contours in the Elastic-Plastic Target at 3.819 ms after Impact

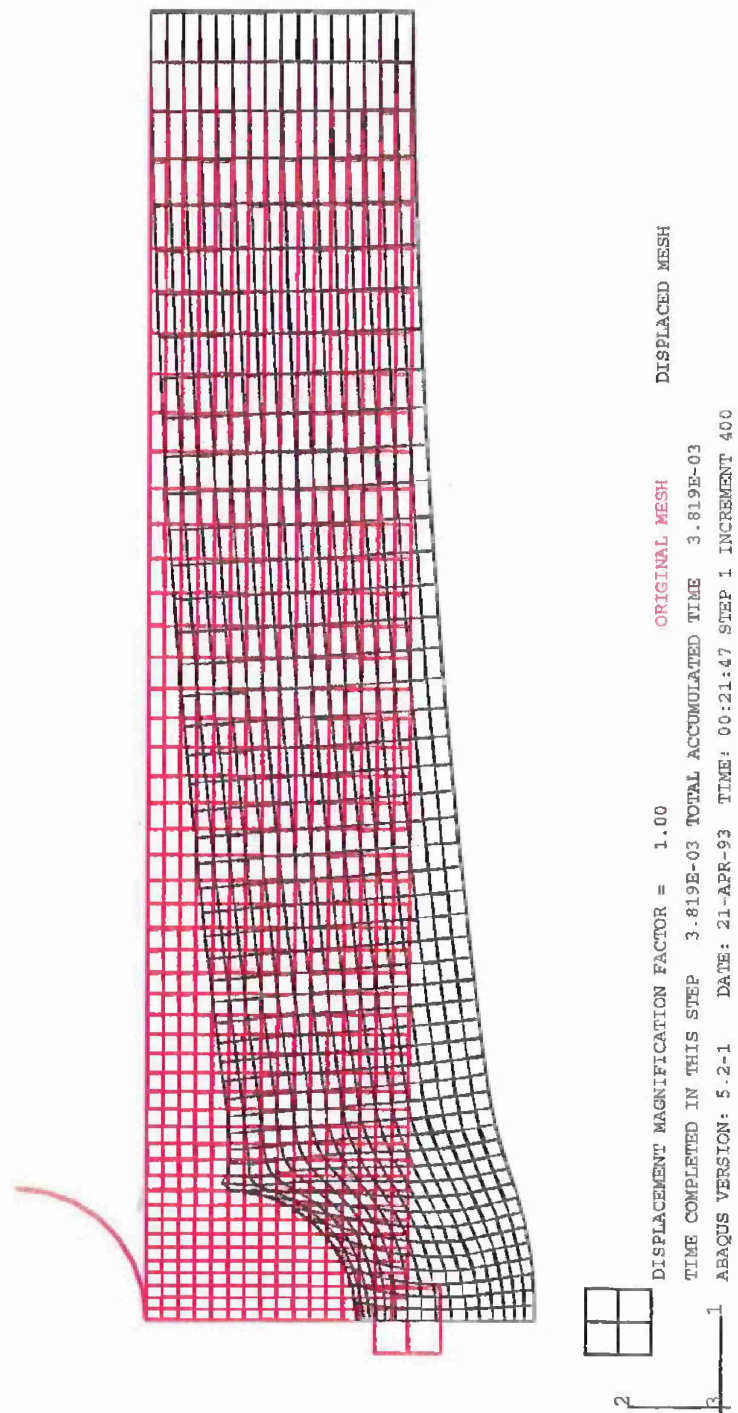


Figure 82. Displaced Mesh at 3.819 ms after Impact

### 5.3.2 High Velocity Impact

High velocity impact is a very localized phenomenon. The boundary conditions have little or no effect on the response or the damage progression. The projectile tends to push the material immediately in front of it and the event takes place in such a short duration that there is very little propagation of the disturbance laterally. As a result, high pressures build in front of the projectile, increasing the density and often playing a significant role in the failure. Since the sequence of events leading to failure is almost impossible to observe and subsequently incorporate in the computational scheme, simpler failure criteria are frequently employed. A good criterion may not represent the actual sequence of events leading to failure; however, it should give a reasonable approximation of the absorbed energy and the post damage condition of the projectile and the target. The simplest criterion is pressure cutoff, which assumes that the material fails instantaneously if the hydrostatic pressure reaches a arbitrary tensile value. For metals it gives reasonably good results. Finding an equivalent damage model for textile composites is one of our goals.

Our initial goal is to optimize the mesh size. We have presented here four examples. The first two examples are simulations of transverse impact with a steel fragment simulation projectile (FSP) at the center of a 6 in. circular composite panel. In example 1 the target is assumed to be elastic and in example 2 it is assumed to be viscoelastic. A sequence of the deformation profiles and the equivalent stress state in the target are presented in Figures 83 to 85, respectively. Figures 86 to 88 represent the equivalent response to impact on a viscoelastic armor. The viscoelastic behavior of the material is assumed to be of the form

$$G(t) = G_0 + (G_\infty - G_0) e^{-\beta t}$$

The decay constant  $\beta$  is of the order of  $10^6$  (i.e., the relaxation time is  $1\mu\text{sec}$ ; compare to impact duration of  $\sim 5\mu\text{sec}$ ). We see that under such circumstances, during deformation the stresses in viscoelastic material is 8 % less than purely elastic material.

Elastic Plate --- DYNA2D Analysis  
time= 0.20000E-05 fringes of effective stress  
dsf = 0.50000E+01



minval= 0.00E+00  
maxval= 0.64E+01  
fringe levels

a= 0.00E+00  
b= 0.12E+00  
c= 0.25E+00  
d= 0.38E+00  
e= 0.50E+00



Figure 83. Effective Stress Contours (GPa) on an Elastic Composite Target 2μS after Impact with a Steel FSP



Elastic Plate --- DYNA2D Analysis  
time= 0.40000E-05 fringes of effective stress  
dsf = 0.50000E+01



minval= 0.00E+00  
maxval= 0.32E+01  
fringe levels

a= 0.00E+00  
b= 0.12E+00  
c= 0.25E+00  
d= 0.38E+00  
e= 0.50E+00

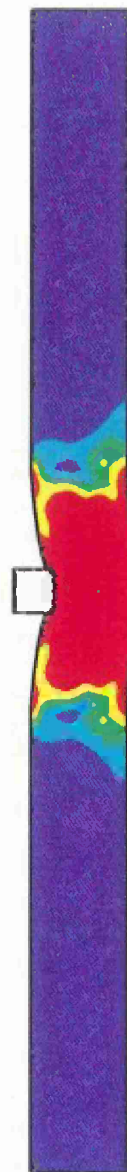


Figure 84. Effective Stress Contours (GPa) on an Elastic Composite Target 4  $\mu$ s after Impact with a Steel FSP

Elastic Plate --- DYNA2D Analysis

time= 0.60000E-05 fringes of effective stress

dsf = 0.50000E+01

minval= 0.00E+00

maxval= 0.11E+01

fringe levels

a= 0.00E+00

b= 0.12E+00

c= 0.25E+00

d= 0.38E+00

e= 0.50E+00

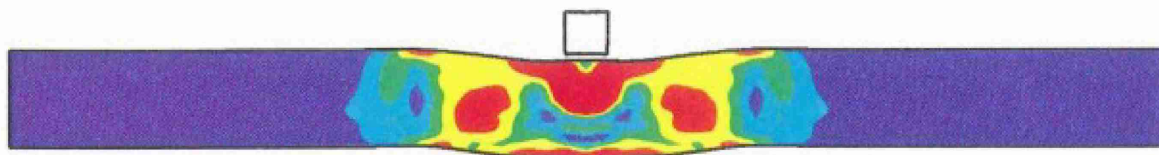


Figure 85. Effective Stress Contours (GPa) on an Elastic Composite Target  
6 $\mu$ S After Impact With a Steel FSP



Viscoelastic Plate --- DYNA2D Analys  
time= 0.20000E-05 fringes of effective stress  
dsf = 0.50000E+01

minval= 0.00E+00  
maxval= 0.59E+01  
fringe levels

a= 0.00E+00  
b= 0.12E+00  
c= 0.25E+00  
d= 0.38E+00  
e= 0.50E+00

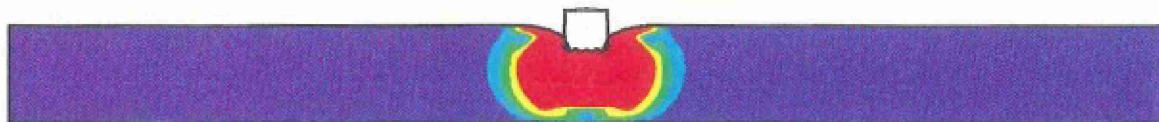


Figure 86. Effective Stress Contours (GPa) on a Visco-Elastic Composite Target  
2 $\mu$ S After Impact With a Steel FSP

Viscoelastic Plate --- DYNA2D Analys  
time= 0.40000E-05 fringes of effective stress  
dsf = 0.50000E+01

minval= 0.00E+00  
maxval= 0.33E+01  
fringe levels

a= 0.00E+00  
b= 0.12E+00  
c= 0.25E+00  
d= 0.38E+00  
e= 0.50E+00

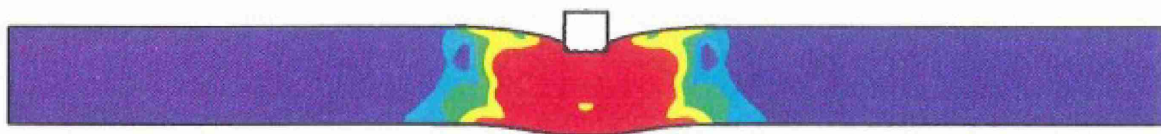


Figure 87. Effective Stress Contours (GPa) on a Visco-Elastic Composite Target  
4 $\mu$ S After Impact With a Steel FSP

Viscoelastic Plate --- DYNA2D Analys  
time= 0.60000E-05 fringes of effective stress  
dsf = 0.50000E+01

minval= 0.00E+00  
maxval= 0.12E+01  
fringe levels

a= 0.00E+00  
b= 0.12E+00  
c= 0.25E+00  
d= 0.38E+00  
e= 0.50E+00

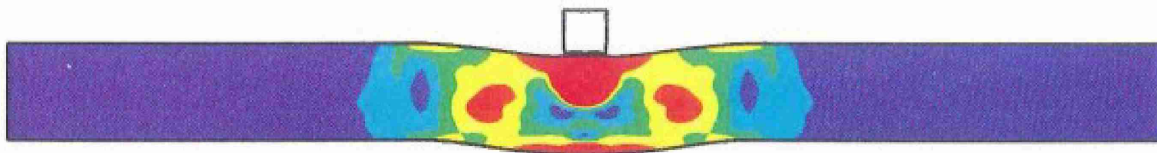


Figure 88. Effective Stress Contours (GPa) on a Visco-Elastic Composite Target  
6 $\mu$ S After Impact With a Steel FSP

From the results we observe that tremendous stresses build up in front of the impactor within the first few micro-seconds of impact. The magnitude of stresses are larger than typical strength values by at least one thousand times. The large size of these stresses is partially due to a high hydrostatic pressure built below the indenter. Failure is very likely to occur. In this early stage, the response is characterized from the material immediately in front of the projectile. The effect of high stresses and pressure on the matrix and the fiber is now experimentally investigated. When the results are known we will incorporate them in our finite element model. In the third example we investigate a elastic-linear strain hardening material and incorporate a pressure based failure criteria. We apply a tensile pressure cutoff, such that if the hydrostatic tension is larger than the cutoff pressure, the material fails. The material is allowed to pressure harden to show the extremely high stresses that develop in high velocity impact. The deformation profile and the equivalent stress contours are presented in Figures 90 to 92. Finally in our last example we simulate the impact of a viscoelastic composite panel by a three-dimensional spherical projectile. The displacements at selected periods of the event are presented in Figures 93 to 95.

It should be noted that impact is a very high strain rate phenomenon and little is known of composite behavior at such strain rates. In general the resin (matrix) should be assumed to have significant rate dependence while the rate dependence of fibers is little for carbon and more significant for glass and Kevlar.

# E-P Hydrodynamic Plate

time= 0.10000E-04 fringes of effective stress

dsf = 0.10000E+01

minval= 0.22E-11  
maxval= 0.69E-01  
fringe levels

a= 0.12E-01

b= 0.23E-01

c= 0.34E-01

d= 0.46E-01

e= 0.58E-01



Figure 89. Effective Stress Contours (GPa) on an Elastic Plastic Composite With A Pressure Cutoff Failure, 10 $\mu$ S After Impact With a Steel FSP

E-P Hydrodynamic Plate

time= 0.15000E-04 fringes of effective stress

dsf = 0.10000E+01

minval= 0.61E-04

maxval= 0.69E-01

fringe levels

a= 0.12E-01

b= 0.23E-01

c= 0.35E-01

d= 0.46E-01

e= 0.58E-01



Figure 90. Effective Stress Contours (GPa) on an Elastic Plastic Composite With A Pressure Cutoff Failure, 15 $\mu$ S After Impact With a Steel FSP

E-P Hydrodynamic Plate

time= 0.20000E-04 fringes of effective stress

dsf = 0.10000E+01



minval= 0.87E-03  
maxval= 0.69E-01  
fringe levels

a= 0.12E-01

b= 0.24E-01

c= 0.35E-01

d= 0.46E-01

e= 0.58E-01



Figure 91. Effective Stress Contours (GPa) on an Elastic Plastic Composite With A Pressure Cutoff Failure, 20 $\mu$ S After Impact With a Steel FSP

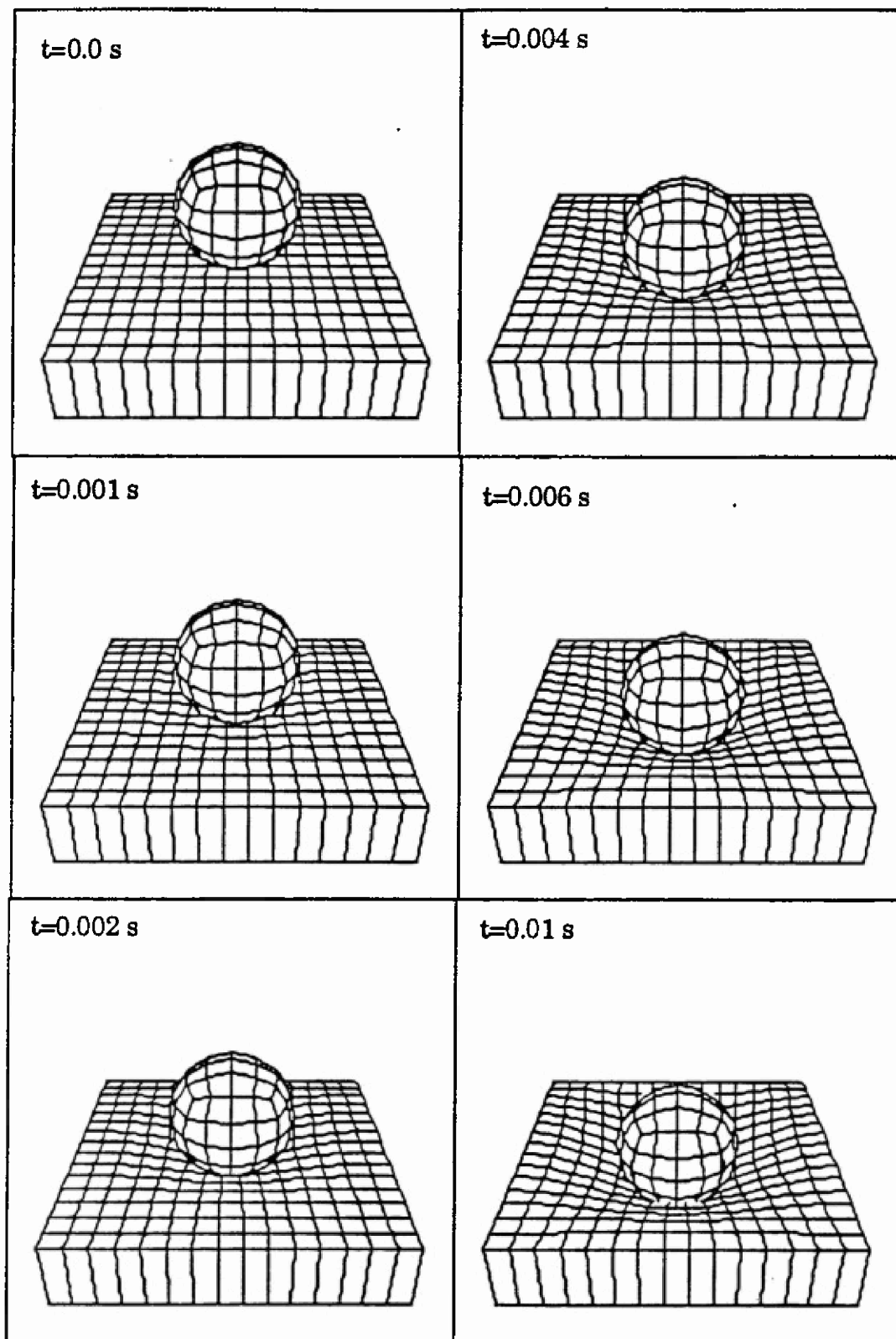


**Figure 92. Displacement of a composite target upon a impact with a spherical steel ball at different time intervals**



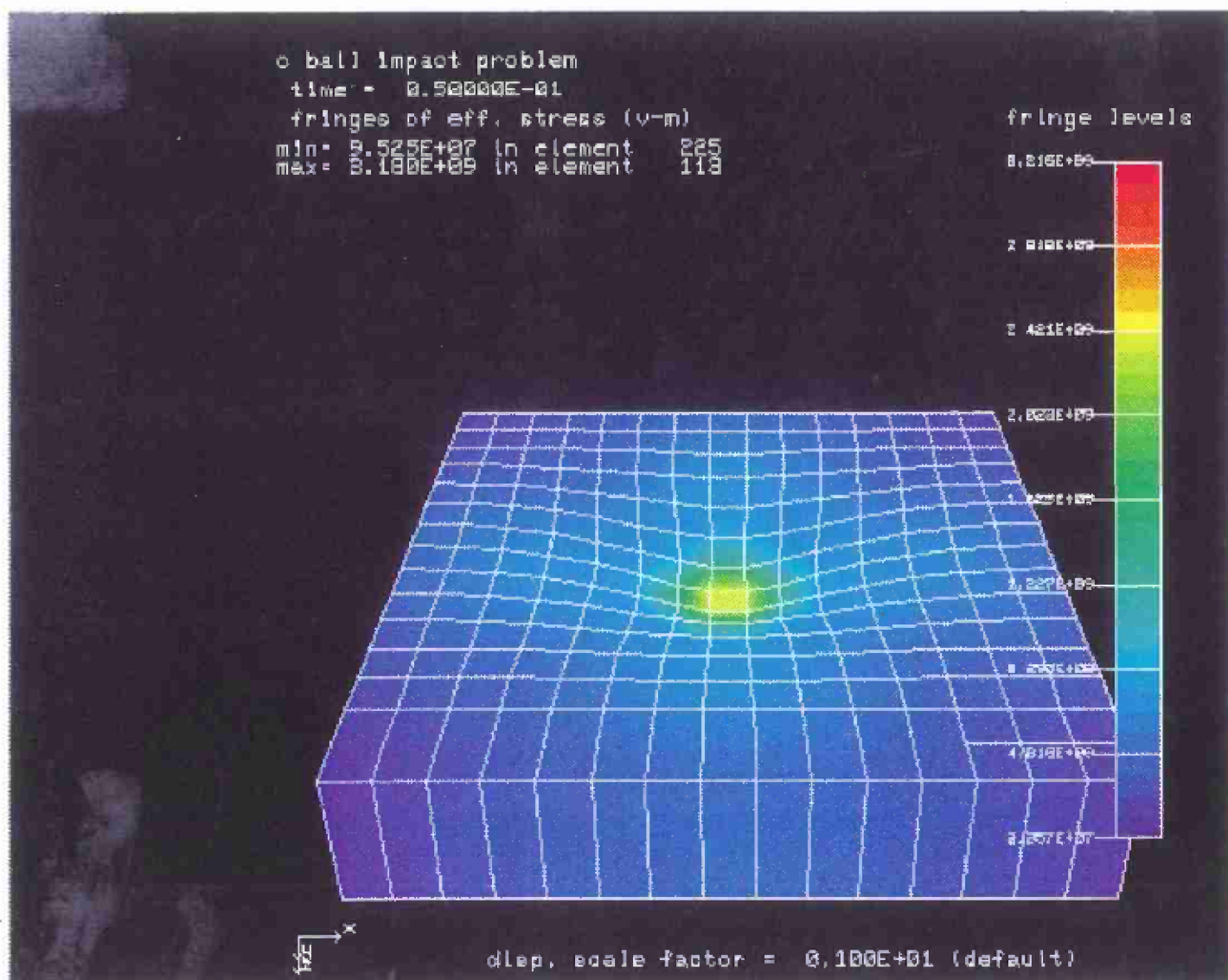


Figure 93. Effective Stress Contours (Pa) on a Viscoelastic Composite 50 ms After Impact with a Spherical Steel Ball

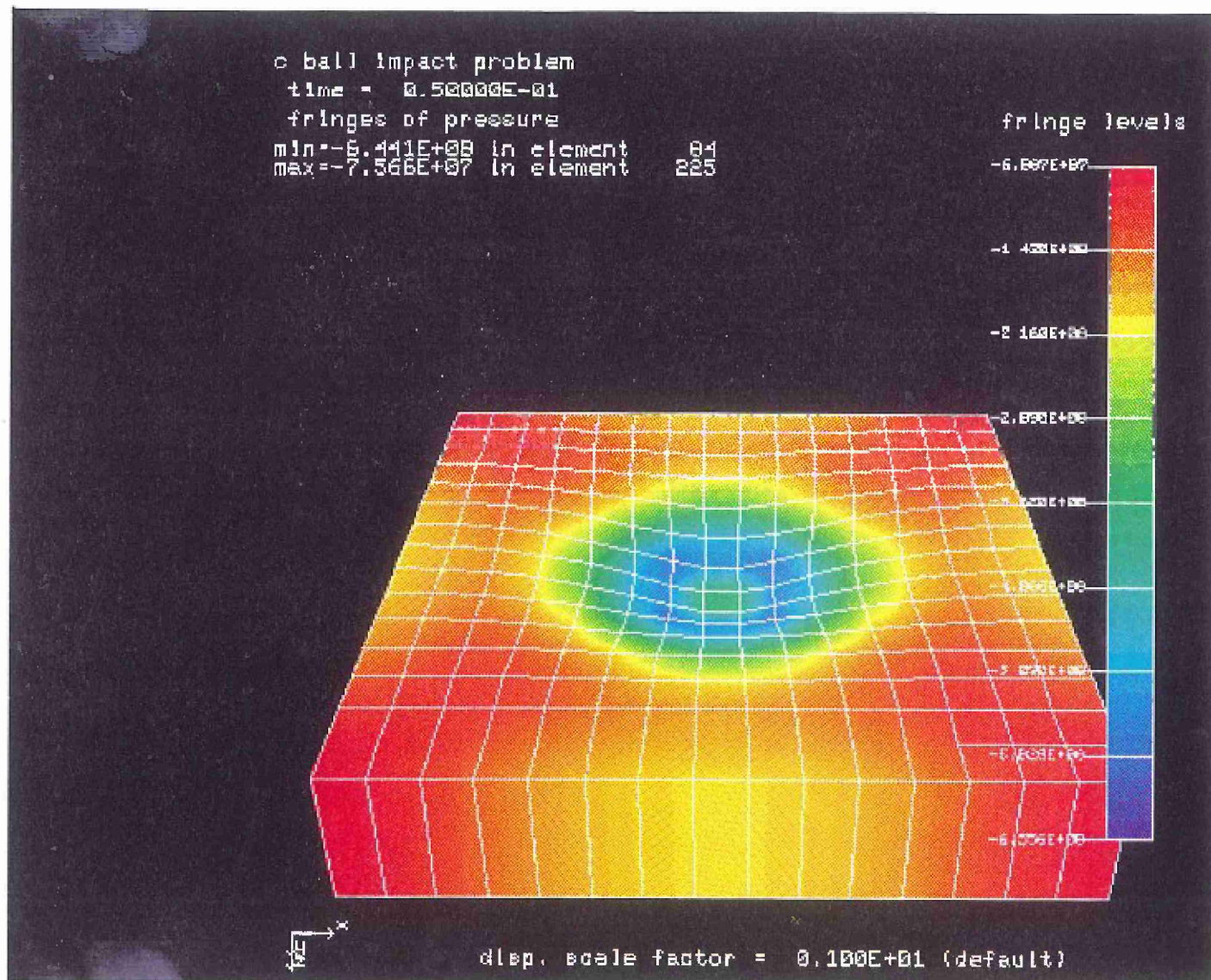


Figure 94. Hydrostatic Stress Contours (Pa) on a Viscoelastic Composite 50 ms After Impact with a Spherical Steel Ball



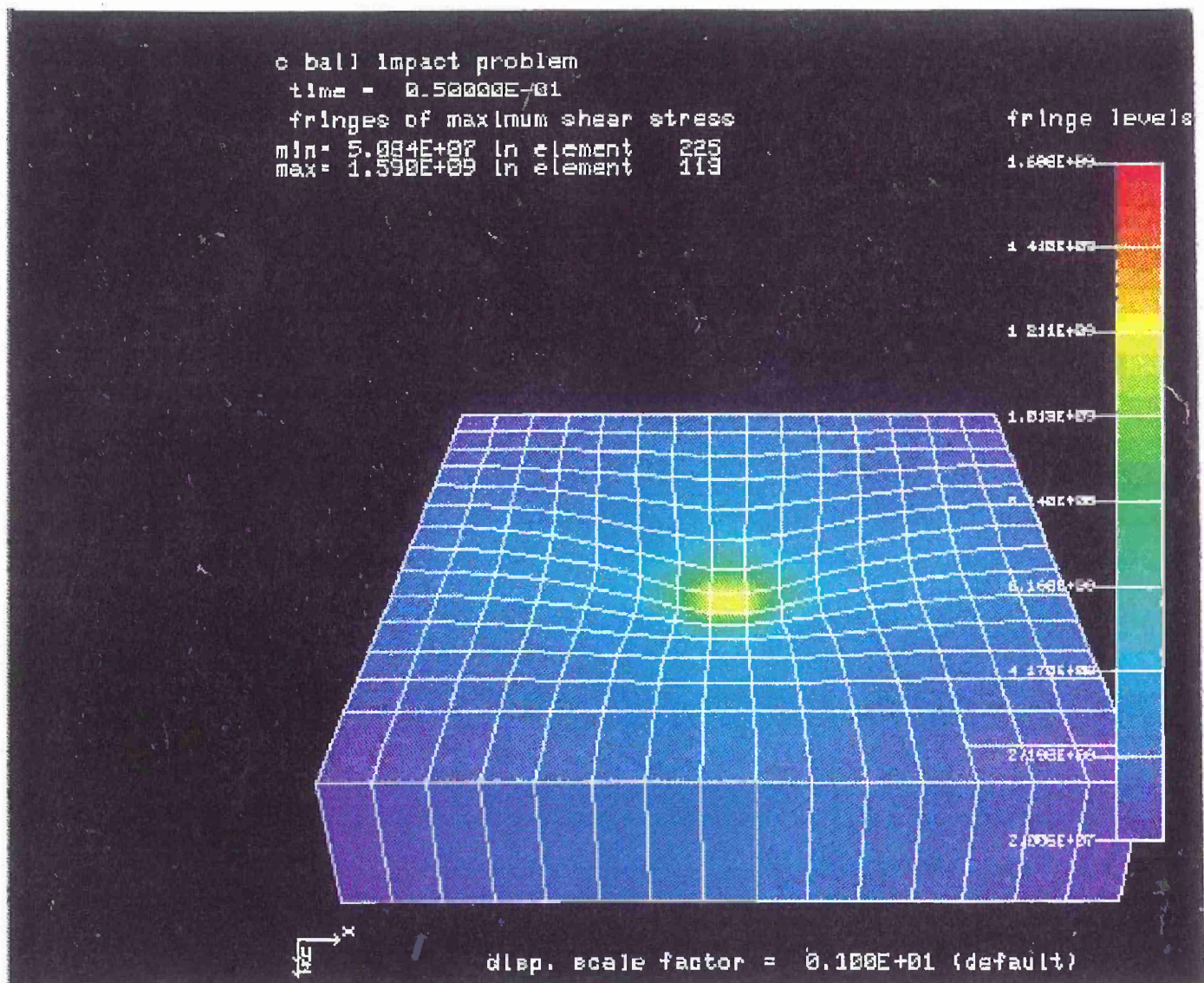


Figure 95. Shear Stress Contours (Pa) on a Viscoelastic Composite 50 ms After Impact with a Spherical Steel Ball

#### 5.4 Future Efforts

Our initial efforts have demonstrated that we are able to carry out numerical simulations of impact on composites. In order to be able to compare numerical predictions with experimental findings, we need to develop a complete anisotropic viscoelastic model with damage for textile composites. Such a model does not exist today.

In the preliminary part of our work we have identified the theoretical framework that can predict the time-dependent behavior of anisotropic composites and have identified the set of material properties that must be determined experimentally in order to complete the model. A summary of the proposed framework is shown in Figure 96. Briefly, based on experimental observations of the dynamic behavior of the neat matrix and unidirectional composites, we will obtain the viscoelastic properties necessary to build an approximate model capable of predicting the viscoelastic properties of textile composites. Suitable corrections depicting the role of interfaces in the energy dissipation process may be necessary.

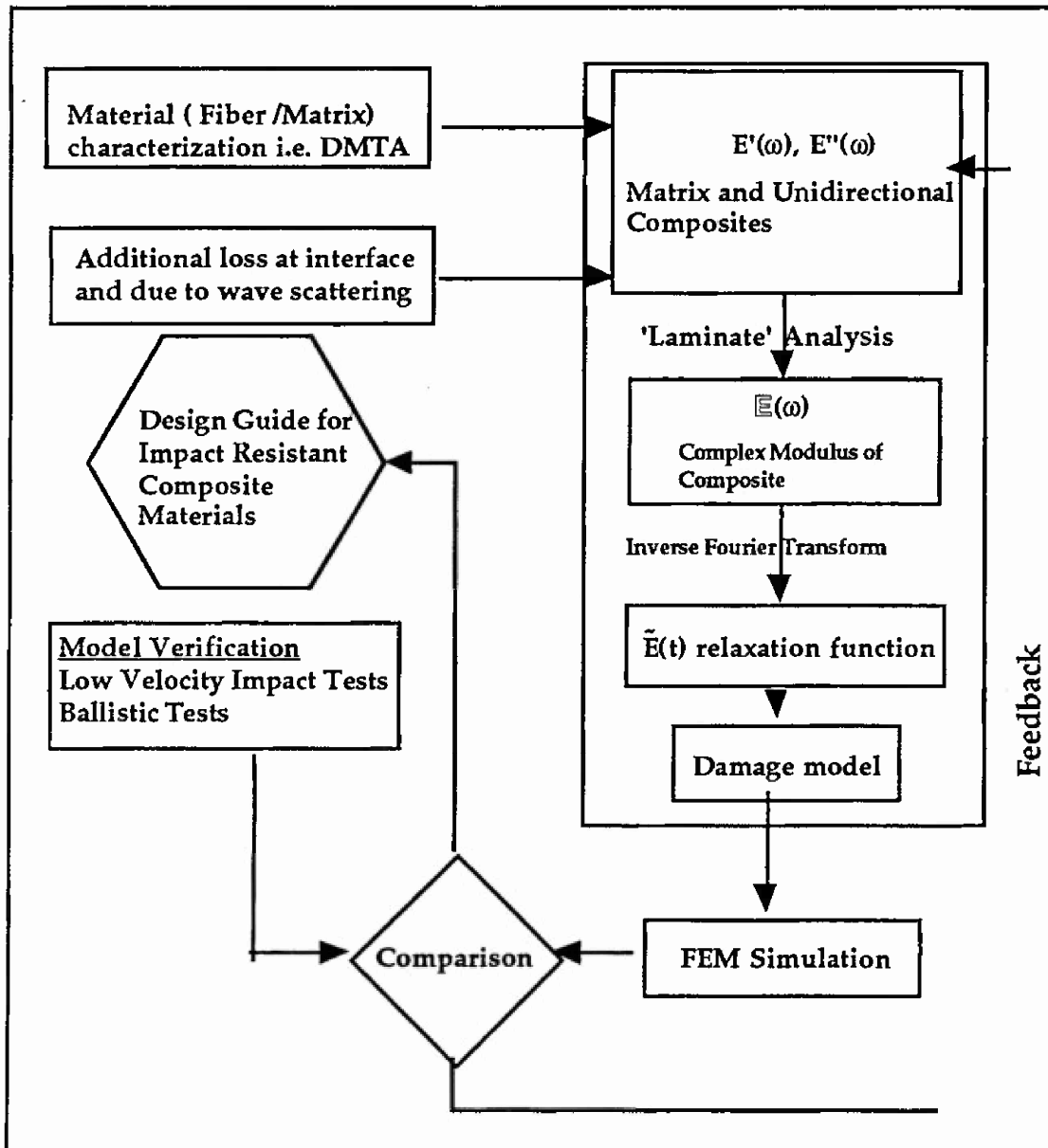
We have started implementing a version of proposed anisotropic viscoelastic model in a finite element code. We expect to have a working version of such model during the next year.

Also, a major effort will be focused on the development of appropriate damage models for textile composites. Guided by the experimental findings from SEM observations of ballistically penetrated specimens, we shall propose approximate damage criteria with the aim of predicting the different failure mechanisms dominating the penetration of textile composites. Of primary importance are: a) matrix cracking, b) fiber debonding, and c) fiber breakage due to the stresses encountered by the composite armor upon penetration. An important aspect of our future work will be the prediction of the properties of partially damaged material. Efforts towards such models will be incorporated in the finite element model.

Based on numerical calculations and related experimental results, we will be able to:

- use data visualization techniques to understand the results of numerical calculations
- relate the energy absorbed with the viscoelastic properties of the composites
- relate the performance of the armor with processing parameters
- provide input in establishing design criteria for viscoelastic armor
- provide guidance for the gradient design concept selection.

## Modeling Impact Behavior of Viscoelastic Composite Materials



### Expected Results

1. Relation of energy absorption to processing parameters.
2. Relation of energy absorption to viscoelastic moduli.
3. Visualization of damage development in viscoelastic armor.
4. Provide guidance for gradient design concept selection.
5. Provide input in establishing design criteria for viscoelastic armor.

**Figure 96. Flow Chart of Future Experimental/Modeling Work**

## References

1. J. N. Chu, "Viscoelastic Properties of 3-D Braided PEEK/Graphite Composites", Ph.D. Thesis, Drexel University, 1992.
2. T. Murayama, Dynamic Mechanical Analysis of Polymeric Material, Elsevier Scientific Publishing Co., Amsterdam, 1978.
3. T. Y. Soong, "Characterizing HDPE Geomembranes by Dynamic Mechanical Analysis", Master Thesis, Drexel University.
4. DuPont Instruments, "TA Instrument Handout".
5. DuPont Instruments, "DuPont 983 Dynamic Mechanical Analysis System".
6. J. W. Song and J. E. Ward, "Fiber Orientation Effect on Dynamic Mechanical and Ballistic Properties of Spectrashield® Composites" in Natick Technical Report NATICK TR-90/039, August, 1990.
7. V. Krishnamurthy, "RF Plasma Modification of Glass Fiber - Polyphenylene Sulfide Interface", Ph. D. Thesis, Drexel University, Philadelphia, PA 1988.
8. L. S. Penn and S. M. Lee, Journal of Fiber Science and Technology, vol. 17, 1982, pp. 91-97.
9. L. S. Penn, F. A. Bystry and H. J. Marchionni, Polymer Composites, vol. 4, 1983, pp. 26-31.
10. L. S. Penn and S. M. Lee, Journal of Composites Technology and Research, JCTRER, Vol., No. 1, Spring 1989, pp. 23-30.
11. G. Rostami, "Surface Modification, Interfacial testing and Matrix Processing of Fiber Reinforced Composites" Ph. D. Thesis, Drexel University, Philadelphia, PA 1988.
12. Cunniff P.M., "Numerical Simulations of the Ballistic Impact of Textile Structures", Technical Report, Natick/TR-92/044., 1992.
13. Hashin Z., et al., "Static and Viscoelastic Behavior of Fiber reinforced Materials and Structures", USAAVLABS Technical Report 68-70.
14. Achenbach J.D., "Theory of Elasticity with Microstructure for Directionally Reinforced Composites", Springer, New York, 1975.
15. Aboudi J., "The Effective Thermomechanical Behavior Of Inelastic Fiber-Reinforced Materials", *Int. J., Eng. Sci.*, **23**, 773-787, 1985.
16. Murakami H., et al., "Development of a Mixture Model for Non-linear Wave Propagation in Fiber-Reinforced Composites", *Int. J. Solids Str.* **29**, 14, 1919-1937, 1992.

17. Liao, David, "Elastic Behavior of 3-D Braided Composite Under Compressive Loading", Ph.D. Dissertation, Drexel University (1990).
18. Adams R. D., "Damping Properties Analysis of Composites", in *ASM Handbook of Engineered Materials*, Vol. 1 "Composites", 1990.
19. Abrate S., "Impact on Laminated Composite Materials", *Appl. Mech. Rev.*, 44, 4, p. 155, 1991.

## APPENDICES

A. Definition Of Complex Modulus

B. Literature Review on Impact Response of Composites

C. Sample Input and Output Files of DYNA3D



## Appendix A. Definition Of Complex Modulus

The definition of the complex modulus is given here. For a linear viscoelastic material the stress-strain relation is given by the hereditary integral:

$$\sigma_{ij}(t) = E_{ijkl}(0)\varepsilon_{ij}(t) + \int_0^t E_{ijkl}(t-\tau)\dot{\varepsilon}_{ij}(\tau)d\tau$$

where  $E_{ijkl}(t)$  is the relaxation moduli tensor and  $E_{ijkl}(0)$  is the instantaneous elasticity tensor. The Fourier transform of this relation gives:

$$\sigma_{ij}(j\omega) = \mathbb{E}_{ijkl}(j\omega)\varepsilon_{kl}(j\omega)$$

where  $\mathbb{E}_{ijkl}(j\omega)$  is the complex (or operational) modulus of the material. The real part of the complex modulus is related to stiffness and is called storage modulus. The imaginary part essentially represents the ability of the material to dissipate energy and it is termed loss modulus.

The complex modulus is related to the Fourier transform of the relaxation moduli tensor  $E_{ijkl}(j\omega)$ :

$$\mathbb{E}_{ijkl}(j\omega) = j\omega E_{ijkl}(j\omega)$$

The inverse Fourier Transform is necessary to recover the relaxation moduli tensor from the complex modulus. The complex modulus can be calculated from DMA measurements. In a bending configuration such as that employed in our experimental work two components of the modulus can be probed\*, namely  $E_{1111}$  and  $E_{1122}$  (1 is the direction along the axis of the specimen and 2 is the through thickness direction). It is obvious that  $E_{1111}$  reflects a strong contribution of the fibers while  $E_{1122}$  depends strongly on the matrix behavior ( $E_{1111} > E_{1122}$ ).

Proper selection of specimen geometry is necessary in order to identify independently these two components. One must be very careful because usual suggested dimensions from the DMA manufacturer refer to isotropic materials (metals, polymers etc.) in which  $E_{1111}$  and  $E_{1122}$  are of the same order of magnitude.

The variation of each of the components of the relaxation moduli tensor, can be approximated by an series of exponentials (Prony series):

$$E(t) = E_r + \sum_{j=1}^n E_j \exp\left(-\frac{t}{\tau_j}\right)$$

---

\* More accurately, the 1111 and 1122 components of the inverse of the complex modulus i.e.,  $\mathbb{E}^{-1}$ .

where  $E_r$  is the relaxed part, and  $\tau_j$  are the characteristic relaxation times. Then the corresponding component of the complex modulus is given by

$$\mathbb{E} = E_r + \sum_{j=1}^n \frac{E_j \omega^2 \tau^2}{1 + \omega^2 \tau^2} + j \sum_{j=1}^n \frac{E_j \omega \tau}{1 + \omega^2 \tau^2}$$

An Arrhenius equation or the WLF equation can be used to take advantage of the time temperature equivalence in characterizing the viscoelastic material.\*\*

Also, attention must be paid to the interpretation of the results of the DMA. The typical DMA set up provides a flexural modulus. The correspondence between the flexural modulus and the axial (tensile) modulus depends on the geometry. Deviations can be significant if the characteristic microstructural length of the composite (e.g., the unit cell) is large compared to the thickness of the specimen.

---

\*\* Margaritis, G. and McGarry G. "Viscoelastic Analysis of Thin Polymer Films in Electronic Packages." *Sampe Quarterly*, Vol 24, No. 3, pp. 2-8, 1993.

## Appendix B. Literature Review on Impact Response of Composites

### 1 AST

AUTHOR: Jih, C. J.; Sun, C. T.

TITLE: Prediction of delamination in composite laminates subjected to low velocity impact

SOURCE: Journal of Composite Materials (ISSN 0021-9983)  
v27 no7 p684-701 '93

CONTAINS: bibliography; diagrams

### SUBJECTS COVERED:

Delamination

### 2 AST

AUTHOR: Green, E. Rhian

TITLE: Response of a fiber composite laminate to a time-varying surface line load

SOURCE: Journal of Applied Mechanics (ISSN 0021-8936) v60  
p217-21 March '93

### SUBJECTS COVERED:

Fiber composites/Stresses

Impact

### 3 AST

AUTHOR: Carman, G. P.; Lesko, J. J.; Reifsnider, K. L.

TITLE: Micromechanical model of composite materials subjected to ball indentation

SOURCE: Journal of Composite Materials (ISSN 0021-9983)  
v27 no3 p303-29 '93

CONTAINS: bibliography; illustration(s); diagrams

### SUBJECTS COVERED:

Interfacial stresses

Composite materials/Mathematical models

Impact tests

### 4 AST

AUTHOR: Lee, S-W. R.; Sun, C. T.

TITLE: A quasi-static penetration model for composite laminates

SOURCE: Journal of Composite Materials (ISSN 0021-9983)  
v27 no3 p251-71 '93

CONTAINS: bibliography; illustration(s); diagrams

### SUBJECTS COVERED:

Laminates/Failure

Impact tests

### 5 AST

AUTHOR: Rajalingam, P.; Baker, W. E.

**TITLE:** The role of functional polymers in ground rubber tire-polyethylene composite

**SOURCE:** Rubber Chemistry and Technology (ISSN 0035-9475)

v65 p908-16 November/December '92

**CONTAINS:** bibliography

**SUBJECTS COVERED:**

Impact tests

Tires, Rubber/Recycling

Polymer matrix composites/Strength

**6 AST**

**AUTHOR:** Hamstad, M. A.; Whittaker, J. W.; Brosey, W. D.

**TITLE:** Correlation of residual strength with acoustic emission from impact-damaged composite structures under constant biaxial load

**SOURCE:** Journal of Composite Materials (ISSN 0021-9983)

v26 no15 p2307-28 '92

**CONTAINS:** bibliography; illustration(s); diagrams

**SUBJECTS COVERED:**

Impact tests

Composite materials/Testing

Acoustic emission testing

Residual stress

**7 AST**

**AUTHOR:** Kim, Chun-Gon; Jun, Eui-Jin

**TITLE:** Impact resistance of composite laminated sandwich plates

**SOURCE:** Journal of Composite Materials (ISSN 0021-9983)

v26 no15 p2247-61 '92

**CONTAINS:** bibliography; illustration(s); diagrams

**SUBJECTS COVERED:**

Sandwich construction/Failure

Impact strength

Delamination

**8 AST**

**AUTHOR:** Shi, Y. B.; Hull, D.

**TITLE:** Fracture of delaminated unidirectional composite beams

**SOURCE:** Journal of Composite Materials (ISSN 0021-9983)

v26 no15 p2172-95 '92

**CONTAINS:** bibliography; illustration(s); diagrams

**SUBJECTS COVERED:**

Delamination

Impact tests

Composite beams/Testing

9 AST

AUTHOR: Datta, S. K.; Ju, T. H.; Shah, A. H.

TITLE: Scattering of an impact wave by a crack in a composite plate

SOURCE: Journal of Applied Mechanics (ISSN 0021-8936) v59

p596-603 September '92

CONTAINS: bibliography; diagram

SUBJECTS COVERED:

Elastic wave scattering/Mathematical models

Ultrasonic testing

Polymer matrix composites/Failure

10 AST

AUTHOR: Strait, Larry H.; Karasek, Mark L.; Amateau, Maurice F.

TITLE: Effects of seawater immersion on the impact resistance of glass fiber reinforced epoxy composites

SOURCE: Journal of Composite Materials (ISSN 0021-9983)

v26 no14 p2118-33 '92

CONTAINS: bibliography (p2132-3)

SUBJECTS COVERED:

Polymer matrix composites/Glass fiber reinforcement

Composite materials, Effect of sea water on

Impact tests

11 AST

AUTHOR: Lee, S.; Wadsworth, J.; Sherby, O. D.

TITLE: Impact properties of a laminated composite based on ultrahigh carbon steel and a Ni-Si-steel

SOURCE: Journal of Engineering Materials and Technology

(ISSN 0094-4289) v114 p278-81 July '92

CONTAINS: bibliography; illustration(s)

SUBJECTS COVERED:

Laminated metals/Testing

Carbon steel/Temperature effect

Notched bar testing

12 AST

AUTHOR: Kim, C. G.; Jun, E. J.

TITLE: Measurement of impact delamination by deply technique

SOURCE: Experimental Techniques (ISSN 0732-8818) v16

p26-8 July/August '92

CONTAINS: illustration(s); diagram

SUBJECTS COVERED:

Delamination

Impact strength

Composite materials/Failure

13 AST

AUTHOR: Olsson, Robin

TITLE: Impact response of orthotropic composite plates predicted from a one-parameter differential equation

SOURCE: AIAA Journal (ISSN 0001-1452) v30 p1587-96 June '92

CONTAINS: bibliography; diagrams

SUBJECTS COVERED:

Orthotropic plates/Mathematical models

Differential equations/Numerical solutions

Impact/Mathematical models

14 AST

AUTHOR: Choi, Hyung Yun; Wang, Hong Sheng; Chang, Fu-Kuo

TITLE: Effect of laminate configuration and impactor's mass on the initial impact damage of graphite/epoxy composite plates due to line-loading impact

SOURCE: Journal of Composite Materials (ISSN 0021-9983) v26 no6 p804-27 '92

CONTAINS: bibliography; diagrams

SUBJECTS COVERED:

Impact tests

Laminates/Testing

Polymer matrix composites/Carbon fiber reinforcement

15 AST

AUTHOR: Mittelman, A.

TITLE: Low-energy repetitive impact in carbon-epoxy composite

SOURCE: Journal of Materials Science (ISSN 0022-2461) v27 p2458-62 May 1 '92

CONTAINS: bibliography; illustration(s); diagrams

SUBJECTS COVERED:

Polymer matrix composites/Carbon fiber reinforcement

Impact tests

16 AST

AUTHOR: Bogdanovich, Alexander E.; Iarve, Endel V.

TITLE: Numerical analysis of impact deformation and failure in composite plates

SOURCE: Journal of Composite Materials (ISSN 0021-9983) v26 no4 p520-45 '92

CONTAINS: bibliography; diagrams

SUBJECTS COVERED:

Impact tests

Elastic deformation/Mathematical models  
Plates, Elastic/Mathematical models

17 AST

AUTHOR: Doong, Ji-Liang; Lin, Shyh-Nung S.; Marcus, H.  
L.

TITLE: Residual stress effect on impact properties of Gr/Al metal matrix  
composite

SOURCE: Journal of Materials Science (ISSN 0022-2461) v27  
p1369-74 March 1 '92

CONTAINS: bibliography; illustration(s); diagram

SUBJECTS COVERED:

Aluminum composites

Residual stress

Impact tests

18 AST

AUTHOR: Jegley, Dawn C.; Lopez, Osvaldo F.

TITLE: Effect of composite fabrication method on structural response and impact  
damage

SOURCE: AIAA Journal (ISSN 0001-1452) v30 p205-13  
January '92

CONTAINS: bibliography; illustration(s); diagrams

SUBJECTS COVERED:

Impact tests

Fiber composites/Failure

Compression tests

19 AST

AUTHOR: Pang, S. S.; Zhao, Y.; Yang, C.

TITLE: Impact response of composite laminates with a hemispherical indenter

SOURCE: Polymer Engineering and Science (ISSN 0032-3888)  
v31 p1461-6 October '91

CONTAINS: bibliography; diagrams

SUBJECTS COVERED:

Impact tests

Laminates/Testing

20 AST

AUTHOR: Scott, R. F.; Lee, S.; Poon, C.

TITLE: Impact and compression response of composite materials containing  
fortifiers

SOURCE: Polymer Engineering and Science (ISSN 0032-3888)  
v31 p1310-15 September '91

CONTAINS: bibliography; illustration(s); diagram

**SUBJECTS COVERED:**

Polymer matrix composites/Carbon fiber reinforcement  
Compression tests  
Impact tests

**21 AST**

**AUTHOR:** Wang, Hao; Vu-Khanh, Toan  
**TITLE:** Impact-induced delamination in [0<sub>sub5</sub>], 90<sub>sub5</sub>, 0<sub>sub5</sub>] carbon fiber/polyetheretherketone composite laminates  
**SOURCE:** Polymer Engineering and Science (ISSN 0032-3888) v31 p1301-9 September '91  
**CONTAINS:** bibliography; illustration(s); diagrams

**SUBJECTS COVERED:**

Delamination  
Polymer matrix composites/Carbon fiber reinforcement  
Impact tests

**22 AST**

**AUTHOR:** Pang, S. S.; Kailasam, A. A.  
**TITLE:** A study of impact response of composite pipe  
**SOURCE:** Journal of Energy Resources Technology (ISSN 0195-0738) v113 p182-8 September '91  
**CONTAINS:** bibliography; diagrams

**SUBJECTS COVERED:**

Polymer matrix composites/Glass fiber reinforcement  
Impact strength  
Pipes/Testing

**23 AST**

**AUTHOR:** Akimune, Yoshio  
**TITLE:** Impact damage and strength degradation in a silicon carbide reinforced silicon nitride composite  
**SOURCE:** Journal of the American Ceramic Society (ISSN 0002-7820) v73 p3019-25 October '90  
**CONTAINS:** bibliography; illustration(s); diagrams

**SUBJECTS COVERED:**

Ceramic matrix composites/Silicon carbide fiber reinforcement  
Impact strength  
Silicon nitride/Strength

**24 AST**

**AUTHOR:** Gong, J. C.; Sankar, B. V.  
**TITLE:** Impact properties of three-dimensional braided graphite/epoxy composites  
**SOURCE:** Journal of Composite Materials (ISSN 0021-9983) v25 p715-31 June '91



CONTAINS: bibliography; illustration(s)

SUBJECTS COVERED:

Composite materials/Testing  
Impact tests

25 AST

AUTHOR: Lin, H. J.; Lee, Y. J.

TITLE: Use of statical indentation laws in the impact analysis of composite laminated plates and shells

SOURCE: Journal of Applied Mechanics (ISSN 0021-8936) v57  
p787-9 September '90

SUBJECTS COVERED:

Composite construction/Failure  
Impact tests

26 AST

AUTHOR: Adams, D. F.; Adams, L. G.

TITLE: A tensile impact test apparatus for composite materials

SOURCE: Experimental Mechanics (ISSN 0014-4851) v29  
p466-73 December '89

CONTAINS: bibliography; illustration(s); diagrams

SUBJECTS COVERED:

Composite materials/Testing  
Impact tests  
Testing machines

27 AST

AUTHOR: Chang, C.; Sun, C. T.:(Chin-teh):1939-

TITLE: Determining transverse impact force on a composite laminate by signal deconvolution

SOURCE: Experimental Mechanics (ISSN 0014-4851) v29  
p414-19 December '89

CONTAINS: bibliography; diagram

SUBJECTS COVERED:

Composite materials  
Impact  
Deconvolution (Mathematics)

28 AST

AUTHOR: Brown, J. R.; Chappell, P. J. C.; Egglestone, G.  
T.

TITLE: A gas-gun facility for material impact studies using low-velocity, low-mass projectiles

SOURCE: Journal of Physics. E, Scientific Instruments  
(ISSN 0022-3735) v22 p771-4 September '89

CONTAINS: bibliography; diagram

SUBJECTS COVERED:

Impact tests

Composite materials/Testing

Projectiles/Testing

29 AST

AUTHOR: Hong, S.; Liu, D.

TITLE: On the relationship between impact energy and delamination area

SOURCE: Experimental Mechanics (ISSN 0014-4851) v29

p115-20 June '89

CONTAINS: bibliography; diagrams

SUBJECTS COVERED:

Delamination

Impact strength

Composite materials/Testing

30 AST

AUTHOR: Lewis, Clifford F.

TITLE: New ideas in composite testing

SOURCE: Materials Engineering (ISSN 0025-5319) v106

p43-5 August '89

CONTAINS: diagrams

SUBJECTS COVERED:

Impact tests

Composite materials/Testing

Shear strength

31 AST

AUTHOR: Yener, M.; Wolcott, E.

TITLE: Damage assessment analysis of composite pressure vessels subjected to random impact loading

SOURCE: Journal of Pressure Vessel Technology (ISSN

0094-9930) v111 p124-9 May '89

CONTAINS: bibliography; diagrams

SUBJECTS COVERED:

Composite materials/Failure

Fracture strength

Fracture mechanics/Finite element method

32 AST

AUTHOR: Russell, S. S.; Sutton, M. A.; Chen, H. S.:

(Hsi-shu)

TITLE: Image correlation quantitative nondestructive evaluation of impact and fabrication damage in a glass fiber-reinforced composite system

SOURCE: Materials Evaluation (ISSN 0025-5327) v47 p550-7

May '89

CONTAINS: bibliography; illustration(s); diagrams

SUBJECTS COVERED:

Polymer matrix composites/Stresses

Deformation (Mechanics)/Finite element method

Image analysis

33 AST

AUTHOR: Bachrach, William E.; Hansen, R. Scott

TITLE: Mixed finite-element method for composite cylinder subjected to impact

SOURCE: AIAA Journal (ISSN 0001-1452) v27 p632-8 May '89

CONTAINS: bibliography; diagrams

SUBJECTS COVERED:

Variational principles

Structural engineering/Finite element method

Cylinders/Failure

34 AST

AUTHOR: Potet, P.; Bathias, C.; Degriigny, B.

TITLE: Quantitative characterization of impact damage in composite materials: a comparison of computerized vibrothermography and x-ray tomography

SOURCE: Materials Evaluation (ISSN 0025-5327) v46

p1050-1+ July '88

CONTAINS: bibliography; illustration(s); diagrams

SUBJECTS COVERED:

Tomography/Industrial use

Composite materials/Failure

Thermography

35 AST

AUTHOR: Chiem, Chi-Yuen; Liu, Zeng-Gang

TITLE: The relationship between tensile strength and shear strength in composite materials subjected to high strain rates

SOURCE: Journal of Engineering Materials and Technology

(ISSN 0094-4289) v110 p191-4 April '88

CONTAINS: bibliography; illustration(s); diagrams

SUBJECTS COVERED:

Polymer matrix composites/Carbon fiber reinforcement

Shear strength

Impact strength

36 AST

AUTHOR: Christoforou, A. P.; Swanson, S. R.

TITLE: Strength loss in composite cylinders under impact  
SOURCE: Journal of Engineering Materials and Technology  
(ISSN 0094-4289) v110 p180-4 April '88  
CONTAINS: bibliography; illustration(s); diagrams

SUBJECTS COVERED:

Polymer matrix composites/Carbon fiber reinforcement  
Cylinders/Failure  
Impact strength

37 AST

AUTHOR: Crockford, William W.; Little, Dallas N.  
TITLE: A model for predicting fracture toughness of a cementitious particulate composite molded under impact pressure  
SOURCE: Journal of Testing and Evaluation (ISSN 0090-3973)  
v15 p211-18 July '87  
CONTAINS: bibliography; diagrams

SUBJECTS COVERED:

Testing/Statistical methods  
Fracture mechanics  
Soil-cement mixtures

38 AST

AUTHOR: Potet, P.; Jeannin, P.; Bathias, C.  
TITLE: The use of digital image processing in vibrothermographic detection of impact damage in composite materials  
SOURCE: Materials Evaluation (ISSN 0025-5327) v45  
p466-70 April '87  
CONTAINS: bibliography; illustration(s); diagram

SUBJECTS COVERED:

Infrared imaging systems  
Composite materials/Failure

39 AST

AUTHOR: Schmueser, D. W.; Wickliffe, L. E.  
TITLE: Impact energy absorption of continuous fiber composite tubes  
SOURCE: Journal of Engineering Materials and Technology  
(ISSN 0094-4289) v109 p72-7 January '87  
CONTAINS: bibliography; illustration(s)

SUBJECTS COVERED:

Automotive materials/Composites  
Impact tests  
Tubes, Plastic/Testing

40 AST

AUTHOR: Gardiner, D. S.; Pearson, L. H.

TITLE: Acoustic-emission monitoring of composite damage occurring under static and impact loading

SOURCE: Experimental Techniques (ISSN 0732-8818) v9

p22-8 November '85

CONTAINS: bibliography; illustration(s); diagram

SUBJECTS COVERED:

Acoustic emission testing

Composite materials/Failure

Static loads

41 AST

AUTHOR: Shivakumar, K. N.; Elber, W.; Illg, W.

TITLE: Prediction of impact force and duration due to low-velocity impact on circular composite laminates

SOURCE: Journal of Applied Mechanics (ISSN 0021-8936) v52

p674-80 September '85

CONTAINS: bibliography; diagrams

SUBJECTS COVERED:

Impact

Laminates/Failure

Contact problems (Mechanics)

42 AST

AUTHOR: O'Connor, Colin; Pritchard, Ross W.

TITLE: Impact studies on small composite girder bridge

SOURCE: Journal of Structural Engineering (ISSN 0733-9445)

v111 p641-53 March '85 Discussion. 113:884-8 Ap

'87

CONTAINS: bibliography; diagrams

SUBJECTS COVERED:

Bridges, Iron and steel/Stresses

Impact

43 AST

AUTHOR: Tan, T. M.; Sun, C. T.

TITLE: Use of static indentation laws in the impact analysis of laminated composite plates

SOURCE: Journal of Applied Mechanics (ISSN 0021-8936) v52

p6-12 March '85

CONTAINS: bibliography; diagrams

SUBJECTS COVERED:

Composite materials/Failure

Polymer matrix composites

Impact

44 AST

TITLE: [Symposium on Instrumented Impact Testing of Plastics and Composite Materials, Houston, TX, Mar. 11-12; with program]

SOURCE: ASTM Standardization News (ISSN 0090-1210) v12  
p54 October '84

SUBJECTS COVERED:

Impact

Plastics/Testing

Composite materials/Testing

45 AST

TITLE: Composite aloft: 6X impact; 1/2 weight (Avtek 400)

SOURCE: Modern Plastics (ISSN 0026-8275) v60 p40+  
September '83

CONTAINS: illustration(s)

SUBJECTS COVERED:

Airplane materials/Plastics

Polymer matrix composites

1 AST

AUTHOR: Hsieh, C. Y.; Nagarajan, S.; Zee, R. H.

TITLE: Infrared thermographic analysis of polymer composites during ballistic impact

SOURCE: Review of Scientific Instruments (ISSN 0034-6748)  
v63 pt1 p2296-304 April '92

CONTAINS: bibliography; illustration(s); diagrams

SUBJECTS COVERED:

Polymer matrix composites/Testing

Thermography

Temperature distribution

2 AST

AUTHOR: Patil, M. S.; Singh, Haridwar:1949-

1 AST

AUTHOR: Jih, C. J.; Sun, C. T.

TITLE: Prediction of delamination in composite laminates subjected to low velocity impact

SOURCE: Journal of Composite Materials (ISSN 0021-9983)  
v27 no7 p684-701 '93

CONTAINS: bibliography; diagrams

SUBJECTS COVERED:

Delamination

2 AST

**AUTHOR:** Green, E. Rhian

**TITLE:** Response of a fiber composite laminate to a time-varying surface line load

**SOURCE:** Journal of Applied Mechanics (ISSN 0021-8936) v60

p217-21 March '93

**SUBJECTS COVERED:**

Fiber composites/Stresses

Impact

**3 AST**

**AUTHOR:** Carman, G. P.; Lesko, J. J.; Reifsnider, K. L.

**TITLE:** Micromechanical model of composite materials subjected to ball indentation

**SOURCE:** Journal of Composite Materials (ISSN 0021-9983)

v27 no3 p303-29 '93

**CONTAINS:** bibliography; illustration(s); diagrams

**SUBJECTS COVERED:**

Interfacial stresses

Composite materials/Mathematical models

Impact tests

**4 AST**

**AUTHOR:** Lee, S-W. R.; Sun, C. T.

**TITLE:** A quasi-static penetration model for composite laminates

**SOURCE:** Journal of Composite Materials (ISSN 0021-9983)

v27 no3 p251-71 '93

**CONTAINS:** bibliography; illustration(s); diagrams

**SUBJECTS COVERED:**

Laminates/Failure

Impact tests

**5 AST**

**AUTHOR:** Rajalingam, P.; Baker, W. E.

**TITLE:** The role of functional polymers in ground rubber tire-polyethylene composite

**SOURCE:** Rubber Chemistry and Technology (ISSN 0035-9475)

v65 p908-16 November/December '92

**CONTAINS:** bibliography

**SUBJECTS COVERED:**

Impact tests

Tires, Rubber/Recycling

Polymer matrix composites/Strength

**6 AST**

**AUTHOR:** Hamstad, M. A.; Whittaker, J. W.; Brosey, W. D.

**TITLE:** Correlation of residual strength with acoustic emission from impact-damaged composite structures under constant biaxial load

**SOURCE:** Journal of Composite Materials (ISSN 0021-9983)

v26 no15 p2307-28 '92

**CONTAINS:** bibliography; illustration(s); diagrams

**SUBJECTS COVERED:**

Impact tests

Composite materials/Testing

Acoustic emission testing

Residual stress

**7 AST**

**AUTHOR:** Kim, Chun-Gon; Jun, Eui-Jin

**TITLE:** Impact resistance of composite laminated sandwich plates

**SOURCE:** Journal of Composite Materials (ISSN 0021-9983)

v26 no15 p2247-61 '92

**CONTAINS:** bibliography; illustration(s); diagrams

**SUBJECTS COVERED:**

Sandwich construction/Failure

Impact strength

Delamination

**8 AST**

**AUTHOR:** Shi, Y. B.; Hull, D.

**TITLE:** Fracture of delaminated unidirectional composite beams

**SOURCE:** Journal of Composite Materials (ISSN 0021-9983)

v26 no15 p2172-95 '92

**CONTAINS:** bibliography; illustration(s); diagrams

**SUBJECTS COVERED:**

Delamination

Impact tests

Composite beams/Testing

**9 AST**

**AUTHOR:** Datta, S. K.; Ju, T. H.; Shah, A. H.

**TITLE:** Scattering of an impact wave by a crack in a composite plate

**SOURCE:** Journal of Applied Mechanics (ISSN 0021-8936) v59

p596-603 September '92

**CONTAINS:** bibliography; diagram

**SUBJECTS COVERED:**

Elastic wave scattering/Mathematical models

Ultrasonic testing

Polymer matrix composites/Failure

**10 AST**



AUTHOR: Strait, Larry H.; Karasek, Mark L.; Amateau, Maurice F.

TITLE: Effects of seawater immersion on the impact resistance of glass fiber reinforced epoxy composites

SOURCE: Journal of Composite Materials (ISSN 0021-9983) v26 no14 p2118-33 '92

CONTAINS: bibliography (p2132-3)

SUBJECTS COVERED:

Polymer matrix composites/Glass fiber reinforcement  
Composite materials, Effect of sea water on  
Impact tests

11 AST

AUTHOR: Lee, S.; Wadsworth, J.; Sherby, O. D.

TITLE: Impact properties of a laminated composite based on ultrahigh carbon steel and a Ni-Si-steel

SOURCE: Journal of Engineering Materials and Technology (ISSN 0094-4289) v114 p278-81 July '92

CONTAINS: bibliography; illustration(s)

SUBJECTS COVERED:

Laminated metals/Testing  
Carbon steel/Temperature effect  
Notched bar testing

12 AST

AUTHOR: Kim, C. G.; Jun, E. J.

TITLE: Measurement of impact delamination by deply technique

SOURCE: Experimental Techniques (ISSN 0732-8818) v16 p26-8 July/August '92

CONTAINS: illustration(s); diagram

SUBJECTS COVERED:

Delamination  
Impact strength  
Composite materials/Failure

13 AST

AUTHOR: Olsson, Robin

TITLE: Impact response of orthotropic composite plates predicted from a one-parameter differential equation

SOURCE: AIAA Journal (ISSN 0001-1452) v30 p1587-96 June '92

CONTAINS: bibliography; diagrams

SUBJECTS COVERED:

Orthotropic plates/Mathematical models  
Differential equations/Numerical solutions

## Impact/Mathematical models

14 AST

AUTHOR: Choi, Hyung Yun; Wang, Hong Sheng; Chang, Fu-Kuo

TITLE: Effect of laminate configuration and impactor's mass on the initial impact damage of graphite/epoxy composite plates due to line-loading impact

SOURCE: Journal of Composite Materials (ISSN 0021-9983)

v26 no6 p804-27 '92

CONTAINS: bibliography; diagrams

### SUBJECTS COVERED:

Impact tests

Laminates/Testing

Polymer matrix composites/Carbon fiber reinforcement

15 AST

AUTHOR: Mittelman, A.

TITLE: Low-energy repetitive impact in carbon-epoxy composite

SOURCE: Journal of Materials Science (ISSN 0022-2461) v27

p2458-62 May 1 '92

CONTAINS: bibliography; illustration(s); diagrams

### SUBJECTS COVERED:

Polymer matrix composites/Carbon fiber reinforcement

Impact tests

16 AST

AUTHOR: Bogdanovich, Alexander E.; Iarve, Endel V.

TITLE: Numerical analysis of impact deformation and failure in composite plates

SOURCE: Journal of Composite Materials (ISSN 0021-9983)

v26 no4 p520-45 '92

CONTAINS: bibliography; diagrams

### SUBJECTS COVERED:

Impact tests

Elastic deformation/Mathematical models

Plates, Elastic/Mathematical models

17 AST

AUTHOR: Doong, Ji-Liang; Lin, Shyh-Nung S.; Marcus, H. L.

TITLE: Residual stress effect on impact properties of Gr/Al metal matrix composite

SOURCE: Journal of Materials Science (ISSN 0022-2461) v27

p1369-74 March 1 '92

CONTAINS: bibliography; illustration(s); diagram

### SUBJECTS COVERED:

Aluminum composites

Residual stress  
Impact tests

18 AST

AUTHOR: Jegley, Dawn C.; Lopez, Osvaldo F.

TITLE: Effect of composite fabrication method on structural response and impact damage

SOURCE: AIAA Journal (ISSN 0001-1452) v30 p205-13

January '92

CONTAINS: bibliography; illustration(s); diagrams

SUBJECTS COVERED:

Impact tests

Fiber composites/Failure

Compression tests

19 AST

AUTHOR: Pang, S. S.; Zhao, Y.; Yang, C.

TITLE: Impact response of composite laminates with a hemispherical indenter

SOURCE: Polymer Engineering and Science (ISSN 0032-3888)

v31 p1461-6 October '91

CONTAINS: bibliography; diagrams

SUBJECTS COVERED:

Impact tests

Laminates/Testing

20 AST

AUTHOR: Scott, R. F.; Lee, S.; Poon, C.

TITLE: Impact and compression response of composite materials containing fortifiers

SOURCE: Polymer Engineering and Science (ISSN 0032-3888)

v31 p1310-15 September '91

CONTAINS: bibliography; illustration(s); diagram

SUBJECTS COVERED:

Polymer matrix composites/Carbon fiber reinforcement

Compression tests

Impact tests

21 AST

AUTHOR: Wang, Hao; Vu-Khanh, Toan

TITLE: Impact-induced delamination in [0<sup>sub5</sup>], 90<sup>sub5</sup>, 0<sup>sub5</sup>] carbon fiber/polyetheretherketone composite laminates

SOURCE: Polymer Engineering and Science (ISSN 0032-3888)

v31 p1301-9 September '91

CONTAINS: bibliography; illustration(s); diagrams

SUBJECTS COVERED:

Delamination  
Polymer matrix composites/Carbon fiber reinforcement  
Impact tests

22 AST

AUTHOR: Pang, S. S.; Kailasam, A. A.  
TITLE: A study of impact response of composite pipe  
SOURCE: Journal of Energy Resources Technology (ISSN  
0195-0738) v113 p182-8 September '91  
CONTAINS: bibliography; diagrams

SUBJECTS COVERED:

Polymer matrix composites/Glass fiber reinforcement  
Impact strength  
Pipes/Testing

23 AST

AUTHOR: Akimune, Yoshio  
TITLE: Impact damage and strength degradation in a silicon carbide reinforced  
silicon nitride composite  
SOURCE: Journal of the American Ceramic Society (ISSN  
0002-7820) v73 p3019-25 October '90  
CONTAINS: bibliography; illustration(s); diagrams

SUBJECTS COVERED:

Ceramic matrix composites/Silicon carbide fiber reinforcement  
Impact strength  
Silicon nitride/Strength

24 AST

AUTHOR: Gong, J. C.; Sankar, B. V.  
TITLE: Impact properties of three-dimensional braided graphite/epoxy  
composites  
SOURCE: Journal of Composite Materials (ISSN 0021-9983)  
v25 p715-31 June '91  
CONTAINS: bibliography; illustration(s)

SUBJECTS COVERED:

Composite materials/Testing  
Impact tests

25 AST

AUTHOR: Lin, H. J.; Lee, Y. J.  
TITLE: Use of statical indentation laws in the impact analysis of composite  
laminated plates and shells  
SOURCE: Journal of Applied Mechanics (ISSN 0021-8936) v57  
p787-9 September '90

SUBJECTS COVERED:

Composite construction/Failure  
Impact tests

26 AST

AUTHOR: Adams, D. F.; Adams, L. G.

TITLE: A tensile impact test apparatus for composite materials

SOURCE: Experimental Mechanics (ISSN 0014-4851) v29  
p466-73 December '89

CONTAINS: bibliography; illustration(s); diagrams

SUBJECTS COVERED:

Composite materials/Testing

Impact tests

Testing machines

27 AST

AUTHOR: Chang, C.; Sun, C. T.:(Chin-teh):1939-

TITLE: Determining transverse impact force on a composite laminate by signal deconvolution

SOURCE: Experimental Mechanics (ISSN 0014-4851) v29  
p414-19 December '89

CONTAINS: bibliography; diagram

SUBJECTS COVERED:

Composite materials

Impact

Deconvolution (Mathematics)

28 AST

AUTHOR: Brown, J. R.; Chappell, P. J. C.; Egglestone, G.  
T.

TITLE: A gas-gun facility for material impact studies using low-velocity, low-mass projectiles

SOURCE: Journal of Physics. E, Scientific Instruments  
(ISSN 0022-3735) v22 p771-4 September '89

CONTAINS: bibliography; diagram

SUBJECTS COVERED:

Impact tests

Composite materials/Testing

Projectiles/Testing

29 AST

AUTHOR: Hong, S.; Liu, D.

TITLE: On the relationship between impact energy and delamination area

SOURCE: Experimental Mechanics (ISSN 0014-4851) v29  
p115-20 June '89

CONTAINS: bibliography; diagrams

**SUBJECTS COVERED:**

Delamination  
Impact strength  
Composite materials/Testing

30 AST

AUTHOR: Lewis, Clifford F.  
TITLE: New ideas in composite testing  
SOURCE: Materials Engineering (ISSN 0025-5319) v106  
p43-5 August '89  
CONTAINS: diagrams

**SUBJECTS COVERED:**

Impact tests  
Composite materials/Testing  
Shear strength

31 AST

AUTHOR: Yener, M.; Wolcott, E.  
TITLE: Damage assessment analysis of composite pressure vessels subjected to random impact loading  
SOURCE: Journal of Pressure Vessel Technology (ISSN 0094-9930) v111 p124-9 May '89  
CONTAINS: bibliography; diagrams

**SUBJECTS COVERED:**

Composite materials/Failure  
Fracture strength  
Fracture mechanics/Finite element method

32 AST

AUTHOR: Russell, S. S.; Sutton, M. A.; Chen, H. S.:  
(Hsi-shu)  
TITLE: Image correlation quantitative nondestructive evaluation of impact and fabrication damage in a glass fiber-reinforced composite system  
SOURCE: Materials Evaluation (ISSN 0025-5327) v47 p550-7  
May '89  
CONTAINS: bibliography; illustration(s); diagrams

**SUBJECTS COVERED:**

Polymer matrix composites/Stresses  
Deformation (Mechanics)/Finite element method  
Image analysis

33 AST

AUTHOR: Bachrach, William E.; Hansen, R. Scott  
TITLE: Mixed finite-element method for composite cylinder subjected to impact  
SOURCE: AIAA Journal (ISSN 0001-1452) v27 p632-8 May '89

CONTAINS: bibliography; diagrams

SUBJECTS COVERED:

Variational principles

Structural engineering/Finite element method

Cylinders/Failure

34 AST

AUTHOR: Potet, P.; Bathias, C.; Degriigny, B.

TITLE: Quantitative characterization of impact damage in composite materials: a comparison of computerized vibrothermography and x-ray tomography

SOURCE: Materials Evaluation (ISSN 0025-5327) v46

p1050-1+ July '88

CONTAINS: bibliography; illustration(s); diagrams

SUBJECTS COVERED:

Tomography/Industrial use

Composite materials/Failure

Thermography

35 AST

AUTHOR: Chiem, Chi-Yuen; Liu, Zeng-Gang

TITLE: The relationship between tensile strength and shear strength in composite materials subjected to high strain rates

SOURCE: Journal of Engineering Materials and Technology

(ISSN 0094-4289) v110 p191-4 April '88

CONTAINS: bibliography; illustration(s); diagrams

SUBJECTS COVERED:

Polymer matrix composites/Carbon fiber reinforcement

Shear strength

Impact strength

36 AST

AUTHOR: Christoforou, A. P.; Swanson, S. R.

TITLE: Strength loss in composite cylinders under impact

SOURCE: Journal of Engineering Materials and Technology

(ISSN 0094-4289) v110 p180-4 April '88

CONTAINS: bibliography; illustration(s); diagrams

SUBJECTS COVERED:

Polymer matrix composites/Carbon fiber reinforcement

Cylinders/Failure

Impact strength

37 AST

AUTHOR: Crockford, William W.; Little, Dallas N.

TITLE: A model for predicting fracture toughness of a cementitious particulate composite molded under impact pressure

SOURCE: Journal of Testing and Evaluation (ISSN 0090-3973)  
v15 p211-18 July '87  
CONTAINS: bibliography; diagrams

SUBJECTS COVERED:  
Testing/Statistical methods  
Fracture mechanics  
Soil-cement mixtures

38 AST

AUTHOR: Potet, P.; Jeannin, P.; Bathias, C.  
TITLE: The use of digital image processing in vibrothermographic detection of impact damage in composite materials  
SOURCE: Materials Evaluation (ISSN 0025-5327) v45  
p466-70 April '87  
CONTAINS: bibliography; illustration(s); diagram

SUBJECTS COVERED:  
Infrared imaging systems  
Composite materials/Failure

39 AST

AUTHOR: Schmueser, D. W.; Wickliffe, L. E.  
TITLE: Impact energy absorption of continuous fiber composite tubes  
SOURCE: Journal of Engineering Materials and Technology  
(ISSN 0094-4289) v109 p72-7 January '87  
CONTAINS: bibliography; illustration(s)

SUBJECTS COVERED:  
Automotive materials/Composites  
Impact tests  
Tubes, Plastic/Testing

40 AST

AUTHOR: Gardiner, D. S.; Pearson, L. H.  
TITLE: Acoustic-emission monitoring of composite damage occurring under static and impact loading  
SOURCE: Experimental Techniques (ISSN 0732-8818) v9  
p22-8 November '85  
CONTAINS: bibliography; illustration(s); diagram

SUBJECTS COVERED:  
Acoustic emission testing  
Composite materials/Failure  
Static loads

41 AST

AUTHOR: Shivakumar, K. N.; Elber, W.; Illg, W.



TITLE: Prediction of impact force and duration due to low-velocity impact on circular composite laminates

SOURCE: Journal of Applied Mechanics (ISSN 0021-8936) v52  
p674-80 September '85

CONTAINS: bibliography; diagrams

SUBJECTS COVERED:

Impact

Laminates/Failure

Contact problems (Mechanics)

42 AST

AUTHOR: O'Connor, Colin; Pritchard, Ross W.

TITLE: Impact studies on small composite girder bridge

SOURCE: Journal of Structural Engineering (ISSN 0733-9445)  
v111 p641-53 March '85 Discussion. 113:884-8 Ap '87

CONTAINS: bibliography; diagrams

SUBJECTS COVERED:

Bridges, Iron and steel/Stresses

Impact

43 AST

AUTHOR: Tan, T. M.; Sun, C. T.

TITLE: Use of static indentation laws in the impact analysis of laminated composite plates

SOURCE: Journal of Applied Mechanics (ISSN 0021-8936) v52  
p6-12 March '85

CONTAINS: bibliography; diagrams

SUBJECTS COVERED:

Composite materials/Failure

Polymer matrix composites

Impact

44 AST

TITLE: [Symposium on Instrumented Impact Testing of Plastics and Composite Materials, Houston, TX, Mar. 11-12; with program]

SOURCE: ASTM Standardization News (ISSN 0090-1210) v12  
p54 October '84

SUBJECTS COVERED:

Impact

Plastics/Testing

Composite materials/Testing

45 AST

TITLE: Composite aloft: 6X impact; 1/2 weight (Avtek 400)

SOURCE: Modern Plastics (ISSN 0026-8275) v60 p40+

September '83  
CONTAINS: illustration(s)

SUBJECTS COVERED:  
Airplane materials/Plastics  
Polymer matrix composites

4 AST

AUTHOR: Roylance, Michael H.  
TITLE: Depositional and diagenetic history of a Pennsylvanian algal-mound complex: Bug and Papoose Canyon fields, Paradox basin, Utah and Colorado  
SOURCE: AAPG Bulletin (ISSN 0149-1423) v74 p1087-99 July '90  
CONTAINS: bibliography; illustration(s); maps; diagrams

SUBJECTS COVERED:  
Petroleum geology/Utah  
Petroleum geology/Colorado

5 AST

AUTHOR: Hashemi, S. M. R.; Roylance, B. J.  
TITLE: The effect of fluid inertia and cavitation on the performance of oscillatory squeeze-film bearings  
SOURCE: Proceedings of the Institution of Mechanical Engineers. Part C, Journal of Mechanical Engineering Science (ISSN 0954-4062) v204 noC2 p99-108 '90  
CONTAINS: bibliography; diagrams

SUBJECTS COVERED:  
Gas turbines/Bearings  
Squeeze films  
Cavitation

6 AST

AUTHOR: Hashemi, S. M. R.; Roylance, B. J.  
TITLE: Analysis of an oscillatory oil squeeze film including effects of fluid inertia  
SOURCE: Tribology Transactions (ISSN 1040-2004) v32 p461-8 October '89  
CONTAINS: bibliography; diagram

SUBJECTS COVERED:  
Squeeze films  
Newtonian flow  
Inertia (Mechanics)

7 AST

AUTHOR: Hashemi, S. M. R.; Roylance, B. J.  
TITLE: Steady-state behavior of squeeze film bearings subjected to harmonic excitation-including fluid inertia and system effects

SOURCE: Tribology Transactions (ISSN 1040-2004) v32  
p431-8 October '89  
CONTAINS: bibliography; diagrams

**SUBJECTS COVERED:**

Squeeze films  
Steady state systems  
Newtonian flow

8 AST

AUTHOR: Fullerton, Rhonda; Roylance, David  
TITLE: Cure analysis of printed wiring boards containing reactive adhesive layers  
SOURCE: Polymer Engineering and Science (ISSN 0032-3888)  
v28 p372-6 March '88  
CONTAINS: bibliography; diagrams

**SUBJECTS COVERED:**

Printed circuits  
Resinous products/Curing  
Heat transmission/Finite element method

9 AST

AUTHOR: Mead, Joey; Singh, Sachchida; Roylance, David  
TITLE: Nonlinear response and thermomechanicochemical degradation of a urethane elastomer  
SOURCE: Polymer Engineering and Science (ISSN 0032-3888)  
v27 p131-40 January '87  
CONTAINS: bibliography; illustration(s); diagrams

**SUBJECTS COVERED:**

Polyurethane rubber/Failure  
Load (Mechanics)  
Motor vehicles, Military

10 AST

AUTHOR: Popli, Rakesh; Roylance, David  
TITLE: A thermodynamic prediction of tie chain length distribution in drawn semicrystalline polymers  
SOURCE: Polymer Engineering and Science (ISSN 0032-3888)  
v25 p828-33 September '85  
CONTAINS: bibliography; diagrams

**SUBJECTS COVERED:**

Chemical chains  
Polymers/Fracture  
Thermodynamics

1/2/1 of 45

DIALOG No: 03578381 EI Monthly No: EIM9303-018494  
Title: Effects of freezing on impact properties of RTM composites, and their applications in offshore structures.  
Author: Pope, Gregory J.; Karbhari, Vistasp M.  
Corporate Source: Univ of Delaware, Newark, DE, USA  
Conference Title: Proceedings of the International Conference on Civil Engineering in the Oceans V  
Conference Location: College Station, TX, USA Conference Date: 1992 Nov 2-5  
Conference Sponsor: ASCE; Texas A & M Univ, Dep of Civil Engineering; Offshore Technology Research Cent (OTRC)  
Source: Civil Engineering in the Oceans V. Publ by ASCE, New York, NY, USA. p 828-839  
Publication Year: 1992  
ISBN: 0-87262-908-2  
Language: English  
Conference Number: 17632  
Document Type: PA; (Conference Paper) Treatment Code: A; (Applications); X; (Experimental)  
Descriptors: \*OFFSHORE STRUCTURES; PLASTIC BUILDING MATERIALS; TRANSFER MOLDING; POLYMERS; COMPOSITE MATERIALS; IMPACT TESTING; FREEZING  
Identifiers: RESIN TRANSFER MOLDING (RTM) COMPOSITES; IMPACT PROPERTIES  
EI Classification Codes: 674 (Other Marine Craft); 415 (Metals, Wood & Other Structural Materials); 817 (Plastics, Products & Applications); 815 (Plastics & Polymeric Materials); 422 (Materials Testing)

1/2/1 of 45

DIALOG No: 03578381 EI Monthly No: EIM9303-018494  
Title: Effects of freezing on impact properties of RTM composites, and their applications in offshore structures.  
Author: Pope, Gregory J.; Karbhari, Vistasp M.  
Corporate Source: Univ of Delaware, Newark, DE, USA  
Conference Title: Proceedings of the International Conference on Civil Engineering in the Oceans V  
Conference Location: College Station, TX, USA Conference Date: 1992 Nov 2-5  
Conference Sponsor: ASCE; Texas A & M Univ, Dep of Civil Engineering; Offshore Technology Research Cent (OTRC)  
Source: Civil Engineering in the Oceans V. Publ by ASCE, New York, NY, USA. p 828-839  
Publication Year: 1992  
ISBN: 0-87262-908-2  
Language: English  
Conference Number: 17632  
Document Type: PA; (Conference Paper) Treatment Code: A; (Applications); X; (Experimental)  
Descriptors: \*OFFSHORE STRUCTURES; PLASTIC BUILDING MATERIALS; TRANSFER

MOLDING; POLYMERS; COMPOSITE MATERIALS; IMPACT TESTING;  
FREEZING

Identifiers: RESIN TRANSFER MOLDING (RTM) COMPOSITES; IMPACT  
PROPERTIES

EI Classification Codes: 674 (Other Marine Craft); 415 (Metals, Wood &  
Other Structural Materials); 817 (Plastics, Products & Applications); 815  
(Plastics & Polymeric Materials); 422 (Materials Testing)

1/2/2 of 45

DIALOG No: 03576555 EI Monthly No: EIM9303-016668

Title: Finite element analysis of revolute manipulators with link and joint  
compliance by joint-beam elements.

Author: Yang, Zhijia; Sadler, J. P.

Corporate Source: Univ of Kentucky, Lexington, KS, USA

Conference Title: 22nd Biennial Mechanisms Conference

Conference Location: Scottsdale, AZ, USA Conference Date: 1992 Sep 13-16

Conference Sponsor: ASME

Source: Robotics, Spatial Mechanisms, and Mechanical Systems American  
Society

of Mechanical Engineers, Design Engineering Division (Publication) DE v 45.

Publ by ASME, New York, NY, USA. p 619-625

Publication Year: 1992

CODEN: AMEDEH

Language: English

Conference Number: 17561

Document Type: PA; (Conference Paper) Treatment Code: T; (Theoretical)

Descriptors: \*MANIPULATORS; FINITE ELEMENT METHOD; BEAMS AND  
GIRDERS;

DYNAMICS; POSITION CONTROL

Identifiers: REVOLUTE MANIPULATORS; JOINT-BEAM ELEMENTS;

DYNAMICALLY INDUCED

POSITIONING ERRORS; LINK FLEXIBILITY; COMPLETELY FLEXIBLE  
MANIPULATORS

EI Classification Codes: 731 (Automatic Control Principles); 921 (Applied  
Mathematics); 408 (Structural Design); 931 (Applied Physics)

1/2/3 of 45

DIALOG No: 03575433 EI Monthly No: EIM9303-015546

Title: Impact damage assessment of composites.

Author: Girshovich, Simon; Gottesman, Tamara; Rosenthal, Hans; Drukker,  
Esther; Steinberg, Yechill

Corporate Source: Israel Aircraft Industries Ltd, Isr

Conference Title: International Symposium on Damage Detection and Quality  
Assurance in Composite Materials

Conference Location: San Antonio, TX, USA Conference Date: 1990 Nov 13-14

Conference Sponsor: ASTM

Source: ASTM Special Technical Publication n 1128. Publ by ASTM,  
Philadelphia, PA, USA. p 183-199

Publication Year: 1992

CODEN: ASTTA8 ISSN: 0066-0558 ISBN: 0-8031-1474-5

Language: English

Conference Number: 17466

Document Type: PA; (Conference Paper) Treatment Code: X; (Experimental)

Descriptors: \*COMPOSITE MATERIALS; STRUCTURAL ANALYSIS; X RAY ANALYSIS;

LAMINATED COMPOSITES

Identifiers: COMPOSITE IMPACT DAMAGE ASSESSMENT; SIMPLIFIED DAMAGE MODEL;

COMPOSITE LAMINATE STRUCTURAL PERFORMANCE; X-RAY MICROFOCUS TECHNIQUE

EI Classification Codes: 421 (Materials Properties); 408 (Structural Design); 931 (Applied Physics); 422 (Materials Testing); 415 (Metals, Wood & Other Structural Materials)

1/2/4 of 45

DIALOG No: 03575426 EI Monthly No: EIM9303-015539

Title: Defect classifications in composites using ultrasonic nondestructive evaluation techniques.

Author: Steiner, Karl V.

Corporate Source: Univ of Delaware, Newark, DE, USA

Conference Title: International Symposium on Damage Detection and Quality Assurance in Composite Materials

Conference Location: San Antonio, TX, USA Conference Date: 1990 Nov 13-14

Conference Sponsor: ASTM

Source: ASTM Special Technical Publication n 1128. Publ by ASTM, Philadelphia, PA, USA. p 72-84

Publication Year: 1992

CODEN: ASTTA8 ISSN: 0066-0558 ISBN: 0-8031-1474-5

Language: English

Conference Number: 17466

Document Type: PA; (Conference Paper) Treatment Code: X; (Experimental)

Descriptors: \*NONDESTRUCTIVE EXAMINATION; ULTRASONICS; COMPOSITE STRUCTURES;

FAILURE ANALYSIS; FIBERS

Identifiers: ULTRASONIC NONDESTRUCTIVE EVALUATION TECHNIQUES; COMPOSITE

DEFECT CLASSIFICATION; FLAW CRITICALITY ISSUE; COMPOSITE STRUCTURE

CHARACTERIZATION; FLAW GROWTH MODELS

EI Classification Codes: 422 (Materials Testing); 753 (Sound Technology & Ultrasonics); 421 (Materials Properties); 415 (Metals, Wood & Other Structural Materials)

1/2/5 of 45

DIALOG No: 03574837 EI Monthly No: EIM9303-014950

Title: Effect of different impact time histories on the response of a fibre composite plate.

Author: Green, E. Rhian

Corporate Source: Univ of Leicester, Leicester, Engl  
 Conference Title: Winter Annual Meeting of the American Society of Mechanical Engineers  
 Conference Location: Atlanta, GA, USA Conference Date: 1991 Dec 1-6  
 Conference Sponsor: ASME  
 Source: Enhancing Analysis Techniques for Composite Materials American Society of Mechanical Engineers (Publication) NDE v 10. Publ by ASME, New York, NY, USA. p 9-21  
 Publication Year: 1991  
 CODEN: AMENED ISBN: 0-7918-0837-8  
 Language: English  
 Conference Number: 17358  
 Document Type: PA; (Conference Paper) Treatment Code: T; (Theoretical); X; (Experimental)  
 Descriptors: \*COMPOSITE MATERIALS; IMPACT TESTING; ELASTICITY; MATHEMATICAL MODELS; FIBER REINFORCED MATERIALS; LAMINATES; COMPUTERS  
 Identifiers: IMPACT TIME HISTORIES; FIBER COMPOSITE PLATES; DELTA FUNCTION  
 LINE LOAD; FIBRE-REINFORCED MATERIAL; CROSS-PLY CONFIGURATION; ELASTIC CONTINUUM  
 EI Classification Codes: 415 (Metals, Wood & Other Structural Materials); 422 (Materials Testing); 421 (Materials Properties); 921 (Applied Mathematics); 723 (Computer Software)

1/2/6 of 45

DIALOG No: 03571506 EI Monthly No: EIM9303-011619  
 Title: Fabrication, testing, and evaluation of high-thermal-conductivity, lightweight polymer composites reinforced with pitch-graphite fibers as heat sinks for high-density packaging applications.  
 Author: Ibrahim, A. Mahammad  
 Corporate Source: Martin Marietta Lab, Baltimore, MD, USA  
 Conference Title: 6th International SAMPE Electronics Conference  
 Conference Location: Baltimore, MD, USA Conference Date: 1992 Jun 22-25  
 Source: International SAMPE Electronics Conference v 6 1992. p 556-567  
 Publication Year: 1992  
 CODEN: ISECE8 ISBN: 0-938994-65-4  
 Language: English  
 Conference Number: 17353  
 Document Type: JA; (Journal Article) Treatment Code: X; (Experimental); A; (Applications)  
 Descriptors: \*GRAPHITE FIBER REINFORCED PLASTICS; FABRICATION; THERMAL CONDUCTIVITY; EVALUATION; ELECTRONICS PACKAGING; HEAT SINKS; ORDNANCE  
 Identifiers: LIGHT WEIGHT POLYMER SOMPOSITES; PITCH GRAPHITE FIBERS; HIGH

DENSITY PACKAGING; MULTICHIP MODULES (MCM); CHIP ON BOARD;  
SMART WEAPON SYSTEMS

EI Classification Codes: 812 (Ceramics & Refractories); 817 (Plastics,  
Products & Applications); 714 (Electronic Components); 641 (Heat &  
Thermodynamics); 404 (Military Engineering); 421 (Materials Properties)

1/2/7 of 45

DIALOG No: 03571484 EI Monthly No: EIM9303-011597

Title: Applications of advanced composites for satellite packaging for  
improved electronic component thermal management.

Author: Glatz, J. J.; Vrable, D. L.; Schmedake, T.; Johnson, C.

Corporate Source: SPARTA Inc, San Diego, CA, USA

Conference Title: 6th International SAMPE Electronics Conference

Conference Location: Baltimore, MD, USA Conference Date: 1992 Jun 22-25

Source: International SAMPE Electronics Conference v 6 1992. p 334-366

Publication Year: 1992

CODEN: ISECE8 ISBN: 0-938994-65-4

Language: English

Conference Number: 17353

Document Type: JA; (Journal Article) Treatment Code: X; (Experimental); A;  
(Applications)

Descriptors: \*METALLIC MATRIX COMPOSITES; ELECTRONICS

PACKAGING; SATELLITES;

RELIABILITY; SPACECRAFT EQUIPMENT; THERMAL CONDUCTIVITY;

ELECTRONIC EQUIPMENT

Identifiers: THERMAL MANAGEMENT (TM); SPACECRAFT ELECTRONICS;  
ELECTRONICS

RELIABILITY; ADVANCED COMPOSITES TM; ORGANIC MATRIX

COMPOSITES; COST

EFFECTIVENESS

EI Classification Codes: 540 (METAL GROUPS); 715 (General Electronic  
Equipment); 655 (Spacecraft); 641 (Heat & Thermodynamics); 817 (Plastics,  
Products & Applications)

1/2/8 of 45

DIALOG No: 03571482 EI Monthly No: EIM9303-011595

Title: Manufacture and test of advanced composite standard electronic  
modules.

Author: Glatz, J.; Whatley, W.; Hook, M.

Corporate Source: SPARTA Inc, San Diego, CA, USA

Conference Title: 6th International SAMPE Electronics Conference

Conference Location: Baltimore, MD, USA Conference Date: 1992 Jun 22-25

Source: International SAMPE Electronics Conference v 6 1992. p 308-319

Publication Year: 1992

CODEN: ISECE8 ISBN: 0-938994-65-4

Language: English

Conference Number: 17353

Document Type: JA; (Journal Article) Treatment Code: X; (Experimental); A;  
(Applications)



Descriptors: \*METALLIC MATRIX COMPOSITES; ELECTRONICS PACKAGING;  
ENVIRONMENTAL TESTING; AVIONICS; HEAT SINKS; DESIGN  
Identifiers: STANDARD ELECTRONIC MODULES (SEM); THERMAL MANAGEMENT (TM); NAVY  
AVIONICS; TOTAL DISSIPATED POWER  
EI Classification Codes: 540 (METAL GROUPS); 715 (General Electronic Equipment); 652 (Aircraft); 404 (Military Engineering); 641 (Heat & Thermodynamics); 423 (General Materials Properties & Testing)

1/2/9 of 45

DIALOG No: 03571466 EI Monthly No: EIM9303-011579  
Title: EMI shielding of advanced composite enclosures.  
Author: Glatz, J. J.; Morgan, R.; Neiswinger, D.  
Corporate Source: SPARTA Inc, San Diego, CA, USA  
Conference Title: 6th International SAMPE Electronics Conference  
Conference Location: Baltimore, MD, USA Conference Date: 1992 Jun 22-25  
Source: International SAMPE Electronics Conference v 6 1992. p 131-145  
Publication Year: 1992  
CODEN: ISECE8 ISBN: 0-938994-65-4  
Language: English  
Conference Number: 17353  
Document Type: JA; (Journal Article) Treatment Code: X; (Experimental); A; (Applications)  
Descriptors: \*ELECTROMAGNETIC SHIELDING; NONMETALLIC MATRIX COMPOSITES;  
ENCLOSURES; AVIONICS; ELECTRONICS PACKAGING; REINFORCED PLASTICS; METALS  
Identifiers: ADVANCED COMPOSITE ENCLOSURES; AVIONICS ENCLOSURES; METAL REINFORCED PLASTICS; AIR TRANSPORTABLE RACK (ATR); ELECTROMAGNETIC INTERFERENCE (EMI); EMI SHIELDING  
EI Classification Codes: 711 (Electromagnetic Waves); 817 (Plastics, Products & Applications); 652 (Aircraft); 715 (General Electronic Equipment); 423 (General Materials Properties & Testing); 541 (Aluminum & Alloys)

1/2/10 of 45

DIALOG No: 03569738 EI Monthly No: EI9303027060  
Title: Numerical modelling of normal impact on ceramic composite armours.  
Author: Cortes, R.; Navarro, C.; Martinez, M. A.; Rodriguez, J.; Sanchez-Galvez, V.  
Corporate Source: Polytechnic Univ of Madrid, Madrid, Spain  
Source: International Journal of Impact Engineering v 12 n 4 1992 p 639-651  
Publication Year: 1992  
CODEN: IJIED4 ISSN: 0734-743X  
Language: English  
Document Type: JA; (Journal Article) Treatment Code: A; (Applications); T; (Theoretical); A; (Applications); T; (Theoretical)

Descriptors: \*ARMOR; IMPACT RESISTANCE; COMPOSITE STRUCTURES;  
CERAMIC  
MATERIALS; PLATE METAL; NUMERICAL ANALYSIS; FAILURE  
(MECHANICAL)  
Identifiers: CERAMIC COMPOSITE ARMOURS; MACROSCOPIC MATERIAL  
BEHAVIOUR;  
PENETRATION PROCESS; COMPUTATIONAL CELL; DAMAGE EVOLUTION  
EQUATION; YIELD  
STRESS  
EI Classification Codes: 404 (Military Engineering); 408 (Structural  
Design); 812 (Ceramics & Refractories); 921 (Applied Mathematics); 931  
(Applied Physics)

1/2/11 of 45

DIALOG No: 03569732 EI Monthly No: EI9303037141  
Title: Response of simulated propellant and explosives to projectile impact -  
III. Experimental and numerical results of warhead penetration and  
fragmentation.  
Author: Yuan, Wenxue; Goldsmith, Werner  
Corporate Source: Univ of California, Berkeley, CA, USA  
Source: International Journal of Impact Engineering v 12 n 4 1992 p 533-558  
Publication Year: 1992  
CODEN: IJIED4 ISSN: 0734-743X  
Language: English  
Document Type: JA; (Journal Article) Treatment Code: A; (Applications); T;  
(Theoretical); X; (Experimental); A; (Applications); T; (Theoretical); X;  
(Experimental)  
Descriptors: \*PROPELLANTS; MATHEMATICAL MODELS; COMPUTER  
SOFTWARE; PLATES  
(STRUCTURAL COMPONENTS); FRACTURE; PROJECTILES; FINITE  
DIFFERENCE METHOD  
Identifiers: WARHEAD PENETRATION; FRAGMENTATION; COMPUTER  
SOFTWARE  
AUTODYN(FRAG); MICROFRACTURE; FRAGMENTATION PROCESSES;  
DYNA2D  
EI Classification Codes: 804 (Chemical Products); 921 (Applied Mathematics);  
723 (Computer Software); 931 (Applied Physics)

1/2/12 of 45

DIALOG No: 03569531 EI Monthly No: EI9303028636  
Title: Study on the dynamic behaviours of polymer-cement composite material.  
Author: Wu, Huimin; Fang, Pin  
Corporate Source: Dep of Civil Engineering  
Source: Journal of Hunan University v 19 n 5 Oct 1992 p 111-119  
Publication Year: 1992  
CODEN: HDAXE3 ISSN: 1000-2472  
Language: English  
Document Type: JA; (Journal Article) Treatment Code: T; (Theoretical)

Descriptors: \*COMPOSITE MATERIALS; POLYMERS; CEMENTS;  
COPOLYMERS; MECHANICAL  
PROPERTIES; EMULSIONS; WAVE PROPAGATION  
Identifiers: PORTLAND CEMENT; ALUMINOUS CEMENT; STYRENE  
METHACRYLATE  
COPOLYMER EMULSIONS; DYNAMIC CHARACTERISTICS  
EI Classification Codes: 415 (Metals, Wood & Other Structural Materials);  
815 (Plastics & Polymeric Materials); 412 (Concrete); 931 (Applied Physics)

1/2/13 of 45

DIALOG No: 03568713 EI Monthly No: EI9303026674

Title: Finite elements analysis of flexural edge wave for composite fan  
blades.

Author: Okumura, Hidehito; Miyachi, Toshio; Fukuda, Masahiro; Nakamura,  
Takashi; Ohtake, Kunihiro

Corporate Source: Natl Aerospace Lab, Tokyo, Jpn

Source: SAE (Society of Automotive Engineers) Transactions v 100 n Sect 1 pt  
2 1991, 912048 p 2208-2215

CODEN: SAETA5 ISSN: 0096-736X ISBN: 1-56091-272-3

Language: English

Document Type: JA; (Journal Article) Treatment Code: A; (Applications); T;  
(Theoretical)

Descriptors: \*AIRCRAFT ENGINES; TURBOMACHINE BLADES; FANS;  
FINITE ELEMENT

METHOD; MATHEMATICAL MODELS; DYNAMIC RESPONSE; COMPUTER  
SIMULATION

Identifiers: FLEXURAL EDGE WAVE; COMPOSITE FAN BLADES; ADVANCED  
TURBOPROP

(ATP); HIGHER ORDER FLEXURAL WAVE

EI Classification Codes: 653 (Aircraft Engines); 921 (Applied Mathematics);  
723 (Computer Software); 931 (Applied Physics); 408 (Structural Design)

1/2/14 of 45

DIALOG No: 03567111 EI Monthly No: EI9303028165

Title: Interaction mechanisms between ceramic particles and atomized metallic  
droplets.

Author: Wu, Yue; Lavernia, Enrique J.

Corporate Source: Univ of California-Irvine, Irvine, CA, USA

Source: Metallurgical Transactions A (Physical Metallurgy and Materials  
Science) v 23A n 10 Oct 1992 p 2923-2937

Publication Year: 1992

CODEN: MTTABN ISSN: 0360-2133

Language: English

Document Type: JA; (Journal Article) Treatment Code: X; (Experimental)

Descriptors: \*CERAMIC MATERIALS; PARTICLES (PARTICULATE  
MATTER); ALUMINUM

ALLOYS; METALLIC MATRIX COMPOSITES; SILICON CARBIDE; POWDERS;  
SOLIDIFICATION

Identifiers: INTERACTION MECHANISMS; CERAMIC PARTICLES;  
ATOMIZED METALLIC  
DROPLETS; ALUMINUM SILICON ALLOYS  
EI Classification Codes: 812 (Ceramics & Refractories); 541 (Aluminum &  
Alloys); 415 (Metals, Wood & Other Structural Materials); 804 (Chemical  
Products); 531 (Metallurgy & Metallography)

1/2/15 of 45

DIALOG No: 03566999 EI Monthly No: EI9303035360  
Title: Fracture behavior of stainless steel-toughened NiAl composite plate.  
Author: Nardone, Vincent C.  
Corporate Source: United Technologies Research Cent, Hartford, CT, USA  
Source: Metallurgical Transactions A (Physical Metallurgy and Materials  
Science) v 23A n 2 Feb 1992 p 563-572  
Publication Year: 1992  
CODEN: MTTABN ISSN: 0360-2133  
Language: English  
Document Type: JA; (Journal Article) Treatment Code: X; (Experimental)  
Descriptors: \*NICKEL ALLOYS; COMPOSITE MATERIALS; TENSILE  
TESTING; FRACTURE;  
TOUGHENING; CRACK PROPAGATION; METAL EXTRUSION  
Identifiers: NICKEL ALUMINUM ALLOYS; STAINLESS STEEL  
TOUGHENING; TRANSVERSE  
ORIENTATION; CHARPY IMPACT TESTING; CRACK GROWTH DIRECTION;  
BORON CARBIDE  
EI Classification Codes: 548 (Nickel & Alloys); 415 (Metals, Wood & Other  
Structural Materials); 931 (Applied Physics); 535 (Rolling, Forging &  
Forming); 804 (Chemical Products)

1/2/16 of 45

DIALOG No: 03565418 EI Monthly No: EI9303036439  
Title: Scattering of an impact wave by a crack in a composite plate.  
Author: Datta, S. K.; Ju, T. H.; Shah, A. H.  
Corporate Source: Univ of Colorado, Boulder, CO, USA  
Source: Journal of Applied Mechanics, Transactions ASME v 59 n 3 Sep 1992 p  
596-603  
Publication Year: 1992  
CODEN: JAMCAV ISSN: 0021-8936  
Language: English  
Document Type: JA; (Journal Article) Treatment Code: T; (Theoretical)  
Descriptors: \*PLATES (STRUCTURAL COMPONENTS); COMPOSITE  
MATERIALS; FINITE  
ELEMENT METHOD; CRACK PROPAGATION  
Identifiers: COMPLETE PLATE CRACK WAVE IMPACT; IMPACT WAVE  
SCATTERING; CRACK-  
TIP SINGULARITY; BICONJUGATE GRADIENT METHOD; EIGHT-NODE  
TRANSITION ELEMENTS;  
UNSYMMETRIC COMPLEX MATRIX EQUATIONS  
EI Classification Codes: 408 (Structural Design); 921 (Applied Mathematics);

421 (Materials Properties)

1/2/17 of 45

DIALOG No: 03565063 EI Monthly No: EI9303028581

Title: Glass fibre reinforced water-resistant gypsum-based composites.

Author: Singh, Manjit; Garg, Mridul

Corporate Source: Central Building Research Inst, Roorkee, India

Source: Cement & Concrete Composites v 14 n 1 1992 p 23-32

Publication Year: 1992

CODEN: CCOCEG ISSN: 0958-9465

Language: English

Document Type: JA; (Journal Article) Treatment Code: X; (Experimental)

Descriptors: \*COMPOSITE MATERIALS; GLASS FIBERS; OPTIMIZATION;  
STRENGTH OF

MATERIALS

Identifiers: WATER-RESISTANT GYPSUM-BASED COMPOSITES; GLASS  
FIBER REINFORCED

COMPOSITES; PLAIN PLASTE COMPOSITES; GYPSUM BINDER

COMPOSITES; GLASS FIBER

OPTIMIZATION; GYPSUM COMPOSITE DURABILITY

EI Classification Codes: 421 (Materials Properties); 921 (Applied

Mathematics); 422 (Materials Testing)

1/2/18 of 45

DIALOG No: 03564825 EI Monthly No: EI9303038992

Title: User's experience with a new composite solder mask system.

Author: Penot, J. M.; Tatsos, P.

Corporate Source: Alcatel CIT, Normandy, Fr

Source: Circuit World v 18 n 4 Aug 1992 p 57-60

Publication Year: 1992

CODEN: CIWODV ISSN: 0305-6120

Language: English

Document Type: JA; (Journal Article) Treatment Code: A; (Applications); T;  
(Theoretical); X; (Experimental)

Descriptors: \*SOLDERING; PRINTED CIRCUIT BOARDS; PRINTED CIRCUIT  
MANUFACTURE;

ENVIRONMENTAL IMPACT; ELECTRIC CONDUCTORS; COATINGS;

SURFACE MOUNT TECHNOLOGY

Identifiers: FRANCE; ALCATEL PRODUCTION PLANT; PHOTODEFINABLE  
SYSTEMS; SOLDER

MASKS; FINE LINE CIRCUITS

EI Classification Codes: 538 (Welding & Bonding); 713 (Electronic Circuits);

454 (Environmental Engineering); 704 (Electric Components & Equipment); 535

(Rolling, Forging & Forming); 715 (General Electronic Equipment)

1/2/19 of 45

DIALOG No: 03563846 EI Monthly No: EI9303033356

Title: Experimental study of the strength degradation of GFRP laminates  
subject to ballistic normal impact.

Author: Jenq, Syh-Tsang; Yang, Shih-Ming; Wu, Jeng-Da  
Corporate Source: Natl Cheng Kung Univ, Tainan, Taiwan  
Source: Chung-Kuo Chi Hsueh Kung Ch'eng Hsueh Pao/Journal of the Chinese Society of Mechanical Engineers v 13 n 1 Feb 1992 p 1-9  
Publication Year: 1992  
CODEN: CCHPEK ISSN: 0257-9731  
Language: English  
Document Type: JA; (Journal Article) Treatment Code: X; (Experimental)  
Descriptors: \*LAMINATES; DEGRADATION; STRENGTH OF MATERIALS; BALLISTICS; IMPACT TESTING  
Identifiers: S-GLASS/EPOXY (FIBERITE HY-E 9134B) LAMINATES; TIP-ENDED CYLINDRICAL IMPACTOR; ULTRASONIC C-SCANNING  
EI Classification Codes: 415 (Metals, Wood & Other Structural Materials); 931 (Applied Physics); 422 (Materials Testing); 753 (Sound Technology & Ultrasonics)

1/2/20 of 45

DIALOG No: 03560487 EI Monthly No: EIM9302-008916  
Title: Automotive exterior body panels with polyurea and the reaction injection molding (RIM) process.  
Author: Wharfield, R. D.  
Corporate Source: General Motors Corp, Flint, MI, USA  
Conference Title: Polyurethanes World Congress 1991  
Conference Location: Nice, Fr Conference Date: 1991 Sep 24-26  
Conference Sponsor: SPI; European Isocyanate Producers Assoc  
Source: Polyurethanes World Congr 91. Publ by Technomic Publ Co Inc, Lancaster, PA, USA. p 661-668  
Publication Year: 1991  
Language: English  
Conference Number: 17401  
Document Type: PA; (Conference Paper) Treatment Code: G; (General Review); A; (Applications)  
Descriptors: \*POLYMERS; POLYURETHANES; AUTOMOBILE MATERIALS; AUTOMOBILE PARTS AND EQUIPMENT; AUTOMOBILE BODIES; REACTION INJECTION MOLDING; PHYSICAL PROPERTIES  
Identifiers: AUTOMOTIVE EXTERIOR BODY PANELS; POLYUREA; DISTINCTNESS OF IMAGE; COMPUTER MODELS; BUSINESS PLANT ASSESSMENT; DIMENSIONAL VERIFICATION  
EI Classification Codes: 818 (Rubber & Elastomers); 815 (Plastics & Polymeric Materials); 662 (Automotive Design & Manufacture); 931 (Applied Physics); 816 (Plastics, Plant Equipment & Processes)

1/2/21 of 45

DIALOG No: 03560460 EI Monthly No: EIM9302-008889  
Title: New interior car components made from polyurethane composites by structural bonding.  
Author: Belle, R.; Blank, N.  
Corporate Source: Teroson GmbH, Heidelberg, Ger  
Conference Title: Polyurethanes World Congress 1991  
Conference Location: Nice, Fr Conference Date: 1991 Sep 24-26  
Conference Sponsor: SPI; European Isocyanate Producers Assoc  
Source: Polyurethanes World Congr 91. Publ by Technomic Publ Co Inc, Lancaster, PA, USA. p 440-449  
Publication Year: 1991  
Language: English  
Conference Number: 17401  
Document Type: PA; (Conference Paper) Treatment Code: X; (Experimental); A; (Applications)  
Descriptors: \*COMPOSITE MATERIALS; POLYURETHANES; AUTOMOBILE PARTS AND EQUIPMENT; BONDING; AUTOMOBILE SEATS; ADHESIVES; RHEOLOGY  
Identifiers: INTERIOR CAR COMPONENTS; STRUCTURAL BONDING; SEAT BACKRESTS; REACTIVITY; CURING SPEED; TEROKAL 806  
EI Classification Codes: 818 (Rubber & Elastomers); 415 (Metals, Wood & Other Structural Materials); 662 (Automotive Design & Manufacture); 802 (Chemical Apparatus & Plants); 804 (Chemical Products)

1/2/22 of 45

DIALOG No: 03558919 EI Monthly No: EIM9302-007348  
Title: Accuracy and precision of well casing surveys and water-level measurements and their impact on water-level contour maps.  
Author: Schalla, Ronald; Lewis, Alan K.; Bates, Derrick J.  
Corporate Source: Pacific Northwest Lab, Richland, WA, USA  
Conference Title: International Symposium on Mapping and Geographic Information Systems  
Conference Location: San Francisco, CA, USA Conference Date: 1990 Jun 21-22  
Conference Sponsor: ASTM, Committee D-18 on Soil & Rock; US Geological Survey  
Source: ASTM Special Technical Publication n 1126. Publ by ASTM, Philadelphia, PA, USA. p 295-309  
Publication Year: 1992  
CODEN: ASTTA8 ISSN: 0066-0558  
Language: English  
Conference Number: 17250  
Document Type: PA; (Conference Paper) Treatment Code: G; (General Review); A; (Applications)  
Descriptors: \*MAPS; GROUNDWATER; WATER LEVELS; MEASUREMENTS; MAPPING; HYDROGRAPHIC SURVEYS; NATURAL SCIENCES COMPUTING

Identifiers: WELL CASING SURVEYS; WATER LEVEL CONTOUR MAPS;  
ACCURACY;  
PRECISION; DATA QUALITY OBJECTIVES; GEOGRAPHIC INFORMATION  
SYSTEM

EI Classification Codes: 405 (Construction Equipment & Methods); 943  
(Mechanical & Miscellaneous Measuring Instruments); 723 (Computer  
Software);  
444 (Water Resources)

1/2/23 of 45

DIALOG No: 03558447 EI Monthly No: EIM9302-006876

Title: Analysis related to the impact of composite panels.

Author: Perry, Ronald; Palazotto, Anthony; Sandhu, Raghbor

Corporate Source: Air Force Inst of Technology, WPAFB, OH, USA

Conference Title: Proceedings of the 3rd International Conference on  
Engineering, Construction, and Operations in Space III

Conference Location: Denver, CO, USA Conference Date: 1992 May 31-Jun 4

Source: Proc 3 Int Conf Eng Constr Oper Space III. Publ by ASCE, New York,  
NY, USA. p 1286-1296

Publication Year: 1992

ISBN: 0-87262-868-x

Language: English

Conference Number: 16701

Document Type: PA; (Conference Paper) Treatment Code: T; (Theoretical); A;  
(Applications)

Descriptors: \*COMPOSITE STRUCTURES; STRUCTURAL ANALYSIS;  
MATHEMATICAL MODELS;

SHELLS (STRUCTURES); SPACE RESEARCH

Identifiers: COMPOSITE PANELS; LOW VELOCITY IMPACT; TRANSVERSE  
SHEAR

EI Classification Codes: 408 (Structural Design); 921 (Applied Mathematics);  
656 (Space Flight)

1/2/24 of 45

DIALOG No: 03558446 EI Monthly No: EIM9302-006875

Title: Measuring vibration in an advanced composite beam with localized  
internal fiber-optic strain sensors.

Author: Jensen, David W.; Cory, John M. Jr.

Corporate Source: Pennsylvania State Univ, University Park, PA, USA

Conference Title: Proceedings of the 3rd International Conference on  
Engineering, Construction, and Operations in Space III

Conference Location: Denver, CO, USA Conference Date: 1992 May 31-Jun 4

Source: Proc 3 Int Conf Eng Constr Oper Space III. Publ by ASCE, New York,  
NY, USA. p 1273-1285

Publication Year: 1992

ISBN: 0-87262-868-x

Language: English

Conference Number: 16701

Document Type: PA; (Conference Paper) Treatment Code: T; (Theoretical); X;



(Experimental)

Descriptors: \*COMPOSITE BEAMS AND GIRDERS; VIBRATION

MEASUREMENT;

MATHEMATICAL MODELS; FIBER OPTIC SENSORS; STRAIN; STRUCTURAL ANALYSIS

Identifiers: ADVANCED COMPOSITES; FIBER OPTIC STRAIN SENSORS; NATURAL

FREQUENCY; MODAL AMPLITUDE

EI Classification Codes: 408 (Structural Design); 921 (Applied Mathematics); 943 (Mechanical & Miscellaneous Measuring Instruments); 941 (Acoustical & Optical Measuring Instruments)

1/2/25 of 45

DIALOG No: 03557652 EI Monthly No: EIM9302-006081

Title: Resistance of carbon-based materials for the ITER divertor under different radiation fluxes.

Author: Burtseva, T. A.; Chugunov, O. K.; Dovguchits, E. F.; Komarov, V. L.; Mazul, I. V.; Mitrofansky, A. A.; Persin, M. I.; Prokofiev, Yu. G.; Sokolov, V. A.; Trofimchuk, E. I.; Zav'jalsky, L. P.

Corporate Source: D.V. Efremov Inst, St. Petersburg, Russia

Conference Title: Proceedings of the 5th International Conference on Fusion Reactor Materials - ICFRM-5

Conference Location: Clearwater, FL, USA Conference Date: 1991 Nov 17-22

Source: Journal of Nuclear Materials v 191-94 pt A Sep 1992. p 309-314

Publication Year: 1992

CODEN: JNUMAM ISSN: 0022-3115

Language: English

Conference Number: 17541

Document Type: JA; (Journal Article) Treatment Code: A; (Applications); X; (Experimental)

Descriptors: \*COMPOSITE MATERIALS; CARBON; RADIATION EFFECTS; DOSIMETRY; IONS;

ELECTRONS; NEUTRONS

Identifiers: INTERNATIONAL THERMONUCLEAR EXPERIMENTAL REACTOR (ITER);

DIVERTORS; THERMAL SHOCK RESISTANCE; PLASMA DISRUPTIONS; THERMAL EROSION;

CRACKING RESISTANCE

EI Classification Codes: 804 (Chemical Products); 622 (Radioactive Materials); 932 (High Energy, Nuclear & Plasma Physics); 931 (Applied Physics); 421 (Materials Properties); 621 (Nuclear Reactors)

1/2/26 of 45

DIALOG No: 03555901 EI Monthly No: EI9302018343

Title: Study of the physical properties of epoxy resin composites reinforced with knitted glass fiber fabrics.

Author: Chou, Shen; Wu, Chi-Jen

Corporate Source: Natl Taiwan Inst of Technology, Taipei, Taiwan

Source: Journal of Reinforced Plastics and Composites v 11 n 11 Nov 1992 p

1239-1250

Publication Year: 1992

CODEN: JRPCDW ISSN: 0731-6844

Language: English

Document Type: JA; (Journal Article) Treatment Code: A; (Applications); X; (Experimental)

Descriptors: \*GLASS FIBER REINFORCED PLASTICS; EPOXY RESINS; MECHANICAL

PROPERTIES; STRENGTH OF MATERIALS; KNIT FABRICS

Identifiers: EPOXY RESIN COMPOSITES; KNITTED GLASS FIBER FABRICS; RIB STITCH

STRUCTURAL FABRIC (RSSF) COMPOSITE; PLAIN WEAVE STRUCTURAL FABRIC (PWSF) COMPOSITE

EI Classification Codes: 817 (Plastics, Products & Applications); 815

(Plastics & Polymeric Materials); 421 (Materials Properties); 819 (Textile & Fiber Technology)

1/2/27 of 45

DIALOG No: 03555899 EI Monthly No: EI9302015658

Title: Correlation of residual strength with acoustic emission from impact-damaged composite structures under constant biaxial load.

Author: Hamstad, M. A.; Whittaker, J. W.; Brosey, W. D.

Corporate Source: Univ of Denver, Denver, CO, USA

Source: Journal of Composite Materials v 26 n 15 1992 p 2307-2328

Publication Year: 1992

CODEN: JCOMBI ISSN: 0021-9983

Language: English

Document Type: JA; (Journal Article) Treatment Code: T; (Theoretical)

Descriptors: \*COMPOSITE STRUCTURES; IMPACT TESTING; LOADS (FORCES); RESIDUAL

STRESSES; ACOUSTIC EMISSION TESTING

Identifiers: IMPACT DAMAGE; RESIDUAL STRENGTH; BIAXIAL TEST SPECIMEN; STATIC LOAD

EI Classification Codes: 408 (Structural Design); 421 (Materials Properties)

1/2/28 of 45

DIALOG No: 03555895 EI Monthly No: EI9302022243

Title: Impact resistance of composite laminated sandwich plates.

Author: Kim, Chun-Gon; Jun, Eui-Jin

Corporate Source: Korea Advanced Inst of Science and Technology, Taejon, Korea

Source: Journal of Composite Materials v 26 n 15 1992 p 2247-2261

Publication Year: 1992

CODEN: JCOMBI ISSN: 0021-9983

Language: English

Document Type: JA; (Journal Article) Treatment Code: T; (Theoretical); X;

(Experimental)

Descriptors: \*PLATES (STRUCTURAL COMPONENTS); LAMINATED COMPOSITES; IMPACT RESISTANCE; SANDWICH STRUCTURES; INTERFACES (MATERIALS); STRENGTH OF MATERIALS

Identifiers: COMPOSITE LAMINATED SANDWICH PLATES; IMPACT DELAMINATION; GRAPHITE/EPOXY FACES; NOMEX HONEYCOMB CORE; DEPLY TECHNIQUE

EI Classification Codes: 408 (Structural Design); 421 (Materials Properties)

1/2/29 of 45

DIALOG No: 03555892 EI Monthly No: EI9302015629

Title: Fracture of delaminated unidirectional composite beams.

Author: Shi, Y. B.; Hull, D.

Corporate Source: Univ of Liverpool, Liverpool, UK

Source: Journal of Composite Materials v 26 n 15 1992 p 2172-2195

Publication Year: 1992

CODEN: JCOMBI ISSN: 0021-9983

Language: English

Document Type: JA; (Journal Article) Treatment Code: T; (Theoretical); X; (Experimental)

Descriptors: \*COMPOSITE BEAMS AND GIRDERS; FRACTURE; LAMINATED COMPOSITES;

FIBER REINFORCED MATERIALS; MATHEMATICAL MODELS;

MICROSCOPIC EXAMINATION;

THERMOANALYSIS

Identifiers: DELAMINATED UNIDIRECTIONAL COMPOSITE BEAMS;

THERMAL DEPLY

CHARACTERIZATIONS; CRACKED BEAM CONFIGURATION; GENERAL BEAM GEOMETRY

EI Classification Codes: 408 (Structural Design); 421 (Materials Properties); 921 (Applied Mathematics); 741 (Optics & Optical Devices)

1/2/30 of 45

DIALOG No: 03555584 EI Monthly No: EI9302021061

Title: NiAl-based microstructurally toughened composites.

Author: Nardone, Vincent C.; Strife, James R.

Corporate Source: United Technologies Research Cent, E. Hartford, CT, USA

Source: Metallurgical Transactions A (Physical Metallurgy and Materials Science) v 22A n 1 Jan 1991 p 183-189

Publication Year: 1991

CODEN: MTTABN ISSN: 0360-2133

Language: English

Document Type: JA; (Journal Article) Treatment Code: X; (Experimental)

Descriptors: \*NICKEL ALLOYS; METALLIC MATRIX COMPOSITES; COMPOSITE MATERIALS;

TOUGHENING; MECHANICAL PROPERTIES; CRACK PROPAGATION;  
TENSILE TESTING

Identifiers: NICKEL ALUMINUM ALLOYS; MICROSTRUCTURALLY  
TOUGHENING; IMPACT  
TESTING

EI Classification Codes: 548 (Nickel & Alloys); 415 (Metals, Wood & Other  
Structural Materials); 931 (Applied Physics)

1/2/31 of 45

DIALOG No: 03555583 EI Monthly No: EI9302014327

Title: Microstructurally toughened particulate-reinforced aluminum matrix  
composites.

Author: Nardone, Vincent C.; Strife, James R.; Prewo, K. M.

Corporate Source: United Technologies Research Cent, E. Hartford, CT, USA

Source: Metallurgical Transactions A (Physical Metallurgy and Materials  
Science) v 22A n 1 Jan 1991 p 171-182

Publication Year: 1991

CODEN: MTTABN ISSN: 0360-2133

Language: English

Document Type: JA; (Journal Article) Treatment Code: X; (Experimental)

Descriptors: \*ALUMINUM ALLOYS; METALLIC MATRIX COMPOSITES;  
COMPOSITE

MATERIALS; SILICON CARBIDE; PARTICLES (PARTICULATE MATTER);  
SEGREGATION

(METALLOGRAPHY); TOUGHENING

Identifiers: PARTICULATE REINFORCED ALUMINUM; ENERGY  
ABSORPTION; DAMAGE

TOLERANCE; CRACK FRONT DEFLECTION LENGTH

EI Classification Codes: 541 (Aluminum & Alloys); 415 (Metals, Wood & Other  
Structural Materials); 804 (Chemical Products); 531 (Metallurgy &  
Metallography); 931 (Applied Physics)

1/2/32 of 45

DIALOG No: 03553827 EI Monthly No: EI9302013902

Title: Penetration of impact waves in a six-ply fibre composite laminate.

Author: Rogerson, G. A.

Corporate Source: Univ of Nottingham, Nottingham, England

Source: Journal of Sound and Vibration v 158 n 1 Oct 8 1992 p 105-120

Publication Year: 1992

CODEN: JSVIAG ISSN: 0022-460X

Language: English

Document Type: JA; (Journal Article) Treatment Code: T; (Theoretical)

Descriptors: \*ACOUSTIC WAVES; COMPOSITE MATERIALS;  
MATHEMATICAL MODELS;

ELASTICITY; INTEGRAL EQUATIONS; COMPUTERS

Identifiers: IMPACT WAVES; SIX-PLY FIBRE COMPOSITE LAMINATE;  
IMPULSIVE LINE

LOAD; TRANSVERSELY ISOTROPIC ELASTIC MATERIAL; INTEGRAL  
TRANSFORMS; PROPAGATOR

## MATRIX METHOD

EI Classification Codes: 751 (Acoustics); 415 (Metals, Wood & Other Structural Materials); 921 (Applied Mathematics); 421 (Materials Properties); 723 (Computer Software)

1/2/33 of 45

DIALOG No: 03553389 EI Monthly No: EI9302017701

Title: Characterization of damage modes in impacted thermoset and thermoplastic composites.

Author: Srinivasan, K.; Jackson, W. C.; Smith, B. T.; Hinkley, J. A.

Corporate Source: Old Dominion Univ, Norfolk, VA, USA

Source: Journal of Reinforced Plastics and Composites v 11 n 10 Oct 1992 p 1111-1126

Publication Year: 1992

CODEN: JRPCDW ISSN: 0731-6844

Language: English

Document Type: JA; (Journal Article) Treatment Code: X; (Experimental)

Descriptors: \*FIBER REINFORCED PLASTICS; MECHANICAL PROPERTIES; IMPACT

RESISTANCE; IMPACT TESTING; MICROSCOPIC EXAMINATION;

CHARACTERIZATION;

THERMOPLASTICS

Identifiers: DAMAGE PROPAGATION; IMPACT INDUCED DAMAGE; POST IMPACT

COMPRESSION; DAMAGE TOLERANCE

EI Classification Codes: 817 (Plastics, Products & Applications); 421

(Materials Properties); 741 (Optics & Optical Devices); 815 (Plastics &

Polymeric Materials)

1/2/34 of 45

DIALOG No: 03552303 EI Monthly No: EI9302021102

Title: Laminated material for impact noise abatement and its applications.

Author: Rivin, Eugene I.

Corporate Source: Wayne State Univ, Detroit, MI, USA

Source: Noise Control Engineering Journal v 38 n 3 May-Jun 1992 p 127-131

Publication Year: 1992

CODEN: NCEJD5 ISSN: 0736-2501

Language: English

Document Type: JA; (Journal Article) Treatment Code: A; (Applications); X; (Experimental)

Descriptors: \*NOISE ABATEMENT; SOUND INSULATING MATERIALS; ACOUSTIC WAVE

ABSORPTION; SOUND INSULATING MATERIALS; LAMINATED

COMPOSITES; PUNCH PRESSES

Identifiers: IMPACT NOISE; LOAD DEFLECTION; IMPACT DAMPERS; REPETITIVE

IMPACTS

EI Classification Codes: 751 (Acoustics); 603 (Machine Tools)

1/2/35 of 45

DIALOG No: 03552284 EI Monthly No: EI9302015079

Title: Effect of titanate coupling agent on electromagnetic interference shielding effectiveness and mechanical properties of PC-ABS-NCF composite.

Author: Chiang, Wen-Yen; Chiang, Yung-Shin

Corporate Source: Tatung Inst of Technology, Taipei, Taiwan

Source: Journal of Applied Polymer Science v 46 n 4 Oct 5 1992 p 673-681

Publication Year: 1992

CODEN: JAPNAB ISSN: 0021-8995

Language: English

Document Type: JA; (Journal Article) Treatment Code: X; (Experimental); A; (Applications)

Descriptors: \*CARBON FIBER REINFORCED PLASTICS; TITANIUM COMPOUNDS;

ELECTROMAGNETIC SHIELDING; MECHANICAL PROPERTIES;

POLYCARBONATES; ABS RESINS;

COATED MATERIALS

Identifiers: TITANATE COUPLING AGENT; COUPLING AGENT EFFECTS; NICKEL COATED

CARBON FIBER (NCF); POLYCARBONATE (PC); ACRYLONITRILE

BUTADIENE STYRENE (ABS);

PC ABS NCF COMPOSITE

EI Classification Codes: 817 (Plastics, Products & Applications); 804

(Chemical Products); 711 (Electromagnetic Waves); 421 (Materials Properties);

548 (Nickel & Alloys); 741 (Optics & Optical Devices)

1/2/36 of 45

DIALOG No: 03551695 EI Monthly No: EI9302019146

Title: Impact damage and residual tension strength of a thick graphite/epoxy rocket motor case.

Author: Poe, C. C. Jr.

Corporate Source: NASA, Hampton, VA, USA

Source: Journal of Spacecraft and Rockets v 29 n 3 May-Jun 1992 p 394-404

Publication Year: 1992

CODEN: JSCRAG ISSN: 0022-4650

Language: English

Document Type: JA; (Journal Article) Treatment Code: X; (Experimental); T; (Theoretical)

Descriptors: \*IMPACT TESTING; GRAPHITE FIBER REINFORCED PLASTICS; BOOSTERS

(ROCKET); EPOXY RESINS; RESIDUAL STRESSES; SAFETY FACTOR; STRENGTH OF MATERIALS

Identifiers: IMPACT DAMAGE; RESIDUAL TENSION STRENGTH; ROCKET MOTOR CASE;

GRAPHITE EPOXY CASE; BOOSTER MOTORS; THICK COMPOSITE CASES

EI Classification Codes: 421 (Materials Properties); 422 (Materials

Testing); 817 (Plastics, Products & Applications); 654 (Rockets & Rocket

Propulsion)

1/2/37 of 45

DIALOG No: 03551619 EI Monthly No: EI9302019580

Title: Impact properties of a laminated composite based on ultrahigh carbon steel and brass.

Author: Lee, S.; Oyama, T.; Wadsworth, J.; Sherby, O. D.

Corporate Source: Natl Central Univ, Chung, Taiwan

Source: Materials Science & Engineering A: Structural Materials: Properties, Microstructure and Processing v A154 n 2 Jul 15 1992 p 133-137

Publication Year: 1992

CODEN: MSAPE3 ISSN: 0921-5093

Language: English

Document Type: JA; (Journal Article) Treatment Code: X; (Experimental)

Descriptors: \*LAMINATED COMPOSITES; BIMETALS; CARBON STEEL; BRASS; IMPACT

TESTING; CRACK PROPAGATION; FRACTURE MECHANICS

Identifiers: LAMINATED METAL COMPOSITES; STEEL/BRASS LAMINATED COMPOSITES;

PRESS-BONDED METAL LAMINATES; NOTCH IMPACT TESTING;

ULTRAHIGH CARBON STEEL;

NOTCH PROPAGATION BLUNTING

EI Classification Codes: 531 (Metallurgy & Metallography); 545 (Iron & Steel); 546 (Lead, Tin, Zinc, Antimony & Alloys); 421 (Materials Properties)

1/2/38 of 45

DIALOG No: 00015326 EI Monthly No: EIM9301-005326

Title: The impact of new applications on thermal properties data requirements.

Author: Tye, R. P.; Maesono, A.

Conference Title: Intersociety Conference on Thermal Phenomena in Electronic Systems - I-THERM '92

Conference Location: Austin, TX, USA Conference Date: 1992 Feb 5-8

Conference Sponsor: IEEE Components, Hybrids, & Manufacturing Technology Soc; ASME; ISHM; NIST

Source: Intersoc Conf Therm Phenom Electr Syst I THERM 92. Publ by IEEE, IEEE Service Center, Piscataway, NJ, USA (IEEE cat n 92CH3096-5). p 253-256

Publication Year: 1992

ISBN: 0-7803-0503-5

Language: English

Conference Number: 17469

Document Type: PA; (Conference Paper) Treatment Code: A; (Applications); T; (Theoretical)

Descriptors: \*THERMAL VARIABLES MEASUREMENT; ELECTRONICS PACKAGING; DESIGN; PERFORMANCE

Identifiers: THERMAL ANALYSIS; ELECTRONICS PACKAGING THERMOANALYSIS; THERMAL PARAMETER MEASUREMENT

EI Classification Codes: 944 (Moisture, Pressure & Temperature, & Radiation Measuring Instruments); 714 (Electronic Components)

1/2/39 of 45

DIALOG No: 00014659 EI Monthly No: EIM9301-004659

Title: Impact response of a single edge crack in an orthotropic strip.

Author: Shindo, Yasuhide; Higaki, Hiroaki; Nozaki, Hideaki

Corporate Source: Tohoku Univ, Sendai, Jpn

Conference Title: 1992 ASME Summer Mechanics and Materials Meeting

Conference Location: Tempe, AZ, USA Conference Date: 1992 Apr 28-May 1

Source: American Society of Mechanical Engineers (Paper). Publ by ASME, New York, NY, USA, 92-APM-22. p 1-6

Publication Year: 1992

CODEN: ASMSA4 ISSN: 0402-1215

Language: English

Conference Number: 17382

Document Type: PA; (Conference Paper) Treatment Code: T; (Theoretical)

Descriptors: \*CRACK PROPAGATION; FIBER REINFORCED MATERIALS; LAPLACE

TRANSFORMS; FOURIER TRANSFORMS; INTEGRAL EQUATIONS; STRESSES; DYNAMICS

Identifiers: SINGLE EDGE CRACK IMPACT RESPONSE; MATERIAL ORTHOTROPY;

NUMERICAL LAPLACE INVERSION; DAUL INTEGRAL EQUATIONS; FREDHOLM INTEGRAL

EQUATIONS; ORTHOTROPIC STRIP

EI Classification Codes: 421 (Materials Properties); 921 (Applied

Mathematics); 408 (Structural Design); 931 (Applied Physics)

1/2/40 of 45

DIALOG No: 00014036 EI Monthly No: EIM9301-004036

Title: Methodology for evaluating dredged material alternatives using risk-cost analysis under uncertainty.

Author: Stansbury, J.; Bogardi, I.; Kelly, W. E.

Corporate Source: Univ of Nebraska--Lincoln, Lincoln, NE, USA

Conference Title: Proceedings of the 5th Conference on Risk-Based Decision Making in Water Resources

Conference Location: Santa Barbara, CA, USA Conference Date: 1991 Nov 3-8

Conference Sponsor: Engineering Foundation; ASCE

Source: Risk-Based Decision Making in Water Resources V, Proceedings of the Conference. Publ by ASCE, New York, NY, USA. p 236-259

Publication Year: 1992

CODEN: 85NBAV ISBN: 0-87262-899-X

Language: English

Conference Number: 17355

Document Type: PA; (Conference Paper) Treatment Code: A; (Applications); T; (Theoretical)

Descriptors: \*DREDGING; HAZARDOUS MATERIALS; ENVIRONMENTAL IMPACT; HEALTH

RISKS; RISK ASSESSMENT; WASTE DISPOSAL; COSTS



Identifiers: CONTAMINATED DREDGED MATERIAL DISPOSAL; RISK-COST  
TRADEOFF

ANALYSIS; COMPOSITE PROGRAMMING; MULTICRITERIA DECISION  
MAKING (MCDM) METHOD

EI Classification Codes: 407 (Maritime & Port Structures); 454  
(Environmental Engineering); 914 (Safety Engineering); 723 (Computer  
Software); 921 (Applied Mathematics)

1/2/41 of 45

DIALOG No: 00007470 EI Monthly No: EI9301002918

Title: Wear characteristics of sintered diamond composite during circular  
sawing.

Author: Liao, Y. S.; Luo, S. Y.

Corporate Source: Natl Taiwan Univ, Taipei, Taiwan

Source: Wear v 157 n 2 Sep 15 1992 p 325-337

Publication Year: 1992

CODEN: WEARAH ISSN: 0043-1648

Language: English

Document Type: JA; (Journal Article) Treatment Code: A; (Applications); X;  
(Experimental)

Descriptors: \*DIAMOND CUTTING TOOLS; WEAR OF MATERIALS;

GRANITE; SAWING;

SCANNING ELECTRON MICROSCOPY; X RAY ANALYSIS; COMPOSITE  
MATERIALS

Identifiers: SINTERED DIAMOND COMPOSITE SEGMENTED SAWBLADES;  
CIRCULAR SAWING

EI Classification Codes: 603 (Machine Tools); 421 (Materials Properties);

741 (Optics & Optical Devices); 801 (Chemical Analysis & Physical Chemistry)

1/2/42 of 45

DIALOG No: 00004043 EI Monthly No: EI9301009699

Title: Study on the application of quick-lime consolidated briquette piles in  
loose sandy soils.

Author: Ito, Takao; Asada, Akie; Konno, Tatsuo

Corporate Source: Tohoku Inst of Technology, Sendai, Jpn

Source: Soils and Foundations v 32 n 2 Jun 1992 p 57-66

Publication Year: 1992

CODEN: SOIFBE ISSN: 0038-0806

Language: English

Document Type: JA; (Journal Article) Treatment Code: A; (Applications); X;  
(Experimental)

Descriptors: \*PILES; EARTHQUAKES; BUILDINGS; EARTHQUAKE  
RESISTANCE; SOIL

LIQUEFACTION; STABILIZATION; LIME

Identifiers: QUICKLIME; BRIQUETTE PILES; LOOSE SANDY SOILS;  
UNDERGROUND

STRUCTURES; QUICKLIME CONSOLIDATED BRIQUETTE

EI Classification Codes: 406 (Highway Engineering); 407 (Maritime & Port  
Structures); 483 (Soil Mechanics & Foundations); 402 (Buildings & Towers);

484 (Seismology)

1/2/43 of 45

DIALOG No: 00001261 EI Monthly No: EI9301006680

Title: Residual tensile strength prediction on a ply-by-ply basis for laminates containing impact damage.

Author: Tian, Z.; Swanson, S. R.

Corporate Source: Univ of Utah, Salt Lake City, UT

Source: Journal of Composite Materials v 26 n 8 1992 p 1193-1206

Publication Year: 1992

CODEN: JCOMBI ISSN: 0021-9983

Language: English

Document Type: JA; (Journal Article) Treatment Code: T; (Theoretical)

Descriptors: \*LAMINATED COMPOSITES; FINITE ELEMENT METHOD;  
STRUCTURAL LOADS

Identifiers: RESIDUAL TENSILE STRENGTH; IMPACT LOADING; THROUGH-THICKNESS  
DAMAGE

EI Classification Codes: 415 (Metals, Wood & Other Structural Materials);  
921 (Applied Mathematics); 408 (Structural Design)

1/2/44 of 45

DIALOG No: 00001052 EI Monthly No: EI9301009804

Title: Impact wave propagation in a thick composite plate using dynamic moire interferometry.

Author: Epstein, J. S.; Deason, V. A.; Abdallah, M. G.

Corporate Source: Idaho Natl Engineering Lab, Idaho Falls, ID, USA

Source: Optics and Lasers in Engineering v 17 n 1 1992 p 35-46

Publication Year: 1992

CODEN: OLENDN ISSN: 0143-8166

Language: English

Document Type: JA; (Journal Article) Treatment Code: T; (Theoretical); A;  
(Applications); X; (Experimental)

Descriptors: \*PLATES (STRUCTURAL COMPONENTS); MOIRE FRINGES;  
INTERFEROMETRY;

GRAPHITE FIBERS; DISTANCE MEASUREMENT; COMPOSITE MATERIALS;  
LIGHT PROPAGATION

Identifiers: THICK PLATES; MOIRE INTERFEROMETRY; DYNAMIC  
INTERFEROMETRY;

IMPACT WAVES; COMPOSITE PLATES; DISPLACEMENT SENSITIVITY

EI Classification Codes: 408 (Structural Design); 741 (Optics & Optical  
Devices); 941 (Acoustical & Optical Measuring Instruments)

1/2/45 of 45

DIALOG No: 00000412 EI Monthly No: EI9301000642

Title: Safety and survivability in formula one motor racing.

Author: Savage, Gary

Corporate Source: McLaren Intl

Source: Metals and Materials (Institute of Metals) v 8 n 3 Mar 1992 p 147-153

Publication Year: 1992  
CODEN: MMIMEQ ISSN: 0266-7185  
Language: English  
Document Type: JA; (Journal Article) Treatment Code: X; (Experimental)  
Descriptors: \*AUTOMOBILE BODIES; AUTOMOBILE SAFETY DEVICES;  
ACCIDENT  
PREVENTION; COMPOSITE MATERIALS; CRASHWORTHINESS; CARBON  
FIBERS  
Identifiers: FORMULA ONE MOTOR RACING; CARBON FIBER CHASSIS;  
DRIVER  
SURVIVABILITY  
EI Classification Codes: 662 (Automotive Design & Manufacture); 914 (Safety  
Engineering); 804 (Chemical Products); 415 (Metals, Wood & Other Structural  
Materials)

2/2/1 of 16  
DIALOG No: 03569734 EI Monthly No: EI9303032570  
Title: Ballistic limit for shielded plates subjected to hypervelocity impact.  
Author: Angel, Y. C.; Whitney, J. P.  
Corporate Source: William Marsh Rice Univ, Houston, TX, USA  
Source: International Journal of Impact Engineering v 12 n 4 1992 p 573-583  
Publication Year: 1992  
CODEN: IJIED4 ISSN: 0734-743X  
Language: English  
Document Type: JA; (Journal Article) Treatment Code: A; (Applications); T;  
(Theoretical); A; (Applications); T; (Theoretical)  
Descriptors: \*IMPACT RESISTANCE; BALLISTICS; PLATES (STRUCTURAL  
COMPONENTS);  
PROJECTILES; MATHEMATICAL MODELS; VELOCITY; SHIELDING  
Identifiers: HYPERVELOCITY IMPACT; BALLISTIC LIMIT; CRITICAL  
PROJECTILE  
RADIUS  
EI Classification Codes: 408 (Structural Design); 931 (Applied Physics);  
921 (Applied Mathematics)

2/2/2 of 16  
DIALOG No: 03569462 EI Monthly No: EI9303030914  
Title: Ballistic impact characteristics of aramid fabrics: The influence of interface  
friction.  
Author: Briscoe, B. J.; Motamedi, F.  
Corporate Source: Imperial Coll of Science, Technology and Medicine, London,  
UK  
Source: Wear v 158 n 1-2 Oct 15 1992 p 229-247  
Publication Year: 1992  
CODEN: WEARAH ISSN: 0043-1648  
Language: English  
Document Type: JA; (Journal Article) Treatment Code: T; (Theoretical); X;  
(Experimental); T; (Theoretical); X; (Experimental)

Descriptors: \*FABRICS; BALLISTICS; IMPACT TESTING; FRICTION;  
INTERFACES  
(MATERIALS); ORGANIC POLYMERS; DEFORMATION  
Identifiers: ARAMID FABRICS; BALLISTIC CAPTURE; SURFACE FRICTION;  
SOXHLET  
EXTRACTION; POLYDIMETHYL SILOXANE TREATMENT; INTERFIBER  
INTERYARN FRICTION  
EI Classification Codes: 819 (Textile & Fiber Technology); 931 (Applied  
Physics); 421 (Materials Properties); 815 (Plastics & Polymeric Materials);  
607 (Lubricants & Lubrication); 921 (Applied Mathematics)

2/2/3 of 16

DIALOG No: 03568487 EI Monthly No: EI9303038517

Title: Temperature dependence and magnetic field dependence of quantum point  
contacts in Si-inversion layers.

Author: Wang, S. L.; van Son, P. C.; van Wees, B. J.; Klapwijk, T. M.

Corporate Source: Univ of Groningen, Groningen, Neth

Source: Superlattices and Microstructures v 12 n 2 1992 p 191-193

Publication Year: 1992

CODEN: SUMIEK ISSN: 0749-6036

Language: English

Document Type: JA; (Journal Article) Treatment Code: A; (Applications); X;  
(Experimental)

Descriptors: \*SEMICONDUCTOR QUANTUM WELLS; BALLISTICS;  
MAGNETIC FIELD EFFECTS;  
THERMAL EFFECTS; HALL EFFECT; QUANTUM THEORY; MOSFET  
DEVICES

Identifiers: BALLISTIC TRANSPORT; SILICON INVERSION LAYERS

EI Classification Codes: 714 (Electronic Components); 931 (Applied Physics);

701 (Electricity & Magnetism); 942 (Electrical & Electronic Measuring  
Instruments)

2/2/4 of 16

DIALOG No: 03563846 EI Monthly No: EI9303033356

Title: Experimental study of the strength degradation of GFRP laminates  
subject to ballistic normal impact.

Author: Jenq, Syh-Tsang; Yang, Shih-Ming; Wu, Jeng-Da

Corporate Source: Natl Cheng Kung Univ, Tainan, Taiwan

Source: Chung-Kuo Chi Hsueh Kung Ch'eng Hsueh Pao/Journal of the Chinese  
Society of Mechanical Engineers v 13 n 1 Feb 1992 p 1-9

Publication Year: 1992

CODEN: CCHPEK ISSN: 0257-9731

Language: English

Document Type: JA; (Journal Article) Treatment Code: X; (Experimental)

Descriptors: \*LAMINATES; DEGRADATION; STRENGTH OF MATERIALS;  
BALLISTICS;  
IMPACT TESTING

Identifiers: S-GLASS/EPOXY (FIBERITE HY-E 9134B) LAMINATES; TIP-  
ENDED

CYLINDRICAL IMPACTOR; ULTRASONIC C-SCANNING

EI Classification Codes: 415 (Metals, Wood & Other Structural Materials); 931 (Applied Physics); 422 (Materials Testing); 753 (Sound Technology & Ultrasonics)

2/2/5 of 16

DIALOG No: 03563665 EI Monthly No: EI9303027285

Title: On the flight of a golf ball in the vertical plane.

Author: Stengel, Robert F.

Corporate Source: Princeton Univ, Princeton, NJ, USA

Source: Dynamics and Control v 2 n 2 Apr 1992 p 147-159

Publication Year: 1992

CODEN: DYCOEL ISSN: 0925-4668

Language: English

Document Type: JA; (Journal Article) Treatment Code: A; (Applications); T; (Theoretical)

Descriptors: \*BALLISTICS; EQUATIONS OF MOTION; RANDOM PROCESSES; SENSITIVITY

ANALYSIS

Identifiers: GOLF BALL FLIGHT; LINEARIZED SENSITIVITY ANALYSIS; WIND

UNCERTAINTY; UNCERTAINTY ASSESSMENT; TIME UNCERTAINTY

EI Classification Codes: 931 (Applied Physics); 922 (Statistical Methods);

921 (Applied Mathematics)

2/2/6 of 16

DIALOG No: 03555016 EI Monthly No: EI9302014468

Title: Effect of clamping rigidity of the armour on ballistic performance.

Author: Dikshit, S. N.; Sundararajan, G.

Corporate Source: Defence Metallurgical Research Lab, Hyderabad, India

Source: Defence Science Journal v 42 n 2 Apr 1992 p 117-120

Publication Year: 1992

CODEN: DSJOAA ISSN: 0011-748X

Language: English

Document Type: JA; (Journal Article) Treatment Code: X; (Experimental)

Descriptors: \*ARMOR; PLATE METAL; BALLISTICS; PROJECTILES; IMPACT RESISTANCE;

MECHANICAL PROPERTIES; PERFORMANCE

Identifiers: CLAMPING RIGIDITY; BALLISTIC TESTING; BALLISTIC DAMAGE; IMPACT

VELOCITY

EI Classification Codes: 404 (Military Engineering); 408 (Structural Design); 931 (Applied Physics)

2/2/7 of 16

DIALOG No: 03552953 EI Monthly No: EI9302023494

Title: Numerical study of the effects of longitudinal acceleration on solid rocket motor internal ballistics.

Author: Gottlieb, J. J.; Greatrix, D. R.

Corporate Source: Univ of Toronto, Ont, Can  
Source: Journal of Fluids Engineering, Transactions of the ASME v 114 n 3 Sep 1992 p 404-410  
Publication Year: 1992  
CODEN: JFEGA4 ISSN: 0098-2202  
Language: English  
Document Type: JA; (Journal Article) Treatment Code: X; (Experimental); T; (Theoretical)  
Descriptors: \*ROCKET ENGINES; BALLISTICS; EQUATIONS OF MOTION; PROPELLANTS;  
COMBUSTION; TWO PHASE FLOW; UNSTEADY FLOW  
Identifiers: ACCELERATING MOTOR CHAMBER; CROSSFLOW-DEPENDENT BURNING-RATE  
EQUATIONS; PROPELLANT COMBUSTION; UNSTEADY TWO-PHASE CORE FLOW; RANDOM CHOICE  
METHOD; CONSTANT FORWARD ACCELERATION  
EI Classification Codes: 654 (Rockets & Rocket Propulsion); 931 (Applied Physics); 521 (Combustion & Fuels); 631 (Fluid Flow & Hydrodynamics); 921 (Applied Mathematics)

2/2/8 of 16

DIALOG No: 03551691 EI Monthly No: EI9302022926  
Title: Predicted flight performance of base-bleed projectiles.  
Author: Danberg, James E.; Nietubicz, Charles J.  
Corporate Source: US Army Ballistic Research Lab, Aberdeen Proving Ground, MD, USA  
Source: Journal of Spacecraft and Rockets v 29 n 3 May-Jun 1992 p 366-372  
Publication Year: 1992  
CODEN: JSCRAG ISSN: 0022-4650  
Language: English  
Document Type: JA; (Journal Article) Treatment Code: X; (Experimental); T; (Theoretical)  
Descriptors: \*PROJECTILES; PERFORMANCE; SOLID PROPELLANTS; GAS GENERATORS;  
EQUATIONS OF MOTION; BALLISTICS; DRAG  
Identifiers: FLIGHT PERFORMANCE PREDICTION; BASE BLEED PROJECTILES;  
PROJECTILE RANGE; SOLID PROPELLANT GAS GENERATOR; NAVIER STOKES EQUATION; MACH NUMBER  
EI Classification Codes: 404 (Military Engineering); 524 (Solid Fuels); 654 (Rockets & Rocket Propulsion); 723 (Computer Software); 921 (Applied Mathematics)

2/2/9 of 16

DIALOG No: 03551683 EI Monthly No: EI9302017500  
Title: Navier-Stokes computations for pointed, spherical, and flat tipped shell at Mach 3.  
Author: Guidos, Bernard J.; Weinacht, Paul; Dolling, David S.

Corporate Source: US Army Ballistic Research Lab, Aberdeen Proving Ground, MD, USA

Source: Journal of Spacecraft and Rockets v 29 n 3 May-Jun 1992 p 305-311

Publication Year: 1992

CODEN: JSCRAG ISSN: 0022-4650

Language: English

Document Type: JA; (Journal Article) Treatment Code: X; (Experimental); T; (Theoretical)

Descriptors: \*EQUATIONS OF MOTION; PROJECTILES; SUPERSONIC AERODYNAMICS;

BALLISTICS; WIND TUNNELS; BOUNDARY LAYER FLOW; TURBULENT FLOW

Identifiers: NAVIER STOKES EQUATION; TANGENT OGIVE CYLINDER; POINTED NOSETIP;

SPHERICAL NOSETIP; FLAT NOSETIP; TURBULENT BOUNDARY LAYER

EI Classification Codes: 931 (Applied Physics); 404 (Military Engineering); 651 (Aerodynamics); 723 (Computer Software)

2/2/10 of 16

DIALOG No: 00014611 EI Monthly No: EIM9301-004611

Title: Response of a cylindrical section to an internal blast.

Author: Das Gupta, Aaron

Corporate Source: U.S. Army Ballistic Research Lab, Aberdeen Proving Ground, MD, USA

Conference Title: Proceedings of the 1992 ASME International Computers in Engineering Conference and Exposition

Conference Location: San Francisco, CA, USA Conference Date: 1992 Aug 2-6

Conference Sponsor: ASME

Source: Computers in Engineering, Proceedings of the International Computers in Engineering Conference and Exhibit v 2. Publ by ASME, New York, NY, USA. p 181-184

Publication Year: 1992

CODEN: COENEF ISBN: 0-7918-0935-8

Language: English

Conference Number: 17381

Document Type: PA; (Conference Paper) Treatment Code: T; (Theoretical); X; (Experimental)

Descriptors: \*BALLISTICS; CYLINDERS (CONTAINERS); DYNAMIC RESPONSE;

STRUCTURAL DESIGN; BLAST RESISTANCE; MATHEMATICAL MODELS; EQUATIONS OF MOTION

Identifiers: TRANSIENT RESPONSE; STRUCTURAL INTEGRITY; CUBE ROOT SCALING LAW;

FRIEDLANDER EXPONENTIAL DECAY

EI Classification Codes: 404 (Military Engineering); 931 (Applied Physics);

408 (Structural Design); 921 (Applied Mathematics)

2/2/11 of 16

DIALOG No: 00014609 EI Monthly No: EIM9301-004609

Title: Penetration by long rods.  
Author: Gillis, Peter P.; House, Joel W.; Jones, S. E.  
Corporate Source: Univ of Kentucky, Lexington, KY, USA  
Conference Title: Proceedings of the 1992 ASME International Computers in Engineering Conference and Exposition  
Conference Location: San Francisco, CA, USA Conference Date: 1992 Aug 2-6  
Conference Sponsor: ASME  
Source: Computers in Engineering, Proceedings of the International Computers in Engineering Conference and Exhibit v 2. Publ by ASME, New York, NY, USA. p 163-172  
Publication Year: 1992  
CODEN: COENEF ISBN: 0-7918-0935-8  
Language: English  
Conference Number: 17381  
Document Type: PA; (Conference Paper) Treatment Code: T; (Theoretical); X; (Experimental)  
Descriptors: \*BALLISTICS; ARMOR; MATHEMATICAL MODELS; EQUATIONS OF MOTION; INTERFACES (MATERIALS); MILITARY ENGINEERING  
Identifiers: TARGET PENETRATION; ROD EROSION; MUSHROOM STRAIN  
EI Classification Codes: 404 (Military Engineering); 931 (Applied Physics); 921 (Applied Mathematics)

2/2/12 of 16

DIALOG No: 00014608 EI Monthly No: EIM9301-004608  
Title: Shock damage to sensitive components in an armored vehicle.  
Author: Das Gupta, Aaron; Santiago, Joseph M.; Wisniewski, Henry L.  
Corporate Source: U.S. Army Lab Command, Aberdeen Proving Ground, MD, USA  
Conference Title: Proceedings of the 1992 ASME International Computers in Engineering Conference and Exposition  
Conference Location: San Francisco, CA, USA Conference Date: 1992 Aug 2-6  
Conference Sponsor: ASME  
Source: Computers in Engineering, Proceedings of the International Computers in Engineering Conference and Exhibit v 2. Publ by ASME, New York, NY, USA. p 153-161  
Publication Year: 1992  
CODEN: COENEF ISBN: 0-7918-0935-8  
Language: English  
Conference Number: 17381  
Document Type: PA; (Conference Paper) Treatment Code: G; (General Review); X; (Experimental)  
Descriptors: \*MILITARY VEHICLES; ARMOR; IMPACT RESISTANCE; LOADS (FORCES); BALLISTICS; DYNAMIC RESPONSE; STRUCTURAL DESIGN  
Identifiers: ARMORED VEHICLE; SHOCK DAMAGE; BALLISTIC SHOCK PROPAGATION;



ARMORED PERSONNEL CARRIER (APC) M113

EI Classification Codes: 404 (Military Engineering); 662 (Automotive Design & Manufacture); 633 (Vacuum Technology); 408 (Structural Design); 931 (Applied Physics)

2/2/13 of 16

DIALOG No: 00006201 EI Monthly No: EI9301011170

Title: Ballistic and elastic mean free paths determined by magnetic electron focusing effect in GaAs/AlGaAs.

Author: Takaoka, S.; Tsukagoshi, K.; Wakayama, S.; Murase, K.; Gamo, K.; Namba, S.

Corporate Source: Osaka Univ, Toyonaka, Jpn

Source: Solid State Communications v 83 n 10 Sep 1992 p 775-777

Publication Year: 1992

CODEN: SSCOAA ISSN: 0038-1098

Language: English

Document Type: JA; (Journal Article) Treatment Code: T; (Theoretical); X; (Experimental)

Descriptors: \*SEMICONDUCTING GALLIUM COMPOUNDS;  
SEMICONDUCTING ALUMINUM

COMPOUNDS; SEMICONDUCTOR DEVICES; ELECTRONS; BALLISTICS

Identifiers: GALLIUM ARSENIDE; ELASTIC MEAN FREE PATHS; BALLISTIC  
MEAN FREE

PATHS; MAGNETIC ELECTRON FOCUSING; MULTITERMINAL

SEMICONDUCTOR DEVICES;

ELECTRON CONCENTRATIONS

EI Classification Codes: 712 (Electronic & Thermionic Materials); 714

(Electronic Components); 933 (Solid State Physics)

2/2/14 of 16

DIALOG No: 00005853 EI Monthly No: EI9301010862

Title: Unsteady internal ballistic calculations of solid rocket motors.

Author: Tinaztepe, H. Tugrul; Akmandor, I. Sinan; Ucer, Ahmet S.

Corporate Source: Roketsan Missiles Industries Inc, Ankara, Turk

Source: Journal of Propulsion and Power v 8 n 5 Sep-Oct 1992 p 1125-1128

Publication Year: 1992

CODEN: JPPOEL ISSN: 0748-4658

Language: English

Document Type: JA; (Journal Article) Treatment Code: T; (Theoretical)

Descriptors: \*ROCKET ENGINES; BALLISTICS; SOLID PROPELLANTS;  
UNSTEADY FLOW;

COMBUSTION; EFFICIENCY; CALCULATIONS

Identifiers: SOLID ROCKET MOTORS; UNSTEADY INTERNAL BALLISTICS

EI Classification Codes: 654 (Rockets & Rocket Propulsion); 931 (Applied

Physics); 524 (Solid Fuels); 631 (Fluid Flow & Hydrodynamics); 521

(Combustion & Fuels)

2/2/15 of 16

DIALOG No: 00005830 EI Monthly No: EI9301004324

Title: Calculation of particle trajectories in solid-rocket motors with arbitrary acceleration.  
 Author: Sabnis, Jayant S.; de Jong, Frederik J.; Gibeling, Howard J.  
 Corporate Source: Scientific Research Associates, Inc, Glastonbury, CT, USA  
 Source: Journal of Propulsion and Power v 8 n 5 Sep-Oct 1992 p 961-967  
 Publication Year: 1992  
 CODEN: JPPOEL ISSN: 0748-4658  
 Language: English  
 Document Type: JA; (Journal Article) Treatment Code: T; (Theoretical)  
 Descriptors: \*EXHAUST GASES; TWO PHASE FLOW; SOLID PROPELLANTS; ROCKET  
 ENGINES; PARTICLES (PARTICULATE MATTER); BALLISTICS; TRANSITION FLOW  
 Identifiers: SOLID ROCKET MOTORS; PARTICLE TRAJECTORIES; EULERIAN LAGRANGIAN  
 ANALYSIS; NAVIER STOKES EQUATIONS; LINEARIZED BLOCK IMPLICIT SCHEME  
 EI Classification Codes: 612 (Combustion Engines); 631 (Fluid Flow & Hydrodynamics); 524 (Solid Fuels); 654 (Rockets & Rocket Propulsion); 931 (Applied Physics); 921 (Applied Mathematics)

2/2/16 of 16  
 DIALOG No: 00001266 EI Monthly No: EI9301007890  
 Title: Design philosophy of variable mass preformed fragmented missile warhead.  
 Author: Murthy, K. P. S.; Rama Rao, K.; Patkar, M. R.  
 Corporate Source: Armament Research and Development Establishment, Pune, India  
 Source: Defence Science Journal v 42 n 1 Jan 1992 p 29-38  
 Publication Year: 1992  
 CODEN: DSJOAA ISSN: 0011-748X  
 Language: English  
 Document Type: JA; (Journal Article) Treatment Code: A; (Applications); T; (Theoretical)  
 Descriptors: \*MILITARY ENGINEERING; EXPLOSIVES; MISSILES; MILITARY EQUIPMENT;  
 COMPUTER AIDED DESIGN; BALLISTICS  
 Identifiers: VARIABLE MASS; FRAGMENTED MISSILE WARHEADS; GROUND TARGETS  
 EI Classification Codes: 404 (Military Engineering); 723 (Computer Software)

## Appendix C.

### Sample Input and Output Files of DYNA3D Analysis of High Velocity Impact of a Steel Ball on a Composite Target

#### Dyna3d Sample Input File

```
c ball impact problem                                     88 large
*                                                         88 large
*
*----- ANALYSIS INPUT DATA FOR DYNA3D 88 -----*
*
* Generated by Ingrid - Version # 1992a      (04/05/92)
*
*----- CONTROL CARD #1 -----*
*
* number of materials[1] nodal points[2] solid hexahedron elements[3] beam
* elements[4] 4-node shell elements[5] 8-node solid shell elements[6]
*   2       937       481       0       0       0
*
*----- CONTROL CARD #2 -----*
*
* number of time history blocks for nodes[1] hexahedron elements[2] beam
* elements[3] shell elements[4] thick shell elements[5] and report interval[6]
*   0       0       0       0       0       0
*
*----- CONTROL CARD #3 -----*
*
* number of nodes in DYNA3D-JOY interface[1] number of sliding boundary
* planes[2] sliding boundary planes w/ failure[3] points in density vs depth
* curve[4] brode function flag[5] number of rigid body merge cards[6]
* nodal coordinate format[7]
*   0       0       0       0       0       0e20.0
*
*----- CONTROL CARD #4 -----*
*
* number of load curves[1] concentrated nodal loads[2] element sides having
* pressure loads applied[3] velocity/acceleration boundary condition cards[4]
* rigid walls (stonewalls)[5] nodal constraint cards[6] initial condition
* parameter[7] sliding interfaces[8] base acceleration in x[9] y[10] and
* z-direction[11] angular velocity about x[12] y[13] and z-axis[14] number of
* solid hexahedron elements for momentum deposit[15] detonation points[16]
*   0       0       0       0       0       0       1       1       0       0       0       0       0       0       0       0
*
*----- CONTROL CARD #5 -----*
*
* termination time[1] time history dump interval[2] complete dump interval[3]
* time steps between restart dumps[4] time steps between running restart
* dumps[5] initial time step[6] sliding interface penalty factor[7] thermal
* effects option[8] default viscosity flag[9] computed time step factor[10]
* 1.000E-01 1.000E-03 5.000E-02   0   0 0.000E+00 0.000E+00   0   0 0.000E+00
*
*----- CONTROL CARD #6 -----*
*
* number of joint definitions[1] rigid bodies with extra nodes[2] shell-
* solid interfaces[3] tie-breaking shell slidelines[4] tied node sets with
* failure[5] limiting time step load curve number[6] springs-dampers-masses
* flag[7] rigid bodies with inertial properties[8] dump shell strain flag[9]
* shadow burn flag[10] dump hydro variables flag[11] shell update[12]
* thickness[13] and theory options[14] number of nonreflecting
* boundary segments[15]
*   0       0       0       0       0       0       0       0       0       0       0       0       0       0
*
*----- CONTROL CARD #7 -----*
```

```

*
* number of point constraint nodes[1] coordinate systems for constraint
* nodes[2] minimum step factor[3] number of beam integration rules[4]
* maximum integration points for beams[5] number of shell integration rules[6]
* maximum integration points for shells[7] relaxation iterations between
* checks[8] relaxation tolerance[9] dynamic relaxation factor[10] dynamic
* relaxation time step factor[11] 4-node shell time step option[12]
  0    0 0.000E+00    0    0    0    0 250 1.000E-04 9.950E-01    0    0
*
*----- CONTROL CARD #8 -----*
*
* plane stress plasticity[1] printout flag[2] number of 1D slidelines[3]
  1    0    0
*
*----- MATERIAL CARDS -----*
*
  1  61.3000E+02    0  00.0000E+00  00.0000E+00 00.0000E+00 0.000E+00 0.000E+00
material type # 6 (viscoelastic)
 3.667E+10 0.000E+00 0.000E+00 0.000E+00 0.000E+00 0.000E+00 0.000E+00 0.000E+00
 2.200E+10 0.000E+00 0.000E+00 0.000E+00 0.000E+00 0.000E+00 0.000E+00 0.000E+00
 1.760E+10 0.000E+00 0.000E+00 0.000E+00 0.000E+00 0.000E+00 0.000E+00 0.000E+00
 1.000E+06 0.000E+00 0.000E+00 0.000E+00 0.000E+00 0.000E+00 0.000E+00 0.000E+00
 0.000E+00 0.000E+00 0.000E+00 0.000E+00 0.000E+00 0.000E+00 0.000E+00 0.000E+00
 0.000E+00 0.000E+00 0.000E+00 0.000E+00 0.000E+00 0.000E+00 0.000E+00 0.000E+00
  2  18.0000E+03    0  00.0000E+00  00.0000E+00 00.0000E+00 0.000E+00 0.000E+00
material type # 1 (elastic)
 2.000E+11 0.000E+00 0.000E+00 0.000E+00 0.000E+00 0.000E+00 0.000E+00 0.000E+00
 3.000E-01 0.000E+00 0.000E+00 0.000E+00 0.000E+00 0.000E+00 0.000E+00 0.000E+00
 0.000E+00 0.000E+00 0.000E+00 0.000E+00 0.000E+00 0.000E+00 0.000E+00 0.000E+00
 0.000E+00 0.000E+00 0.000E+00 0.000E+00 0.000E+00 0.000E+00 0.000E+00 0.000E+00
 0.000E+00 0.000E+00 0.000E+00 0.000E+00 0.000E+00 0.000E+00 0.000E+00 0.000E+00
 0.000E+00 0.000E+00 0.000E+00 0.000E+00 0.000E+00 0.000E+00 0.000E+00 0.000E+00
*
*----- NODE DEFINITIONS -----*
*
  1  7.-2.50000000000000E+02 -2.50000000000000E+02 1.00000000000000E+02 7.
  2  7.-2.50000000000000E+02 -2.50000000000000E+02 2.00000000000000E+02 7.
  3  7.-2.50000000000000E+02 -2.1666665649414E+02 1.00000000000000E+02 7.
  4  7.-2.50000000000000E+02 -2.1666665649414E+02 2.00000000000000E+02 7.
  5  7.-2.50000000000000E+02 -1.8333334350586E+02 1.00000000000000E+02 7.
  6  7.-2.50000000000000E+02 -1.8333334350586E+02 2.00000000000000E+02 7.
  7  7.-2.4999998474121E+02 -1.5000001525879E+02 9.9999992370605E+01 7.
  8  7.-2.50000000000000E+02 -1.50000000000000E+02 2.00000000000000E+02 7.
  9  7.-2.50000000000000E+02 -1.1666667938232E+02 1.00000000000000E+02 7.
 10  7.-2.50000000000000E+02 -1.1666667938232E+02 2.00000000000000E+02 7.
 11  7.-2.50000000000000E+02 -8.33333343505859E+01 1.00000000000000E+02 7.
 12  7.-2.50000000000000E+02 -8.33333343505859E+01 2.00000000000000E+02 7.
 13  7.-2.50000000000000E+02 -5.0000007629395E+01 1.00000000000000E+02 7.
 14  7.-2.50000000000000E+02 -5.0000007629395E+01 2.00000000000000E+02 7.
 15  7.-2.4999998474121E+02 -1.66666702270508E+01 9.9999992370605E+01 7.
 16  7.-2.50000000000000E+02 -1.6666687011719E+01 2.00000000000000E+02 7.
 17  7.-2.50000000000000E+02 1.6666664123535E+01 1.00000000000000E+02 7.
 18  7.-2.50000000000000E+02 1.6666664123535E+01 2.00000000000000E+02 7.
 19  7.-2.50000000000000E+02 5.0000000000000E+01 1.00000000000000E+02 7.
 20  7.-2.50000000000000E+02 5.0000000000000E+01 2.00000000000000E+02 7.
 21  7.-2.50000000000000E+02 8.3333320617676E+01 1.00000000000000E+02 7.
 22  7.-2.50000000000000E+02 8.3333320617676E+01 2.00000000000000E+02 7.
 23  7.-2.5000001525879E+02 1.1666667175293E+02 1.00000000000000E+02 7.
 24  7.-2.5000001525879E+02 1.1666667175293E+02 2.00000000000000E+02 7.
 25  7.-2.50000000000000E+02 1.5000000000000E+02 1.00000000000000E+02 7.
 26  7.-2.50000000000000E+02 1.5000000000000E+02 2.00000000000000E+02 7.
 27  7.-2.50000000000000E+02 1.8333334350586E+02 1.00000000000000E+02 7.
 28  7.-2.50000000000000E+02 1.8333334350586E+02 2.00000000000000E+02 7.
 29  7.-2.50000000000000E+02 2.1666665649414E+02 1.00000000000000E+02 7.

```

30 7.-2.5000000000000E+02 2.1666665649414E+02 2.0000000000000E+02 7.  
31 7.-2.5000000000000E+02 2.5000000000000E+02 1.0000000000000E+02 7.  
32 7.-2.5000000000000E+02 2.5000000000000E+02 2.0000000000000E+02 7.  
33 7.-2.1666665649414E+02-2.5000000000000E+02 9.9999992370605E+01 7.  
34 7.-2.1666665649414E+02-2.5000000000000E+02 2.0000000000000E+02 7.  
35 0.-2.1666667175293E+02-2.1666667175293E+02 9.9999984741211E+01 7.  
36 0.-2.1666667175293E+02-2.1666667175293E+02 1.9999998474121E+02 7.  
37 0.-2.1666667175293E+02-1.8333332824707E+02 1.0000002288818E+02 7.  
38 0.-2.1666665649414E+02-1.8333334350586E+02 2.0000001525879E+02 7.  
39 0.-2.1666667175293E+02-1.4999996948242E+02 1.0000000000000E+02 7.  
40 0.-2.1666668701172E+02-1.5000000000000E+02 2.0000000000000E+02 7.  
41 0.-2.1666668701172E+02-1.1666664886475E+02 9.9999992370605E+01 7.  
42 0.-2.1666665649414E+02-1.166666412354E+02 2.0000000000000E+02 7.  
43 0.-2.1666665649414E+02-8.3333343505859E+01 1.0000000762939E+02 7.  
44 0.-2.1666665649414E+02-8.3333343505859E+01 2.0000000000000E+02 7.  
45 0.-2.1666667175293E+02-5.0000019073486E+01 1.0000001525879E+02 7.  
46 0.-2.1666668701172E+02-5.0000003814697E+01 1.9999998474121E+02 7.  
47 0.-2.1666664123535E+02-1.6666715621948E+01 1.0000000000000E+02 7.  
48 0.-2.1666667175293E+02-1.6666685104370E+01 2.0000000000000E+02 7.  
49 0.-2.1666665649414E+02 1.6666656494141E+01 9.9999984741211E+01 7.  
50 0.-2.1666667175293E+02 1.6666671752930E+01 2.0000000000000E+02 7.  
51 0.-2.1666667175293E+02 4.9999984741211E+01 9.9999961853027E+01 7.  
52 0.-2.1666668701172E+02 4.9999992370605E+01 2.0000000000000E+02 7.  
53 0.-2.1666667175293E+02 8.3333328247070E+01 1.0000002288818E+02 7.  
54 0.-2.1666665649414E+02 8.3333312988281E+01 2.0000000000000E+02 7.  
55 0.-2.1666667175293E+02 1.166666412354E+02 1.0000000762939E+02 7.  
56 0.-2.1666667175293E+02 1.1666667175293E+02 2.0000001525879E+02 7.  
57 0.-2.1666667175293E+02 1.5000000000000E+02 9.9999992370605E+01 7.  
58 0.-2.1666665649414E+02 1.5000000000000E+02 2.0000000000000E+02 7.  
59 0.-2.1666665649414E+02 1.8333331298828E+02 9.9999984741211E+01 7.  
60 0.-2.1666667175293E+02 1.8333332824707E+02 2.0000001525879E+02 7.  
61 0.-2.1666665649414E+02 2.1666665649414E+02 9.9999992370605E+01 7.  
62 0.-2.1666665649414E+02 2.1666665649414E+02 1.9999998474121E+02 7.  
63 7.-2.1666665649414E+02 2.5000000000000E+02 1.0000000000000E+02 7.  
64 7.-2.1666665649414E+02 2.5000000000000E+02 2.0000000000000E+02 7.  
65 7.-1.8333334350586E+02-2.5000000000000E+02 1.0000000000000E+02 7.  
66 7.-1.8333334350586E+02-2.5000000000000E+02 2.0000000000000E+02 7.  
67 0.-1.8333331298828E+02-2.1666668701172E+02 1.0000002288818E+02 7.  
68 0.-1.8333332824707E+02-2.1666667175293E+02 2.0000001525879E+02 7.  
69 0.-1.8333334350586E+02-1.8333334350586E+02 9.9999992370605E+01 7.  
70 0.-1.8333334350586E+02-1.8333334350586E+02 1.9999998474121E+02 7.  
71 0.-1.8333332824707E+02-1.5000001525879E+02 9.9999977111816E+01 7.  
72 0.-1.8333334350586E+02-1.5000000000000E+02 2.0000000000000E+02 7.  
73 0.-1.8333337402344E+02-1.1666663360596E+02 1.0000000762939E+02 7.  
74 0.-1.8333334350586E+02-1.166666412354E+02 2.0000000000000E+02 7.  
75 0.-1.8333332824707E+02-8.3333374023438E+01 9.9999969482422E+01 7.  
76 0.-1.8333334350586E+02-8.3333358764648E+01 1.9999998474121E+02 7.  
77 0.-1.8333332824707E+02-5.0000022888184E+01 1.0000003814697E+02 7.  
78 0.-1.8333334350586E+02-5.0000022888184E+01 2.0000000000000E+02 7.  
79 0.-1.8333331298828E+02-1.6666690826416E+01 1.0000003051758E+02 7.  
80 0.-1.8333332824707E+02-1.6666675567627E+01 2.0000000000000E+02 7.  
81 0.-1.8333334350586E+02 1.6666648864746E+01 1.0000000000000E+02 7.  
82 0.-1.8333334350586E+02 1.6666656494141E+01 1.9999998474121E+02 7.  
83 0.-1.8333331298828E+02 5.0000011444092E+01 1.0000000000000E+02 7.  
84 0.-1.8333331298828E+02 5.0000011444092E+01 2.0000000000000E+02 7.  
85 0.-1.8333334350586E+02 8.3333320617676E+01 9.9999992370605E+01 7.  
86 0.-1.8333334350586E+02 8.3333320617676E+01 1.9999998474121E+02 7.  
87 0.-1.8333335876465E+02 1.1666664886475E+02 1.0000001525879E+02 7.  
88 0.-1.8333334350586E+02 1.1666664123535E+02 2.0000000000000E+02 7.  
89 0.-1.8333331298828E+02 1.4999998474121E+02 1.0000000000000E+02 7.  
90 0.-1.8333332824707E+02 1.5000000000000E+02 2.0000000000000E+02 7.  
91 0.-1.8333331298828E+02 1.8333332824707E+02 1.0000000762939E+02 7.  
92 0.-1.8333331298828E+02 1.8333332824707E+02 2.0000000000000E+02 7.  
93 0.-1.8333334350586E+02 2.1666665649414E+02 1.0000000000000E+02 7.

94	0.-1.8333334350586E+02	2.1666665649414E+02	2.0000000000000E+02	7.
95	7.-1.8333334350586E+02	2.5000000000000E+02	1.0000000000000E+02	7.
96	7.-1.8333334350586E+02	2.5000000000000E+02	2.0000000000000E+02	7.
97	7.-1.5000001525879E+02	-2.4999998474121E+02	9.9999992370605E+01	7.
98	7.-1.5000000000000E+02	-2.5000000000000E+02	2.0000000000000E+02	7.
99	0.-1.4999998474121E+02	-2.1666670227051E+02	1.0000000000000E+02	7.
100	0.-1.5000001525879E+02	-2.1666667175293E+02	2.0000000000000E+02	7.
101	0.-1.5000003051758E+02	-1.8333331298828E+02	9.9999984741211E+01	7.
102	0.-1.5000001525879E+02	-1.8333332824707E+02	2.0000001525879E+02	7.
103	0.-1.5000001525879E+02	-1.5000000000000E+02	9.9999992370605E+01	7.
104	0.-1.5000001525879E+02	-1.5000000000000E+02	2.0000000000000E+02	7.
105	0.-1.5000001525879E+02	-1.1666664886475E+02	1.0000001525879E+02	7.
106	0.-1.5000000000000E+02	-1.1666666412354E+02	2.0000000000000E+02	7.
107	0.-1.5000001525879E+02	-8.3333343505859E+01	1.0000001525879E+02	7.
108	0.-1.5000001525879E+02	-8.3333343505859E+01	2.0000000000000E+02	7.
109	0.-1.4999998474121E+02	-5.0000034332275E+01	9.9999984741211E+01	7.
110	0.-1.5000000000000E+02	-5.0000019073486E+01	2.0000000000000E+02	7.
111	0.-1.5000000000000E+02	-1.6666673660278E+01	9.9999977111816E+01	7.
112	0.-1.5000000000000E+02	-1.6666673660278E+01	2.0000001525879E+02	7.
113	0.-1.5000001525879E+02	1.6666679382324E+01	1.0000003051758E+02	7.
114	0.-1.5000000000000E+02	1.6666671752930E+01	2.0000000000000E+02	7.
115	0.-1.5000000000000E+02	4.9999984741211E+01	9.9999977111816E+01	7.
116	0.-1.5000001525879E+02	5.0000000000000E+01	2.0000000000000E+02	7.
117	0.-1.5000003051758E+02	8.3333343505859E+01	1.0000002288818E+02	7.
118	0.-1.5000001525879E+02	8.3333328247070E+01	2.0000000000000E+02	7.
119	0.-1.4999998474121E+02	1.1666663360596E+02	9.9999961853027E+01	7.
120	0.-1.5000000000000E+02	1.1666664123535E+02	1.9999998474121E+02	7.
121	0.-1.4999998474121E+02	1.5000001525879E+02	1.0000001525879E+02	7.
122	0.-1.5000000000000E+02	1.5000000000000E+02	2.0000000000000E+02	7.
123	0.-1.5000000000000E+02	1.833334350586E+02	1.0000000762939E+02	7.
124	0.-1.5000000000000E+02	1.833334350586E+02	2.0000001525879E+02	7.
125	0.-1.5000000000000E+02	2.1666667175293E+02	1.0000000000000E+02	7.
126	0.-1.5000000000000E+02	2.1666667175293E+02	1.9999998474121E+02	7.
127	7.-1.5000000000000E+02	2.5000000000000E+02	1.0000000000000E+02	7.
128	7.-1.5000000000000E+02	2.5000000000000E+02	2.0000000000000E+02	7.
129	7.-1.1666667938232E+02	-2.5000000000000E+02	1.0000000000000E+02	7.
130	7.-1.1666667938232E+02	-2.5000000000000E+02	2.0000000000000E+02	7.
131	0.-1.1666664886475E+02	-2.1666668701172E+02	9.9999992370605E+01	7.
132	0.-1.1666666412354E+02	-2.1666665649414E+02	2.0000000000000E+02	7.
133	0.-1.1666664123535E+02	-1.8333335876465E+02	1.0000001525879E+02	7.
134	0.-1.1666667175293E+02	-1.8333332824707E+02	2.0000001525879E+02	7.
135	0.-1.1666664886475E+02	-1.5000001525879E+02	1.0000001525879E+02	7.
136	0.-1.166666412354E+02	-1.5000000000000E+02	2.0000000000000E+02	7.
137	0.-1.1666667175293E+02	-1.1666668701172E+02	1.0000000000000E+02	7.
138	0.-1.1666667175293E+02	-1.1666668701172E+02	2.0000000000000E+02	7.
139	0.-1.1666667938232E+02	-8.3333328247070E+01	1.0000000762939E+02	7.
140	0.-1.1666666412354E+02	-8.3333343505859E+01	2.0000000000000E+02	7.
141	0.-1.1666667175293E+02	-5.0000000000000E+01	1.0000000000000E+02	7.
142	0.-1.1666667175293E+02	-5.0000000000000E+01	2.0000000000000E+02	7.
143	0.-1.1666667938232E+02	-1.6666679382324E+01	1.0000000000000E+02	7.
144	0.-1.1666667938232E+02	-1.6666679382324E+01	2.0000000000000E+02	7.
145	0.-1.1666667175293E+02	1.6666671752930E+01	1.0000000762939E+02	7.
146	0.-1.1666667175293E+02	1.6666671752930E+01	2.0000000000000E+02	7.
147	0.-1.1666665649414E+02	4.9999969482422E+01	9.9999992370605E+01	7.
148	0.-1.1666667938232E+02	4.9999992370605E+01	2.0000000000000E+02	7.
149	0.-1.1666667175293E+02	8.3333328247070E+01	1.0000000762939E+02	7.
150	0.-1.1666667175293E+02	8.3333328247070E+01	2.0000001525879E+02	7.
151	0.-1.1666666412354E+02	1.1666666412354E+02	1.0000000000000E+02	7.
152	0.-1.1666666412354E+02	1.1666666412354E+02	2.0000000000000E+02	7.
153	0.-1.1666667175293E+02	1.5000000000000E+02	1.0000000000000E+02	7.
154	0.-1.1666667175293E+02	1.5000000000000E+02	2.0000000000000E+02	7.
155	0.-1.1666666412354E+02	1.8333332824707E+02	9.9999992370605E+01	7.
156	0.-1.1666666412354E+02	1.8333332824707E+02	2.0000000000000E+02	7.
157	0.-1.1666665649414E+02	2.1666667175293E+02	1.0000000000000E+02	7.

158	0.-1.1666665649414E+02	2.1666667175293E+02	2.0000000000000E+02	7.
159	7.-1.1666667938232E+02	2.5000000000000E+02	1.0000000000000E+02	7.
160	7.-1.1666667938232E+02	2.5000000000000E+02	2.0000000000000E+02	7.
161	7.-8.3333343505859E+01	-2.5000000000000E+02	9.999992370605E+01	7.
162	7.-8.3333343505859E+01	-2.5000000000000E+02	2.0000000000000E+02	7.
163	0.-8.3333343505859E+01	-2.1666665649414E+02	1.0000000762939E+02	7.
164	0.-8.3333343505859E+01	-2.1666665649414E+02	2.0000000000000E+02	7.
165	0.-8.3333366394043E+01	-1.8333332824707E+02	9.999969482422E+01	7.
166	0.-8.3333343505859E+01	-1.8333334350586E+02	1.999998474121E+02	7.
167	0.-8.3333351135254E+01	-1.5000000000000E+02	1.0000000000000E+02	7.
168	0.-8.3333351135254E+01	-1.5000000000000E+02	1.999998474121E+02	7.
169	0.-8.3333328247070E+01	-1.1666669464111E+02	1.0000000762939E+02	7.
170	0.-8.3333343505859E+01	-1.1666667938232E+02	2.0000000000000E+02	7.
171	0.-8.3333343505859E+01	-8.333335876465E+01	1.0000001525879E+02	7.
172	0.-8.3333343505859E+01	-8.333335876465E+01	2.0000000000000E+02	7.
173	0.-8.3333358764648E+01	-4.9999988555908E+01	9.999969482422E+01	7.
174	0.-8.3333343505859E+01	-5.0000003814697E+01	2.0000000000000E+02	7.
175	0.-8.3333343505859E+01	-1.6666687011719E+01	1.0000000762939E+02	7.
176	0.-8.3333343505859E+01	-1.6666687011719E+01	2.0000000000000E+02	7.
177	0.-8.3333358764648E+01	1.6666687011719E+01	1.0000003051758E+02	7.
178	0.-8.3333343505859E+01	1.6666671752930E+01	2.0000001525879E+02	7.
179	0.-8.3333358764648E+01	5.0000011444092E+01	1.0000001525879E+02	7.
180	0.-8.3333343505859E+01	4.9999996185303E+01	2.0000000000000E+02	7.
181	0.-8.3333358764648E+01	8.3333343505859E+01	1.0000003051758E+02	7.
182	0.-8.3333343505859E+01	8.3333328247070E+01	2.0000001525879E+02	7.
183	0.-8.3333366394043E+01	1.1666667175293E+02	1.0000001525879E+02	7.
184	0.-8.3333351135254E+01	1.1666665649414E+02	2.0000000000000E+02	7.
185	0.-8.3333351135254E+01	1.5000000000000E+02	1.0000000000000E+02	7.
186	0.-8.3333351135254E+01	1.5000000000000E+02	2.0000000000000E+02	7.
187	0.-8.3333351135254E+01	1.833334350586E+02	1.0000000000000E+02	7.
188	0.-8.3333351135254E+01	1.833334350586E+02	2.0000000000000E+02	7.
189	0.-8.3333343505859E+01	2.1666665649414E+02	1.0000000000000E+02	7.
190	0.-8.3333343505859E+01	2.1666665649414E+02	2.0000000000000E+02	7.
191	7.-8.3333343505859E+01	2.5000000000000E+02	1.0000000000000E+02	7.
192	7.-8.3333343505859E+01	2.5000000000000E+02	2.0000000000000E+02	7.
193	7.-5.0000007629395E+01	-2.5000000000000E+02	1.0000000000000E+02	7.
194	7.-5.0000007629395E+01	-2.5000000000000E+02	2.0000000000000E+02	7.
195	0.-5.0000026702881E+01	-2.1666667175293E+02	1.0000001525879E+02	7.
196	0.-5.0000011444092E+01	-2.1666668701172E+02	1.999998474121E+02	7.
197	0.-5.0000019073486E+01	-1.8333332824707E+02	1.0000004577637E+02	7.
198	0.-5.0000019073486E+01	-1.833334350586E+02	2.0000001525879E+02	7.
199	0.-5.0000026702881E+01	-1.4999998474121E+02	9.999984741211E+01	7.
200	0.-5.0000011444092E+01	-1.5000000000000E+02	2.0000000000000E+02	7.
201	0.-5.0000007629395E+01	-1.1666667175293E+02	1.0000000000000E+02	7.
202	0.-5.0000007629395E+01	-1.1666667175293E+02	2.0000000000000E+02	7.
203	0.-4.9999996185303E+01	-8.3333358764648E+01	9.999977111816E+01	7.
204	0.-5.0000011444092E+01	-8.3333343505859E+01	2.0000000000000E+02	7.
205	0.-5.0000007629395E+01	-5.0000007629395E+01	1.0000000000000E+02	7.
206	0.-5.0000007629395E+01	-5.0000007629395E+01	2.0000000000000E+02	7.
207	0.-5.000003432275E+01	-1.6666675567627E+01	9.999969482422E+01	7.
208	0.-5.0000019073486E+01	-1.6666690826416E+01	2.0000000000000E+02	7.
209	0.-5.0000015258789E+01	1.6666664123535E+01	1.0000001525879E+02	7.
210	0.-5.0000015258789E+01	1.6666664123535E+01	2.0000000000000E+02	7.
211	0.-5.0000003814697E+01	5.0000011444092E+01	9.999992370605E+01	7.
212	0.-4.9999996185303E+01	5.0000003814697E+01	2.0000000000000E+02	7.
213	0.-5.0000007629395E+01	8.3333328247070E+01	1.0000000000000E+02	7.
214	0.-5.0000007629395E+01	8.3333328247070E+01	2.0000000000000E+02	7.
215	0.-5.0000022888184E+01	1.1666665649414E+02	9.999992370605E+01	7.
216	0.-5.0000015258789E+01	1.1666664886475E+02	2.0000000000000E+02	7.
217	0.-5.0000019073486E+01	1.5000000000000E+02	1.0000000000000E+02	7.
218	0.-5.0000015258789E+01	1.5000000000000E+02	2.0000000000000E+02	7.
219	0.-5.000003432275E+01	1.8333332824707E+02	9.999984741211E+01	7.
220	0.-5.0000030517578E+01	1.8333334350586E+02	2.0000000000000E+02	7.
221	0.-4.9999992370605E+01	2.1666667175293E+02	1.0000001525879E+02	7.

222	0.-4.9999992370605E+01	2.1666665649414E+02	2.0000000000000E+02	7.
223	7.-5.0000007629395E+01	2.5000000000000E+02	1.0000000000000E+02	7.
224	7.-5.0000007629395E+01	2.5000000000000E+02	2.0000000000000E+02	7.
225	7.-1.6666702270508E+01	-2.4999998474121E+02	9.9999992370605E+01	7.
226	7.-1.6666687011719E+01	-2.5000000000000E+02	2.0000000000000E+02	7.
227	0.-1.6666715621948E+01	-2.1666664123535E+02	1.0000000762939E+02	7.
228	0.-1.6666685104370E+01	-2.1666667175293E+02	2.0000001525879E+02	7.
229	0.-1.6666690826416E+01	-1.8333331298828E+02	1.0000003814697E+02	7.
230	0.-1.6666675567627E+01	-1.8333332824707E+02	2.0000001525879E+02	7.
231	0.-1.6666673660278E+01	-1.5000000000000E+02	9.9999969482422E+01	7.
232	0.-1.6666673660278E+01	-1.5000000000000E+02	2.0000000000000E+02	7.
233	0.-1.6666679382324E+01	-1.1666667938232E+02	1.0000000000000E+02	7.
234	0.-1.6666679382324E+01	-1.1666667938232E+02	2.0000000000000E+02	7.
235	0.-1.6666687011719E+01	-8.3333343505859E+01	1.0000001525879E+02	7.
236	0.-1.6666687011719E+01	-8.3333343505859E+01	2.0000001525879E+02	7.
237	0.-1.6666675567627E+01	-5.0000026702881E+01	9.9999969482422E+01	7.
238	0.-1.6666690826416E+01	-5.0000011444092E+01	2.0000000000000E+02	7.
239	0.-1.6666690826416E+01	-1.6666690826416E+01	1.0000002288818E+02	7.
240	0.-1.6666690826416E+01	-1.6666690826416E+01	1.9999998474121E+02	7.
241	0.-1.6666694641113E+01	1.6666664123535E+01	9.9999984741211E+01	7.
242	0.-1.6666687011719E+01	1.6666656494141E+01	2.0000000000000E+02	7.
243	0.-1.6666687011719E+01	5.0000000000000E+01	9.9999977111816E+01	7.
244	0.-1.6666679382324E+01	4.9999992370605E+01	2.0000000000000E+02	7.
245	0.-1.6666702270508E+01	8.3333343505859E+01	1.0000003051758E+02	7.
246	0.-1.6666687011719E+01	8.3333328247070E+01	2.0000000000000E+02	7.
247	0.-1.6666679382324E+01	1.1666665649414E+02	1.0000000762939E+02	7.
248	0.-1.6666679382324E+01	1.1666667175293E+02	2.0000001525879E+02	7.
249	0.-1.6666675567627E+01	1.5000000000000E+02	1.0000000000000E+02	7.
250	0.-1.6666671752930E+01	1.5000000000000E+02	2.0000000000000E+02	7.
251	0.-1.6666683197021E+01	1.8333332824707E+02	1.0000000000000E+02	7.
252	0.-1.6666687011719E+01	1.8333332824707E+02	2.0000000000000E+02	7.
253	0.-1.6666685104370E+01	2.1666667175293E+02	9.9999984741211E+01	7.
254	0.-1.6666687011719E+01	2.1666665649414E+02	2.0000000000000E+02	7.
255	7.-1.6666687011719E+01	2.5000000000000E+02	1.0000000000000E+02	7.
256	7.-1.6666687011719E+01	2.5000000000000E+02	2.0000000000000E+02	7.
257	7.1.6666664123535E+01	-2.5000000000000E+02	9.9999992370605E+01	7.
258	7.1.6666664123535E+01	-2.5000000000000E+02	2.0000000000000E+02	7.
259	0.1.6666654586792E+01	-2.1666664123535E+02	9.9999977111816E+01	7.
260	0.1.6666669845581E+01	-2.1666667175293E+02	2.0000000000000E+02	7.
261	0.1.6666652679443E+01	-1.8333334350586E+02	1.0000000762939E+02	7.
262	0.1.6666660308838E+01	-1.8333334350586E+02	2.0000000000000E+02	7.
263	0.1.6666681289673E+01	-1.5000001525879E+02	1.0000003051758E+02	7.
264	0.1.6666673660278E+01	-1.5000000000000E+02	2.0000000000000E+02	7.
265	0.1.6666671752930E+01	-1.1666667175293E+02	1.0000000762939E+02	7.
266	0.1.6666671752930E+01	-1.1666667175293E+02	2.0000000000000E+02	7.
267	0.1.6666687011719E+01	-8.3333358764648E+01	1.0000002288818E+02	7.
268	0.1.6666671752930E+01	-8.3333343505859E+01	2.0000001525879E+02	7.
269	0.1.6666667938232E+01	-5.0000000000000E+01	1.0000000762939E+02	7.
270	0.1.6666667938232E+01	-5.0000000000000E+01	2.0000000000000E+02	7.
271	0.1.6666667938232E+01	-1.6666694641113E+01	9.9999984741211E+01	7.
272	0.1.6666660308838E+01	-1.6666687011719E+01	2.0000000000000E+02	7.
273	0.1.6666671752930E+01	1.6666667938232E+01	9.9999992370605E+01	7.
274	0.1.6666671752930E+01	1.6666667938232E+01	2.0000000000000E+02	7.
275	0.1.6666683197021E+01	4.9999984741211E+01	9.9999992370605E+01	7.
276	0.1.6666667938232E+01	5.0000000000000E+01	2.0000000000000E+02	7.
277	0.1.6666671752930E+01	8.3333320617676E+01	1.0000000762939E+02	7.
278	0.1.6666671752930E+01	8.3333320617676E+01	2.0000000000000E+02	7.
279	0.1.6666671752930E+01	1.1666667175293E+02	1.0000000000000E+02	7.
280	0.1.6666671752930E+01	1.1666667175293E+02	2.0000000000000E+02	7.
281	0.1.6666675567627E+01	1.5000001525879E+02	9.9999992370605E+01	7.
282	0.1.6666671752930E+01	1.5000000000000E+02	2.0000000000000E+02	7.
283	0.1.6666671752930E+01	1.8333334350586E+02	9.9999984741211E+01	7.
284	0.1.6666664123535E+01	1.8333334350586E+02	2.0000000000000E+02	7.
285	0.1.6666671752930E+01	2.1666665649414E+02	9.9999992370605E+01	7.



286	0.	1.6666671752930E+01	2.1666665649414E+02	2.0000000000000E+02	7.
287	7.	1.6666664123535E+01	2.5000000000000E+02	1.0000000000000E+02	7.
288	7.	1.6666664123535E+01	2.5000000000000E+02	2.0000000000000E+02	7.
289	7.	5.0000000000000E+01	-2.5000000000000E+02	1.0000000762939E+02	7.
290	7.	5.0000000000000E+01	-2.5000000000000E+02	2.0000000000000E+02	7.
291	0.	4.9999977111816E+01	-2.1666665649414E+02	9.9999961853027E+01	7.
292	0.	4.9999984741211E+01	-2.1666668701172E+02	1.999996948242E+02	7.
293	0.	4.9999996185303E+01	-1.8333331298828E+02	1.0000000000000E+02	7.
294	0.	4.9999996185303E+01	-1.8333331298828E+02	2.0000001525879E+02	7.
295	0.	4.9999984741211E+01	-1.4999996948242E+02	9.9999977111816E+01	7.
296	0.	5.0000000000000E+01	-1.5000000000000E+02	2.0000000000000E+02	7.
297	0.	4.9999969482422E+01	-1.1666667175293E+02	9.999992370605E+01	7.
298	0.	4.9999992370605E+01	-1.1666669464111E+02	2.0000000000000E+02	7.
299	0.	5.0000007629395E+01	-8.3333366394043E+01	1.0000002288818E+02	7.
300	0.	4.9999992370605E+01	-8.3333343505859E+01	2.0000000000000E+02	7.
301	0.	5.0000007629395E+01	-5.0000003814697E+01	1.0000000000000E+02	7.
302	0.	5.0000000000000E+01	-4.9999996185303E+01	2.0000000000000E+02	7.
303	0.	4.9999996185303E+01	-1.6666694641113E+01	9.9999984741211E+01	7.
304	0.	4.9999988555908E+01	-1.6666687011719E+01	2.0000000000000E+02	7.
305	0.	4.9999980926514E+01	1.6666679382324E+01	9.999992370605E+01	7.
306	0.	4.9999996185303E+01	1.6666664123535E+01	2.0000000000000E+02	7.
307	0.	4.9999996185303E+01	5.0000000000000E+01	9.999992370605E+01	7.
308	0.	4.9999996185303E+01	5.0000000000000E+01	2.0000000000000E+02	7.
309	0.	4.9999992370605E+01	8.3333320617676E+01	1.0000002288818E+02	7.
310	0.	4.9999992370605E+01	8.3333320617676E+01	2.0000000000000E+02	7.
311	0.	5.0000007629395E+01	1.1666664886475E+02	9.9999984741211E+01	7.
312	0.	5.0000000000000E+01	1.1666665649414E+02	2.0000000000000E+02	7.
313	0.	5.0000003814697E+01	1.5000001525879E+02	9.999992370605E+01	7.
314	0.	5.0000007629395E+01	1.5000000000000E+02	2.0000000000000E+02	7.
315	0.	5.0000000000000E+01	1.8333332824707E+02	1.0000000000000E+02	7.
316	0.	5.0000000000000E+01	1.8333332824707E+02	2.0000000000000E+02	7.
317	0.	5.0000000000000E+01	2.1666667175293E+02	1.0000000762939E+02	7.
318	0.	5.0000000000000E+01	2.1666667175293E+02	2.0000000000000E+02	7.
319	7.	5.0000000000000E+01	2.5000000000000E+02	1.0000000000000E+02	7.
320	7.	5.0000000000000E+01	2.5000000000000E+02	2.0000000000000E+02	7.
321	7.	8.3333320617676E+01	-2.5000000000000E+02	9.999992370605E+01	7.
322	7.	8.3333320617676E+01	-2.5000000000000E+02	2.0000000000000E+02	7.
323	0.	8.3333335876465E+01	-2.1666667175293E+02	1.0000001525879E+02	7.
324	0.	8.3333312988281E+01	-2.1666664123535E+02	1.9999984741211E+02	7.
325	0.	8.3333320617676E+01	-1.8333332824707E+02	9.999992370605E+01	7.
326	0.	8.3333328247070E+01	-1.8333334350586E+02	1.9999984741211E+02	7.
327	0.	8.3333335876465E+01	-1.5000001525879E+02	1.0000001525879E+02	7.
328	0.	8.3333328247070E+01	-1.5000000000000E+02	2.0000000000000E+02	7.
329	0.	8.3333328247070E+01	-1.1666667175293E+02	9.999992370605E+01	7.
330	0.	8.3333328247070E+01	-1.1666667175293E+02	2.0000000000000E+02	7.
331	0.	8.3333343505859E+01	-8.3333366394043E+01	1.0000002288818E+02	7.
332	0.	8.3333328247070E+01	-8.3333343505859E+01	2.0000001525879E+02	7.
333	0.	8.3333328247070E+01	-5.0000007629395E+01	9.999992370605E+01	7.
334	0.	8.3333328247070E+01	-5.0000007629395E+01	1.9999984741211E+02	7.
335	0.	8.3333343505859E+01	-1.6666702270508E+01	1.0000002288818E+02	7.
336	0.	8.3333328247070E+01	-1.6666687011719E+01	2.0000000000000E+02	7.
337	0.	8.3333320617676E+01	1.6666671752930E+01	1.0000000762939E+02	7.
338	0.	8.3333320617676E+01	1.6666671752930E+01	2.0000000000000E+02	7.
339	0.	8.3333320617676E+01	4.9999992370605E+01	1.0000000762939E+02	7.
340	0.	8.3333320617676E+01	4.9999992370605E+01	2.0000000000000E+02	7.
341	0.	8.3333328247070E+01	8.3333328247070E+01	1.0000000762939E+02	7.
342	0.	8.3333328247070E+01	8.3333328247070E+01	2.0000000000000E+02	7.
343	0.	8.3333320617676E+01	1.1666664886475E+02	1.0000000762939E+02	7.
344	0.	8.3333328247070E+01	1.1666665649414E+02	2.0000000000000E+02	7.
345	0.	8.3333320617676E+01	1.5000000000000E+02	9.999992370605E+01	7.
346	0.	8.3333320617676E+01	1.5000000000000E+02	2.0000000000000E+02	7.
347	0.	8.3333328247070E+01	1.8333334350586E+02	1.0000000000000E+02	7.
348	0.	8.3333328247070E+01	1.8333334350586E+02	2.0000000000000E+02	7.
349	0.	8.3333320617676E+01	2.1666665649414E+02	9.9999984741211E+01	7.

350	0.	8.3333320617676E+01	2.1666665649414E+02	2.0000000000000E+02	7.
351	7.	8.3333320617676E+01	2.5000000000000E+02	1.0000000000000E+02	7.
352	7.	8.3333320617676E+01	2.5000000000000E+02	2.0000000000000E+02	7.
353	7.	1.1666667175293E+02	-2.5000001525879E+02	1.0000000762939E+02	7.
354	7.	1.1666667175293E+02	-2.5000001525879E+02	2.0000000000000E+02	7.
355	0.	1.1666666412354E+02	-2.1666665649414E+02	1.0000000762939E+02	7.
356	0.	1.1666667175293E+02	-2.1666667175293E+02	2.0000001525879E+02	7.
357	0.	1.1666667175293E+02	-1.8333334350586E+02	1.0000002288818E+02	7.
358	0.	1.1666665649414E+02	-1.8333334350586E+02	2.0000001525879E+02	7.
359	0.	1.1666664123535E+02	-1.4999998474121E+02	9.9999969482422E+01	7.
360	0.	1.1666664123535E+02	-1.5000001525879E+02	2.0000000000000E+02	7.
361	0.	1.1666666412354E+02	-1.1666667938232E+02	1.0000000762939E+02	7.
362	0.	1.1666666412354E+02	-1.1666667938232E+02	2.0000001525879E+02	7.
363	0.	1.1666667175293E+02	-8.3333366394043E+01	1.0000002288818E+02	7.
364	0.	1.1666665649414E+02	-8.3333351135254E+01	2.0000000000000E+02	7.
365	0.	1.1666665649414E+02	-5.0000015258789E+01	9.999992370605E+01	7.
366	0.	1.1666665649414E+02	-5.0000007629395E+01	1.9999998474121E+02	7.
367	0.	1.1666665649414E+02	-1.6666671752930E+01	1.0000001525879E+02	7.
368	0.	1.1666667175293E+02	-1.6666671752930E+01	2.0000001525879E+02	7.
369	0.	1.1666667175293E+02	1.6666671752930E+01	1.0000000762939E+02	7.
370	0.	1.1666667175293E+02	1.6666671752930E+01	2.0000000000000E+02	7.
371	0.	1.1666664886475E+02	5.0000007629395E+01	9.9999984741211E+01	7.
372	0.	1.1666665649414E+02	5.0000000000000E+01	2.0000000000000E+02	7.
373	0.	1.1666664886475E+02	8.3333320617676E+01	1.0000002288818E+02	7.
374	0.	1.1666665649414E+02	8.3333328247070E+01	2.0000000000000E+02	7.
375	0.	1.1666666412354E+02	1.1666666412354E+02	1.0000000762939E+02	7.
376	0.	1.1666666412354E+02	1.1666666412354E+02	2.0000001525879E+02	7.
377	0.	1.1666664886475E+02	1.4999998474121E+02	1.0000000762939E+02	7.
378	0.	1.1666664886475E+02	1.5000000000000E+02	2.0000000000000E+02	7.
379	0.	1.1666664123535E+02	1.833331298828E+02	9.9999984741211E+01	7.
380	0.	1.1666664123535E+02	1.833331298828E+02	2.0000000000000E+02	7.
381	0.	1.1666667175293E+02	2.1666667175293E+02	1.0000000000000E+02	7.
382	0.	1.1666667175293E+02	2.1666667175293E+02	2.0000000000000E+02	7.
383	7.	1.1666667175293E+02	2.5000001525879E+02	1.0000000000000E+02	7.
384	7.	1.1666667175293E+02	2.5000001525879E+02	2.0000000000000E+02	7.
385	7.	1.5000000000000E+02	-2.5000000000000E+02	1.0000000000000E+02	7.
386	7.	1.5000000000000E+02	-2.5000000000000E+02	2.0000000000000E+02	7.
387	0.	1.5000000000000E+02	-2.1666668701172E+02	9.999992370605E+01	7.
388	0.	1.5000000000000E+02	-2.1666668701172E+02	2.0000000000000E+02	7.
389	0.	1.4999998474121E+02	-1.8333329772949E+02	1.0000000000000E+02	7.
390	0.	1.5000000000000E+02	-1.833331298828E+02	2.0000000000000E+02	7.
391	0.	1.4999998474121E+02	-1.5000001525879E+02	9.999992370605E+01	7.
392	0.	1.5000000000000E+02	-1.5000000000000E+02	2.0000000000000E+02	7.
393	0.	1.5000000000000E+02	-1.1666668701172E+02	1.0000000762939E+02	7.
394	0.	1.5000000000000E+02	-1.1666668701172E+02	2.0000001525879E+02	7.
395	0.	1.5000000000000E+02	-8.3333351135254E+01	1.0000000000000E+02	7.
396	0.	1.5000000000000E+02	-8.3333351135254E+01	2.0000000000000E+02	7.
397	0.	1.5000000000000E+02	-5.0000019073486E+01	1.0000000000000E+02	7.
398	0.	1.5000000000000E+02	-5.0000015258789E+01	2.0000000000000E+02	7.
399	0.	1.5000000000000E+02	-1.6666683197021E+01	1.0000000000000E+02	7.
400	0.	1.5000000000000E+02	-1.6666679382324E+01	2.0000000000000E+02	7.
401	0.	1.5000000000000E+02	1.6666675567627E+01	1.0000000000000E+02	7.
402	0.	1.5000000000000E+02	1.6666671752930E+01	2.0000000000000E+02	7.
403	0.	1.5000001525879E+02	5.0000003814697E+01	9.999992370605E+01	7.
404	0.	1.5000000000000E+02	5.0000007629395E+01	2.0000000000000E+02	7.
405	0.	1.5000000000000E+02	8.3333312988281E+01	9.9999984741211E+01	7.
406	0.	1.5000000000000E+02	8.3333312988281E+01	2.0000000000000E+02	7.
407	0.	1.5000000000000E+02	1.1666664886475E+02	1.0000000000000E+02	7.
408	0.	1.5000000000000E+02	1.1666664886475E+02	2.0000000000000E+02	7.
409	0.	1.5000000000000E+02	1.5000000000000E+02	1.0000000000000E+02	7.
410	0.	1.5000000000000E+02	1.5000000000000E+02	2.0000000000000E+02	7.
411	0.	1.5000000000000E+02	1.8333332824707E+02	1.0000000000000E+02	7.
412	0.	1.5000000000000E+02	1.8333332824707E+02	2.0000000000000E+02	7.
413	0.	1.5000000000000E+02	2.1666667175293E+02	1.0000000000000E+02	7.

414	0.	1.5000000000000E+02	2.1666667175293E+02	2.0000000000000E+02	7.
415	7.	1.5000000000000E+02	2.5000000000000E+02	1.0000000000000E+02	7.
416	7.	1.5000000000000E+02	2.5000000000000E+02	2.0000000000000E+02	7.
417	7.	1.8333334350586E+02	-2.5000000000000E+02	1.0000000000000E+02	7.
418	7.	1.8333334350586E+02	-2.5000000000000E+02	2.0000000000000E+02	7.
419	0.	1.8333331298828E+02	-2.1666665649414E+02	9.9999977111816E+01	7.
420	0.	1.8333332824707E+02	-2.1666667175293E+02	2.0000000000000E+02	7.
421	0.	1.8333331298828E+02	-1.8333334350586E+02	9.999992370605E+01	7.
422	0.	1.8333332824707E+02	-1.8333332824707E+02	1.999998474121E+02	7.
423	0.	1.8333331298828E+02	-1.5000000000000E+02	1.0000000000000E+02	7.
424	0.	1.8333331298828E+02	-1.5000000000000E+02	2.0000000000000E+02	7.
425	0.	1.8333332824707E+02	-1.1666666412354E+02	1.0000000000000E+02	7.
426	0.	1.8333334350586E+02	-1.1666666412354E+02	2.0000000000000E+02	7.
427	0.	1.8333334350586E+02	-8.3333351135254E+01	1.0000000000000E+02	7.
428	0.	1.8333334350586E+02	-8.3333351135254E+01	2.0000000000000E+02	7.
429	0.	1.8333332824707E+02	-5.0000034332275E+01	9.999984741211E+01	7.
430	0.	1.8333334350586E+02	-5.0000030517578E+01	2.0000000000000E+02	7.
431	0.	1.8333332824707E+02	-1.6666683197021E+01	1.0000000000000E+02	7.
432	0.	1.8333332824707E+02	-1.6666687011719E+01	2.0000000000000E+02	7.
433	0.	1.8333334350586E+02	1.6666671752930E+01	9.999992370605E+01	7.
434	0.	1.8333334350586E+02	1.6666664123535E+01	2.0000000000000E+02	7.
435	0.	1.8333332824707E+02	5.0000000000000E+01	1.0000000000000E+02	7.
436	0.	1.8333332824707E+02	5.0000000000000E+01	2.0000000000000E+02	7.
437	0.	1.8333334350586E+02	8.3333320617676E+01	1.0000000000000E+02	7.
438	0.	1.8333334350586E+02	8.3333320617676E+01	2.0000000000000E+02	7.
439	0.	1.8333331298828E+02	1.1666664123535E+02	9.999984741211E+01	7.
440	0.	1.8333331298828E+02	1.1666664123535E+02	2.0000000000000E+02	7.
441	0.	1.8333332824707E+02	1.5000000000000E+02	1.0000000000000E+02	7.
442	0.	1.8333332824707E+02	1.5000000000000E+02	2.0000000000000E+02	7.
443	0.	1.8333332824707E+02	1.8333332824707E+02	9.999984741211E+01	7.
444	0.	1.8333332824707E+02	1.8333332824707E+02	2.0000000000000E+02	7.
445	0.	1.8333334350586E+02	2.1666667175293E+02	1.0000001525879E+02	7.
446	0.	1.8333334350586E+02	2.1666667175293E+02	2.0000000000000E+02	7.
447	7.	1.8333334350586E+02	2.5000000000000E+02	1.0000000000000E+02	7.
448	7.	1.8333334350586E+02	2.5000000000000E+02	2.0000000000000E+02	7.
449	7.	2.1666665649414E+02	-2.5000000000000E+02	1.0000000000000E+02	7.
450	7.	2.1666665649414E+02	-2.5000000000000E+02	2.0000000000000E+02	7.
451	0.	2.1666665649414E+02	-2.1666665649414E+02	9.999992370605E+01	7.
452	0.	2.1666665649414E+02	-2.1666665649414E+02	1.999998474121E+02	7.
453	0.	2.1666665649414E+02	-1.8333334350586E+02	1.0000000000000E+02	7.
454	0.	2.1666665649414E+02	-1.8333334350586E+02	2.0000000000000E+02	7.
455	0.	2.1666668701172E+02	-1.5000000000000E+02	1.0000001525879E+02	7.
456	0.	2.1666668701172E+02	-1.5000000000000E+02	2.0000000000000E+02	7.
457	0.	2.1666665649414E+02	-1.1666668701172E+02	9.999984741211E+01	7.
458	0.	2.1666665649414E+02	-1.1666668701172E+02	1.999998474121E+02	7.
459	0.	2.1666665649414E+02	-8.3333343505859E+01	1.0000000000000E+02	7.
460	0.	2.1666665649414E+02	-8.3333343505859E+01	2.0000000000000E+02	7.
461	0.	2.1666667175293E+02	-4.999992370605E+01	1.0000001525879E+02	7.
462	0.	2.1666667175293E+02	-4.999992370605E+01	2.0000000000000E+02	7.
463	0.	2.1666665649414E+02	-1.6666685104370E+01	9.999984741211E+01	7.
464	0.	2.1666665649414E+02	-1.6666687011719E+01	2.0000000000000E+02	7.
465	0.	2.1666665649414E+02	1.6666671752930E+01	1.0000000000000E+02	7.
466	0.	2.1666665649414E+02	1.6666671752930E+01	2.0000000000000E+02	7.
467	0.	2.1666667175293E+02	5.0000000000000E+01	1.0000000000000E+02	7.
468	0.	2.1666667175293E+02	5.0000000000000E+01	2.0000000000000E+02	7.
469	0.	2.1666665649414E+02	8.3333320617676E+01	9.999984741211E+01	7.
470	0.	2.1666665649414E+02	8.3333320617676E+01	2.0000000000000E+02	7.
471	0.	2.1666665649414E+02	1.1666664886475E+02	9.999992370605E+01	7.
472	0.	2.1666667175293E+02	1.166666412354E+02	2.0000000000000E+02	7.
473	0.	2.1666667175293E+02	1.5000000000000E+02	1.0000000000000E+02	7.
474	0.	2.1666667175293E+02	1.5000000000000E+02	2.0000000000000E+02	7.
475	0.	2.1666667175293E+02	1.8333334350586E+02	1.0000001525879E+02	7.
476	0.	2.1666667175293E+02	1.8333334350586E+02	2.0000001525879E+02	7.
477	0.	2.1666665649414E+02	2.1666665649414E+02	9.999984741211E+01	7.

478	0.	2.1666665649414E+02	2.1666665649414E+02	2.0000000000000E+02	7.
479	7.	2.1666665649414E+02	2.5000000000000E+02	1.0000000000000E+02	7.
480	7.	2.1666665649414E+02	2.5000000000000E+02	2.0000000000000E+02	7.
481	7.	2.5000000000000E+02	-2.5000000000000E+02	1.0000000000000E+02	7.
482	7.	2.5000000000000E+02	-2.5000000000000E+02	2.0000000000000E+02	7.
483	7.	2.5000000000000E+02	-2.1666665649414E+02	1.0000000000000E+02	7.
484	7.	2.5000000000000E+02	-2.1666665649414E+02	2.0000000000000E+02	7.
485	7.	2.5000000000000E+02	-1.8333334350586E+02	1.0000000000000E+02	7.
486	7.	2.5000000000000E+02	-1.8333334350586E+02	2.0000000000000E+02	7.
487	7.	2.5000000000000E+02	-1.5000000000000E+02	1.0000000000000E+02	7.
488	7.	2.5000000000000E+02	-1.5000000000000E+02	2.0000000000000E+02	7.
489	7.	2.5000000000000E+02	-1.1666667938232E+02	1.0000000000000E+02	7.
490	7.	2.5000000000000E+02	-1.1666667938232E+02	2.0000000000000E+02	7.
491	7.	2.5000000000000E+02	-8.3333343505859E+01	1.0000000000000E+02	7.
492	7.	2.5000000000000E+02	-8.3333343505859E+01	2.0000000000000E+02	7.
493	7.	2.5000000000000E+02	-5.0000007629395E+01	1.0000000000000E+02	7.
494	7.	2.5000000000000E+02	-5.0000007629395E+01	2.0000000000000E+02	7.
495	7.	2.5000000000000E+02	-1.6666687011719E+01	1.0000000000000E+02	7.
496	7.	2.5000000000000E+02	-1.6666687011719E+01	2.0000000000000E+02	7.
497	7.	2.5000000000000E+02	1.6666664123535E+01	1.0000000000000E+02	7.
498	7.	2.5000000000000E+02	1.6666664123535E+01	2.0000000000000E+02	7.
499	7.	2.5000000000000E+02	5.0000000000000E+01	1.0000000000000E+02	7.
500	7.	2.5000000000000E+02	5.0000000000000E+01	2.0000000000000E+02	7.
501	7.	2.5000000000000E+02	8.3333320617676E+01	1.0000000000000E+02	7.
502	7.	2.5000000000000E+02	8.3333320617676E+01	2.0000000000000E+02	7.
503	7.	2.5000001525879E+02	1.1666667175293E+02	1.0000000000000E+02	7.
504	7.	2.5000001525879E+02	1.1666667175293E+02	2.0000000000000E+02	7.
505	7.	2.5000000000000E+02	1.5000000000000E+02	1.0000000000000E+02	7.
506	7.	2.5000000000000E+02	1.5000000000000E+02	2.0000000000000E+02	7.
507	7.	2.5000000000000E+02	1.8333334350586E+02	1.0000000000000E+02	7.
508	7.	2.5000000000000E+02	1.8333334350586E+02	2.0000000000000E+02	7.
509	7.	2.5000000000000E+02	2.1666665649414E+02	1.0000000000000E+02	7.
510	7.	2.5000000000000E+02	2.1666665649414E+02	2.0000000000000E+02	7.
511	7.	2.5000000000000E+02	2.5000000000000E+02	1.0000000000000E+02	7.
512	7.	2.5000000000000E+02	2.5000000000000E+02	2.0000000000000E+02	7.
513	0.-5.7735031127930E+01	-5.7735031127930E+01	-5.7735031127930E+01	-5.7735031127930E+01	7.
514	0.-6.7388732910156E+01	-6.7388732910156E+01	-3.0290544509888E+01	-6.7388732910156E+01	7.
515	0.-7.0710678100586E+01	-7.0710678100586E+01	0.0000000000000E+00	-7.0710678100586E+01	7.
516	0.-6.7388732910156E+01	-3.0290544509888E+01	-6.7388732910156E+01	-6.7388732910156E+01	7.
517	0.-8.5871849060059E+01	-3.6235507965088E+01	-3.6235515594482E+01	-8.5871849060059E+01	7.
518	0.-9.2387962341309E+01	-3.8268344879150E+01	0.0000000000000E+00	-9.2387962341309E+01	7.
519	0.-7.0710678100586E+01	0.0000000000000E+00	-7.0710678100586E+01	-7.0710678100586E+01	7.
520	0.-9.2387962341309E+01	0.0000000000000E+00	-3.8268344879150E+01	-9.2387962341309E+01	7.
521	0.-1.0000000000000E+02	0.0000000000000E+00	0.0000000000000E+00	-1.0000000000000E+02	7.
522	0.-5.3867515563965E+01	-5.3867515563965E+01	-5.3867515563965E+01	-5.3867515563965E+01	7.
523	0.-5.8694374084473E+01	-5.8694374084473E+01	-2.7645271301270E+01	-5.8694374084473E+01	7.
524	0.-6.0355339050293E+01	-6.0355339050293E+01	0.0000000000000E+00	-6.0355339050293E+01	7.
525	0.-5.8694374084473E+01	-2.7645271301270E+01	-5.8694374084473E+01	-5.8694374084473E+01	7.
526	0.-6.7935928344727E+01	-3.0617759704590E+01	-3.0617752075195E+01	-6.7935928344727E+01	7.
527	0.-7.1193969726562E+01	-3.1634174346924E+01	0.0000000000000E+00	-7.1193969726562E+01	7.
528	0.-6.0355339050293E+01	0.0000000000000E+00	-6.0355339050293E+01	-6.0355339050293E+01	7.
529	0.-7.1193969726562E+01	0.0000000000000E+00	-3.1634174346924E+01	-7.1193969726562E+01	7.
530	0.-7.5000000000000E+01	0.0000000000000E+00	0.0000000000000E+00	-7.5000000000000E+01	7.
531	0.-5.0000000000000E+01	-5.0000000000000E+01	-5.0000000000000E+01	-5.0000000000000E+01	7.
532	0.-5.0000000000000E+01	-5.0000000000000E+01	-2.5000000000000E+01	-5.0000000000000E+01	7.
533	0.-5.0000000000000E+01	-5.0000000000000E+01	0.0000000000000E+00	-5.0000000000000E+01	7.
534	0.-5.0000000000000E+01	-2.5000000000000E+01	-5.0000000000000E+01	-5.0000000000000E+01	7.
535	0.-5.0000000000000E+01	-2.5000000000000E+01	-2.5000000000000E+01	-5.0000000000000E+01	7.
536	0.-5.0000000000000E+01	-2.5000000000000E+01	0.0000000000000E+00	-5.0000000000000E+01	7.
537	0.-5.0000000000000E+01	0.0000000000000E+00	-5.0000000000000E+01	-5.0000000000000E+01	7.
538	0.-5.0000000000000E+01	0.0000000000000E+00	-2.5000000000000E+01	-5.0000000000000E+01	7.
539	0.-5.0000000000000E+01	0.0000000000000E+00	0.0000000000000E+00	-5.0000000000000E+01	7.
540	0.-6.7388732910156E+01	-6.7388732910156E+01	3.0290544509888E+01	-6.7388732910156E+01	7.
541	0.-5.7735031127930E+01	-5.7735031127930E+01	5.7735031127930E+01	-5.7735031127930E+01	7.

542	0.-8.5871849060059E+01-3.6235507965088E+01	3.6235515594482E+01	7.
543	0.-6.7388732910156E+01-3.0290544509888E+01	6.7388732910156E+01	7.
544	0.-9.2387962341309E+01 0.0000000000000E+00	3.8268344879150E+01	7.
545	0.-7.0710678100586E+01 0.0000000000000E+00	7.0710678100586E+01	7.
546	0.-5.8694374084473E+01-5.8694374084473E+01	2.7645271301270E+01	7.
547	0.-5.3867515563965E+01-5.3867515563965E+01	5.3867515563965E+01	7.
548	0.-6.7935928344727E+01-3.0617752075195E+01	3.0617752075195E+01	7.
549	0.-5.8694374084473E+01-2.7645271301270E+01	5.8694374084473E+01	7.
550	0.-7.1193969726562E+01 0.0000000000000E+00	3.1634174346924E+01	7.
551	0.-6.0355339050293E+01 0.0000000000000E+00	6.0355339050293E+01	7.
552	0.-5.0000000000000E+01-5.0000000000000E+01	2.5000000000000E+01	7.
553	0.-5.0000000000000E+01-5.0000000000000E+01	5.0000000000000E+01	7.
554	0.-5.0000000000000E+01-2.5000000000000E+01	2.5000000000000E+01	7.
555	0.-5.0000000000000E+01-2.5000000000000E+01	5.0000000000000E+01	7.
556	0.-5.0000000000000E+01 0.0000000000000E+00	2.5000000000000E+01	7.
557	0.-5.0000000000000E+01 0.0000000000000E+00	5.0000000000000E+01	7.
558	0.-6.7388732910156E+01 3.0290542602539E+01-6.7388732910156E+01	7.	
559	0.-8.5871849060059E+01 3.6235507965088E+01-3.6235515594482E+01	7.	
560	0.-9.2387962341309E+01 3.8268344879150E+01 0.0000000000000E+00	7.	
561	0.-5.7735031127930E+01 5.7735031127930E+01-5.7735031127930E+01	7.	
562	0.-6.7388732910156E+01 6.7388732910156E+01-3.0290544509888E+01	7.	
563	0.-7.0710678100586E+01 7.0710678100586E+01 0.0000000000000E+00	7.	
564	0.-5.8694374084473E+01 2.7645271301270E+01-5.8694374084473E+01	7.	
565	0.-6.7935928344727E+01 3.0617759704590E+01-3.0617759704590E+01	7.	
566	0.-7.1193969726562E+01 3.1634174346924E+01 0.0000000000000E+00	7.	
567	0.-5.3867515563965E+01 5.3867515563965E+01-5.3867515563965E+01	7.	
568	0.-5.8694374084473E+01 5.8694374084473E+01-2.7645271301270E+01	7.	
569	0.-6.0355339050293E+01 6.0355339050293E+01 0.0000000000000E+00	7.	
570	0.-5.0000000000000E+01 2.5000000000000E+01-5.0000000000000E+01	7.	
571	0.-5.0000000000000E+01 2.5000000000000E+01-2.5000000000000E+01	7.	
572	0.-5.0000000000000E+01 2.5000000000000E+01 0.0000000000000E+00	7.	
573	0.-5.0000000000000E+01 5.0000000000000E+01-5.0000000000000E+01	7.	
574	0.-5.0000000000000E+01 5.0000000000000E+01-2.5000000000000E+01	7.	
575	0.-5.0000000000000E+01 5.0000000000000E+01 0.0000000000000E+00	7.	
576	0.-8.5871849060059E+01 3.6235507965088E+01 3.6235515594482E+01	7.	
577	0.-6.7388732910156E+01 3.0290542602539E+01 6.7388732910156E+01	7.	
578	0.-6.7388732910156E+01 6.7388732910156E+01 3.0290544509888E+01	7.	
579	0.-5.7735031127930E+01 5.7735031127930E+01 5.7735031127930E+01	7.	
580	0.-6.7935928344727E+01 3.0617752075195E+01 3.0617759704590E+01	7.	
581	0.-5.8694374084473E+01 2.7645271301270E+01 5.8694374084473E+01	7.	
582	0.-5.8694374084473E+01 5.8694374084473E+01 2.7645271301270E+01	7.	
583	0.-5.3867515563965E+01 5.3867515563965E+01 5.3867515563965E+01	7.	
584	0.-5.0000000000000E+01 2.5000000000000E+01 2.5000000000000E+01	7.	
585	0.-5.0000000000000E+01 2.5000000000000E+01 5.0000000000000E+01	7.	
586	0.-5.0000000000000E+01 5.0000000000000E+01 2.5000000000000E+01	7.	
587	0.-5.0000000000000E+01 5.0000000000000E+01 5.0000000000000E+01	7.	
588	0.-5.7735031127930E+01-5.7735031127930E+01-5.7735031127930E+01	7.	
589	0.-6.7388732910156E+01-6.7388732910156E+01-3.0290544509888E+01	7.	
590	0.-7.0710678100586E+01-7.0710678100586E+01 0.0000000000000E+00	7.	
591	0.-5.3867515563965E+01-5.3867515563965E+01-5.3867515563965E+01	7.	
592	0.-5.8694374084473E+01-5.8694374084473E+01-2.7645271301270E+01	7.	
593	0.-6.0355339050293E+01-6.0355339050293E+01 0.0000000000000E+00	7.	
594	0.-3.0290544509888E+01-6.7388732910156E+01-6.7388732910156E+01	7.	
595	0.-3.6235507965088E+01-8.5871849060059E+01-3.6235515594482E+01	7.	
596	0.-3.8268344879150E+01-9.2387962341309E+01 0.0000000000000E+00	7.	
597	0.-2.7645271301270E+01-5.8694366455078E+01-5.8694366455078E+01	7.	
598	0.-3.0617759704590E+01-6.7935928344727E+01-3.0617752075195E+01	7.	
599	0.-3.1634174346924E+01-7.1193969726562E+01 0.0000000000000E+00	7.	
600	0.-2.5000000000000E+01-5.0000000000000E+01-5.0000000000000E+01	7.	
601	0.-2.5000000000000E+01-5.0000000000000E+01-2.5000000000000E+01	7.	
602	0.-2.5000000000000E+01-5.0000000000000E+01 0.0000000000000E+00	7.	
603	0. 0.0000000000000E+00-7.0710678100586E+01-7.0710678100586E+01	7.	
604	0. 0.0000000000000E+00-9.2387962341309E+01-3.8268344879150E+01	7.	
605	0. 0.0000000000000E+00-1.0000000000000E+02 0.0000000000000E+00	7.	

606	0. 0.00000000000000E+00-6.0355339050293E+01-6.0355339050293E+01	7.
607	0. 0.00000000000000E+00-7.1193969726562E+01-3.1634174346924E+01	7.
608	0. 0.00000000000000E+00-7.50000000000000E+01 0.00000000000000E+00	7.
609	0. 0.00000000000000E+00-5.00000000000000E+01-5.00000000000000E+01	7.
610	0. 0.00000000000000E+00-5.00000000000000E+01-2.50000000000000E+01	7.
611	0. 0.00000000000000E+00-5.00000000000000E+01 0.00000000000000E+00	7.
612	0.-6.7388732910156E+01-6.7388732910156E+01 3.0290544509888E+01	7.
613	0.-5.7735031127930E+01-5.7735031127930E+01 5.7735031127930E+01	7.
614	0.-5.8694374084473E+01-5.8694374084473E+01 2.7645271301270E+01	7.
615	0.-5.3867515563965E+01-5.3867515563965E+01 5.3867515563965E+01	7.
616	0.-3.6235507965088E+01-8.5871849060059E+01 3.6235515594482E+01	7.
617	0.-3.0290544509888E+01-6.7388732910156E+01 6.7388732910156E+01	7.
618	0.-3.0617752075195E+01-6.7935928344727E+01 3.0617752075195E+01	7.
619	0.-2.7645271301270E+01-5.8694366455078E+01 5.8694366455078E+01	7.
620	0.-2.50000000000000E+01-5.00000000000000E+01 2.50000000000000E+01	7.
621	0.-2.50000000000000E+01-5.00000000000000E+01 5.00000000000000E+01	7.
622	0. 0.00000000000000E+00-9.2387962341309E+01 3.8268344879150E+01	7.
623	0. 0.00000000000000E+00-7.0710678100586E+01 7.0710678100586E+01	7.
624	0. 0.00000000000000E+00-7.1193969726562E+01 3.1634174346924E+01	7.
625	0. 0.00000000000000E+00-6.0355339050293E+01 6.0355339050293E+01	7.
626	0. 0.00000000000000E+00-5.00000000000000E+01 2.50000000000000E+01	7.
627	0. 0.00000000000000E+00-5.00000000000000E+01 5.00000000000000E+01	7.
628	0.-5.7735031127930E+01-5.7735031127930E+01-5.7735031127930E+01	7.
629	0.-5.3867515563965E+01-5.3867515563965E+01-5.3867515563965E+01	7.
630	0.-6.7388732910156E+01-3.0290544509888E+01-6.7388732910156E+01	7.
631	0.-5.8694366455078E+01-2.7645271301270E+01-5.8694366455078E+01	7.
632	0.-7.0710678100586E+01 0.00000000000000E+00-7.0710678100586E+01	7.
633	0.-6.0355339050293E+01 0.00000000000000E+00-6.0355339050293E+01	7.
634	0.-3.0290544509888E+01-6.7388732910156E+01-6.7388732910156E+01	7.
635	0.-2.7645271301270E+01-5.8694366455078E+01-5.8694366455078E+01	7.
636	0.-3.6235511779785E+01-3.6235519409180E+01-8.5871856689453E+01	7.
637	0.-3.0617752075195E+01-3.0617759704590E+01-6.7935928344727E+01	7.
638	0.-2.50000000000000E+01-2.50000000000000E+01-5.00000000000000E+01	7.
639	0.-3.8268344879150E+01 0.00000000000000E+00-9.2387962341309E+01	7.
640	0.-3.1634174346924E+01 0.00000000000000E+00-7.1193969726562E+01	7.
641	0.-2.50000000000000E+01 0.00000000000000E+00-5.00000000000000E+01	7.
642	0. 0.00000000000000E+00-7.0710678100586E+01-7.0710678100586E+01	7.
643	0. 0.00000000000000E+00-6.0355339050293E+01-6.0355339050293E+01	7.
644	0. 0.00000000000000E+00-3.8268344879150E+01-9.2387962341309E+01	7.
645	0. 0.00000000000000E+00-3.1634174346924E+01-7.1193969726562E+01	7.
646	0. 0.00000000000000E+00-2.50000000000000E+01-5.00000000000000E+01	7.
647	0. 0.00000000000000E+00 0.00000000000000E+00-1.00000000000000E+02	7.
648	0. 0.00000000000000E+00 0.00000000000000E+00-7.50000000000000E+01	7.
649	0. 0.00000000000000E+00 0.00000000000000E+00-5.00000000000000E+01	7.
650	0.-2.50000000000000E+01-2.50000000000000E+01-2.50000000000000E+01	7.
651	0.-2.50000000000000E+01-2.50000000000000E+01 0.00000000000000E+00	7.
652	0.-2.50000000000000E+01 0.00000000000000E+00-2.50000000000000E+01	7.
653	0.-2.50000000000000E+01 0.00000000000000E+00 0.00000000000000E+00	7.
654	0. 0.00000000000000E+00-2.50000000000000E+01-2.50000000000000E+01	7.
655	0. 0.00000000000000E+00-2.50000000000000E+01 0.00000000000000E+00	7.
656	0. 0.00000000000000E+00 0.00000000000000E+00-2.50000000000000E+01	7.
657	0. 0.00000000000000E+00 0.00000000000000E+00 0.00000000000000E+00	7.
658	0.-2.50000000000000E+01-2.50000000000000E+01 2.50000000000000E+01	7.
659	0.-2.50000000000000E+01-2.50000000000000E+01 5.00000000000000E+01	7.
660	0.-2.50000000000000E+01 0.00000000000000E+00 2.50000000000000E+01	7.
661	0.-2.50000000000000E+01 0.00000000000000E+00 5.00000000000000E+01	7.
662	0. 0.00000000000000E+00-2.50000000000000E+01 2.50000000000000E+01	7.
663	0. 0.00000000000000E+00-2.50000000000000E+01 5.00000000000000E+01	7.
664	0. 0.00000000000000E+00 0.00000000000000E+00 2.50000000000000E+01	7.
665	0. 0.00000000000000E+00 0.00000000000000E+00 5.00000000000000E+01	7.
666	0.-5.3867515563965E+01-5.3867515563965E+01 5.3867515563965E+01	7.
667	0.-5.7735031127930E+01-5.7735031127930E+01 5.7735031127930E+01	7.
668	0.-5.8694366455078E+01-2.7645271301270E+01 5.8694366455078E+01	7.
669	0.-6.7388732910156E+01-3.0290544509888E+01 6.7388732910156E+01	7.

670	0.-6.0355339050293E+01	0.0000000000000E+00	6.0355339050293E+01	7.
671	0.-7.0710678100586E+01	0.0000000000000E+00	7.0710678100586E+01	7.
672	0.-2.7645271301270E+01	-5.8694366455078E+01	5.8694366455078E+01	7.
673	0.-3.0290544509888E+01	-6.7388732910156E+01	6.7388732910156E+01	7.
674	0.-3.0617752075195E+01	-3.0617759704590E+01	6.7935913085938E+01	7.
675	0.-3.6235511779785E+01	-3.6235519409180E+01	8.5871856689453E+01	7.
676	0.-3.1634174346924E+01	0.0000000000000E+00	7.1193969726562E+01	7.
677	0.-3.8268344879150E+01	0.0000000000000E+00	9.2387962341309E+01	7.
678	0.0.0000000000000E+00	-6.0355339050293E+01	6.0355339050293E+01	7.
679	0.0.0000000000000E+00	-7.0710678100586E+01	7.0710678100586E+01	7.
680	0.0.0000000000000E+00	-3.1634174346924E+01	7.1193969726562E+01	7.
681	0.0.0000000000000E+00	-3.8268344879150E+01	9.2387962341309E+01	7.
682	0.0.0000000000000E+00	0.0000000000000E+00	7.5000000000000E+01	7.
683	0.0.0000000000000E+00	0.0000000000000E+00	1.0000000000000E+02	7.
684	0.-6.7388732910156E+01	3.0290542602539E+01	-6.7388732910156E+01	7.
685	0.-5.8694366455078E+01	2.7645271301270E+01	-5.8694366455078E+01	7.
686	0.-5.7735031127930E+01	5.7735031127930E+01	-5.7735031127930E+01	7.
687	0.-5.3867515563965E+01	5.3867515563965E+01	-5.3867515563965E+01	7.
688	0.-3.6235515594482E+01	3.6235515594482E+01	-8.5871864318848E+01	7.
689	0.-3.0617759704590E+01	3.0617759704590E+01	-6.7935928344727E+01	7.
690	0.-2.5000000000000E+01	2.5000000000000E+01	-5.0000000000000E+01	7.
691	0.-3.0290544509888E+01	6.7388732910156E+01	-6.7388732910156E+01	7.
692	0.-2.7645271301270E+01	5.8694366455078E+01	-5.8694366455078E+01	7.
693	0.-2.5000000000000E+01	5.0000000000000E+01	-5.0000000000000E+01	7.
694	0.0.0000000000000E+00	3.8268344879150E+01	-9.2387962341309E+01	7.
695	0.0.0000000000000E+00	3.1634174346924E+01	-7.1193969726562E+01	7.
696	0.0.0000000000000E+00	2.5000000000000E+01	-5.0000000000000E+01	7.
697	0.0.0000000000000E+00	7.0710678100586E+01	-7.0710678100586E+01	7.
698	0.0.0000000000000E+00	6.0355339050293E+01	-6.0355339050293E+01	7.
699	0.0.0000000000000E+00	5.0000000000000E+01	-5.0000000000000E+01	7.
700	0.-2.5000000000000E+01	2.5000000000000E+01	-2.5000000000000E+01	7.
701	0.-2.5000000000000E+01	2.5000000000000E+01	0.0000000000000E+00	7.
702	0.-2.5000000000000E+01	5.0000000000000E+01	-2.5000000000000E+01	7.
703	0.-2.5000000000000E+01	5.0000000000000E+01	0.0000000000000E+00	7.
704	0.0.0000000000000E+00	2.5000000000000E+01	-2.5000000000000E+01	7.
705	0.0.0000000000000E+00	2.5000000000000E+01	0.0000000000000E+00	7.
706	0.0.0000000000000E+00	5.0000000000000E+01	-2.5000000000000E+01	7.
707	0.0.0000000000000E+00	5.0000000000000E+01	0.0000000000000E+00	7.
708	0.-2.5000000000000E+01	2.5000000000000E+01	2.5000000000000E+01	7.
709	0.-2.5000000000000E+01	2.5000000000000E+01	5.0000000000000E+01	7.
710	0.-2.5000000000000E+01	5.0000000000000E+01	2.5000000000000E+01	7.
711	0.-2.5000000000000E+01	5.0000000000000E+01	5.0000000000000E+01	7.
712	0.0.0000000000000E+00	2.5000000000000E+01	2.5000000000000E+01	7.
713	0.0.0000000000000E+00	2.5000000000000E+01	5.0000000000000E+01	7.
714	0.0.0000000000000E+00	5.0000000000000E+01	2.5000000000000E+01	7.
715	0.0.0000000000000E+00	5.0000000000000E+01	5.0000000000000E+01	7.
716	0.-5.8694366455078E+01	2.7645271301270E+01	5.8694366455078E+01	7.
717	0.-6.7388732910156E+01	3.0290542602539E+01	6.7388732910156E+01	7.
718	0.-5.3867515563965E+01	5.3867515563965E+01	5.3867515563965E+01	7.
719	0.-5.7735031127930E+01	5.7735031127930E+01	5.7735031127930E+01	7.
720	0.-3.0617759704590E+01	3.0617759704590E+01	6.7935928344727E+01	7.
721	0.-3.6235515594482E+01	3.6235515594482E+01	8.5871864318848E+01	7.
722	0.-2.7645271301270E+01	5.8694366455078E+01	5.8694366455078E+01	7.
723	0.-3.0290544509888E+01	6.7388732910156E+01	6.7388732910156E+01	7.
724	0.0.0000000000000E+00	3.1634174346924E+01	7.1193969726562E+01	7.
725	0.0.0000000000000E+00	3.8268344879150E+01	9.2387962341309E+01	7.
726	0.0.0000000000000E+00	6.0355339050293E+01	6.0355339050293E+01	7.
727	0.0.0000000000000E+00	7.0710678100586E+01	7.0710678100586E+01	7.
728	0.-5.3867515563965E+01	5.3867515563965E+01	-5.3867515563965E+01	7.
729	0.-5.8694374084473E+01	5.8694374084473E+01	-2.7645271301270E+01	7.
730	0.-6.0355339050293E+01	6.0355339050293E+01	0.0000000000000E+00	7.
731	0.-5.7735031127930E+01	5.7735031127930E+01	-5.7735031127930E+01	7.
732	0.-6.7388732910156E+01	6.7388732910156E+01	-3.0290544509888E+01	7.
733	0.-7.0710678100586E+01	7.0710678100586E+01	0.0000000000000E+00	7.



734	0.-2.7645271301270E+01	5.8694366455078E+01	-5.8694366455078E+01	7.
735	0.-3.0617759704590E+01	6.7935928344727E+01	-3.0617759704590E+01	7.
736	0.-3.1634174346924E+01	7.1193969726562E+01	0.0000000000000E+00	7.
737	0.-3.0290544509888E+01	6.7388732910156E+01	-6.7388732910156E+01	7.
738	0.-3.6235507965088E+01	8.5871849060059E+01	-3.6235515594482E+01	7.
739	0.-3.8268344879150E+01	9.2387962341309E+01	0.0000000000000E+00	7.
740	0.0.0000000000000E+00	6.0355339050293E+01	-6.0355339050293E+01	7.
741	0.0.0000000000000E+00	7.1193969726562E+01	-3.1634174346924E+01	7.
742	0.0.0000000000000E+00	7.5000000000000E+01	0.0000000000000E+00	7.
743	0.0.0000000000000E+00	7.0710678100586E+01	-7.0710678100586E+01	7.
744	0.0.0000000000000E+00	9.2387962341309E+01	-3.8268344879150E+01	7.
745	0.0.0000000000000E+00	1.0000000000000E+02	0.0000000000000E+00	7.
746	0.-5.8694374084473E+01	5.8694374084473E+01	2.7645271301270E+01	7.
747	0.-5.3867515563965E+01	5.3867515563965E+01	5.3867515563965E+01	7.
748	0.-6.7388732910156E+01	6.7388732910156E+01	3.0290544509888E+01	7.
749	0.-5.7735031127930E+01	5.7735031127930E+01	5.7735031127930E+01	7.
750	0.-3.0617752075195E+01	6.7935928344727E+01	3.0617759704590E+01	7.
751	0.-2.7645271301270E+01	5.8694366455078E+01	5.8694366455078E+01	7.
752	0.-3.6235507965088E+01	8.5871849060059E+01	3.6235515594482E+01	7.
753	0.-3.0290544509888E+01	6.7388732910156E+01	6.7388732910156E+01	7.
754	0.0.0000000000000E+00	7.1193969726562E+01	3.1634174346924E+01	7.
755	0.0.0000000000000E+00	6.0355339050293E+01	6.0355339050293E+01	7.
756	0.0.0000000000000E+00	9.2387962341309E+01	3.8268344879150E+01	7.
757	0.0.0000000000000E+00	7.0710678100586E+01	7.0710678100586E+01	7.
758	0.3.0290542602539E+01	-6.7388732910156E+01	-6.7388732910156E+01	7.
759	0.3.6235507965088E+01	-8.5871849060059E+01	-3.6235515594482E+01	7.
760	0.3.8268344879150E+01	-9.2387962341309E+01	0.0000000000000E+00	7.
761	0.2.7645271301270E+01	-5.8694366455078E+01	-5.8694366455078E+01	7.
762	0.3.0617759704590E+01	-6.7935928344727E+01	-3.0617752075195E+01	7.
763	0.3.1634174346924E+01	-7.1193969726562E+01	0.0000000000000E+00	7.
764	0.2.5000000000000E+01	-5.0000000000000E+01	-5.0000000000000E+01	7.
765	0.2.5000000000000E+01	-5.0000000000000E+01	-2.5000000000000E+01	7.
766	0.2.5000000000000E+01	-5.0000000000000E+01	0.0000000000000E+00	7.
767	0.5.7735031127930E+01	-5.7735031127930E+01	-5.7735031127930E+01	7.
768	0.6.7388732910156E+01	-6.7388732910156E+01	-3.0290544509888E+01	7.
769	0.7.0710678100586E+01	-7.0710678100586E+01	0.0000000000000E+00	7.
770	0.5.3867515563965E+01	-5.3867515563965E+01	-5.3867515563965E+01	7.
771	0.5.8694374084473E+01	-5.8694374084473E+01	-2.7645271301270E+01	7.
772	0.6.0355339050293E+01	-6.0355339050293E+01	0.0000000000000E+00	7.
773	0.5.0000000000000E+01	-5.0000000000000E+01	-5.0000000000000E+01	7.
774	0.5.0000000000000E+01	-5.0000000000000E+01	-2.5000000000000E+01	7.
775	0.5.0000000000000E+01	-5.0000000000000E+01	0.0000000000000E+00	7.
776	0.3.6235507965088E+01	-8.5871849060059E+01	3.6235515594482E+01	7.
777	0.3.0290542602539E+01	-6.7388732910156E+01	6.7388732910156E+01	7.
778	0.3.0617752075195E+01	-6.7935928344727E+01	3.0617752075195E+01	7.
779	0.2.7645271301270E+01	-5.8694366455078E+01	5.8694366455078E+01	7.
780	0.2.5000000000000E+01	-5.0000000000000E+01	2.5000000000000E+01	7.
781	0.2.5000000000000E+01	-5.0000000000000E+01	5.0000000000000E+01	7.
782	0.6.7388732910156E+01	-6.7388732910156E+01	3.0290544509888E+01	7.
783	0.5.7735031127930E+01	-5.7735031127930E+01	5.7735031127930E+01	7.
784	0.5.8694374084473E+01	-5.8694374084473E+01	2.7645271301270E+01	7.
785	0.5.3867515563965E+01	-5.3867515563965E+01	5.3867515563965E+01	7.
786	0.5.0000000000000E+01	-5.0000000000000E+01	2.5000000000000E+01	7.
787	0.5.0000000000000E+01	-5.0000000000000E+01	5.0000000000000E+01	7.
788	0.3.0290542602539E+01	-6.7388732910156E+01	-6.7388732910156E+01	7.
789	0.2.7645271301270E+01	-5.8694366455078E+01	-5.8694366455078E+01	7.
790	0.3.6235511779785E+01	-3.6235519409180E+01	-8.5871856689453E+01	7.
791	0.3.0617752075195E+01	-3.0617759704590E+01	-6.7935928344727E+01	7.
792	0.2.5000000000000E+01	-2.5000000000000E+01	-5.0000000000000E+01	7.
793	0.3.8268344879150E+01	0.0000000000000E+00	-9.2387962341309E+01	7.
794	0.3.1634174346924E+01	0.0000000000000E+00	-7.1193969726562E+01	7.
795	0.2.5000000000000E+01	0.0000000000000E+00	-5.0000000000000E+01	7.
796	0.5.7735031127930E+01	-5.7735031127930E+01	-5.7735031127930E+01	7.
797	0.5.3867515563965E+01	-5.3867515563965E+01	-5.3867515563965E+01	7.



798	0. 6.7388732910156E+01-3.0290544509888E+01-6.7388732910156E+01	7.
799	0. 5.8694366455078E+01-2.7645271301270E+01-5.8694366455078E+01	7.
800	0. 5.0000000000000E+01-2.5000000000000E+01-5.0000000000000E+01	7.
801	0. 7.0710678100586E+01 0.0000000000000E+00-7.0710678100586E+01	7.
802	0. 6.0355339050293E+01 0.0000000000000E+00-6.0355339050293E+01	7.
803	0. 5.0000000000000E+01 0.0000000000000E+00-5.0000000000000E+01	7.
804	0. 2.5000000000000E+01-2.5000000000000E+01-2.5000000000000E+01	7.
805	0. 2.5000000000000E+01-2.5000000000000E+01 0.0000000000000E+00	7.
806	0. 2.5000000000000E+01 0.0000000000000E+00-2.5000000000000E+01	7.
807	0. 2.5000000000000E+01 0.0000000000000E+00 0.0000000000000E+00	7.
808	0. 5.0000000000000E+01-2.5000000000000E+01-2.5000000000000E+01	7.
809	0. 5.0000000000000E+01-2.5000000000000E+01 0.0000000000000E+00	7.
810	0. 5.0000000000000E+01 0.0000000000000E+00-2.5000000000000E+01	7.
811	0. 5.0000000000000E+01 0.0000000000000E+00 0.0000000000000E+00	7.
812	0. 2.5000000000000E+01-2.5000000000000E+01 2.5000000000000E+01	7.
813	0. 2.5000000000000E+01-2.5000000000000E+01 5.0000000000000E+01	7.
814	0. 2.5000000000000E+01 0.0000000000000E+00 2.5000000000000E+01	7.
815	0. 2.5000000000000E+01 0.0000000000000E+00 5.0000000000000E+01	7.
816	0. 5.0000000000000E+01-2.5000000000000E+01 2.5000000000000E+01	7.
817	0. 5.0000000000000E+01-2.5000000000000E+01 5.0000000000000E+01	7.
818	0. 5.0000000000000E+01 0.0000000000000E+00 2.5000000000000E+01	7.
819	0. 5.0000000000000E+01 0.0000000000000E+00 5.0000000000000E+01	7.
820	0. 2.7645271301270E+01-5.8694366455078E+01 5.8694366455078E+01	7.
821	0. 3.0290542602539E+01-6.7388732910156E+01 6.7388732910156E+01	7.
822	0. 3.0617752075195E+01-3.0617759704590E+01 6.7935928344727E+01	7.
823	0. 3.6235511779785E+01-3.6235519409180E+01 8.5871856689453E+01	7.
824	0. 3.1634174346924E+01 0.0000000000000E+00 7.1193969726562E+01	7.
825	0. 3.8268344879150E+01 0.0000000000000E+00 9.2387962341309E+01	7.
826	0. 5.3867515563965E+01-5.3867515563965E+01 5.3867515563965E+01	7.
827	0. 5.7735031127930E+01-5.7735031127930E+01 5.7735031127930E+01	7.
828	0. 5.8694366455078E+01-2.7645271301270E+01 5.8694366455078E+01	7.
829	0. 6.7388732910156E+01-3.0290544509888E+01 6.7388732910156E+01	7.
830	0. 6.0355339050293E+01 0.0000000000000E+00 6.0355339050293E+01	7.
831	0. 7.0710678100586E+01 0.0000000000000E+00 7.0710678100586E+01	7.
832	0. 3.6235515594482E+01 3.6235515594482E+01-8.5871864318848E+01	7.
833	0. 3.0617759704590E+01 3.0617759704590E+01-6.7935928344727E+01	7.
834	0. 2.5000000000000E+01 2.5000000000000E+01-5.0000000000000E+01	7.
835	0. 3.0290542602539E+01 6.7388732910156E+01-6.7388732910156E+01	7.
836	0. 2.7645271301270E+01 5.8694366455078E+01-5.8694366455078E+01	7.
837	0. 2.5000000000000E+01 5.0000000000000E+01-5.0000000000000E+01	7.
838	0. 6.7388732910156E+01 3.0290542602539E+01-6.7388732910156E+01	7.
839	0. 5.8694366455078E+01 2.7645271301270E+01-5.8694366455078E+01	7.
840	0. 5.0000000000000E+01 2.5000000000000E+01-5.0000000000000E+01	7.
841	0. 5.7735031127930E+01 5.7735031127930E+01-5.7735031127930E+01	7.
842	0. 5.3867515563965E+01 5.3867515563965E+01-5.3867515563965E+01	7.
843	0. 5.0000000000000E+01 5.0000000000000E+01-5.0000000000000E+01	7.
844	0. 2.5000000000000E+01 2.5000000000000E+01-2.5000000000000E+01	7.
845	0. 2.5000000000000E+01 2.5000000000000E+01 0.0000000000000E+00	7.
846	0. 2.5000000000000E+01 5.0000000000000E+01-2.5000000000000E+01	7.
847	0. 2.5000000000000E+01 5.0000000000000E+01 0.0000000000000E+00	7.
848	0. 5.0000000000000E+01 2.5000000000000E+01-2.5000000000000E+01	7.
849	0. 5.0000000000000E+01 2.5000000000000E+01 0.0000000000000E+00	7.
850	0. 5.0000000000000E+01 5.0000000000000E+01-2.5000000000000E+01	7.
851	0. 5.0000000000000E+01 5.0000000000000E+01 0.0000000000000E+00	7.
852	0. 2.5000000000000E+01 2.5000000000000E+01 2.5000000000000E+01	7.
853	0. 2.5000000000000E+01 2.5000000000000E+01 5.0000000000000E+01	7.
854	0. 2.5000000000000E+01 5.0000000000000E+01 2.5000000000000E+01	7.
855	0. 2.5000000000000E+01 5.0000000000000E+01 5.0000000000000E+01	7.
856	0. 5.0000000000000E+01 2.5000000000000E+01 2.5000000000000E+01	7.
857	0. 5.0000000000000E+01 2.5000000000000E+01 5.0000000000000E+01	7.
858	0. 5.0000000000000E+01 5.0000000000000E+01 2.5000000000000E+01	7.
859	0. 5.0000000000000E+01 5.0000000000000E+01 5.0000000000000E+01	7.
860	0. 3.0617759704590E+01 3.0617759704590E+01 6.7935913085938E+01	7.
861	0. 3.6235515594482E+01 3.6235515594482E+01 8.5871864318848E+01	7.

862	0.	2.7645271301270E+01	5.8694366455078E+01	5.8694366455078E+01	7.
863	0.	3.0290542602539E+01	6.7388732910156E+01	6.7388732910156E+01	7.
864	0.	5.8694366455078E+01	2.7645271301270E+01	5.8694366455078E+01	7.
865	0.	6.7388732910156E+01	3.0290542602539E+01	6.7388732910156E+01	7.
866	0.	5.3867515563965E+01	5.3867515563965E+01	5.3867515563965E+01	7.
867	0.	5.7735031127930E+01	5.7735031127930E+01	5.7735031127930E+01	7.
868	0.	2.7645271301270E+01	5.8694366455078E+01-5.8694366455078E+01		7.
869	0.	3.0617759704590E+01	6.7935928344727E+01-3.0617759704590E+01		7.
870	0.	3.1634174346924E+01	7.1193969726562E+01	0.0000000000000E+00	7.
871	0.	3.0290542602539E+01	6.7388732910156E+01-6.7388732910156E+01		7.
872	0.	3.6235507965088E+01	8.5871849060059E+01-3.6235515594482E+01		7.
873	0.	3.8268344879150E+01	9.2387962341309E+01	0.0000000000000E+00	7.
874	0.	5.3867515563965E+01	5.3867515563965E+01-5.3867515563965E+01		7.
875	0.	5.8694374084473E+01	5.8694374084473E+01-2.7645271301270E+01		7.
876	0.	6.0355339050293E+01	6.0355339050293E+01	0.0000000000000E+00	7.
877	0.	5.7735031127930E+01	5.7735031127930E+01-5.7735031127930E+01		7.
878	0.	6.7388732910156E+01	6.7388732910156E+01-3.0290544509888E+01		7.
879	0.	7.0710678100586E+01	7.0710678100586E+01	0.0000000000000E+00	7.
880	0.	3.0617752075195E+01	6.7935928344727E+01	3.0617759704590E+01	7.
881	0.	2.7645271301270E+01	5.8694366455078E+01	5.8694366455078E+01	7.
882	0.	3.6235507965088E+01	8.5871849060059E+01	3.6235515594482E+01	7.
883	0.	3.0290542602539E+01	6.7388732910156E+01	6.7388732910156E+01	7.
884	0.	5.8694374084473E+01	5.8694374084473E+01	2.7645271301270E+01	7.
885	0.	5.3867515563965E+01	5.3867515563965E+01	5.3867515563965E+01	7.
886	0.	6.7388732910156E+01	6.7388732910156E+01	3.0290544509888E+01	7.
887	0.	5.7735031127930E+01	5.7735031127930E+01	5.7735031127930E+01	7.
888	0.	5.3867515563965E+01-5.3867515563965E+01			7.
889	0.	5.8694374084473E+01-5.8694374084473E+01			7.
890	0.	6.0355339050293E+01-6.0355339050293E+01			7.
891	0.	5.8694374084473E+01-2.7645271301270E+01			7.
892	0.	6.7935928344727E+01-3.0617759704590E+01			7.
893	0.	7.1193969726562E+01-3.1634174346924E+01			7.
894	0.	6.0355339050293E+01	0.0000000000000E+00-6.0355339050293E+01		7.
895	0.	7.1193969726562E+01	0.0000000000000E+00-3.1634174346924E+01		7.
896	0.	7.5000000000000E+01	0.0000000000000E+00	0.0000000000000E+00	7.
897	0.	5.7735031127930E+01-5.7735031127930E+01			7.
898	0.	6.7388732910156E+01-6.7388732910156E+01			7.
899	0.	7.0710678100586E+01-7.0710678100586E+01			7.
900	0.	6.7388732910156E+01-3.0290544509888E+01			7.
901	0.	8.5871849060059E+01-3.6235507965088E+01			7.
902	0.	9.2387962341309E+01-3.8268344879150E+01			7.
903	0.	7.0710678100586E+01	0.0000000000000E+00-7.0710678100586E+01		7.
904	0.	9.2387962341309E+01	0.0000000000000E+00-3.8268344879150E+01		7.
905	0.	1.0000000000000E+02	0.0000000000000E+00	0.0000000000000E+00	7.
906	0.	5.8694374084473E+01-5.8694374084473E+01			7.
907	0.	5.3867515563965E+01-5.3867515563965E+01			7.
908	0.	6.7935928344727E+01-3.0617752075195E+01			7.
909	0.	5.8694374084473E+01-2.7645271301270E+01			7.
910	0.	7.1193969726562E+01	0.0000000000000E+00	3.1634174346924E+01	7.
911	0.	6.0355339050293E+01	0.0000000000000E+00	6.0355339050293E+01	7.
912	0.	6.7388732910156E+01-6.7388732910156E+01			7.
913	0.	5.7735031127930E+01-5.7735031127930E+01			7.
914	0.	8.5871849060059E+01-3.6235507965088E+01			7.
915	0.	6.7388732910156E+01-3.0290544509888E+01			7.
916	0.	9.2387962341309E+01	0.0000000000000E+00	3.8268344879150E+01	7.
917	0.	7.0710678100586E+01	0.0000000000000E+00	7.0710678100586E+01	7.
918	0.	5.8694374084473E+01	2.7645271301270E+01-5.8694374084473E+01		7.
919	0.	6.7935928344727E+01	3.0617759704590E+01-3.0617759704590E+01		7.
920	0.	7.1193969726562E+01	3.1634174346924E+01	0.0000000000000E+00	7.
921	0.	5.3867515563965E+01	5.3867515563965E+01-5.3867515563965E+01		7.
922	0.	5.8694374084473E+01	5.8694374084473E+01-2.7645271301270E+01		7.
923	0.	6.0355339050293E+01	6.0355339050293E+01	0.0000000000000E+00	7.
924	0.	6.7388732910156E+01	3.0290542602539E+01-6.7388732910156E+01		7.
925	0.	8.5871849060059E+01	3.6235507965088E+01-3.6235515594482E+01		7.

926 0. 9.2387962341309E+01 3.8268344879150E+01 0.0000000000000E+00 7.  
 927 0. 5.7735031127930E+01 5.7735031127930E+01-5.7735031127930E+01 7.  
 928 0. 6.7388732910156E+01 6.7388732910156E+01-3.0290544509888E+01 7.  
 929 0. 7.0710678100586E+01 7.0710678100586E+01 0.0000000000000E+00 7.  
 930 0. 6.7935913085938E+01 3.0617752075195E+01 3.0617759704590E+01 7.  
 931 0. 5.8694374084473E+01 2.7645271301270E+01 5.8694374084473E+01 7.  
 932 0. 5.8694374084473E+01 5.8694374084473E+01 2.7645271301270E+01 7.  
 933 0. 5.3867515563965E+01 5.3867515563965E+01 5.3867515563965E+01 7.  
 934 0. 8.5871849060059E+01 3.6235507965088E+01 3.6235515594482E+01 7.  
 935 0. 6.7388732910156E+01 3.0290542602539E+01 6.7388732910156E+01 7.  
 936 0. 6.7388732910156E+01 6.7388732910156E+01 3.0290544509888E+01 7.  
 937 0. 5.7735031127930E+01 5.7735031127930E+01 5.7735031127930E+01 7.

\*

\*----- ELEMENT CARDS FOR SOLID ELEMENTS -----\*

\*

1	1	1	33	35	3	2	34	36	4
2	1	33	65	67	35	34	66	68	36
3	1	65	97	99	67	66	98	100	68
4	1	97	129	131	99	98	130	132	100
5	1	129	161	163	131	130	162	164	132
6	1	161	193	195	163	162	194	196	164
7	1	193	225	227	195	194	226	228	196
8	1	225	257	259	227	226	258	260	228
9	1	257	289	291	259	258	290	292	260
10	1	289	321	323	291	290	322	324	292
11	1	321	353	355	323	322	354	356	324
12	1	353	385	387	355	354	386	388	356
13	1	385	417	419	387	386	418	420	388
14	1	417	449	451	419	418	450	452	420
15	1	449	481	483	451	450	482	484	452
16	1	3	35	37	5	4	36	38	6
17	1	35	67	69	37	36	68	70	38
18	1	67	99	101	69	68	100	102	70
19	1	99	131	133	101	100	132	134	102
20	1	131	163	165	133	132	164	166	134
21	1	163	195	197	165	164	196	198	166
22	1	195	227	229	197	196	228	230	198
23	1	227	259	261	229	228	260	262	230
24	1	259	291	293	261	260	292	294	262
25	1	291	323	325	293	292	324	326	294
26	1	323	355	357	325	324	356	358	326
27	1	355	387	389	357	356	388	390	358
28	1	387	419	421	389	388	420	422	390
29	1	419	451	453	421	420	452	454	422
30	1	451	483	485	453	452	484	486	454
31	1	5	37	39	7	6	38	40	8
32	1	37	69	71	39	38	70	72	40
33	1	69	101	103	71	70	102	104	72
34	1	101	133	135	103	102	134	136	104
35	1	133	165	167	135	134	166	168	136
36	1	165	197	199	167	166	198	200	168
37	1	197	229	231	199	198	230	232	200
38	1	229	261	263	231	230	262	264	232
39	1	261	293	295	263	262	294	296	264
40	1	293	325	327	295	294	326	328	296
41	1	325	357	359	327	326	358	360	328
42	1	357	389	391	359	358	390	392	360
43	1	389	421	423	391	390	422	424	392
44	1	421	453	455	423	422	454	456	424
45	1	453	485	487	455	454	486	488	456
46	1	7	39	41	9	8	40	42	10
47	1	39	71	73	41	40	72	74	42
48	1	71	103	105	73	72	104	106	74
49	1	103	135	137	105	104	136	138	106

50	1	135	167	169	137	136	168	170	138
51	1	167	199	201	169	168	200	202	170
52	1	199	231	233	201	200	232	234	202
53	1	231	263	265	233	232	264	266	234
54	1	263	295	297	265	264	296	298	266
55	1	295	327	329	297	296	328	330	298
56	1	327	359	361	329	328	360	362	330
57	1	359	391	393	361	360	392	394	362
58	1	391	423	425	393	392	424	426	394
59	1	423	455	457	425	424	456	458	426
60	1	455	487	489	457	456	488	490	458
61	1	9	41	43	11	10	42	44	12
62	1	41	73	75	43	42	74	76	44
63	1	73	105	107	75	74	106	108	76
64	1	105	137	139	107	106	138	140	108
65	1	137	169	171	139	138	170	172	140
66	1	169	201	203	171	170	202	204	172
67	1	201	233	235	203	202	234	236	204
68	1	233	265	267	235	234	266	268	236
69	1	265	297	299	267	266	298	300	268
70	1	297	329	331	299	298	330	332	300
71	1	329	361	363	331	330	362	364	332
72	1	361	393	395	363	362	394	396	364
73	1	393	425	427	395	394	426	428	396
74	1	425	457	459	427	426	458	460	428
75	1	457	489	491	459	458	490	492	460
76	1	11	43	45	13	12	44	46	14
77	1	43	75	77	45	44	76	78	46
78	1	75	107	109	77	76	108	110	78
79	1	107	139	141	109	108	140	142	110
80	1	139	171	173	141	140	172	174	142
81	1	171	203	205	173	172	204	206	174
82	1	203	235	237	205	204	236	238	206
83	1	235	267	269	237	236	268	270	238
84	1	267	299	301	269	268	300	302	270
85	1	299	331	333	301	300	332	334	302
86	1	331	363	365	333	332	364	366	334
87	1	363	395	397	365	364	396	398	366
88	1	395	427	429	397	396	428	430	398
89	1	427	459	461	429	428	460	462	430
90	1	459	491	493	461	460	492	494	462
91	1	13	45	47	15	14	46	48	16
92	1	45	77	79	47	46	78	80	48
93	1	77	109	111	79	78	110	112	80
94	1	109	141	143	111	110	142	144	112
95	1	141	173	175	143	142	174	176	144
96	1	173	205	207	175	174	206	208	176
97	1	205	237	239	207	206	238	240	208
98	1	237	269	271	239	238	270	272	240
99	1	269	301	303	271	270	302	304	272
100	1	301	333	335	303	302	334	336	304
101	1	333	365	367	335	334	366	368	336
102	1	365	397	399	367	366	398	400	368
103	1	397	429	431	399	398	430	432	400
104	1	429	461	463	431	430	462	464	432
105	1	461	493	495	463	462	494	496	464
106	1	15	47	49	17	16	48	50	18
107	1	47	79	81	49	48	80	82	50
108	1	79	111	113	81	80	112	114	82
109	1	111	143	145	113	112	144	146	114
110	1	143	175	177	145	144	176	178	146
111	1	175	207	209	177	176	208	210	178
112	1	207	239	241	209	208	240	242	210
113	1	239	271	273	241	240	272	274	242

114	1	271	303	305	273	272	304	306	274
115	1	303	335	337	305	304	336	338	306
116	1	335	367	369	337	336	368	370	338
117	1	367	399	401	369	368	400	402	370
118	1	399	431	433	401	400	432	434	402
119	1	431	463	465	433	432	464	466	434
120	1	463	495	497	465	464	496	498	466
121	1	17	49	51	19	18	50	52	20
122	1	49	81	83	51	50	82	84	52
123	1	81	113	115	83	82	114	116	84
124	1	113	145	147	115	114	146	148	116
125	1	145	177	179	147	146	178	180	148
126	1	177	209	211	179	178	210	212	180
127	1	209	241	243	211	210	242	244	212
128	1	241	273	275	243	242	274	276	244
129	1	273	305	307	275	274	306	308	276
130	1	305	337	339	307	306	338	340	308
131	1	337	369	371	339	338	370	372	340
132	1	369	401	403	371	370	402	404	372
133	1	401	433	435	403	402	434	436	404
134	1	433	465	467	435	434	466	468	436
135	1	465	497	499	467	466	498	500	468
136	1	19	51	53	21	20	52	54	22
137	1	51	83	85	53	52	84	86	54
138	1	83	115	117	85	84	116	118	86
139	1	115	147	149	117	116	148	150	118
140	1	147	179	181	149	148	180	182	150
141	1	179	211	213	181	180	212	214	182
142	1	211	243	245	213	212	244	246	214
143	1	243	275	277	245	244	276	278	246
144	1	275	307	309	277	276	308	310	278
145	1	307	339	341	309	308	340	342	310
146	1	339	371	373	341	340	372	374	342
147	1	371	403	405	373	372	404	406	374
148	1	403	435	437	405	404	436	438	406
149	1	435	467	469	437	436	468	470	438
150	1	467	499	501	469	468	500	502	470
151	1	21	53	55	23	22	54	56	24
152	1	53	85	87	55	54	86	88	56
153	1	85	117	119	87	86	118	120	88
154	1	117	149	151	119	118	150	152	120
155	1	149	181	183	151	150	182	184	152
156	1	181	213	215	183	182	214	216	184
157	1	213	245	247	215	214	246	248	216
158	1	245	277	279	247	246	278	280	248
159	1	277	309	311	279	278	310	312	280
160	1	309	341	343	311	310	342	344	312
161	1	341	373	375	343	342	374	376	344
162	1	373	405	407	375	374	406	408	376
163	1	405	437	439	407	406	438	440	408
164	1	437	469	471	439	438	470	472	440
165	1	469	501	503	471	470	502	504	472
166	1	23	55	57	25	24	56	58	26
167	1	55	87	89	57	56	88	90	58
168	1	87	119	121	89	88	120	122	90
169	1	119	151	153	121	120	152	154	122
170	1	151	183	185	153	152	184	186	154
171	1	183	215	217	185	184	216	218	186
172	1	215	247	249	217	216	248	250	218
173	1	247	279	281	249	248	280	282	250
174	1	279	311	313	281	280	312	314	282
175	1	311	343	345	313	312	344	346	314
176	1	343	375	377	345	344	376	378	346
177	1	375	407	409	377	376	408	410	378

178	1	407	439	441	409	408	440	442	410
179	1	439	471	473	441	440	472	474	442
180	1	471	503	505	473	472	504	506	474
181	1	25	57	59	27	26	58	60	28
182	1	57	89	91	59	58	90	92	60
183	1	89	121	123	91	90	122	124	92
184	1	121	153	155	123	122	154	156	124
185	1	153	185	187	155	154	186	188	156
186	1	185	217	219	187	186	218	220	188
187	1	217	249	251	219	218	250	252	220
188	1	249	281	283	251	250	282	284	252
189	1	281	313	315	283	282	314	316	284
190	1	313	345	347	315	314	346	348	316
191	1	345	377	379	347	346	378	380	348
192	1	377	409	411	379	378	410	412	380
193	1	409	441	443	411	410	442	444	412
194	1	441	473	475	443	442	474	476	444
195	1	473	505	507	475	474	506	508	476
196	1	27	59	61	29	28	60	62	30
197	1	59	91	93	61	60	92	94	62
198	1	91	123	125	93	92	124	126	94
199	1	123	155	157	125	124	156	158	126
200	1	155	187	189	157	156	188	190	158
201	1	187	219	221	189	188	220	222	190
202	1	219	251	253	221	220	252	254	222
203	1	251	283	285	253	252	284	286	254
204	1	283	315	317	285	284	316	318	286
205	1	315	347	349	317	316	348	350	318
206	1	347	379	381	349	348	380	382	350
207	1	379	411	413	381	380	412	414	382
208	1	411	443	445	413	412	444	446	414
209	1	443	475	477	445	444	476	478	446
210	1	475	507	509	477	476	508	510	478
211	1	29	61	63	31	30	62	64	32
212	1	61	93	95	63	62	94	96	64
213	1	93	125	127	95	94	126	128	96
214	1	125	157	159	127	126	158	160	128
215	1	157	189	191	159	158	190	192	160
216	1	189	221	223	191	190	222	224	192
217	1	221	253	255	223	222	254	256	224
218	1	253	285	287	255	254	286	288	256
219	1	285	317	319	287	286	318	320	288
220	1	317	349	351	319	318	350	352	320
221	1	349	381	383	351	350	382	384	352
222	1	381	413	415	383	382	414	416	384
223	1	413	445	447	415	414	446	448	416
224	1	445	477	479	447	446	478	480	448
225	1	477	509	511	479	478	510	512	480
226	2	513	522	525	516	514	523	526	517
227	2	522	531	534	525	523	532	535	526
228	2	516	525	528	519	517	526	529	520
229	2	525	534	537	528	526	535	538	529
230	2	514	523	526	517	515	524	527	518
231	2	523	532	535	526	524	533	536	527
232	2	517	526	529	520	518	527	530	521
233	2	526	535	538	529	527	536	539	530
234	2	515	524	527	518	516	525	528	519
235	2	524	533	536	527	525	534	537	528
236	2	518	527	530	521	519	528	531	524
237	2	527	536	539	530	528	537	540	531
238	2	540	546	548	542	540	547	550	543
239	2	546	552	554	548	546	553	556	549
240	2	542	548	550	544	542	549	552	545
241	2	548	554	556	550	548	555	558	551

242	2	519	528	564	558	520	529	565	559
243	2	528	537	570	564	529	538	571	565
244	2	558	564	567	561	559	565	568	562
245	2	564	570	573	567	565	571	574	568
246	2	520	529	565	559	521	530	566	560
247	2	529	538	571	565	530	539	572	566
248	2	559	565	568	562	560	566	569	563
249	2	565	571	574	568	566	572	575	569
250	2	521	530	566	560	544	550	580	576
251	2	530	539	572	566	550	556	584	580
252	2	560	566	569	563	576	580	582	578
253	2	566	572	575	569	580	584	586	582
254	2	544	550	580	576	545	551	581	577
255	2	550	556	584	580	551	557	585	581
256	2	576	580	582	578	577	581	583	579
257	2	580	584	586	582	581	585	587	583
258	2	588	594	597	591	589	595	598	592
259	2	594	603	606	597	595	604	607	598
260	2	591	597	600	531	592	598	601	532
261	2	597	606	609	600	598	607	610	601
262	2	589	595	598	592	590	596	599	593
263	2	595	604	607	598	596	605	608	599
264	2	592	598	601	532	593	599	602	533
265	2	598	607	610	601	599	608	611	602
266	2	590	596	599	593	612	616	618	614
267	2	596	605	608	599	616	622	624	618
268	2	593	599	602	533	614	618	620	552
269	2	599	608	611	602	618	624	626	620
270	2	612	616	618	614	613	617	619	615
271	2	616	622	624	618	617	623	625	619
272	2	614	618	620	552	615	619	621	553
273	2	618	624	626	620	619	625	627	621
274	2	628	634	636	630	629	635	637	631
275	2	634	642	644	636	635	643	645	637
276	2	630	636	639	632	631	637	640	633
277	2	636	644	647	639	637	645	648	640
278	2	629	635	637	631	531	600	638	534
279	2	635	643	645	637	600	609	646	638
280	2	631	637	640	633	534	638	641	537
281	2	637	645	648	640	638	646	649	641
282	2	531	600	638	534	532	601	650	535
283	2	600	609	646	638	601	610	654	650
284	2	534	638	641	537	535	650	652	538
285	2	638	646	649	641	650	654	656	652
286	2	532	601	650	535	533	602	651	536
287	2	601	610	654	650	602	611	655	651
288	2	535	650	652	538	536	651	653	539
289	2	650	654	656	652	651	655	657	653
290	2	533	602	651	536	552	620	658	554
291	2	602	611	655	651	620	626	662	658
292	2	536	651	653	539	554	658	660	556
293	2	651	655	657	653	658	662	664	660
294	2	552	620	658	554	553	621	659	555
295	2	620	626	662	658	621	627	663	659
296	2	554	658	660	556	555	659	661	557
297	2	658	662	664	660	659	663	665	661
298	2	553	621	659	555	666	672	674	668
299	2	621	627	663	659	672	678	680	674
300	2	555	659	661	557	668	674	676	670
301	2	659	663	665	661	674	680	682	676
302	2	666	672	674	668	667	673	675	669
303	2	672	678	680	674	673	679	681	675
304	2	668	674	676	670	669	675	677	671
305	2	674	680	682	676	675	681	683	677

306	2	632	639	688	684	633	640	689	685
307	2	639	647	694	688	640	648	695	689
308	2	684	688	691	686	685	689	692	687
309	2	688	694	697	691	689	695	698	692
310	2	633	640	689	685	537	641	690	570
311	2	640	648	695	689	641	649	696	690
312	2	685	689	692	687	570	690	693	573
313	2	689	695	698	692	690	696	699	693
314	2	537	641	690	570	538	652	700	571
315	2	641	649	696	690	652	656	704	700
316	2	570	690	693	573	571	700	702	574
317	2	690	696	699	693	700	704	706	702
318	2	538	652	700	571	539	653	701	572
319	2	652	656	704	700	653	657	705	701
320	2	571	700	702	574	572	701	703	575
321	2	700	704	706	702	701	705	707	703
322	2	539	653	701	572	556	660	708	584
323	2	653	657	705	701	660	664	712	708
324	2	572	701	703	575	584	708	710	586
325	2	701	705	707	703	708	712	714	710
326	2	556	660	708	584	557	661	709	585
327	2	660	664	712	708	661	665	713	709
328	2	584	708	710	586	585	709	711	587
329	2	708	712	714	710	709	713	715	711
330	2	557	661	709	585	670	676	720	716
331	2	661	665	713	709	676	682	724	720
332	2	585	709	711	587	716	720	722	718
333	2	709	713	715	711	720	724	726	722
334	2	670	676	720	716	671	677	721	717
335	2	676	682	724	720	677	683	725	721
336	2	716	720	722	718	717	721	723	719
337	2	720	724	726	722	721	725	727	723
338	2	573	693	734	728	574	702	735	729
339	2	693	699	740	734	702	706	741	735
340	2	728	734	737	731	729	735	738	732
341	2	734	740	743	737	735	741	744	738
342	2	574	702	735	729	575	703	736	730
343	2	702	706	741	735	703	707	742	736
344	2	729	735	738	732	730	736	739	733
345	2	735	741	744	738	736	742	745	739
346	2	575	703	736	730	586	710	750	746
347	2	703	707	742	736	710	714	754	750
348	2	730	736	739	733	746	750	752	748
349	2	736	742	745	739	750	754	756	752
350	2	586	710	750	746	587	711	751	747
351	2	710	714	754	750	711	715	755	751
352	2	746	750	752	748	747	751	753	749
353	2	750	754	756	752	751	755	757	753
354	2	603	758	761	606	604	759	762	607
355	2	758	767	770	761	759	768	771	762
356	2	606	761	764	609	607	762	765	610
357	2	761	770	773	764	762	771	774	765
358	2	604	759	762	607	605	760	763	608
359	2	759	768	771	762	760	769	772	763
360	2	607	762	765	610	608	763	766	611
361	2	762	771	774	765	763	772	775	766
362	2	605	760	763	608	622	776	778	624
363	2	760	769	772	763	776	782	784	778
364	2	608	763	766	611	624	778	780	626
365	2	763	772	775	766	778	784	786	780
366	2	622	776	778	624	623	777	779	625
367	2	776	782	784	778	777	783	785	779
368	2	624	778	780	626	625	779	781	627
369	2	778	784	786	780	779	785	787	781



370	2	642	788	790	644	643	789	791	645
371	2	788	796	798	790	789	797	799	791
372	2	644	790	793	647	645	791	794	648
373	2	790	798	801	793	791	799	802	794
374	2	643	789	791	645	609	764	792	646
375	2	789	797	799	791	764	773	800	792
376	2	645	791	794	648	646	792	795	649
377	2	791	799	802	794	792	800	803	795
378	2	609	764	792	646	610	765	804	654
379	2	764	773	800	792	765	774	808	804
380	2	646	792	795	649	654	804	806	656
381	2	792	800	803	795	804	808	810	806
382	2	610	765	804	654	611	766	805	655
383	2	765	774	808	804	766	775	809	805
384	2	654	804	806	656	655	805	807	657
385	2	804	808	810	806	805	809	811	807
386	2	611	766	805	655	626	780	812	662
387	2	766	775	809	805	780	786	816	812
388	2	655	805	807	657	662	812	814	664
389	2	805	809	811	807	812	816	818	814
390	2	626	780	812	662	627	781	813	663
391	2	780	786	816	812	781	787	817	813
392	2	662	812	814	664	663	813	815	665
393	2	812	816	818	814	813	817	819	815
394	2	627	781	813	663	678	820	822	680
395	2	781	787	817	813	820	826	828	822
396	2	663	813	815	665	680	822	824	682
397	2	813	817	819	815	822	828	830	824
398	2	678	820	822	680	679	821	823	681
399	2	820	826	828	822	821	827	829	823
400	2	680	822	824	682	681	823	825	683
401	2	822	828	830	824	823	829	831	825
402	2	647	793	832	694	648	794	833	695
403	2	793	801	838	832	794	802	839	833
404	2	694	832	835	697	695	833	836	698
405	2	832	838	841	835	833	839	842	836
406	2	648	794	833	695	649	795	834	696
407	2	794	802	839	833	795	803	840	834
408	2	695	833	836	698	696	834	837	699
409	2	833	839	842	836	834	840	843	837
410	2	649	795	834	696	656	806	844	704
411	2	795	803	840	834	806	810	848	844
412	2	696	834	837	699	704	844	846	706
413	2	834	840	843	837	844	848	850	846
414	2	656	806	844	704	657	807	845	705
415	2	806	810	848	844	807	811	849	845
416	2	704	844	846	706	705	845	847	707
417	2	844	848	850	846	845	849	851	847
418	2	657	807	845	705	664	814	852	712
419	2	807	811	849	845	814	818	856	852
420	2	705	845	847	707	712	852	854	714
421	2	845	849	851	847	852	856	858	854
422	2	664	814	852	712	665	815	853	713
423	2	814	818	856	852	815	819	857	853
424	2	712	852	854	714	713	853	855	715
425	2	852	856	858	854	853	857	859	855
426	2	665	815	853	713	682	824	860	724
427	2	815	819	857	853	824	830	864	860
428	2	713	853	855	715	724	860	862	726
429	2	853	857	859	855	860	864	866	862
430	2	682	824	860	724	683	825	861	725
431	2	824	830	864	860	825	831	865	861
432	2	724	860	862	726	725	861	863	727
433	2	860	864	866	862	861	865	867	863

434	2	699	837	868	740	706	846	869	741
435	2	837	843	874	868	846	850	875	869
436	2	740	868	871	743	741	869	872	744
437	2	868	874	877	871	869	875	878	872
438	2	706	846	869	741	707	847	870	742
439	2	846	850	875	869	847	851	876	870
440	2	741	869	872	744	742	870	873	745
441	2	869	875	878	872	870	876	879	873
442	2	707	847	870	742	714	854	880	754
443	2	847	851	876	870	854	858	884	880
444	2	742	870	873	745	754	880	882	756
445	2	870	876	879	873	880	884	886	882
446	2	714	854	880	754	715	855	881	755
447	2	854	858	884	880	855	859	885	881
448	2	754	880	882	756	755	881	883	757
449	2	880	884	886	882	881	885	887	883
450	2	773	888	891	800	774	889	892	808
451	2	888	897	900	891	889	898	901	892
452	2	800	891	894	803	808	892	895	810
453	2	891	900	903	894	892	901	904	895
454	2	774	889	892	808	775	890	893	809
455	2	889	898	901	892	890	899	902	893
456	2	808	892	895	810	809	893	896	811
457	2	892	901	904	895	893	902	905	896
458	2	775	890	893	809	786	906	908	816
459	2	890	899	902	893	906	912	914	908
460	2	809	893	896	811	816	908	910	818
461	2	893	902	905	896	908	914	916	910
462	2	786	906	908	816	787	907	909	817
463	2	906	912	914	908	907	913	915	909
464	2	816	908	910	818	817	909	911	819
465	2	908	914	916	910	909	915	917	911
466	2	803	894	918	840	810	895	919	848
467	2	894	903	924	918	895	904	925	919
468	2	840	918	921	843	848	919	922	850
469	2	918	924	927	921	919	925	928	922
470	2	810	895	919	848	811	896	920	849
471	2	895	904	925	919	896	905	926	920
472	2	848	919	922	850	849	920	923	851
473	2	919	925	928	922	920	926	929	923
474	2	811	896	920	849	818	910	930	856
475	2	896	905	926	920	910	916	934	930
476	2	849	920	923	851	856	930	932	858
477	2	920	926	929	923	930	934	936	932
478	2	818	910	930	856	819	911	931	857
479	2	910	916	934	930	911	917	935	931
480	2	856	930	932	858	857	931	933	859
481	2	930	934	936	932	931	935	937	933

\*  
\*----- ELEMENT CARDS FOR 8-NODE SOLID SHELL ELEMENTS -----\*

\*  
\*----- INITIAL CONDITIONS -----\*

\*  
1 0.000E+00 0.000E+00 0.000E+00  
2 0.000E+00 0.000E+00 0.000E+00  
3 0.000E+00 0.000E+00 0.000E+00  
4 0.000E+00 0.000E+00 0.000E+00  
5 0.000E+00 0.000E+00 0.000E+00  
6 0.000E+00 0.000E+00 0.000E+00  
7 0.000E+00 0.000E+00 0.000E+00  
8 0.000E+00 0.000E+00 0.000E+00  
9 0.000E+00 0.000E+00 0.000E+00  
10 0.000E+00 0.000E+00 0.000E+00

206

[illegible]

208

209

210

[illegible]



212

213

214

215

216

217

218

219



907 0.000E+00 0.000E+00 1.000E+03  
 908 0.000E+00 0.000E+00 1.000E+03  
 909 0.000E+00 0.000E+00 1.000E+03  
 910 0.000E+00 0.000E+00 1.000E+03  
 911 0.000E+00 0.000E+00 1.000E+03  
 912 0.000E+00 0.000E+00 1.000E+03  
 913 0.000E+00 0.000E+00 1.000E+03  
 914 0.000E+00 0.000E+00 1.000E+03  
 915 0.000E+00 0.000E+00 1.000E+03  
 916 0.000E+00 0.000E+00 1.000E+03  
 917 0.000E+00 0.000E+00 1.000E+03  
 918 0.000E+00 0.000E+00 1.000E+03  
 919 0.000E+00 0.000E+00 1.000E+03  
 920 0.000E+00 0.000E+00 1.000E+03  
 921 0.000E+00 0.000E+00 1.000E+03  
 922 0.000E+00 0.000E+00 1.000E+03  
 923 0.000E+00 0.000E+00 1.000E+03  
 924 0.000E+00 0.000E+00 1.000E+03  
 925 0.000E+00 0.000E+00 1.000E+03  
 926 0.000E+00 0.000E+00 1.000E+03  
 927 0.000E+00 0.000E+00 1.000E+03  
 928 0.000E+00 0.000E+00 1.000E+03  
 929 0.000E+00 0.000E+00 1.000E+03  
 930 0.000E+00 0.000E+00 1.000E+03  
 931 0.000E+00 0.000E+00 1.000E+03  
 932 0.000E+00 0.000E+00 1.000E+03  
 933 0.000E+00 0.000E+00 1.000E+03  
 934 0.000E+00 0.000E+00 1.000E+03  
 935 0.000E+00 0.000E+00 1.000E+03  
 936 0.000E+00 0.000E+00 1.000E+03  
 937 0.000E+00 0.000E+00 1.000E+03

\*

\*----- SLIDING INTERFACE DEFINITIONS -----\*

\*

48	225	3	0.000E+00	0.000E+00	0.000E+00	0	0	00.0E+000.0E+00
1	515	540	542	518				
2	540	541	543	542				
3	518	542	544	521				
4	542	543	545	544				
5	521	544	576	560				
6	544	545	577	576				
7	560	576	578	563				
8	576	577	579	578				
9	899	902	914	912				
10	912	914	915	913				
11	902	905	916	914				
12	914	916	917	915				
13	905	926	934	916				
14	916	934	935	917				
15	926	929	936	934				
16	934	936	937	935				
17	590	596	616	612				
18	612	616	617	613				
19	596	605	622	616				
20	616	622	623	617				
21	605	760	776	622				
22	622	776	777	623				
23	760	769	782	776				
24	776	782	783	777				
25	733	748	752	739				
26	748	749	753	752				
27	739	752	756	745				
28	752	753	757	756				
29	745	756	882	873				

30	756	757	883	882
31	873	882	886	879
32	882	883	887	886
33	667	673	675	669
34	669	675	677	671
35	671	677	721	717
36	717	721	723	719
37	673	679	681	675
38	675	681	683	677
39	677	683	725	721
40	721	725	727	723
41	679	821	823	681
42	681	823	825	683
43	683	825	861	725
44	725	861	863	727
45	821	827	829	823
46	823	829	831	825
47	825	831	865	861
48	861	865	867	863
1	1	3	35	33
2	3	5	37	35
3	5	7	39	37
4	7	9	41	39
5	9	11	43	41
6	11	13	45	43
7	13	15	47	45
8	15	17	49	47
9	17	19	51	49
10	19	21	53	51
11	21	23	55	53
12	23	25	57	55
13	25	27	59	57
14	27	29	61	59
15	29	31	63	61
16	33	35	67	65
17	35	37	69	67
18	37	39	71	69
19	39	41	73	71
20	41	43	75	73
21	43	45	77	75
22	45	47	79	77
23	47	49	81	79
24	49	51	83	81
25	51	53	85	83
26	53	55	87	85
27	55	57	89	87
28	57	59	91	89
29	59	61	93	91
30	61	63	95	93
31	65	67	99	97
32	67	69	101	99
33	69	71	103	101
34	71	73	105	103
35	73	75	107	105
36	75	77	109	107
37	77	79	111	109
38	79	81	113	111
39	81	83	115	113
40	83	85	117	115
41	85	87	119	117
42	87	89	121	119
43	89	91	123	121
44	91	93	125	123
45	93	95	127	125

46	97	99	131	129
47	99	101	133	131
48	101	103	135	133
49	103	105	137	135
50	105	107	139	137
51	107	109	141	139
52	109	111	143	141
53	111	113	145	143
54	113	115	147	145
55	115	117	149	147
56	117	119	151	149
57	119	121	153	151
58	121	123	155	153
59	123	125	157	155
60	125	127	159	157
61	129	131	163	161
62	131	133	165	163
63	133	135	167	165
64	135	137	169	167
65	137	139	171	169
66	139	141	173	171
67	141	143	175	173
68	143	145	177	175
69	145	147	179	177
70	147	149	181	179
71	149	151	183	181
72	151	153	185	183
73	153	155	187	185
74	155	157	189	187
75	157	159	191	189
76	161	163	195	193
77	163	165	197	195
78	165	167	199	197
79	167	169	201	199
80	169	171	203	201
81	171	173	205	203
82	173	175	207	205
83	175	177	209	207
84	177	179	211	209
85	179	181	213	211
86	181	183	215	213
87	183	185	217	215
88	185	187	219	217
89	187	189	221	219
90	189	191	223	221
91	193	195	227	225
92	195	197	229	227
93	197	199	231	229
94	199	201	233	231
95	201	203	235	233
96	203	205	237	235
97	205	207	239	237
98	207	209	241	239
99	209	211	243	241
100	211	213	245	243
101	213	215	247	245
102	215	217	249	247
103	217	219	251	249
104	219	221	253	251
105	221	223	255	253
106	225	227	259	257
107	227	229	261	259
108	229	231	263	261
109	231	233	265	263

110	233	235	267	265
111	235	237	269	267
112	237	239	271	269
113	239	241	273	271
114	241	243	275	273
115	243	245	277	275
116	245	247	279	277
117	247	249	281	279
118	249	251	283	281
119	251	253	285	283
120	253	255	287	285
121	257	259	291	289
122	259	261	293	291
123	261	263	295	293
124	263	265	297	295
125	265	267	299	297
126	267	269	301	299
127	269	271	303	301
128	271	273	305	303
129	273	275	307	305
130	275	277	309	307
131	277	279	311	309
132	279	281	313	311
133	281	283	315	313
134	283	285	317	315
135	285	287	319	317
136	289	291	323	321
137	291	293	325	323
138	293	295	327	325
139	295	297	329	327
140	297	299	331	329
141	299	301	333	331
142	301	303	335	333
143	303	305	337	335
144	305	307	339	337
145	307	309	341	339
146	309	311	343	341
147	311	313	345	343
148	313	315	347	345
149	315	317	349	347
150	317	319	351	349
151	321	323	355	353
152	323	325	357	355
153	325	327	359	357
154	327	329	361	359
155	329	331	363	361
156	331	333	365	363
157	333	335	367	365
158	335	337	369	367
159	337	339	371	369
160	339	341	373	371
161	341	343	375	373
162	343	345	377	375
163	345	347	379	377
164	347	349	381	379
165	349	351	383	381
166	353	355	387	385
167	355	357	389	387
168	357	359	391	389
169	359	361	393	391
170	361	363	395	393
171	363	365	397	395
172	365	367	399	397
173	367	369	401	399

174	369	371	403	401
175	371	373	405	403
176	373	375	407	405
177	375	377	409	407
178	377	379	411	409
179	379	381	413	411
180	381	383	415	413
181	385	387	419	417
182	387	389	421	419
183	389	391	423	421
184	391	393	425	423
185	393	395	427	425
186	395	397	429	427
187	397	399	431	429
188	399	401	433	431
189	401	403	435	433
190	403	405	437	435
191	405	407	439	437
192	407	409	441	439
193	409	411	443	441
194	411	413	445	443
195	413	415	447	445
196	417	419	451	449
197	419	421	453	451
198	421	423	455	453
199	423	425	457	455
200	425	427	459	457
201	427	429	461	459
202	429	431	463	461
203	431	433	465	463
204	433	435	467	465
205	435	437	469	467
206	437	439	471	469
207	439	441	473	471
208	441	443	475	473
209	443	445	477	475
210	445	447	479	477
211	449	451	483	481
212	451	453	485	483
213	453	455	487	485
214	455	457	489	487
215	457	459	491	489
216	459	461	493	491
217	461	463	495	493
218	463	465	497	495
219	465	467	499	497
220	467	469	501	499
221	469	471	503	501
222	471	473	505	503
223	473	475	507	505
224	475	477	509	507
225	477	479	511	509

# Dyna3d Sample Output File

c ball impact problem

\*\*\*\*\*

```

*****  **  **  *  **  *****  *****  *****
*****  **  **  **  **  *****  *****  *****
**  ***  **  **  ***  **  ***  ***  **  **  ***
**  **  **  **  ****  **  **  **  **  **  **  **
**  **  ****  **  **  **  **  **  ****  **  **
**  **  **  **  **  **  **  ****  **  **  **
**  **  **  **  ****  ****  ****  **  **  **
**  ***  **  **  **  ***  **  **  ***  ***  **  ***
*****  **  **  **  **  **  **  ****  ****  ****
*****  **  **  *  **  **  **  ****  ****  ****

```

\*\*\*\*\*

dyna3d (version 3.2.3 ) compiled 6/04/92

code input version =1988  
formats =large

## control information

number of materials.....	2
number of nodes.....	937
number of solid elements.....	481
number of beam elements.....	0
number of shell elements.....	0
number of thick shell elements.....	0
number of interface segments for linking.....	0
output interval for interface file.....	0.0000E+00
factor for minimum shell element time step....	0.0000E+00
number of nodal time history blocks.....	0
number of solid element time history blocks....	0
number of beam element time history blocks....	0
number of shell element time history blocks....	0
number of thick shell element time hist blocks.	0
problem status report interval in printer file.	1000
number of sliding boundary planes.....	0
number of sliding boundary planes w/ failure ..	0

number of points in density vs. depth curve....	0
overpressure option (eq.0 no, eq.1 yes).....	0
number of rigid body merge cards.....	0
number of cross section definitions.....	0
output interval for cross section forces.....	0.00E+00
number of load curves.....	0
number of concentrated load cards.....	0
number of traction cards.....	0
number of prescribed velocity cards.....	0
number of rigid wall definitions.....	0
number of nodal constraint cards .....	0
initialization of velocities.....	1
eq.0, velocities are initialized to zero	
eq.1, initial velocities are read in	
number of sliding interface definitions.....	1
x-dir base acceleration.....	0
eq.0, no	
eq.1, yes	
y-dir base acceleration.....	0
eq.0, no	
eq.1, yes	
z-dir base acceleration.....	0
eq.0, no	
eq.1, yes	
x-dir angular velocity.....	0
eq.0, no	
eq.1, yes	
y-dir angular velocity.....	0
eq.0, no	
eq.1, yes	
z-dir angular velocity.....	0
eq.0, no	
eq.1, yes	
no. of solid elements for momentum depositeon...	0
number of detonation points.....	0
termination time.....	0.10E+00
time step between dumps of time history data...	0.10E-02
time step between dumps of complete state data.	0.50E-01

```

number of time steps between restart dumps.....999999

no. of time steps between running rstrt dumps..999999

initial time step size..... 0.00E+00
    eq.0.0, dyna3d picks initial step size

scale factor for sliding interface penalties... 0.10E+00

thermal effects option..... 0
    eq.0: no thermal effects
    eq.n: nodal temps scaled by load ftn -n-
    lt.0: nodal temps are on disk file

    eq.-9999: nodal temps are in input

viscosity reset option..... 0
    eq.0: default viscosities set by dyna3d
    eq.1: default viscosities read in

time step scale factor..... 0.90E+00

number of rigid body joints..... 0

number of extra node blocks..... 0

number of shell-solid interfaces..... 0

number of tie-breaking shell slidelines..... 0

number of blocks of tied nodes with failure.... 0

load curve for maximum timestep..... 0

spring-damper input option..... 0
    eq.0: no input
    eq.1: discrete springs and dampers defined

number of rigid body inertia definitions..... 0

shell strain dump flag..... 0

hughes-liu normal computation options..... -1
    eq.-2: unique nodal fibers per hughes-liu
    eq.-1: compute normals each time step
    eq.0 : default set to -1
    eq.1 : compute on restart
    eq.n : compute on restart and every nth step

thickness modification for membrane strains.... 0
    eq.0: no
    eq.1: yes

shell formulation basis..... 2
    eq.1: hughes-liu shell theory
    eq.2: belytschko-lin-tsay shell theory
    eq.3: bc12
    eq.4: c0-triangular element
    eq.5: membrane element
    eq.6: yase

```



number of non-reflecting boundary segments.....	0
number of single point constraint nodes.....	0
number of spc coordinate system definitions....	0
reduction factor for tsmn.....	0.00E+00
# of user specified beam integration rules.....	0
max number of integration points reqd (beams) .	0
# of user specified shell integration rules....	0
max number of integration points reqd (shells).	0
convergence check interval (dynamic relaxation)	250
convergence tolerance for dynamic relaxation...	0.10E-03
time step size calculation for 4-node shells...	0
eq.0: based on longest element side	
eq.1: based on longest element diagonal	
eq.2: based on bar wave speed max side	
iterative plane stress plasticity for shells ..	1
eq.1: vectorized with three iterates	
eq.2: nonvectorized iterations as needed	
eq.3: noniterative approximate radial return	
time zero printout of element time step size .	0
eq.0: no printout	
eq.1: print dt for each element at t=0	
number of ld slidelines.....	0
mass coef. for rayleigh damping .....	0.00E+00
number of matls for stif. rayleigh damping.....	0

1

## m a t e r i a l   d e f i n i t i o n

### material models

eq.1	isotropic elastic
eq.2	orthotropic elastic
eq.3	kinematic/isotropic elastic-plastic
eq.4	thermo-elastic-plastic
eq.5	soil and crushable foam
eq.6	viscoelastic
eq.7	blatz-ko hyperelastic rubber
eq.8	high explosive
eq.9	fluid material
eq.10	isotropic elastic-plastic hydrodynamic
eq.11	steinberg-guinan high-rate elastic-plastic
eq.12	isotropic elastic-plastic
eq.13	elastic-plastic with failure
eq.14	soil and crushable foam with failure
eq.15	johnson/cook elastic-plastic
eq.16	concrete/geological material
eq.17	elastic-plastic with oriented cracks

- eq.18 power law isotropic elastic-plastic
- eq.19 strain rate dependent elastic-plastic
- eq.20 rigid
- eq.21 thermal orthotropic elastic
- eq.22 fiber composite with damage
- eq.23 thermal orthotropic elastic w/ variable props
- eq.24 rate-dependent tabular elastic-plastic
- eq.25 extended two-invariant geologic cap
- eq.26 crushable metallic honeycomb
- eq.27 compressible mooney-rivlin hyperelastic rubber
- eq.28 resultant plasticity
- eq.29 not currently available
- eq.30 closed form update elastic-plastic for shells
- eq.31 frazer-nash hyperelastic rubber
- eq.32 ramberg osgood elastic-plastic
- eq.33 hill general anisotropic plasticity
- eq.34 hill normal anisotropic plasticity for shells
- eq.35 elastic-plastic with forming limit diagram

#### equation-of-state models

- eq.1 linear polynomial
- eq.2 jwl high explosive
- eq.3 sack high explosive
- eq.4 gruneisen
- eq.5 ratio of polynomials
- eq.6 linear polynomial with energy deposition
- eq.7 initiation and reaction in he
- eq.8 compaction
- eq.9 tabulated
- eq.10 not currently available
- eq.11 pore collapse

#### hourglass viscosity models

- eq.1 standard
- eq.2 flanagan-belytschko viscous form
- eq.3 full flanagan-belytschko viscous form  
(belytschko constant stress elements)
- eq.4 flanagan-belytschko stiffness form
- eq.5 full flanagan-belytschko stiffness form  
(belytschko constant stress elements)

#### bulk viscosity models

- eq.1 standard

#### default viscosities

hourglass viscosity type.....	1
hourglass viscosity coefficient.....	0.1000E+00
bulk viscosity type.....	1
quadratic bulk viscosity coefficient..	0.1440E+01
linear bulk viscosity coefficient.....	0.6000E-01

material type # 6 (viscoelastic)

material constants set number .... 1

```

material model ..... 6
equation-of-state model .... 0
hourglass viscosity model .. 1
bulk viscosity model ..... 1

den ..... = 0.1300E+03
hourglass viscosity ..... = 0.1000E+00
quadratic bulk viscosity ..... = 0.1440E+01
linear bulk viscosity ..... = 0.6000E-01
element type ..... = 0
  eq.0: 8-node solid element
  eq.1: 2-node beam or truss element
  eq.2: 4-node membrane or shell element
  eq.3: 8-node membrane or shell element

standard dyna3d viscoelastic model
bulk ..... = 0.3667E+11
short time shear modulus ..... = 0.2200E+11
long time shear modulus ..... = 0.1760E+11
decay constant ..... = 0.1000E+07

```

material type # 1 (elastic)

material constants set number .... 2

```

material model ..... 1
equation-of-state model .... 0
hourglass viscosity model .. 1
bulk viscosity model ..... 1

den ..... = 0.8000E+04
hourglass viscosity ..... = 0.1000E+00
quadratic bulk viscosity ..... = 0.1440E+01
linear bulk viscosity ..... = 0.6000E-01
element type ..... = 0
  eq.0: 8-node solid element
  eq.1: 2-node beam or truss element
  eq.2: 4-node membrane or shell element
  eq.3: 8-node membrane or shell element

e ..... = 0.2000E+12
vnu ..... = 0.3000E+00

```

1 n o d a l p o i n t c o o r d i n a t e s

np	type	x-ord	y-ord	z-ord	
1	7.0	-0.2500E+03	-0.2500E+03	0.1000E+03	7.0
2	7.0	-0.2500E+03	-0.2500E+03	0.2000E+03	7.0
3	7.0	-0.2500E+03	-0.2167E+03	0.1000E+03	7.0
4	7.0	-0.2500E+03	-0.2167E+03	0.2000E+03	7.0
5	7.0	-0.2500E+03	-0.1833E+03	0.1000E+03	7.0
6	7.0	-0.2500E+03	-0.1833E+03	0.2000E+03	7.0
7	7.0	-0.2500E+03	-0.1500E+03	0.1000E+03	7.0
8	7.0	-0.2500E+03	-0.1500E+03	0.2000E+03	7.0
9	7.0	-0.2500E+03	-0.1167E+03	0.1000E+03	7.0
10	7.0	-0.2500E+03	-0.1167E+03	0.2000E+03	7.0
11	7.0	-0.2500E+03	-0.8333E+02	0.1000E+03	7.0

12	7.0	-0.2500E+03	-0.8333E+02	0.2000E+03	7.0
13	7.0	-0.2500E+03	-0.5000E+02	0.1000E+03	7.0
14	7.0	-0.2500E+03	-0.5000E+02	0.2000E+03	7.0
15	7.0	-0.2500E+03	-0.1667E+02	0.1000E+03	7.0
16	7.0	-0.2500E+03	-0.1667E+02	0.2000E+03	7.0
17	7.0	-0.2500E+03	0.1667E+02	0.1000E+03	7.0
18	7.0	-0.2500E+03	0.1667E+02	0.2000E+03	7.0
19	7.0	-0.2500E+03	0.5000E+02	0.1000E+03	7.0
20	7.0	-0.2500E+03	0.5000E+02	0.2000E+03	7.0
21	7.0	-0.2500E+03	0.8333E+02	0.1000E+03	7.0
22	7.0	-0.2500E+03	0.8333E+02	0.2000E+03	7.0
23	7.0	-0.2500E+03	0.1167E+03	0.1000E+03	7.0
24	7.0	-0.2500E+03	0.1167E+03	0.2000E+03	7.0
25	7.0	-0.2500E+03	0.1500E+03	0.1000E+03	7.0
26	7.0	-0.2500E+03	0.1500E+03	0.2000E+03	7.0
27	7.0	-0.2500E+03	0.1833E+03	0.1000E+03	7.0
28	7.0	-0.2500E+03	0.1833E+03	0.2000E+03	7.0
29	7.0	-0.2500E+03	0.2167E+03	0.1000E+03	7.0
30	7.0	-0.2500E+03	0.2167E+03	0.2000E+03	7.0
31	7.0	-0.2500E+03	0.2500E+03	0.1000E+03	7.0
32	7.0	-0.2500E+03	0.2500E+03	0.2000E+03	7.0
33	7.0	-0.2167E+03	-0.2500E+03	0.1000E+03	7.0
34	7.0	-0.2167E+03	-0.2500E+03	0.2000E+03	7.0
35	0.0	-0.2167E+03	-0.2167E+03	0.1000E+03	7.0
36	0.0	-0.2167E+03	-0.2167E+03	0.2000E+03	7.0
37	0.0	-0.2167E+03	-0.1833E+03	0.1000E+03	7.0
38	0.0	-0.2167E+03	-0.1833E+03	0.2000E+03	7.0
39	0.0	-0.2167E+03	-0.1500E+03	0.1000E+03	7.0
40	0.0	-0.2167E+03	-0.1500E+03	0.2000E+03	7.0
41	0.0	-0.2167E+03	-0.1167E+03	0.1000E+03	7.0
42	0.0	-0.2167E+03	-0.1167E+03	0.2000E+03	7.0
43	0.0	-0.2167E+03	-0.8333E+02	0.1000E+03	7.0
44	0.0	-0.2167E+03	-0.8333E+02	0.2000E+03	7.0
45	0.0	-0.2167E+03	-0.5000E+02	0.1000E+03	7.0
46	0.0	-0.2167E+03	-0.5000E+02	0.2000E+03	7.0
47	0.0	-0.2167E+03	-0.1667E+02	0.1000E+03	7.0
48	0.0	-0.2167E+03	-0.1667E+02	0.2000E+03	7.0
49	0.0	-0.2167E+03	0.1667E+02	0.1000E+03	7.0
50	0.0	-0.2167E+03	0.1667E+02	0.2000E+03	7.0

1 n o d a 1 p o i n t c o o r d i n a t e s

np	type	x-ord	y-ord	z-ord	
51	0.0	-0.2167E+03	0.5000E+02	0.1000E+03	7.0
52	0.0	-0.2167E+03	0.5000E+02	0.2000E+03	7.0
53	0.0	-0.2167E+03	0.8333E+02	0.1000E+03	7.0
54	0.0	-0.2167E+03	0.8333E+02	0.2000E+03	7.0
55	0.0	-0.2167E+03	0.1167E+03	0.1000E+03	7.0
56	0.0	-0.2167E+03	0.1167E+03	0.2000E+03	7.0
57	0.0	-0.2167E+03	0.1500E+03	0.1000E+03	7.0
58	0.0	-0.2167E+03	0.1500E+03	0.2000E+03	7.0
59	0.0	-0.2167E+03	0.1833E+03	0.1000E+03	7.0
60	0.0	-0.2167E+03	0.1833E+03	0.2000E+03	7.0
61	0.0	-0.2167E+03	0.2167E+03	0.1000E+03	7.0
62	0.0	-0.2167E+03	0.2167E+03	0.2000E+03	7.0
63	7.0	-0.2167E+03	0.2500E+03	0.1000E+03	7.0
64	7.0	-0.2167E+03	0.2500E+03	0.2000E+03	7.0
65	7.0	-0.1833E+03	-0.2500E+03	0.1000E+03	7.0
66	7.0	-0.1833E+03	-0.2500E+03	0.2000E+03	7.0
67	0.0	-0.1833E+03	-0.2167E+03	0.1000E+03	7.0
68	0.0	-0.1833E+03	-0.2167E+03	0.2000E+03	7.0
69	0.0	-0.1833E+03	-0.1833E+03	0.1000E+03	7.0
70	0.0	-0.1833E+03	-0.1833E+03	0.2000E+03	7.0

71	0.0	-0.1833E+03	-0.1500E+03	0.1000E+03	7.0
72	0.0	-0.1833E+03	-0.1500E+03	0.2000E+03	7.0
73	0.0	-0.1833E+03	-0.1167E+03	0.1000E+03	7.0
74	0.0	-0.1833E+03	-0.1167E+03	0.2000E+03	7.0
75	0.0	-0.1833E+03	-0.8333E+02	0.1000E+03	7.0
76	0.0	-0.1833E+03	-0.8333E+02	0.2000E+03	7.0
77	0.0	-0.1833E+03	-0.5000E+02	0.1000E+03	7.0
78	0.0	-0.1833E+03	-0.5000E+02	0.2000E+03	7.0
79	0.0	-0.1833E+03	-0.1667E+02	0.1000E+03	7.0
80	0.0	-0.1833E+03	-0.1667E+02	0.2000E+03	7.0
81	0.0	-0.1833E+03	0.1667E+02	0.1000E+03	7.0
82	0.0	-0.1833E+03	0.1667E+02	0.2000E+03	7.0
83	0.0	-0.1833E+03	0.5000E+02	0.1000E+03	7.0
84	0.0	-0.1833E+03	0.5000E+02	0.2000E+03	7.0
85	0.0	-0.1833E+03	0.8333E+02	0.1000E+03	7.0
86	0.0	-0.1833E+03	0.8333E+02	0.2000E+03	7.0
87	0.0	-0.1833E+03	0.1167E+03	0.1000E+03	7.0
88	0.0	-0.1833E+03	0.1167E+03	0.2000E+03	7.0
89	0.0	-0.1833E+03	0.1500E+03	0.1000E+03	7.0
90	0.0	-0.1833E+03	0.1500E+03	0.2000E+03	7.0
91	0.0	-0.1833E+03	0.1833E+03	0.1000E+03	7.0
92	0.0	-0.1833E+03	0.1833E+03	0.2000E+03	7.0
93	0.0	-0.1833E+03	0.2167E+03	0.1000E+03	7.0
94	0.0	-0.1833E+03	0.2167E+03	0.2000E+03	7.0
95	7.0	-0.1833E+03	0.2500E+03	0.1000E+03	7.0
96	7.0	-0.1833E+03	0.2500E+03	0.2000E+03	7.0
97	7.0	-0.1500E+03	-0.2500E+03	0.1000E+03	7.0
98	7.0	-0.1500E+03	-0.2500E+03	0.2000E+03	7.0
99	0.0	-0.1500E+03	-0.2167E+03	0.1000E+03	7.0
100	0.0	-0.1500E+03	-0.2167E+03	0.2000E+03	7.0

1 n o d a l   p o i n t   c o o r d i n a t e s

np	type	x-ord	y-ord	z-ord	
101	0.0	-0.1500E+03	-0.1833E+03	0.1000E+03	7.0
102	0.0	-0.1500E+03	-0.1833E+03	0.2000E+03	7.0
103	0.0	-0.1500E+03	-0.1500E+03	0.1000E+03	7.0
104	0.0	-0.1500E+03	-0.1500E+03	0.2000E+03	7.0
105	0.0	-0.1500E+03	-0.1167E+03	0.1000E+03	7.0
106	0.0	-0.1500E+03	-0.1167E+03	0.2000E+03	7.0
107	0.0	-0.1500E+03	-0.8333E+02	0.1000E+03	7.0
108	0.0	-0.1500E+03	-0.8333E+02	0.2000E+03	7.0
109	0.0	-0.1500E+03	-0.5000E+02	0.1000E+03	7.0
110	0.0	-0.1500E+03	-0.5000E+02	0.2000E+03	7.0
111	0.0	-0.1500E+03	-0.1667E+02	0.1000E+03	7.0
112	0.0	-0.1500E+03	-0.1667E+02	0.2000E+03	7.0
113	0.0	-0.1500E+03	0.1667E+02	0.1000E+03	7.0
114	0.0	-0.1500E+03	0.1667E+02	0.2000E+03	7.0
115	0.0	-0.1500E+03	0.5000E+02	0.1000E+03	7.0
116	0.0	-0.1500E+03	0.5000E+02	0.2000E+03	7.0
117	0.0	-0.1500E+03	0.8333E+02	0.1000E+03	7.0
118	0.0	-0.1500E+03	0.8333E+02	0.2000E+03	7.0
119	0.0	-0.1500E+03	0.1167E+03	0.1000E+03	7.0
120	0.0	-0.1500E+03	0.1167E+03	0.2000E+03	7.0
121	0.0	-0.1500E+03	0.1500E+03	0.1000E+03	7.0
122	0.0	-0.1500E+03	0.1500E+03	0.2000E+03	7.0
123	0.0	-0.1500E+03	0.1833E+03	0.1000E+03	7.0
124	0.0	-0.1500E+03	0.1833E+03	0.2000E+03	7.0
125	0.0	-0.1500E+03	0.2167E+03	0.1000E+03	7.0
126	0.0	-0.1500E+03	0.2167E+03	0.2000E+03	7.0
127	7.0	-0.1500E+03	0.2500E+03	0.1000E+03	7.0
128	7.0	-0.1500E+03	0.2500E+03	0.2000E+03	7.0
129	7.0	-0.1167E+03	-0.2500E+03	0.1000E+03	7.0

130	7.0	-0.1167E+03	-0.2500E+03	0.2000E+03	7.0
131	0.0	-0.1167E+03	-0.2167E+03	0.1000E+03	7.0
132	0.0	-0.1167E+03	-0.2167E+03	0.2000E+03	7.0
133	0.0	-0.1167E+03	-0.1833E+03	0.1000E+03	7.0
134	0.0	-0.1167E+03	-0.1833E+03	0.2000E+03	7.0
135	0.0	-0.1167E+03	-0.1500E+03	0.1000E+03	7.0
136	0.0	-0.1167E+03	-0.1500E+03	0.2000E+03	7.0
137	0.0	-0.1167E+03	-0.1167E+03	0.1000E+03	7.0
138	0.0	-0.1167E+03	-0.1167E+03	0.2000E+03	7.0
139	0.0	-0.1167E+03	-0.8333E+02	0.1000E+03	7.0
140	0.0	-0.1167E+03	-0.8333E+02	0.2000E+03	7.0
141	0.0	-0.1167E+03	-0.5000E+02	0.1000E+03	7.0
142	0.0	-0.1167E+03	-0.5000E+02	0.2000E+03	7.0
143	0.0	-0.1167E+03	-0.1667E+02	0.1000E+03	7.0
144	0.0	-0.1167E+03	-0.1667E+02	0.2000E+03	7.0
145	0.0	-0.1167E+03	0.1667E+02	0.1000E+03	7.0
146	0.0	-0.1167E+03	0.1667E+02	0.2000E+03	7.0
147	0.0	-0.1167E+03	0.5000E+02	0.1000E+03	7.0
148	0.0	-0.1167E+03	0.5000E+02	0.2000E+03	7.0
149	0.0	-0.1167E+03	0.8333E+02	0.1000E+03	7.0
150	0.0	-0.1167E+03	0.8333E+02	0.2000E+03	7.0

1 n o d a l   p o i n t   c o o r d i n a t e s

np	type	x-ord	y-ord	z-ord	
151	0.0	-0.1167E+03	0.1167E+03	0.1000E+03	7.0
152	0.0	-0.1167E+03	0.1167E+03	0.2000E+03	7.0
153	0.0	-0.1167E+03	0.1500E+03	0.1000E+03	7.0
154	0.0	-0.1167E+03	0.1500E+03	0.2000E+03	7.0
155	0.0	-0.1167E+03	0.1833E+03	0.1000E+03	7.0
156	0.0	-0.1167E+03	0.1833E+03	0.2000E+03	7.0
157	0.0	-0.1167E+03	0.2167E+03	0.1000E+03	7.0
158	0.0	-0.1167E+03	0.2167E+03	0.2000E+03	7.0
159	7.0	-0.1167E+03	0.2500E+03	0.1000E+03	7.0
160	7.0	-0.1167E+03	0.2500E+03	0.2000E+03	7.0
161	7.0	-0.8333E+02	-0.2500E+03	0.1000E+03	7.0
162	7.0	-0.8333E+02	-0.2500E+03	0.2000E+03	7.0
163	0.0	-0.8333E+02	-0.2167E+03	0.1000E+03	7.0
164	0.0	-0.8333E+02	-0.2167E+03	0.2000E+03	7.0
165	0.0	-0.8333E+02	-0.1833E+03	0.1000E+03	7.0
166	0.0	-0.8333E+02	-0.1833E+03	0.2000E+03	7.0
167	0.0	-0.8333E+02	-0.1500E+03	0.1000E+03	7.0
168	0.0	-0.8333E+02	-0.1500E+03	0.2000E+03	7.0
169	0.0	-0.8333E+02	-0.1167E+03	0.1000E+03	7.0
170	0.0	-0.8333E+02	-0.1167E+03	0.2000E+03	7.0
171	0.0	-0.8333E+02	-0.8333E+02	0.1000E+03	7.0
172	0.0	-0.8333E+02	-0.8333E+02	0.2000E+03	7.0
173	0.0	-0.8333E+02	-0.5000E+02	0.1000E+03	7.0
174	0.0	-0.8333E+02	-0.5000E+02	0.2000E+03	7.0
175	0.0	-0.8333E+02	-0.1667E+02	0.1000E+03	7.0
176	0.0	-0.8333E+02	-0.1667E+02	0.2000E+03	7.0
177	0.0	-0.8333E+02	0.1667E+02	0.1000E+03	7.0
178	0.0	-0.8333E+02	0.1667E+02	0.2000E+03	7.0
179	0.0	-0.8333E+02	0.5000E+02	0.1000E+03	7.0
180	0.0	-0.8333E+02	0.5000E+02	0.2000E+03	7.0
181	0.0	-0.8333E+02	0.8333E+02	0.1000E+03	7.0
182	0.0	-0.8333E+02	0.8333E+02	0.2000E+03	7.0
183	0.0	-0.8333E+02	0.1167E+03	0.1000E+03	7.0
184	0.0	-0.8333E+02	0.1167E+03	0.2000E+03	7.0
185	0.0	-0.8333E+02	0.1500E+03	0.1000E+03	7.0
186	0.0	-0.8333E+02	0.1500E+03	0.2000E+03	7.0
187	0.0	-0.8333E+02	0.1833E+03	0.1000E+03	7.0
188	0.0	-0.8333E+02	0.1833E+03	0.2000E+03	7.0

189	0.0	-0.8333E+02	0.2167E+03	0.1000E+03	7.0
190	0.0	-0.8333E+02	0.2167E+03	0.2000E+03	7.0
191	7.0	-0.8333E+02	0.2500E+03	0.1000E+03	7.0
192	7.0	-0.8333E+02	0.2500E+03	0.2000E+03	7.0
193	7.0	-0.5000E+02	-0.2500E+03	0.1000E+03	7.0
194	7.0	-0.5000E+02	-0.2500E+03	0.2000E+03	7.0
195	0.0	-0.5000E+02	-0.2167E+03	0.1000E+03	7.0
196	0.0	-0.5000E+02	-0.2167E+03	0.2000E+03	7.0
197	0.0	-0.5000E+02	-0.1833E+03	0.1000E+03	7.0
198	0.0	-0.5000E+02	-0.1833E+03	0.2000E+03	7.0
199	0.0	-0.5000E+02	-0.1500E+03	0.1000E+03	7.0
200	0.0	-0.5000E+02	-0.1500E+03	0.2000E+03	7.0

1 n o d a l   p o i n t   c o o r d i n a t e s

np	type	x-ord	y-ord	z-ord	
201	0.0	-0.5000E+02	-0.1167E+03	0.1000E+03	7.0
202	0.0	-0.5000E+02	-0.1167E+03	0.2000E+03	7.0
203	0.0	-0.5000E+02	-0.8333E+02	0.1000E+03	7.0
204	0.0	-0.5000E+02	-0.8333E+02	0.2000E+03	7.0
205	0.0	-0.5000E+02	-0.5000E+02	0.1000E+03	7.0
206	0.0	-0.5000E+02	-0.5000E+02	0.2000E+03	7.0
207	0.0	-0.5000E+02	-0.1667E+02	0.1000E+03	7.0
208	0.0	-0.5000E+02	-0.1667E+02	0.2000E+03	7.0
209	0.0	-0.5000E+02	0.1667E+02	0.1000E+03	7.0
210	0.0	-0.5000E+02	0.1667E+02	0.2000E+03	7.0
211	0.0	-0.5000E+02	0.5000E+02	0.1000E+03	7.0
212	0.0	-0.5000E+02	0.5000E+02	0.2000E+03	7.0
213	0.0	-0.5000E+02	0.8333E+02	0.1000E+03	7.0
214	0.0	-0.5000E+02	0.8333E+02	0.2000E+03	7.0
215	0.0	-0.5000E+02	0.1167E+03	0.1000E+03	7.0
216	0.0	-0.5000E+02	0.1167E+03	0.2000E+03	7.0
217	0.0	-0.5000E+02	0.1500E+03	0.1000E+03	7.0
218	0.0	-0.5000E+02	0.1500E+03	0.2000E+03	7.0
219	0.0	-0.5000E+02	0.1833E+03	0.1000E+03	7.0
220	0.0	-0.5000E+02	0.1833E+03	0.2000E+03	7.0
221	0.0	-0.5000E+02	0.2167E+03	0.1000E+03	7.0
222	0.0	-0.5000E+02	0.2167E+03	0.2000E+03	7.0
223	7.0	-0.5000E+02	0.2500E+03	0.1000E+03	7.0
224	7.0	-0.5000E+02	0.2500E+03	0.2000E+03	7.0
225	7.0	-0.1667E+02	-0.2500E+03	0.1000E+03	7.0
226	7.0	-0.1667E+02	-0.2500E+03	0.2000E+03	7.0
227	0.0	-0.1667E+02	-0.2167E+03	0.1000E+03	7.0
228	0.0	-0.1667E+02	-0.2167E+03	0.2000E+03	7.0
229	0.0	-0.1667E+02	-0.1833E+03	0.1000E+03	7.0
230	0.0	-0.1667E+02	-0.1833E+03	0.2000E+03	7.0
231	0.0	-0.1667E+02	-0.1500E+03	0.1000E+03	7.0
232	0.0	-0.1667E+02	-0.1500E+03	0.2000E+03	7.0
233	0.0	-0.1667E+02	-0.1167E+03	0.1000E+03	7.0
234	0.0	-0.1667E+02	-0.1167E+03	0.2000E+03	7.0
235	0.0	-0.1667E+02	-0.8333E+02	0.1000E+03	7.0
236	0.0	-0.1667E+02	-0.8333E+02	0.2000E+03	7.0
237	0.0	-0.1667E+02	-0.5000E+02	0.1000E+03	7.0
238	0.0	-0.1667E+02	-0.5000E+02	0.2000E+03	7.0
239	0.0	-0.1667E+02	-0.1667E+02	0.1000E+03	7.0
240	0.0	-0.1667E+02	-0.1667E+02	0.2000E+03	7.0
241	0.0	-0.1667E+02	0.1667E+02	0.1000E+03	7.0
242	0.0	-0.1667E+02	0.1667E+02	0.2000E+03	7.0
243	0.0	-0.1667E+02	0.5000E+02	0.1000E+03	7.0
244	0.0	-0.1667E+02	0.5000E+02	0.2000E+03	7.0
245	0.0	-0.1667E+02	0.8333E+02	0.1000E+03	7.0
246	0.0	-0.1667E+02	0.8333E+02	0.2000E+03	7.0
247	0.0	-0.1667E+02	0.1167E+03	0.1000E+03	7.0

248	0.0	-0.1667E+02	0.1167E+03	0.2000E+03	7.0
249	0.0	-0.1667E+02	0.1500E+03	0.1000E+03	7.0
250	0.0	-0.1667E+02	0.1500E+03	0.2000E+03	7.0

l n o d a l   p o i n t   c o o r d i n a t e s

np	type	x-ord	y-ord	z-ord	
251	0.0	-0.1667E+02	0.1833E+03	0.1000E+03	7.0
252	0.0	-0.1667E+02	0.1833E+03	0.2000E+03	7.0
253	0.0	-0.1667E+02	0.2167E+03	0.1000E+03	7.0
254	0.0	-0.1667E+02	0.2167E+03	0.2000E+03	7.0
255	7.0	-0.1667E+02	0.2500E+03	0.1000E+03	7.0
256	7.0	-0.1667E+02	0.2500E+03	0.2000E+03	7.0
257	7.0	0.1667E+02	-0.2500E+03	0.1000E+03	7.0
258	7.0	0.1667E+02	-0.2500E+03	0.2000E+03	7.0
259	0.0	0.1667E+02	-0.2167E+03	0.1000E+03	7.0
260	0.0	0.1667E+02	-0.2167E+03	0.2000E+03	7.0
261	0.0	0.1667E+02	-0.1833E+03	0.1000E+03	7.0
262	0.0	0.1667E+02	-0.1833E+03	0.2000E+03	7.0
263	0.0	0.1667E+02	-0.1500E+03	0.1000E+03	7.0
264	0.0	0.1667E+02	-0.1500E+03	0.2000E+03	7.0
265	0.0	0.1667E+02	-0.1167E+03	0.1000E+03	7.0
266	0.0	0.1667E+02	-0.1167E+03	0.2000E+03	7.0
267	0.0	0.1667E+02	-0.8333E+02	0.1000E+03	7.0
268	0.0	0.1667E+02	-0.8333E+02	0.2000E+03	7.0
269	0.0	0.1667E+02	-0.5000E+02	0.1000E+03	7.0
270	0.0	0.1667E+02	-0.5000E+02	0.2000E+03	7.0
271	0.0	0.1667E+02	-0.1667E+02	0.1000E+03	7.0
272	0.0	0.1667E+02	-0.1667E+02	0.2000E+03	7.0
273	0.0	0.1667E+02	0.1667E+02	0.1000E+03	7.0
274	0.0	0.1667E+02	0.1667E+02	0.2000E+03	7.0
275	0.0	0.1667E+02	0.5000E+02	0.1000E+03	7.0
276	0.0	0.1667E+02	0.5000E+02	0.2000E+03	7.0
277	0.0	0.1667E+02	0.8333E+02	0.1000E+03	7.0
278	0.0	0.1667E+02	0.8333E+02	0.2000E+03	7.0
279	0.0	0.1667E+02	0.1167E+03	0.1000E+03	7.0
280	0.0	0.1667E+02	0.1167E+03	0.2000E+03	7.0
281	0.0	0.1667E+02	0.1500E+03	0.1000E+03	7.0
282	0.0	0.1667E+02	0.1500E+03	0.2000E+03	7.0
283	0.0	0.1667E+02	0.1833E+03	0.1000E+03	7.0
284	0.0	0.1667E+02	0.1833E+03	0.2000E+03	7.0
285	0.0	0.1667E+02	0.2167E+03	0.1000E+03	7.0
286	0.0	0.1667E+02	0.2167E+03	0.2000E+03	7.0
287	7.0	0.1667E+02	0.2500E+03	0.1000E+03	7.0
288	7.0	0.1667E+02	0.2500E+03	0.2000E+03	7.0
289	7.0	0.5000E+02	-0.2500E+03	0.1000E+03	7.0
290	7.0	0.5000E+02	-0.2500E+03	0.2000E+03	7.0
291	0.0	0.5000E+02	-0.2167E+03	0.1000E+03	7.0
292	0.0	0.5000E+02	-0.2167E+03	0.2000E+03	7.0
293	0.0	0.5000E+02	-0.1833E+03	0.1000E+03	7.0
294	0.0	0.5000E+02	-0.1833E+03	0.2000E+03	7.0
295	0.0	0.5000E+02	-0.1500E+03	0.1000E+03	7.0
296	0.0	0.5000E+02	-0.1500E+03	0.2000E+03	7.0
297	0.0	0.5000E+02	-0.1167E+03	0.1000E+03	7.0
298	0.0	0.5000E+02	-0.1167E+03	0.2000E+03	7.0
299	0.0	0.5000E+02	-0.8333E+02	0.1000E+03	7.0
300	0.0	0.5000E+02	-0.8333E+02	0.2000E+03	7.0

l n o d a l   p o i n t   c o o r d i n a t e s

np	type	x-ord	y-ord	z-ord	
301	0.0	0.5000E+02	-0.5000E+02	0.1000E+03	7.0



302	0.0	0.5000E+02	-0.5000E+02	0.2000E+03	7.0
303	0.0	0.5000E+02	-0.1667E+02	0.1000E+03	7.0
304	0.0	0.5000E+02	-0.1667E+02	0.2000E+03	7.0
305	0.0	0.5000E+02	0.1667E+02	0.1000E+03	7.0
306	0.0	0.5000E+02	0.1667E+02	0.2000E+03	7.0
307	0.0	0.5000E+02	0.5000E+02	0.1000E+03	7.0
308	0.0	0.5000E+02	0.5000E+02	0.2000E+03	7.0
309	0.0	0.5000E+02	0.8333E+02	0.1000E+03	7.0
310	0.0	0.5000E+02	0.8333E+02	0.2000E+03	7.0
311	0.0	0.5000E+02	0.1167E+03	0.1000E+03	7.0
312	0.0	0.5000E+02	0.1167E+03	0.2000E+03	7.0
313	0.0	0.5000E+02	0.1500E+03	0.1000E+03	7.0
314	0.0	0.5000E+02	0.1500E+03	0.2000E+03	7.0
315	0.0	0.5000E+02	0.1833E+03	0.1000E+03	7.0
316	0.0	0.5000E+02	0.1833E+03	0.2000E+03	7.0
317	0.0	0.5000E+02	0.2167E+03	0.1000E+03	7.0
318	0.0	0.5000E+02	0.2167E+03	0.2000E+03	7.0
319	7.0	0.5000E+02	0.2500E+03	0.1000E+03	7.0
320	7.0	0.5000E+02	0.2500E+03	0.2000E+03	7.0
321	7.0	0.8333E+02	-0.2500E+03	0.1000E+03	7.0
322	7.0	0.8333E+02	-0.2500E+03	0.2000E+03	7.0
323	0.0	0.8333E+02	-0.2167E+03	0.1000E+03	7.0
324	0.0	0.8333E+02	-0.2167E+03	0.2000E+03	7.0
325	0.0	0.8333E+02	-0.1833E+03	0.1000E+03	7.0
326	0.0	0.8333E+02	-0.1833E+03	0.2000E+03	7.0
327	0.0	0.8333E+02	-0.1500E+03	0.1000E+03	7.0
328	0.0	0.8333E+02	-0.1500E+03	0.2000E+03	7.0
329	0.0	0.8333E+02	-0.1167E+03	0.1000E+03	7.0
330	0.0	0.8333E+02	-0.1167E+03	0.2000E+03	7.0
331	0.0	0.8333E+02	-0.8333E+02	0.1000E+03	7.0
332	0.0	0.8333E+02	-0.8333E+02	0.2000E+03	7.0
333	0.0	0.8333E+02	-0.5000E+02	0.1000E+03	7.0
334	0.0	0.8333E+02	-0.5000E+02	0.2000E+03	7.0
335	0.0	0.8333E+02	-0.1667E+02	0.1000E+03	7.0
336	0.0	0.8333E+02	-0.1667E+02	0.2000E+03	7.0
337	0.0	0.8333E+02	0.1667E+02	0.1000E+03	7.0
338	0.0	0.8333E+02	0.1667E+02	0.2000E+03	7.0
339	0.0	0.8333E+02	0.5000E+02	0.1000E+03	7.0
340	0.0	0.8333E+02	0.5000E+02	0.2000E+03	7.0
341	0.0	0.8333E+02	0.8333E+02	0.1000E+03	7.0
342	0.0	0.8333E+02	0.8333E+02	0.2000E+03	7.0
343	0.0	0.8333E+02	0.1167E+03	0.1000E+03	7.0
344	0.0	0.8333E+02	0.1167E+03	0.2000E+03	7.0
345	0.0	0.8333E+02	0.1500E+03	0.1000E+03	7.0
346	0.0	0.8333E+02	0.1500E+03	0.2000E+03	7.0
347	0.0	0.8333E+02	0.1833E+03	0.1000E+03	7.0
348	0.0	0.8333E+02	0.1833E+03	0.2000E+03	7.0
349	0.0	0.8333E+02	0.2167E+03	0.1000E+03	7.0
350	0.0	0.8333E+02	0.2167E+03	0.2000E+03	7.0

1 n o d a l   p o i n t   c o o r d i n a t e s

np	type	x-ord	y-ord	z-ord	
351	7.0	0.8333E+02	0.2500E+03	0.1000E+03	7.0
352	7.0	0.8333E+02	0.2500E+03	0.2000E+03	7.0
353	7.0	0.1167E+03	-0.2500E+03	0.1000E+03	7.0
354	7.0	0.1167E+03	-0.2500E+03	0.2000E+03	7.0
355	0.0	0.1167E+03	-0.2167E+03	0.1000E+03	7.0
356	0.0	0.1167E+03	-0.2167E+03	0.2000E+03	7.0
357	0.0	0.1167E+03	-0.1833E+03	0.1000E+03	7.0
358	0.0	0.1167E+03	-0.1833E+03	0.2000E+03	7.0
359	0.0	0.1167E+03	-0.1500E+03	0.1000E+03	7.0
360	0.0	0.1167E+03	-0.1500E+03	0.2000E+03	7.0

361	0.0	0.1167E+03	-0.1167E+03	0.1000E+03	7.0
362	0.0	0.1167E+03	-0.1167E+03	0.2000E+03	7.0
363	0.0	0.1167E+03	-0.8333E+02	0.1000E+03	7.0
364	0.0	0.1167E+03	-0.8333E+02	0.2000E+03	7.0
365	0.0	0.1167E+03	-0.5000E+02	0.1000E+03	7.0
366	0.0	0.1167E+03	-0.5000E+02	0.2000E+03	7.0
367	0.0	0.1167E+03	-0.1667E+02	0.1000E+03	7.0
368	0.0	0.1167E+03	-0.1667E+02	0.2000E+03	7.0
369	0.0	0.1167E+03	0.1667E+02	0.1000E+03	7.0
370	0.0	0.1167E+03	0.1667E+02	0.2000E+03	7.0
371	0.0	0.1167E+03	0.5000E+02	0.1000E+03	7.0
372	0.0	0.1167E+03	0.5000E+02	0.2000E+03	7.0
373	0.0	0.1167E+03	0.8333E+02	0.1000E+03	7.0
374	0.0	0.1167E+03	0.8333E+02	0.2000E+03	7.0
375	0.0	0.1167E+03	0.1167E+03	0.1000E+03	7.0
376	0.0	0.1167E+03	0.1167E+03	0.2000E+03	7.0
377	0.0	0.1167E+03	0.1500E+03	0.1000E+03	7.0
378	0.0	0.1167E+03	0.1500E+03	0.2000E+03	7.0
379	0.0	0.1167E+03	0.1833E+03	0.1000E+03	7.0
380	0.0	0.1167E+03	0.1833E+03	0.2000E+03	7.0
381	0.0	0.1167E+03	0.2167E+03	0.1000E+03	7.0
382	0.0	0.1167E+03	0.2167E+03	0.2000E+03	7.0
383	7.0	0.1167E+03	0.2500E+03	0.1000E+03	7.0
384	7.0	0.1167E+03	0.2500E+03	0.2000E+03	7.0
385	7.0	0.1500E+03	-0.2500E+03	0.1000E+03	7.0
386	7.0	0.1500E+03	-0.2500E+03	0.2000E+03	7.0
387	0.0	0.1500E+03	-0.2167E+03	0.1000E+03	7.0
388	0.0	0.1500E+03	-0.2167E+03	0.2000E+03	7.0
389	0.0	0.1500E+03	-0.1833E+03	0.1000E+03	7.0
390	0.0	0.1500E+03	-0.1833E+03	0.2000E+03	7.0
391	0.0	0.1500E+03	-0.1500E+03	0.1000E+03	7.0
392	0.0	0.1500E+03	-0.1500E+03	0.2000E+03	7.0
393	0.0	0.1500E+03	-0.1167E+03	0.1000E+03	7.0
394	0.0	0.1500E+03	-0.1167E+03	0.2000E+03	7.0
395	0.0	0.1500E+03	-0.8333E+02	0.1000E+03	7.0
396	0.0	0.1500E+03	-0.8333E+02	0.2000E+03	7.0
397	0.0	0.1500E+03	-0.5000E+02	0.1000E+03	7.0
398	0.0	0.1500E+03	-0.5000E+02	0.2000E+03	7.0
399	0.0	0.1500E+03	-0.1667E+02	0.1000E+03	7.0
400	0.0	0.1500E+03	-0.1667E+02	0.2000E+03	7.0

1 nodal point coordinates

np	type	x-ord	y-ord	z-ord	
401	0.0	0.1500E+03	0.1667E+02	0.1000E+03	7.0
402	0.0	0.1500E+03	0.1667E+02	0.2000E+03	7.0
403	0.0	0.1500E+03	0.5000E+02	0.1000E+03	7.0
404	0.0	0.1500E+03	0.5000E+02	0.2000E+03	7.0
405	0.0	0.1500E+03	0.8333E+02	0.1000E+03	7.0
406	0.0	0.1500E+03	0.8333E+02	0.2000E+03	7.0
407	0.0	0.1500E+03	0.1167E+03	0.1000E+03	7.0
408	0.0	0.1500E+03	0.1167E+03	0.2000E+03	7.0
409	0.0	0.1500E+03	0.1500E+03	0.1000E+03	7.0
410	0.0	0.1500E+03	0.1500E+03	0.2000E+03	7.0
411	0.0	0.1500E+03	0.1833E+03	0.1000E+03	7.0
412	0.0	0.1500E+03	0.1833E+03	0.2000E+03	7.0
413	0.0	0.1500E+03	0.2167E+03	0.1000E+03	7.0
414	0.0	0.1500E+03	0.2167E+03	0.2000E+03	7.0
415	7.0	0.1500E+03	0.2500E+03	0.1000E+03	7.0
416	7.0	0.1500E+03	0.2500E+03	0.2000E+03	7.0
417	7.0	0.1833E+03	-0.2500E+03	0.1000E+03	7.0
418	7.0	0.1833E+03	-0.2500E+03	0.2000E+03	7.0
419	0.0	0.1833E+03	-0.2167E+03	0.1000E+03	7.0

420	0.0	0.1833E+03	-0.2167E+03	0.2000E+03	7.0
421	0.0	0.1833E+03	-0.1833E+03	0.1000E+03	7.0
422	0.0	0.1833E+03	-0.1833E+03	0.2000E+03	7.0
423	0.0	0.1833E+03	-0.1500E+03	0.1000E+03	7.0
424	0.0	0.1833E+03	-0.1500E+03	0.2000E+03	7.0
425	0.0	0.1833E+03	-0.1167E+03	0.1000E+03	7.0
426	0.0	0.1833E+03	-0.1167E+03	0.2000E+03	7.0
427	0.0	0.1833E+03	-0.8333E+02	0.1000E+03	7.0
428	0.0	0.1833E+03	-0.8333E+02	0.2000E+03	7.0
429	0.0	0.1833E+03	-0.5000E+02	0.1000E+03	7.0
430	0.0	0.1833E+03	-0.5000E+02	0.2000E+03	7.0
431	0.0	0.1833E+03	-0.1667E+02	0.1000E+03	7.0
432	0.0	0.1833E+03	-0.1667E+02	0.2000E+03	7.0
433	0.0	0.1833E+03	0.1667E+02	0.1000E+03	7.0
434	0.0	0.1833E+03	0.1667E+02	0.2000E+03	7.0
435	0.0	0.1833E+03	0.5000E+02	0.1000E+03	7.0
436	0.0	0.1833E+03	0.5000E+02	0.2000E+03	7.0
437	0.0	0.1833E+03	0.8333E+02	0.1000E+03	7.0
438	0.0	0.1833E+03	0.8333E+02	0.2000E+03	7.0
439	0.0	0.1833E+03	0.1167E+03	0.1000E+03	7.0
440	0.0	0.1833E+03	0.1167E+03	0.2000E+03	7.0
441	0.0	0.1833E+03	0.1500E+03	0.1000E+03	7.0
442	0.0	0.1833E+03	0.1500E+03	0.2000E+03	7.0
443	0.0	0.1833E+03	0.1833E+03	0.1000E+03	7.0
444	0.0	0.1833E+03	0.1833E+03	0.2000E+03	7.0
445	0.0	0.1833E+03	0.2167E+03	0.1000E+03	7.0
446	0.0	0.1833E+03	0.2167E+03	0.2000E+03	7.0
447	7.0	0.1833E+03	0.2500E+03	0.1000E+03	7.0
448	7.0	0.1833E+03	0.2500E+03	0.2000E+03	7.0
449	7.0	0.2167E+03	-0.2500E+03	0.1000E+03	7.0
450	7.0	0.2167E+03	-0.2500E+03	0.2000E+03	7.0

1 n o d a l p o i n t c o o r d i n a t e s

np	type	x-ord	y-ord	z-ord	
451	0.0	0.2167E+03	-0.2167E+03	0.1000E+03	7.0
452	0.0	0.2167E+03	-0.2167E+03	0.2000E+03	7.0
453	0.0	0.2167E+03	-0.1833E+03	0.1000E+03	7.0
454	0.0	0.2167E+03	-0.1833E+03	0.2000E+03	7.0
455	0.0	0.2167E+03	-0.1500E+03	0.1000E+03	7.0
456	0.0	0.2167E+03	-0.1500E+03	0.2000E+03	7.0
457	0.0	0.2167E+03	-0.1167E+03	0.1000E+03	7.0
458	0.0	0.2167E+03	-0.1167E+03	0.2000E+03	7.0
459	0.0	0.2167E+03	-0.8333E+02	0.1000E+03	7.0
460	0.0	0.2167E+03	-0.8333E+02	0.2000E+03	7.0
461	0.0	0.2167E+03	-0.5000E+02	0.1000E+03	7.0
462	0.0	0.2167E+03	-0.5000E+02	0.2000E+03	7.0
463	0.0	0.2167E+03	-0.1667E+02	0.1000E+03	7.0
464	0.0	0.2167E+03	-0.1667E+02	0.2000E+03	7.0
465	0.0	0.2167E+03	0.1667E+02	0.1000E+03	7.0
466	0.0	0.2167E+03	0.1667E+02	0.2000E+03	7.0
467	0.0	0.2167E+03	0.5000E+02	0.1000E+03	7.0
468	0.0	0.2167E+03	0.5000E+02	0.2000E+03	7.0
469	0.0	0.2167E+03	0.8333E+02	0.1000E+03	7.0
470	0.0	0.2167E+03	0.8333E+02	0.2000E+03	7.0
471	0.0	0.2167E+03	0.1167E+03	0.1000E+03	7.0
472	0.0	0.2167E+03	0.1167E+03	0.2000E+03	7.0
473	0.0	0.2167E+03	0.1500E+03	0.1000E+03	7.0
474	0.0	0.2167E+03	0.1500E+03	0.2000E+03	7.0
475	0.0	0.2167E+03	0.1833E+03	0.1000E+03	7.0
476	0.0	0.2167E+03	0.1833E+03	0.2000E+03	7.0
477	0.0	0.2167E+03	0.2167E+03	0.1000E+03	7.0
478	0.0	0.2167E+03	0.2167E+03	0.2000E+03	7.0

479	7.0	0.2167E+03	0.2500E+03	0.1000E+03	7.0
480	7.0	0.2167E+03	0.2500E+03	0.2000E+03	7.0
481	7.0	0.2500E+03	-0.2500E+03	0.1000E+03	7.0
482	7.0	0.2500E+03	-0.2500E+03	0.2000E+03	7.0
483	7.0	0.2500E+03	-0.2167E+03	0.1000E+03	7.0
484	7.0	0.2500E+03	-0.2167E+03	0.2000E+03	7.0
485	7.0	0.2500E+03	-0.1833E+03	0.1000E+03	7.0
486	7.0	0.2500E+03	-0.1833E+03	0.2000E+03	7.0
487	7.0	0.2500E+03	-0.1500E+03	0.1000E+03	7.0
488	7.0	0.2500E+03	-0.1500E+03	0.2000E+03	7.0
489	7.0	0.2500E+03	-0.1167E+03	0.1000E+03	7.0
490	7.0	0.2500E+03	-0.1167E+03	0.2000E+03	7.0
491	7.0	0.2500E+03	-0.8333E+02	0.1000E+03	7.0
492	7.0	0.2500E+03	-0.8333E+02	0.2000E+03	7.0
493	7.0	0.2500E+03	-0.5000E+02	0.1000E+03	7.0
494	7.0	0.2500E+03	-0.5000E+02	0.2000E+03	7.0
495	7.0	0.2500E+03	-0.1667E+02	0.1000E+03	7.0
496	7.0	0.2500E+03	-0.1667E+02	0.2000E+03	7.0
497	7.0	0.2500E+03	0.1667E+02	0.1000E+03	7.0
498	7.0	0.2500E+03	0.1667E+02	0.2000E+03	7.0
499	7.0	0.2500E+03	0.5000E+02	0.1000E+03	7.0
500	7.0	0.2500E+03	0.5000E+02	0.2000E+03	7.0

1 n o d a l   p o i n t   c o o r d i n a t e s

np	type	x-ord	y-ord	z-ord	
501	7.0	0.2500E+03	0.8333E+02	0.1000E+03	7.0
502	7.0	0.2500E+03	0.8333E+02	0.2000E+03	7.0
503	7.0	0.2500E+03	0.1167E+03	0.1000E+03	7.0
504	7.0	0.2500E+03	0.1167E+03	0.2000E+03	7.0
505	7.0	0.2500E+03	0.1500E+03	0.1000E+03	7.0
506	7.0	0.2500E+03	0.1500E+03	0.2000E+03	7.0
507	7.0	0.2500E+03	0.1833E+03	0.1000E+03	7.0
508	7.0	0.2500E+03	0.1833E+03	0.2000E+03	7.0
509	7.0	0.2500E+03	0.2167E+03	0.1000E+03	7.0
510	7.0	0.2500E+03	0.2167E+03	0.2000E+03	7.0
511	7.0	0.2500E+03	0.2500E+03	0.1000E+03	7.0
512	7.0	0.2500E+03	0.2500E+03	0.2000E+03	7.0
513	0.0	-0.5774E+02	-0.5774E+02	-0.5774E+02	7.0
514	0.0	-0.6739E+02	-0.6739E+02	-0.3029E+02	7.0
515	0.0	-0.7071E+02	-0.7071E+02	0.0000E+00	7.0
516	0.0	-0.6739E+02	-0.3029E+02	-0.6739E+02	7.0
517	0.0	-0.8587E+02	-0.3624E+02	-0.3624E+02	7.0
518	0.0	-0.9239E+02	-0.3827E+02	0.0000E+00	7.0
519	0.0	-0.7071E+02	0.0000E+00	-0.7071E+02	7.0
520	0.0	-0.9239E+02	0.0000E+00	-0.3827E+02	7.0
521	0.0	-0.1000E+03	0.0000E+00	0.0000E+00	7.0
522	0.0	-0.5387E+02	-0.5387E+02	-0.5387E+02	7.0
523	0.0	-0.5869E+02	-0.5869E+02	-0.2765E+02	7.0
524	0.0	-0.6036E+02	-0.6036E+02	0.0000E+00	7.0
525	0.0	-0.5869E+02	-0.2765E+02	-0.5869E+02	7.0
526	0.0	-0.6794E+02	-0.3062E+02	-0.3062E+02	7.0
527	0.0	-0.7119E+02	-0.3163E+02	0.0000E+00	7.0
528	0.0	-0.6036E+02	0.0000E+00	-0.6036E+02	7.0
529	0.0	-0.7119E+02	0.0000E+00	-0.3163E+02	7.0
530	0.0	-0.7500E+02	0.0000E+00	0.0000E+00	7.0
531	0.0	-0.5000E+02	-0.5000E+02	-0.5000E+02	7.0
532	0.0	-0.5000E+02	-0.5000E+02	-0.2500E+02	7.0
533	0.0	-0.5000E+02	-0.5000E+02	0.0000E+00	7.0
534	0.0	-0.5000E+02	-0.2500E+02	-0.5000E+02	7.0
535	0.0	-0.5000E+02	-0.2500E+02	-0.2500E+02	7.0
536	0.0	-0.5000E+02	-0.2500E+02	0.0000E+00	7.0
537	0.0	-0.5000E+02	0.0000E+00	-0.5000E+02	7.0

538	0.0	-0.5000E+02	0.0000E+00	-0.2500E+02	7.0
539	0.0	-0.5000E+02	0.0000E+00	0.0000E+00	7.0
540	0.0	-0.6739E+02	-0.6739E+02	0.3029E+02	7.0
541	0.0	-0.5774E+02	-0.5774E+02	0.5774E+02	7.0
542	0.0	-0.8587E+02	-0.3624E+02	0.3624E+02	7.0
543	0.0	-0.6739E+02	-0.3029E+02	0.6739E+02	7.0
544	0.0	-0.9239E+02	0.0000E+00	0.3827E+02	7.0
545	0.0	-0.7071E+02	0.0000E+00	0.7071E+02	7.0
546	0.0	-0.5869E+02	-0.5869E+02	0.2765E+02	7.0
547	0.0	-0.5387E+02	-0.5387E+02	0.5387E+02	7.0
548	0.0	-0.6794E+02	-0.3062E+02	0.3062E+02	7.0
549	0.0	-0.5869E+02	-0.2765E+02	0.5869E+02	7.0
550	0.0	-0.7119E+02	0.0000E+00	0.3163E+02	7.0

1 n o d a l   p o i n t   c o o r d i n a t e s

np	type	x-ord	y-ord	z-ord	
551	0.0	-0.6036E+02	0.0000E+00	0.6036E+02	7.0
552	0.0	-0.5000E+02	-0.5000E+02	0.2500E+02	7.0
553	0.0	-0.5000E+02	-0.5000E+02	0.5000E+02	7.0
554	0.0	-0.5000E+02	-0.2500E+02	0.2500E+02	7.0
555	0.0	-0.5000E+02	-0.2500E+02	0.5000E+02	7.0
556	0.0	-0.5000E+02	0.0000E+00	0.2500E+02	7.0
557	0.0	-0.5000E+02	0.0000E+00	0.5000E+02	7.0
558	0.0	-0.6739E+02	0.3029E+02	-0.6739E+02	7.0
559	0.0	-0.8587E+02	0.3624E+02	-0.3624E+02	7.0
560	0.0	-0.9239E+02	0.3827E+02	0.0000E+00	7.0
561	0.0	-0.5774E+02	0.5774E+02	-0.5774E+02	7.0
562	0.0	-0.6739E+02	0.6739E+02	-0.3029E+02	7.0
563	0.0	-0.7071E+02	0.7071E+02	0.0000E+00	7.0
564	0.0	-0.5869E+02	0.2765E+02	-0.5869E+02	7.0
565	0.0	-0.6794E+02	0.3062E+02	-0.3062E+02	7.0
566	0.0	-0.7119E+02	0.3163E+02	0.0000E+00	7.0
567	0.0	-0.5387E+02	0.5387E+02	-0.5387E+02	7.0
568	0.0	-0.5869E+02	0.5869E+02	-0.2765E+02	7.0
569	0.0	-0.6036E+02	0.6036E+02	0.0000E+00	7.0
570	0.0	-0.5000E+02	0.2500E+02	-0.5000E+02	7.0
571	0.0	-0.5000E+02	0.2500E+02	-0.2500E+02	7.0
572	0.0	-0.5000E+02	0.2500E+02	0.0000E+00	7.0
573	0.0	-0.5000E+02	0.5000E+02	-0.5000E+02	7.0
574	0.0	-0.5000E+02	0.5000E+02	-0.2500E+02	7.0
575	0.0	-0.5000E+02	0.5000E+02	0.0000E+00	7.0
576	0.0	-0.8587E+02	0.3624E+02	0.3624E+02	7.0
577	0.0	-0.6739E+02	0.3029E+02	0.6739E+02	7.0
578	0.0	-0.6739E+02	0.6739E+02	0.3029E+02	7.0
579	0.0	-0.5774E+02	0.5774E+02	0.5774E+02	7.0
580	0.0	-0.6794E+02	0.3062E+02	0.3062E+02	7.0
581	0.0	-0.5869E+02	0.2765E+02	0.5869E+02	7.0
582	0.0	-0.5869E+02	0.5869E+02	0.2765E+02	7.0
583	0.0	-0.5387E+02	0.5387E+02	0.5387E+02	7.0
584	0.0	-0.5000E+02	0.2500E+02	0.2500E+02	7.0
585	0.0	-0.5000E+02	0.2500E+02	0.5000E+02	7.0
586	0.0	-0.5000E+02	0.5000E+02	0.2500E+02	7.0
587	0.0	-0.5000E+02	0.5000E+02	0.5000E+02	7.0
588	0.0	-0.5774E+02	-0.5774E+02	-0.5774E+02	7.0
589	0.0	-0.6739E+02	-0.6739E+02	-0.3029E+02	7.0
590	0.0	-0.7071E+02	-0.7071E+02	0.0000E+00	7.0
591	0.0	-0.5387E+02	-0.5387E+02	-0.5387E+02	7.0
592	0.0	-0.5869E+02	-0.5869E+02	-0.2765E+02	7.0
593	0.0	-0.6036E+02	-0.6036E+02	0.0000E+00	7.0
594	0.0	-0.3029E+02	-0.6739E+02	-0.6739E+02	7.0
595	0.0	-0.3624E+02	-0.8587E+02	-0.3624E+02	7.0
596	0.0	-0.3827E+02	-0.9239E+02	0.0000E+00	7.0

597	0.0	-0.2765E+02	-0.5869E+02	-0.5869E+02	7.0
598	0.0	-0.3062E+02	-0.6794E+02	-0.3062E+02	7.0
599	0.0	-0.3163E+02	-0.7119E+02	0.0000E+00	7.0
600	0.0	-0.2500E+02	-0.5000E+02	-0.5000E+02	7.0

1 n o d a l   p o i n t   c o o r d i n a t e s

np	type	x-ord	y-ord	z-ord	
601	0.0	-0.2500E+02	-0.5000E+02	-0.2500E+02	7.0
602	0.0	-0.2500E+02	-0.5000E+02	0.0000E+00	7.0
603	0.0	0.0000E+00	-0.7071E+02	-0.7071E+02	7.0
604	0.0	0.0000E+00	-0.9239E+02	-0.3827E+02	7.0
605	0.0	0.0000E+00	-0.1000E+03	0.0000E+00	7.0
606	0.0	0.0000E+00	-0.6036E+02	-0.6036E+02	7.0
607	0.0	0.0000E+00	-0.7119E+02	-0.3163E+02	7.0
608	0.0	0.0000E+00	-0.7500E+02	0.0000E+00	7.0
609	0.0	0.0000E+00	-0.5000E+02	-0.5000E+02	7.0
610	0.0	0.0000E+00	-0.5000E+02	-0.2500E+02	7.0
611	0.0	0.0000E+00	-0.5000E+02	0.0000E+00	7.0
612	0.0	-0.6739E+02	-0.6739E+02	0.3029E+02	7.0
613	0.0	-0.5774E+02	-0.5774E+02	0.5774E+02	7.0
614	0.0	-0.5869E+02	-0.5869E+02	0.2765E+02	7.0
615	0.0	-0.5387E+02	-0.5387E+02	0.5387E+02	7.0
616	0.0	-0.3624E+02	-0.8587E+02	0.3624E+02	7.0
617	0.0	-0.3029E+02	-0.6739E+02	0.6739E+02	7.0
618	0.0	-0.3062E+02	-0.6794E+02	0.3062E+02	7.0
619	0.0	-0.2765E+02	-0.5869E+02	0.5869E+02	7.0
620	0.0	-0.2500E+02	-0.5000E+02	0.2500E+02	7.0
621	0.0	-0.2500E+02	-0.5000E+02	0.5000E+02	7.0
622	0.0	0.0000E+00	-0.9239E+02	0.3827E+02	7.0
623	0.0	0.0000E+00	-0.7071E+02	0.7071E+02	7.0
624	0.0	0.0000E+00	-0.7119E+02	0.3163E+02	7.0
625	0.0	0.0000E+00	-0.6036E+02	0.6036E+02	7.0
626	0.0	0.0000E+00	-0.5000E+02	0.2500E+02	7.0
627	0.0	0.0000E+00	-0.5000E+02	0.5000E+02	7.0
628	0.0	-0.5774E+02	-0.5774E+02	-0.5774E+02	7.0
629	0.0	-0.5387E+02	-0.5387E+02	-0.5387E+02	7.0
630	0.0	-0.6739E+02	-0.3029E+02	-0.6739E+02	7.0
631	0.0	-0.5869E+02	-0.2765E+02	-0.5869E+02	7.0
632	0.0	-0.7071E+02	0.0000E+00	-0.7071E+02	7.0
633	0.0	-0.6036E+02	0.0000E+00	-0.6036E+02	7.0
634	0.0	-0.3029E+02	-0.6739E+02	-0.6739E+02	7.0
635	0.0	-0.2765E+02	-0.5869E+02	-0.5869E+02	7.0
636	0.0	-0.3624E+02	-0.3624E+02	-0.8587E+02	7.0
637	0.0	-0.3062E+02	-0.3062E+02	-0.6794E+02	7.0
638	0.0	-0.2500E+02	-0.2500E+02	-0.5000E+02	7.0
639	0.0	-0.3827E+02	0.0000E+00	-0.9239E+02	7.0
640	0.0	-0.3163E+02	0.0000E+00	-0.7119E+02	7.0
641	0.0	-0.2500E+02	0.0000E+00	-0.5000E+02	7.0
642	0.0	0.0000E+00	-0.7071E+02	-0.7071E+02	7.0
643	0.0	0.0000E+00	-0.6036E+02	-0.6036E+02	7.0
644	0.0	0.0000E+00	-0.3827E+02	-0.9239E+02	7.0
645	0.0	0.0000E+00	-0.3163E+02	-0.7119E+02	7.0
646	0.0	0.0000E+00	-0.2500E+02	-0.5000E+02	7.0
647	0.0	0.0000E+00	0.0000E+00	-0.1000E+03	7.0
648	0.0	0.0000E+00	0.0000E+00	-0.7500E+02	7.0
649	0.0	0.0000E+00	0.0000E+00	-0.5000E+02	7.0
650	0.0	-0.2500E+02	-0.2500E+02	-0.2500E+02	7.0

1 n o d a l   p o i n t   c o o r d i n a t e s

np	type	x-ord	y-ord	z-ord
----	------	-------	-------	-------

651	0.0	-0.2500E+02	-0.2500E+02	0.0000E+00	7.0
652	0.0	-0.2500E+02	0.0000E+00	-0.2500E+02	7.0
653	0.0	-0.2500E+02	0.0000E+00	0.0000E+00	7.0
654	0.0	0.0000E+00	-0.2500E+02	-0.2500E+02	7.0
655	0.0	0.0000E+00	-0.2500E+02	0.0000E+00	7.0
656	0.0	0.0000E+00	0.0000E+00	-0.2500E+02	7.0
657	0.0	0.0000E+00	0.0000E+00	0.0000E+00	7.0
658	0.0	-0.2500E+02	-0.2500E+02	0.2500E+02	7.0
659	0.0	-0.2500E+02	-0.2500E+02	0.5000E+02	7.0
660	0.0	-0.2500E+02	0.0000E+00	0.2500E+02	7.0
661	0.0	-0.2500E+02	0.0000E+00	0.5000E+02	7.0
662	0.0	0.0000E+00	-0.2500E+02	0.2500E+02	7.0
663	0.0	0.0000E+00	-0.2500E+02	0.5000E+02	7.0
664	0.0	0.0000E+00	0.0000E+00	0.2500E+02	7.0
665	0.0	0.0000E+00	0.0000E+00	0.5000E+02	7.0
666	0.0	-0.5387E+02	-0.5387E+02	0.5387E+02	7.0
667	0.0	-0.5774E+02	-0.5774E+02	0.5774E+02	7.0
668	0.0	-0.5869E+02	-0.2765E+02	0.5869E+02	7.0
669	0.0	-0.6739E+02	-0.3029E+02	0.6739E+02	7.0
670	0.0	-0.6036E+02	0.0000E+00	0.6036E+02	7.0
671	0.0	-0.7071E+02	0.0000E+00	0.7071E+02	7.0
672	0.0	-0.2765E+02	-0.5869E+02	0.5869E+02	7.0
673	0.0	-0.3029E+02	-0.6739E+02	0.6739E+02	7.0
674	0.0	-0.3062E+02	-0.3062E+02	0.6794E+02	7.0
675	0.0	-0.3624E+02	-0.3624E+02	0.8587E+02	7.0
676	0.0	-0.3163E+02	0.0000E+00	0.7119E+02	7.0
677	0.0	-0.3827E+02	0.0000E+00	0.9239E+02	7.0
678	0.0	0.0000E+00	-0.6036E+02	0.6036E+02	7.0
679	0.0	0.0000E+00	-0.7071E+02	0.7071E+02	7.0
680	0.0	0.0000E+00	-0.3163E+02	0.7119E+02	7.0
681	0.0	0.0000E+00	-0.3827E+02	0.9239E+02	7.0
682	0.0	0.0000E+00	0.0000E+00	0.7500E+02	7.0
683	0.0	0.0000E+00	0.0000E+00	0.1000E+03	7.0
684	0.0	-0.6739E+02	0.3029E+02	-0.6739E+02	7.0
685	0.0	-0.5869E+02	0.2765E+02	-0.5869E+02	7.0
686	0.0	-0.5774E+02	0.5774E+02	-0.5774E+02	7.0
687	0.0	-0.5387E+02	0.5387E+02	-0.5387E+02	7.0
688	0.0	-0.3624E+02	0.3624E+02	-0.8587E+02	7.0
689	0.0	-0.3062E+02	0.3062E+02	-0.6794E+02	7.0
690	0.0	-0.2500E+02	0.2500E+02	-0.5000E+02	7.0
691	0.0	-0.3029E+02	0.6739E+02	-0.6739E+02	7.0
692	0.0	-0.2765E+02	0.5869E+02	-0.5869E+02	7.0
693	0.0	-0.2500E+02	0.5000E+02	-0.5000E+02	7.0
694	0.0	0.0000E+00	0.3827E+02	-0.9239E+02	7.0
695	0.0	0.0000E+00	0.3163E+02	-0.7119E+02	7.0
696	0.0	0.0000E+00	0.2500E+02	-0.5000E+02	7.0
697	0.0	0.0000E+00	0.7071E+02	-0.7071E+02	7.0
698	0.0	0.0000E+00	0.6036E+02	-0.6036E+02	7.0
699	0.0	0.0000E+00	0.5000E+02	-0.5000E+02	7.0
700	0.0	-0.2500E+02	0.2500E+02	-0.2500E+02	7.0

inodal point coordinates

np	type	x-ord	y-ord	z-ord	
701	0.0	-0.2500E+02	0.2500E+02	0.0000E+00	7.0
702	0.0	-0.2500E+02	0.5000E+02	-0.2500E+02	7.0
703	0.0	-0.2500E+02	0.5000E+02	0.0000E+00	7.0
704	0.0	0.0000E+00	0.2500E+02	-0.2500E+02	7.0
705	0.0	0.0000E+00	0.2500E+02	0.0000E+00	7.0
706	0.0	0.0000E+00	0.5000E+02	-0.2500E+02	7.0
707	0.0	0.0000E+00	0.5000E+02	0.0000E+00	7.0
708	0.0	-0.2500E+02	0.2500E+02	0.2500E+02	7.0
709	0.0	-0.2500E+02	0.2500E+02	0.5000E+02	7.0

710	0.0	-0.2500E+02	0.5000E+02	0.2500E+02	7.0
711	0.0	-0.2500E+02	0.5000E+02	0.5000E+02	7.0
712	0.0	0.0000E+00	0.2500E+02	0.2500E+02	7.0
713	0.0	0.0000E+00	0.2500E+02	0.5000E+02	7.0
714	0.0	0.0000E+00	0.5000E+02	0.2500E+02	7.0
715	0.0	0.0000E+00	0.5000E+02	0.5000E+02	7.0
716	0.0	-0.5869E+02	0.2765E+02	0.5869E+02	7.0
717	0.0	-0.6739E+02	0.3029E+02	0.6739E+02	7.0
718	0.0	-0.5387E+02	0.5387E+02	0.5387E+02	7.0
719	0.0	-0.5774E+02	0.5774E+02	0.5774E+02	7.0
720	0.0	-0.3062E+02	0.3062E+02	0.6794E+02	7.0
721	0.0	-0.3624E+02	0.3624E+02	0.8587E+02	7.0
722	0.0	-0.2765E+02	0.5869E+02	0.5869E+02	7.0
723	0.0	-0.3029E+02	0.6739E+02	0.6739E+02	7.0
724	0.0	0.0000E+00	0.3163E+02	0.7119E+02	7.0
725	0.0	0.0000E+00	0.3827E+02	0.9239E+02	7.0
726	0.0	0.0000E+00	0.6036E+02	0.6036E+02	7.0
727	0.0	0.0000E+00	0.7071E+02	0.7071E+02	7.0
728	0.0	-0.5387E+02	0.5387E+02	-0.5387E+02	7.0
729	0.0	-0.5869E+02	0.5869E+02	-0.2765E+02	7.0
730	0.0	-0.6036E+02	0.6036E+02	0.0000E+00	7.0
731	0.0	-0.5774E+02	0.5774E+02	-0.5774E+02	7.0
732	0.0	-0.6739E+02	0.6739E+02	-0.3029E+02	7.0
733	0.0	-0.7071E+02	0.7071E+02	0.0000E+00	7.0
734	0.0	-0.2765E+02	0.5869E+02	-0.5869E+02	7.0
735	0.0	-0.3062E+02	0.6794E+02	-0.3062E+02	7.0
736	0.0	-0.3163E+02	0.7119E+02	0.0000E+00	7.0
737	0.0	-0.3029E+02	0.6739E+02	-0.6739E+02	7.0
738	0.0	-0.3624E+02	0.8587E+02	-0.3624E+02	7.0
739	0.0	-0.3827E+02	0.9239E+02	0.0000E+00	7.0
740	0.0	0.0000E+00	0.6036E+02	-0.6036E+02	7.0
741	0.0	0.0000E+00	0.7119E+02	-0.3163E+02	7.0
742	0.0	0.0000E+00	0.7500E+02	0.0000E+00	7.0
743	0.0	0.0000E+00	0.7071E+02	-0.7071E+02	7.0
744	0.0	0.0000E+00	0.9239E+02	-0.3827E+02	7.0
745	0.0	0.0000E+00	0.1000E+03	0.0000E+00	7.0
746	0.0	-0.5869E+02	0.5869E+02	0.2765E+02	7.0
747	0.0	-0.5387E+02	0.5387E+02	0.5387E+02	7.0
748	0.0	-0.6739E+02	0.6739E+02	0.3029E+02	7.0
749	0.0	-0.5774E+02	0.5774E+02	0.5774E+02	7.0
750	0.0	-0.3062E+02	0.6794E+02	0.3062E+02	7.0

1 n o d a l   p o i n t   c o o r d i n a t e s

np	type	x-ord	y-ord	z-ord	
751	0.0	-0.2765E+02	0.5869E+02	0.5869E+02	7.0
752	0.0	-0.3624E+02	0.8587E+02	0.3624E+02	7.0
753	0.0	-0.3029E+02	0.6739E+02	0.6739E+02	7.0
754	0.0	0.0000E+00	0.7119E+02	0.3163E+02	7.0
755	0.0	0.0000E+00	0.6036E+02	0.6036E+02	7.0
756	0.0	0.0000E+00	0.9239E+02	0.3827E+02	7.0
757	0.0	0.0000E+00	0.7071E+02	0.7071E+02	7.0
758	0.0	0.3029E+02	-0.6739E+02	-0.6739E+02	7.0
759	0.0	0.3624E+02	-0.8587E+02	-0.3624E+02	7.0
760	0.0	0.3827E+02	-0.9239E+02	0.0000E+00	7.0
761	0.0	0.2765E+02	-0.5869E+02	-0.5869E+02	7.0
762	0.0	0.3062E+02	-0.6794E+02	-0.3062E+02	7.0
763	0.0	0.3163E+02	-0.7119E+02	0.0000E+00	7.0
764	0.0	0.2500E+02	-0.5000E+02	-0.5000E+02	7.0
765	0.0	0.2500E+02	-0.5000E+02	-0.2500E+02	7.0
766	0.0	0.2500E+02	-0.5000E+02	0.0000E+00	7.0
767	0.0	0.5774E+02	-0.5774E+02	-0.5774E+02	7.0
768	0.0	0.6739E+02	-0.6739E+02	-0.3029E+02	7.0



769	0.0	0.7071E+02	-0.7071E+02	0.0000E+00	7.0
770	0.0	0.5387E+02	-0.5387E+02	-0.5387E+02	7.0
771	0.0	0.5869E+02	-0.5869E+02	-0.2765E+02	7.0
772	0.0	0.6036E+02	-0.6036E+02	0.0000E+00	7.0
773	0.0	0.5000E+02	-0.5000E+02	-0.5000E+02	7.0
774	0.0	0.5000E+02	-0.5000E+02	-0.2500E+02	7.0
775	0.0	0.5000E+02	-0.5000E+02	0.0000E+00	7.0
776	0.0	0.3624E+02	-0.8587E+02	0.3624E+02	7.0
777	0.0	0.3029E+02	-0.6739E+02	0.6739E+02	7.0
778	0.0	0.3062E+02	-0.6794E+02	0.3062E+02	7.0
779	0.0	0.2765E+02	-0.5869E+02	0.5869E+02	7.0
780	0.0	0.2500E+02	-0.5000E+02	0.2500E+02	7.0
781	0.0	0.2500E+02	-0.5000E+02	0.5000E+02	7.0
782	0.0	0.6739E+02	-0.6739E+02	0.3029E+02	7.0
783	0.0	0.5774E+02	-0.5774E+02	0.5774E+02	7.0
784	0.0	0.5869E+02	-0.5869E+02	0.2765E+02	7.0
785	0.0	0.5387E+02	-0.5387E+02	0.5387E+02	7.0
786	0.0	0.5000E+02	-0.5000E+02	0.2500E+02	7.0
787	0.0	0.5000E+02	-0.5000E+02	0.5000E+02	7.0
788	0.0	0.3029E+02	-0.6739E+02	-0.6739E+02	7.0
789	0.0	0.2765E+02	-0.5869E+02	-0.5869E+02	7.0
790	0.0	0.3624E+02	-0.3624E+02	-0.8587E+02	7.0
791	0.0	0.3062E+02	-0.3062E+02	-0.6794E+02	7.0
792	0.0	0.2500E+02	-0.2500E+02	-0.5000E+02	7.0
793	0.0	0.3827E+02	0.0000E+00	-0.9239E+02	7.0
794	0.0	0.3163E+02	0.0000E+00	-0.7119E+02	7.0
795	0.0	0.2500E+02	0.0000E+00	-0.5000E+02	7.0
796	0.0	0.5774E+02	-0.5774E+02	-0.5774E+02	7.0
797	0.0	0.5387E+02	-0.5387E+02	-0.5387E+02	7.0
798	0.0	0.6739E+02	-0.3029E+02	-0.6739E+02	7.0
799	0.0	0.5869E+02	-0.2765E+02	-0.5869E+02	7.0
800	0.0	0.5000E+02	-0.2500E+02	-0.5000E+02	7.0

1 n o d a l   p o i n t   c o o r d i n a t e s

np	type	x-ord	y-ord	z-ord	
801	0.0	0.7071E+02	0.0000E+00	-0.7071E+02	7.0
802	0.0	0.6036E+02	0.0000E+00	-0.6036E+02	7.0
803	0.0	0.5000E+02	0.0000E+00	-0.5000E+02	7.0
804	0.0	0.2500E+02	-0.2500E+02	-0.2500E+02	7.0
805	0.0	0.2500E+02	-0.2500E+02	0.0000E+00	7.0
806	0.0	0.2500E+02	0.0000E+00	-0.2500E+02	7.0
807	0.0	0.2500E+02	0.0000E+00	0.0000E+00	7.0
808	0.0	0.5000E+02	-0.2500E+02	-0.2500E+02	7.0
809	0.0	0.5000E+02	-0.2500E+02	0.0000E+00	7.0
810	0.0	0.5000E+02	0.0000E+00	-0.2500E+02	7.0
811	0.0	0.5000E+02	0.0000E+00	0.0000E+00	7.0
812	0.0	0.2500E+02	-0.2500E+02	0.2500E+02	7.0
813	0.0	0.2500E+02	-0.2500E+02	0.5000E+02	7.0
814	0.0	0.2500E+02	0.0000E+00	0.2500E+02	7.0
815	0.0	0.2500E+02	0.0000E+00	0.5000E+02	7.0
816	0.0	0.5000E+02	-0.2500E+02	0.2500E+02	7.0
817	0.0	0.5000E+02	-0.2500E+02	0.5000E+02	7.0
818	0.0	0.5000E+02	0.0000E+00	0.2500E+02	7.0
819	0.0	0.5000E+02	0.0000E+00	0.5000E+02	7.0
820	0.0	0.2765E+02	-0.5869E+02	0.5869E+02	7.0
821	0.0	0.3029E+02	-0.6739E+02	0.6739E+02	7.0
822	0.0	0.3062E+02	-0.3062E+02	0.6794E+02	7.0
823	0.0	0.3624E+02	-0.3624E+02	0.8587E+02	7.0
824	0.0	0.3163E+02	0.0000E+00	0.7119E+02	7.0
825	0.0	0.3827E+02	0.0000E+00	0.9239E+02	7.0
826	0.0	0.5387E+02	-0.5387E+02	0.5387E+02	7.0
827	0.0	0.5774E+02	-0.5774E+02	0.5774E+02	7.0

828	0.0	0.5869E+02	-0.2765E+02	0.5869E+02	7.0
829	0.0	0.6739E+02	-0.3029E+02	0.6739E+02	7.0
830	0.0	0.6036E+02	0.0000E+00	0.6036E+02	7.0
831	0.0	0.7071E+02	0.0000E+00	0.7071E+02	7.0
832	0.0	0.3624E+02	0.3624E+02	-0.8587E+02	7.0
833	0.0	0.3062E+02	0.3062E+02	-0.6794E+02	7.0
834	0.0	0.2500E+02	0.2500E+02	-0.5000E+02	7.0
835	0.0	0.3029E+02	0.6739E+02	-0.6739E+02	7.0
836	0.0	0.2765E+02	0.5869E+02	-0.5869E+02	7.0
837	0.0	0.2500E+02	0.5000E+02	-0.5000E+02	7.0
838	0.0	0.6739E+02	0.3029E+02	-0.6739E+02	7.0
839	0.0	0.5869E+02	0.2765E+02	-0.5869E+02	7.0
840	0.0	0.5000E+02	0.2500E+02	-0.5000E+02	7.0
841	0.0	0.5774E+02	0.5774E+02	-0.5774E+02	7.0
842	0.0	0.5387E+02	0.5387E+02	-0.5387E+02	7.0
843	0.0	0.5000E+02	0.5000E+02	-0.5000E+02	7.0
844	0.0	0.2500E+02	0.2500E+02	-0.2500E+02	7.0
845	0.0	0.2500E+02	0.2500E+02	0.0000E+00	7.0
846	0.0	0.2500E+02	0.5000E+02	-0.2500E+02	7.0
847	0.0	0.2500E+02	0.5000E+02	0.0000E+00	7.0
848	0.0	0.5000E+02	0.2500E+02	-0.2500E+02	7.0
849	0.0	0.5000E+02	0.2500E+02	0.0000E+00	7.0
850	0.0	0.5000E+02	0.5000E+02	-0.2500E+02	7.0

1 n o d a l   p o i n t   c o o r d i n a t e s

np	type	x-ord	y-ord	z-ord	
851	0.0	0.5000E+02	0.5000E+02	0.0000E+00	7.0
852	0.0	0.2500E+02	0.2500E+02	0.2500E+02	7.0
853	0.0	0.2500E+02	0.2500E+02	0.5000E+02	7.0
854	0.0	0.2500E+02	0.5000E+02	0.2500E+02	7.0
855	0.0	0.2500E+02	0.5000E+02	0.5000E+02	7.0
856	0.0	0.5000E+02	0.2500E+02	0.2500E+02	7.0
857	0.0	0.5000E+02	0.2500E+02	0.5000E+02	7.0
858	0.0	0.5000E+02	0.5000E+02	0.2500E+02	7.0
859	0.0	0.5000E+02	0.5000E+02	0.5000E+02	7.0
860	0.0	0.3062E+02	0.3062E+02	0.6794E+02	7.0
861	0.0	0.3624E+02	0.3624E+02	0.8587E+02	7.0
862	0.0	0.2765E+02	0.5869E+02	0.5869E+02	7.0
863	0.0	0.3029E+02	0.6739E+02	0.6739E+02	7.0
864	0.0	0.5869E+02	0.2765E+02	0.5869E+02	7.0
865	0.0	0.6739E+02	0.3029E+02	0.6739E+02	7.0
866	0.0	0.5387E+02	0.5387E+02	0.5387E+02	7.0
867	0.0	0.5774E+02	0.5774E+02	0.5774E+02	7.0
868	0.0	0.2765E+02	0.5869E+02	-0.5869E+02	7.0
869	0.0	0.3062E+02	0.6794E+02	-0.3062E+02	7.0
870	0.0	0.3163E+02	0.7119E+02	0.0000E+00	7.0
871	0.0	0.3029E+02	0.6739E+02	-0.6739E+02	7.0
872	0.0	0.3624E+02	0.8587E+02	-0.3624E+02	7.0
873	0.0	0.3827E+02	0.9239E+02	0.0000E+00	7.0
874	0.0	0.5387E+02	0.5387E+02	-0.5387E+02	7.0
875	0.0	0.5869E+02	0.5869E+02	-0.2765E+02	7.0
876	0.0	0.6036E+02	0.6036E+02	0.0000E+00	7.0
877	0.0	0.5774E+02	0.5774E+02	-0.5774E+02	7.0
878	0.0	0.6739E+02	0.6739E+02	-0.3029E+02	7.0
879	0.0	0.7071E+02	0.7071E+02	0.0000E+00	7.0
880	0.0	0.3062E+02	0.6794E+02	0.3062E+02	7.0
881	0.0	0.2765E+02	0.5869E+02	0.5869E+02	7.0
882	0.0	0.3624E+02	0.8587E+02	0.3624E+02	7.0
883	0.0	0.3029E+02	0.6739E+02	0.6739E+02	7.0
884	0.0	0.5869E+02	0.5869E+02	0.2765E+02	7.0
885	0.0	0.5387E+02	0.5387E+02	0.5387E+02	7.0
886	0.0	0.6739E+02	0.6739E+02	0.3029E+02	7.0

887	0.0	0.5774E+02	0.5774E+02	0.5774E+02	7.0
888	0.0	0.5387E+02	-0.5387E+02	-0.5387E+02	7.0
889	0.0	0.5869E+02	-0.5869E+02	-0.2765E+02	7.0
890	0.0	0.6036E+02	-0.6036E+02	0.0000E+00	7.0
891	0.0	0.5869E+02	-0.2765E+02	-0.5869E+02	7.0
892	0.0	0.6794E+02	-0.3062E+02	-0.3062E+02	7.0
893	0.0	0.7119E+02	-0.3163E+02	0.0000E+00	7.0
894	0.0	0.6036E+02	0.0000E+00	-0.6036E+02	7.0
895	0.0	0.7119E+02	0.0000E+00	-0.3163E+02	7.0
896	0.0	0.7500E+02	0.0000E+00	0.0000E+00	7.0
897	0.0	0.5774E+02	-0.5774E+02	-0.5774E+02	7.0
898	0.0	0.6739E+02	-0.6739E+02	-0.3029E+02	7.0
899	0.0	0.7071E+02	-0.7071E+02	0.0000E+00	7.0
900	0.0	0.6739E+02	-0.3029E+02	-0.6739E+02	7.0

1 n o d a l p o i n t c o o r d i n a t e s

np	type	x-ord	y-ord	z-ord	
901	0.0	0.8587E+02	-0.3624E+02	-0.3624E+02	7.0
902	0.0	0.9239E+02	-0.3827E+02	0.0000E+00	7.0
903	0.0	0.7071E+02	0.0000E+00	-0.7071E+02	7.0
904	0.0	0.9239E+02	0.0000E+00	-0.3827E+02	7.0
905	0.0	0.1000E+03	0.0000E+00	0.0000E+00	7.0
906	0.0	0.5869E+02	-0.5869E+02	0.2765E+02	7.0
907	0.0	0.5387E+02	-0.5387E+02	0.5387E+02	7.0
908	0.0	0.6794E+02	-0.3062E+02	0.3062E+02	7.0
909	0.0	0.5869E+02	-0.2765E+02	0.5869E+02	7.0
910	0.0	0.7119E+02	0.0000E+00	0.3163E+02	7.0
911	0.0	0.6036E+02	0.0000E+00	0.6036E+02	7.0
912	0.0	0.6739E+02	-0.6739E+02	0.3029E+02	7.0
913	0.0	0.5774E+02	-0.5774E+02	0.5774E+02	7.0
914	0.0	0.8587E+02	-0.3624E+02	0.3624E+02	7.0
915	0.0	0.6739E+02	-0.3029E+02	0.6739E+02	7.0
916	0.0	0.9239E+02	0.0000E+00	0.3827E+02	7.0
917	0.0	0.7071E+02	0.0000E+00	0.7071E+02	7.0
918	0.0	0.5869E+02	0.2765E+02	-0.5869E+02	7.0
919	0.0	0.6794E+02	0.3062E+02	-0.3062E+02	7.0
920	0.0	0.7119E+02	0.3163E+02	0.0000E+00	7.0
921	0.0	0.5387E+02	0.5387E+02	-0.5387E+02	7.0
922	0.0	0.5869E+02	0.5869E+02	-0.2765E+02	7.0
923	0.0	0.6036E+02	0.6036E+02	0.0000E+00	7.0
924	0.0	0.6739E+02	0.3029E+02	-0.6739E+02	7.0
925	0.0	0.8587E+02	0.3624E+02	-0.3624E+02	7.0
926	0.0	0.9239E+02	0.3827E+02	0.0000E+00	7.0
927	0.0	0.5774E+02	0.5774E+02	-0.5774E+02	7.0
928	0.0	0.6739E+02	0.6739E+02	-0.3029E+02	7.0
929	0.0	0.7071E+02	0.7071E+02	0.0000E+00	7.0
930	0.0	0.6794E+02	0.3062E+02	0.3062E+02	7.0
931	0.0	0.5869E+02	0.2765E+02	0.5869E+02	7.0
932	0.0	0.5869E+02	0.5869E+02	0.2765E+02	7.0
933	0.0	0.5387E+02	0.5387E+02	0.5387E+02	7.0
934	0.0	0.8587E+02	0.3624E+02	0.3624E+02	7.0
935	0.0	0.6739E+02	0.3029E+02	0.6739E+02	7.0
936	0.0	0.6739E+02	0.6739E+02	0.3029E+02	7.0
937	0.0	0.5774E+02	0.5774E+02	0.5774E+02	7.0

1

e i g h t n o d e b r i c k e l e m e n t s

c b a l l i m p a c t p r o b l e m

element	material	node1	node2	node3	node4	node5	node6	node7	node8
1	1	1	33	35	3	2	34	36	4
2	1	33	65	67	35	34	66	68	36

3	1	65	97	99	67	66	98	100	68
4	1	97	129	131	99	98	130	132	100
5	1	129	161	163	131	130	162	164	132
6	1	161	193	195	163	162	194	196	164
7	1	193	225	227	195	194	226	228	196
8	1	225	257	259	227	226	258	260	228
9	1	257	289	291	259	258	290	292	260
10	1	289	321	323	291	290	322	324	292
11	1	321	353	355	323	322	354	356	324
12	1	353	385	387	355	354	386	388	356
13	1	385	417	419	387	386	418	420	388
14	1	417	449	451	419	418	450	452	420
15	1	449	481	483	451	450	482	484	452
16	1	3	35	37	5	4	36	38	6
17	1	35	67	69	37	36	68	70	38
18	1	67	99	101	69	68	100	102	70
19	1	99	131	133	101	100	132	134	102
20	1	131	163	165	133	132	164	166	134
21	1	163	195	197	165	164	196	198	166
22	1	195	227	229	197	196	228	230	198
23	1	227	259	261	229	228	260	262	230
24	1	259	291	293	261	260	292	294	262
25	1	291	323	325	293	292	324	326	294
26	1	323	355	357	325	324	356	358	326
27	1	355	387	389	357	356	388	390	358
28	1	387	419	421	389	388	420	422	390
29	1	419	451	453	421	420	452	454	422
30	1	451	483	485	453	452	484	486	454
31	1	5	37	39	7	6	38	40	8
32	1	37	69	71	39	38	70	72	40
33	1	69	101	103	71	70	102	104	72
34	1	101	133	135	103	102	134	136	104
35	1	133	165	167	135	134	166	168	136
36	1	165	197	199	167	166	198	200	168
37	1	197	229	231	199	198	230	232	200
38	1	229	261	263	231	230	262	264	232
39	1	261	293	295	263	262	294	296	264
40	1	293	325	327	295	294	326	328	296
41	1	325	357	359	327	326	358	360	328
42	1	357	389	391	359	358	390	392	360
43	1	389	421	423	391	390	422	424	392
44	1	421	453	455	423	422	454	456	424
45	1	453	485	487	455	454	486	488	456
46	1	7	39	41	9	8	40	42	10
47	1	39	71	73	41	40	72	74	42
48	1	71	103	105	73	72	104	106	74
49	1	103	135	137	105	104	136	138	106
50	1	135	167	169	137	136	168	170	138

1

eight node brick elements

c ball impact problem

element	material	node1	node2	node3	node4	node5	node6	node7	node8
51	1	167	199	201	169	168	200	202	170
52	1	199	231	233	201	200	232	234	202
53	1	231	263	265	233	232	264	266	234
54	1	263	295	297	265	264	296	298	266
55	1	295	327	329	297	296	328	330	298
56	1	327	359	361	329	328	360	362	330
57	1	359	391	393	361	360	392	394	362
58	1	391	423	425	393	392	424	426	394
59	1	423	455	457	425	424	456	458	426
60	1	455	487	489	457	456	488	490	458

61	1	9	41	43	11	10	42	44	12
62	1	41	73	75	43	42	74	76	44
63	1	73	105	107	75	74	106	108	76
64	1	105	137	139	107	106	138	140	108
65	1	137	169	171	139	138	170	172	140
66	1	169	201	203	171	170	202	204	172
67	1	201	233	235	203	202	234	236	204
68	1	233	265	267	235	234	266	268	236
69	1	265	297	299	267	266	298	300	268
70	1	297	329	331	299	298	330	332	300
71	1	329	361	363	331	330	362	364	332
72	1	361	393	395	363	362	394	396	364
73	1	393	425	427	395	394	426	428	396
74	1	425	457	459	427	426	458	460	428
75	1	457	489	491	459	458	490	492	460
76	1	11	43	45	13	12	44	46	14
77	1	43	75	77	45	44	76	78	46
78	1	75	107	109	77	76	108	110	78
79	1	107	139	141	109	108	140	142	110
80	1	139	171	173	141	140	172	174	142
81	1	171	203	205	173	172	204	206	174
82	1	203	235	237	205	204	236	238	206
83	1	235	267	269	237	236	268	270	238
84	1	267	299	301	269	268	300	302	270
85	1	299	331	333	301	300	332	334	302
86	1	331	363	365	333	332	364	366	334
87	1	363	395	397	365	364	396	398	366
88	1	395	427	429	397	396	428	430	398
89	1	427	459	461	429	428	460	462	430
90	1	459	491	493	461	460	492	494	462
91	1	13	45	47	15	14	46	48	16
92	1	45	77	79	47	46	78	80	48
93	1	77	109	111	79	78	110	112	80
94	1	109	141	143	111	110	142	144	112
95	1	141	173	175	143	142	174	176	144
96	1	173	205	207	175	174	206	208	176
97	1	205	237	239	207	206	238	240	208
98	1	237	269	271	239	238	270	272	240
99	1	269	301	303	271	270	302	304	272
100	1	301	333	335	303	302	334	336	304

1  
e i g h t   n o d e   b r i c k   e l e m e n t s

c b a l l   i m p a c t   p r o b l e m

element	material	node1	node2	node3	node4	node5	node6	node7	node8
101	1	333	365	367	335	334	366	368	336
102	1	365	397	399	367	366	398	400	368
103	1	397	429	431	399	398	430	432	400
104	1	429	461	463	431	430	462	464	432
105	1	461	493	495	463	462	494	496	464
106	1	15	47	49	17	16	48	50	18
107	1	47	79	81	49	48	80	82	50
108	1	79	111	113	81	80	112	114	82
109	1	111	143	145	113	112	144	146	114
110	1	143	175	177	145	144	176	178	146
111	1	175	207	209	177	176	208	210	178
112	1	207	239	241	209	208	240	242	210
113	1	239	271	273	241	240	272	274	242
114	1	271	303	305	273	272	304	306	274
115	1	303	335	337	305	304	336	338	306
116	1	335	367	369	337	336	368	370	338
117	1	367	399	401	369	368	400	402	370
118	1	399	431	433	401	400	432	434	402

119	1	431	463	465	433	432	464	466	434
120	1	463	495	497	465	464	496	498	466
121	1	17	49	51	19	18	50	52	20
122	1	49	81	83	51	50	82	84	52
123	1	81	113	115	83	82	114	116	84
124	1	113	145	147	115	114	146	148	116
125	1	145	177	179	147	146	178	180	148
126	1	177	209	211	179	178	210	212	180
127	1	209	241	243	211	210	242	244	212
128	1	241	273	275	243	242	274	276	244
129	1	273	305	307	275	274	306	308	276
130	1	305	337	339	307	306	338	340	308
131	1	337	369	371	339	338	370	372	340
132	1	369	401	403	371	370	402	404	372
133	1	401	433	435	403	402	434	436	404
134	1	433	465	467	435	434	466	468	436
135	1	465	497	499	467	466	498	500	468
136	1	19	51	53	21	20	52	54	22
137	1	51	83	85	53	52	84	86	54
138	1	83	115	117	85	84	116	118	86
139	1	115	147	149	117	116	148	150	118
140	1	147	179	181	149	148	180	182	150
141	1	179	211	213	181	180	212	214	182
142	1	211	243	245	213	212	244	246	214
143	1	243	275	277	245	244	276	278	246
144	1	275	307	309	277	276	308	310	278
145	1	307	339	341	309	308	340	342	310
146	1	339	371	373	341	340	372	374	342
147	1	371	403	405	373	372	404	406	374
148	1	403	435	437	405	404	436	438	406
149	1	435	467	469	437	436	468	470	438
150	1	467	499	501	469	468	500	502	470

1

e i g h t n o d e b r i c k e l e m e n t s

c b a l l i m p a c t p r o b l e m

element	material	node1	node2	node3	node4	node5	node6	node7	node8
151	1	21	53	55	23	22	54	56	24
152	1	53	85	87	55	54	86	88	56
153	1	85	117	119	87	86	118	120	88
154	1	117	149	151	119	118	150	152	120
155	1	149	181	183	151	150	182	184	152
156	1	181	213	215	183	182	214	216	184
157	1	213	245	247	215	214	246	248	216
158	1	245	277	279	247	246	278	280	248
159	1	277	309	311	279	278	310	312	280
160	1	309	341	343	311	310	342	344	312
161	1	341	373	375	343	342	374	376	344
162	1	373	405	407	375	374	406	408	376
163	1	405	437	439	407	406	438	440	408
164	1	437	469	471	439	438	470	472	440
165	1	469	501	503	471	470	502	504	472
166	1	23	55	57	25	24	56	58	26
167	1	55	87	89	57	56	88	90	58
168	1	87	119	121	89	88	120	122	90
169	1	119	151	153	121	120	152	154	122
170	1	151	183	185	153	152	184	186	154
171	1	183	215	217	185	184	216	218	186
172	1	215	247	249	217	216	248	250	218
173	1	247	279	281	249	248	280	282	250
174	1	279	311	313	281	280	312	314	282
175	1	311	343	345	313	312	344	346	314
176	1	343	375	377	345	344	376	378	346

177	1	375	407	409	377	376	408	410	378
178	1	407	439	441	409	408	440	442	410
179	1	439	471	473	441	440	472	474	442
180	1	471	503	505	473	472	504	506	474
181	1	25	57	59	27	26	58	60	28
182	1	57	89	91	59	58	90	92	60
183	1	89	121	123	91	90	122	124	92
184	1	121	153	155	123	122	154	156	124
185	1	153	185	187	155	154	186	188	156
186	1	185	217	219	187	186	218	220	188
187	1	217	249	251	219	218	250	252	220
188	1	249	281	283	251	250	282	284	252
189	1	281	313	315	283	282	314	316	284
190	1	313	345	347	315	314	346	348	316
191	1	345	377	379	347	346	378	380	348
192	1	377	409	411	379	378	410	412	380
193	1	409	441	443	411	410	442	444	412
194	1	441	473	475	443	442	474	476	444
195	1	473	505	507	475	474	506	508	476
196	1	27	59	61	29	28	60	62	30
197	1	59	91	93	61	60	92	94	62
198	1	91	123	125	93	92	124	126	94
199	1	123	155	157	125	124	156	158	126
200	1	155	187	189	157	156	188	190	158

1  
e i g h t n o d e b r i c k e l e m e n t s

c b a l l i m p a c t p r o b l e m

element	material	node1	node2	node3	node4	node5	node6	node7	node8
201	1	187	219	221	189	188	220	222	190
202	1	219	251	253	221	220	252	254	222
203	1	251	283	285	253	252	284	286	254
204	1	283	315	317	285	284	316	318	286
205	1	315	347	349	317	316	348	350	318
206	1	347	379	381	349	348	380	382	350
207	1	379	411	413	381	380	412	414	382
208	1	411	443	445	413	412	444	446	414
209	1	443	475	477	445	444	476	478	446
210	1	475	507	509	477	476	508	510	478
211	1	29	61	63	31	30	62	64	32
212	1	61	93	95	63	62	94	96	64
213	1	93	125	127	95	94	126	128	96
214	1	125	157	159	127	126	158	160	128
215	1	157	189	191	159	158	190	192	160
216	1	189	221	223	191	190	222	224	192
217	1	221	253	255	223	222	254	256	224
218	1	253	285	287	255	254	286	288	256
219	1	285	317	319	287	286	318	320	288
220	1	317	349	351	319	318	350	352	320
221	1	349	381	383	351	350	382	384	352
222	1	381	413	415	383	382	414	416	384
223	1	413	445	447	415	414	446	448	416
224	1	445	477	479	447	446	478	480	448
225	1	477	509	511	479	478	510	512	480
226	2	513	522	525	516	514	523	526	517
227	2	522	531	534	525	523	532	535	526
228	2	516	525	528	519	517	526	529	520
229	2	525	534	537	528	526	535	538	529
230	2	514	523	526	517	515	524	527	518
231	2	523	532	535	526	524	533	536	527
232	2	517	526	529	520	518	527	530	521
233	2	526	535	538	529	527	536	539	530
234	2	515	524	527	518	540	546	548	542

235	2	524	533	536	527	546	552	554	548
236	2	518	527	530	521	542	548	550	544
237	2	527	536	539	530	548	554	556	550
238	2	540	546	548	542	541	547	549	543
239	2	546	552	554	548	547	553	555	549
240	2	542	548	550	544	543	549	551	545
241	2	548	554	556	550	549	555	557	551
242	2	519	528	564	558	520	529	565	559
243	2	528	537	570	564	529	538	571	565
244	2	558	564	567	561	559	565	568	562
245	2	564	570	573	567	565	571	574	568
246	2	520	529	565	559	521	530	566	560
247	2	529	538	571	565	530	539	572	566
248	2	559	565	568	562	560	566	569	563
249	2	565	571	574	568	566	572	575	569
250	2	521	530	566	560	544	550	580	576

1

eight node brick elements

c ball impact problem

element	material	node1	node2	node3	node4	node5	node6	node7	node8
251	2	530	539	572	566	550	556	584	580
252	2	560	566	569	563	576	580	582	578
253	2	566	572	575	569	580	584	586	582
254	2	544	550	580	576	545	551	581	577
255	2	550	556	584	580	551	557	585	581
256	2	576	580	582	578	577	581	583	579
257	2	580	584	586	582	581	585	587	583
258	2	588	594	597	591	589	595	598	592
259	2	594	603	606	597	595	604	607	598
260	2	591	597	600	531	592	598	601	532
261	2	597	606	609	600	598	607	610	601
262	2	589	595	598	592	590	596	599	593
263	2	595	604	607	598	596	605	608	599
264	2	592	598	601	532	593	599	602	533
265	2	598	607	610	601	599	608	611	602
266	2	590	596	599	593	612	616	618	614
267	2	596	605	608	599	616	622	624	618
268	2	593	599	602	533	614	618	620	552
269	2	599	608	611	602	618	624	626	620
270	2	612	616	618	614	613	617	619	615
271	2	616	622	624	618	617	623	625	619
272	2	614	618	620	552	615	619	621	553
273	2	618	624	626	620	619	625	627	621
274	2	628	634	636	630	629	635	637	631
275	2	634	642	644	636	635	643	645	637
276	2	630	636	639	632	631	637	640	633
277	2	636	644	647	639	637	645	648	640
278	2	629	635	637	631	531	600	638	534
279	2	635	643	645	637	600	609	646	638
280	2	631	637	640	633	534	638	641	537
281	2	637	645	648	640	638	646	649	641
282	2	531	600	638	534	532	601	650	535
283	2	600	609	646	638	601	610	654	650
284	2	534	638	641	537	535	650	652	538
285	2	638	646	649	641	650	654	656	652
286	2	532	601	650	535	533	602	651	536
287	2	601	610	654	650	602	611	655	651
288	2	535	650	652	538	536	651	653	539
289	2	650	654	656	652	651	655	657	653
290	2	533	602	651	536	552	620	658	554
291	2	602	611	655	651	620	626	662	658
292	2	536	651	653	539	554	658	660	556



293	2	651	655	657	653	658	662	664	660
294	2	552	620	658	554	553	621	659	555
295	2	620	626	662	658	621	627	663	659
296	2	554	658	660	556	555	659	661	557
297	2	658	662	664	660	659	663	665	661
298	2	553	621	659	555	666	672	674	668
299	2	621	627	663	659	672	678	680	674
300	2	555	659	661	557	668	674	676	670

1

eight node brick elements

c ball impact problem

element	material	node1	node2	node3	node4	node5	node6	node7	node8
301	2	659	663	665	661	674	680	682	676
302	2	666	672	674	668	667	673	675	669
303	2	672	678	680	674	673	679	681	675
304	2	668	674	676	670	669	675	677	671
305	2	674	680	682	676	675	681	683	677
306	2	632	639	688	684	633	640	689	685
307	2	639	647	694	688	640	648	695	689
308	2	684	688	691	686	685	689	692	687
309	2	688	694	697	691	689	695	698	692
310	2	633	640	689	685	537	641	690	570
311	2	640	648	695	689	641	649	696	690
312	2	685	689	692	687	570	690	693	573
313	2	689	695	698	692	690	696	699	693
314	2	537	641	690	570	538	652	700	571
315	2	641	649	696	690	652	656	704	700
316	2	570	690	693	573	571	700	702	574
317	2	690	696	699	693	700	704	706	702
318	2	538	652	700	571	539	653	701	572
319	2	652	656	704	700	653	657	705	701
320	2	571	700	702	574	572	701	703	575
321	2	700	704	706	702	701	705	707	703
322	2	539	653	701	572	556	660	708	584
323	2	653	657	705	701	660	664	712	708
324	2	572	701	703	575	584	708	710	586
325	2	701	705	707	703	708	712	714	710
326	2	556	660	708	584	557	661	709	585
327	2	660	664	712	708	661	665	713	709
328	2	584	708	710	586	585	709	711	587
329	2	708	712	714	710	709	713	715	711
330	2	557	661	709	585	670	676	720	716
331	2	661	665	713	709	676	682	724	720
332	2	585	709	711	587	716	720	722	718
333	2	709	713	715	711	720	724	726	722
334	2	670	676	720	716	671	677	721	717
335	2	676	682	724	720	677	683	725	721
336	2	716	720	722	718	717	721	723	719
337	2	720	724	726	722	721	725	727	723
338	2	573	693	734	728	574	702	735	729
339	2	693	699	740	734	702	706	741	735
340	2	728	734	737	731	729	735	738	732
341	2	734	740	743	737	735	741	744	738
342	2	574	702	735	729	575	703	736	730
343	2	702	706	741	735	703	707	742	736
344	2	729	735	738	732	730	736	739	733
345	2	735	741	744	738	736	742	745	739
346	2	575	703	736	730	586	710	750	746
347	2	703	707	742	736	710	714	754	750
348	2	730	736	739	733	746	750	752	748
349	2	736	742	745	739	750	754	756	752
350	2	586	710	750	746	587	711	751	747

1  
e i g h t n o d e b r i c k e l e m e n t s

c b a l l i m p a c t p r o b l e m

element	material	node1	node2	node3	node4	node5	node6	node7	node8
351	2	710	714	754	750	711	715	755	751
352	2	746	750	752	748	747	751	753	749
353	2	750	754	756	752	751	755	757	753
354	2	603	758	761	606	604	759	762	607
355	2	758	767	770	761	759	768	771	762
356	2	606	761	764	609	607	762	765	610
357	2	761	770	773	764	762	771	774	765
358	2	604	759	762	607	605	760	763	608
359	2	759	768	771	762	760	769	772	763
360	2	607	762	765	610	608	763	766	611
361	2	762	771	774	765	763	772	775	766
362	2	605	760	763	608	622	776	778	624
363	2	760	769	772	763	776	782	784	778
364	2	608	763	766	611	624	778	780	626
365	2	763	772	775	766	778	784	786	780
366	2	622	776	778	624	623	777	779	625
367	2	776	782	784	778	777	783	785	779
368	2	624	778	780	626	625	779	781	627
369	2	778	784	786	780	779	785	787	781
370	2	642	788	790	644	643	789	791	645
371	2	788	796	798	790	789	797	799	791
372	2	644	790	793	647	645	791	794	648
373	2	790	798	801	793	791	799	802	794
374	2	643	789	791	645	609	764	792	646
375	2	789	797	799	791	764	773	800	792
376	2	645	791	794	648	646	792	795	649
377	2	791	799	802	794	792	800	803	795
378	2	609	764	792	646	610	765	804	654
379	2	764	773	800	792	765	774	808	804
380	2	646	792	795	649	654	804	806	656
381	2	792	800	803	795	804	808	810	806
382	2	610	765	804	654	611	766	805	655
383	2	765	774	808	804	766	775	809	805
384	2	654	804	806	656	655	805	807	657
385	2	804	808	810	806	805	809	811	807
386	2	611	766	805	655	626	780	812	662
387	2	766	775	809	805	780	786	816	812
388	2	655	805	807	657	662	812	814	664
389	2	805	809	811	807	812	816	818	814
390	2	626	780	812	662	627	781	813	663
391	2	780	786	816	812	781	787	817	813
392	2	662	812	814	664	663	813	815	665
393	2	812	816	818	814	813	817	819	815
394	2	627	781	813	663	678	820	822	680
395	2	781	787	817	813	820	826	828	822
396	2	663	813	815	665	680	822	824	682
397	2	813	817	819	815	822	828	830	824
398	2	678	820	822	680	679	821	823	681
399	2	820	826	828	822	821	827	829	823
400	2	680	822	824	682	681	823	825	683

1  
e i g h t n o d e b r i c k e l e m e n t s

c b a l l i m p a c t p r o b l e m

element	material	node1	node2	node3	node4	node5	node6	node7	node8
401	2	822	828	830	824	823	829	831	825
402	2	647	793	832	694	648	794	833	695

403	2	793	801	838	832	794	802	839	833
404	2	694	832	835	697	695	833	836	698
405	2	832	838	841	835	833	839	842	836
406	2	648	794	833	695	649	795	834	696
407	2	794	802	839	833	795	803	840	834
408	2	695	833	836	698	696	834	837	699
409	2	833	839	842	836	834	840	843	837
410	2	649	795	834	696	656	806	844	704
411	2	795	803	840	834	806	810	848	844
412	2	696	834	837	699	704	844	846	706
413	2	834	840	843	837	844	848	850	846
414	2	656	806	844	704	657	807	845	705
415	2	806	810	848	844	807	811	849	845
416	2	704	844	846	706	705	845	847	707
417	2	844	848	850	846	845	849	851	847
418	2	657	807	845	705	664	814	852	712
419	2	807	811	849	845	814	818	856	852
420	2	705	845	847	707	712	852	854	714
421	2	845	849	851	847	852	856	858	854
422	2	664	814	852	712	665	815	853	713
423	2	814	818	856	852	815	819	857	853
424	2	712	852	854	714	713	853	855	715
425	2	852	856	858	854	853	857	859	855
426	2	665	815	853	713	682	824	860	724
427	2	815	819	857	853	824	830	864	860
428	2	713	853	855	715	724	860	862	726
429	2	853	857	859	855	860	864	866	862
430	2	682	824	860	724	683	825	861	725
431	2	824	830	864	860	825	831	865	861
432	2	724	860	862	726	725	861	863	727
433	2	860	864	866	862	861	865	867	863
434	2	699	837	868	740	706	846	869	741
435	2	837	843	874	868	846	850	875	869
436	2	740	868	871	743	741	869	872	744
437	2	868	874	877	871	869	875	878	872
438	2	706	846	869	741	707	847	870	742
439	2	846	850	875	869	847	851	876	870
440	2	741	869	872	744	742	870	873	745
441	2	869	875	878	872	870	876	879	873
442	2	707	847	870	742	714	854	880	754
443	2	847	851	876	870	854	858	884	880
444	2	742	870	873	745	754	880	882	756
445	2	870	876	879	873	880	884	886	882
446	2	714	854	880	754	715	855	881	755
447	2	854	858	884	880	855	859	885	881
448	2	754	880	882	756	755	881	883	757
449	2	880	884	886	882	881	885	887	883
450	2	773	888	891	800	774	889	892	808

1

e i g h t n o d e b r i c k e l e m e n t s

c b a l l i m p a c t p r o b l e m

element	material	node1	node2	node3	node4	node5	node6	node7	node8
451	2	888	897	900	891	889	898	901	892
452	2	800	891	894	803	808	892	895	810
453	2	891	900	903	894	892	901	904	895
454	2	774	889	892	808	775	890	893	809
455	2	889	898	901	892	890	899	902	893
456	2	808	892	895	810	809	893	896	811
457	2	892	901	904	895	893	902	905	896
458	2	775	890	893	809	786	906	908	816
459	2	890	899	902	893	906	912	914	908
460	2	809	893	896	811	816	908	910	818

461	2	893	902	905	896	908	914	916	910
462	2	786	906	908	816	787	907	909	817
463	2	906	912	914	908	907	913	915	909
464	2	816	908	910	818	817	909	911	819
465	2	908	914	916	910	909	915	917	911
466	2	803	894	918	840	810	895	919	848
467	2	894	903	924	918	895	904	925	919
468	2	840	918	921	843	848	919	922	850
469	2	918	924	927	921	919	925	928	922
470	2	810	895	919	848	811	896	920	849
471	2	895	904	925	919	896	905	926	920
472	2	848	919	922	850	849	920	923	851
473	2	919	925	928	922	920	926	929	923
474	2	811	896	920	849	818	910	930	856
475	2	896	905	926	920	910	916	934	930
476	2	849	920	923	851	856	930	932	858
477	2	920	926	929	923	930	934	936	932
478	2	818	910	930	856	819	911	931	857
479	2	910	916	934	930	911	917	935	931
480	2	856	930	932	858	857	931	933	859
481	2	930	934	936	932	931	935	937	933

1

# nodal point velocities

np	x-vel	y-vel	z-vel
1	0.0000E+00	0.0000E+00	0.0000E+00
2	0.0000E+00	0.0000E+00	0.0000E+00
3	0.0000E+00	0.0000E+00	0.0000E+00
4	0.0000E+00	0.0000E+00	0.0000E+00
5	0.0000E+00	0.0000E+00	0.0000E+00
6	0.0000E+00	0.0000E+00	0.0000E+00
7	0.0000E+00	0.0000E+00	0.0000E+00
8	0.0000E+00	0.0000E+00	0.0000E+00
9	0.0000E+00	0.0000E+00	0.0000E+00
10	0.0000E+00	0.0000E+00	0.0000E+00
11	0.0000E+00	0.0000E+00	0.0000E+00
12	0.0000E+00	0.0000E+00	0.0000E+00
13	0.0000E+00	0.0000E+00	0.0000E+00
14	0.0000E+00	0.0000E+00	0.0000E+00
15	0.0000E+00	0.0000E+00	0.0000E+00
16	0.0000E+00	0.0000E+00	0.0000E+00
17	0.0000E+00	0.0000E+00	0.0000E+00
18	0.0000E+00	0.0000E+00	0.0000E+00
19	0.0000E+00	0.0000E+00	0.0000E+00
20	0.0000E+00	0.0000E+00	0.0000E+00
21	0.0000E+00	0.0000E+00	0.0000E+00
22	0.0000E+00	0.0000E+00	0.0000E+00
23	0.0000E+00	0.0000E+00	0.0000E+00
24	0.0000E+00	0.0000E+00	0.0000E+00
25	0.0000E+00	0.0000E+00	0.0000E+00
26	0.0000E+00	0.0000E+00	0.0000E+00
27	0.0000E+00	0.0000E+00	0.0000E+00
28	0.0000E+00	0.0000E+00	0.0000E+00
29	0.0000E+00	0.0000E+00	0.0000E+00
30	0.0000E+00	0.0000E+00	0.0000E+00
31	0.0000E+00	0.0000E+00	0.0000E+00
32	0.0000E+00	0.0000E+00	0.0000E+00
33	0.0000E+00	0.0000E+00	0.0000E+00
34	0.0000E+00	0.0000E+00	0.0000E+00
35	0.0000E+00	0.0000E+00	0.0000E+00
36	0.0000E+00	0.0000E+00	0.0000E+00

37	0.0000E+00	0.0000E+00	0.0000E+00
38	0.0000E+00	0.0000E+00	0.0000E+00
39	0.0000E+00	0.0000E+00	0.0000E+00
40	0.0000E+00	0.0000E+00	0.0000E+00
41	0.0000E+00	0.0000E+00	0.0000E+00
42	0.0000E+00	0.0000E+00	0.0000E+00
43	0.0000E+00	0.0000E+00	0.0000E+00
44	0.0000E+00	0.0000E+00	0.0000E+00
45	0.0000E+00	0.0000E+00	0.0000E+00
46	0.0000E+00	0.0000E+00	0.0000E+00
47	0.0000E+00	0.0000E+00	0.0000E+00
48	0.0000E+00	0.0000E+00	0.0000E+00
49	0.0000E+00	0.0000E+00	0.0000E+00
50	0.0000E+00	0.0000E+00	0.0000E+00

1

# nodal point velocities

np	x-vel	y-vel	z-vel
51	0.0000E+00	0.0000E+00	0.0000E+00
52	0.0000E+00	0.0000E+00	0.0000E+00
53	0.0000E+00	0.0000E+00	0.0000E+00
54	0.0000E+00	0.0000E+00	0.0000E+00
55	0.0000E+00	0.0000E+00	0.0000E+00
56	0.0000E+00	0.0000E+00	0.0000E+00
57	0.0000E+00	0.0000E+00	0.0000E+00
58	0.0000E+00	0.0000E+00	0.0000E+00
59	0.0000E+00	0.0000E+00	0.0000E+00
60	0.0000E+00	0.0000E+00	0.0000E+00
61	0.0000E+00	0.0000E+00	0.0000E+00
62	0.0000E+00	0.0000E+00	0.0000E+00
63	0.0000E+00	0.0000E+00	0.0000E+00
64	0.0000E+00	0.0000E+00	0.0000E+00
65	0.0000E+00	0.0000E+00	0.0000E+00
66	0.0000E+00	0.0000E+00	0.0000E+00
67	0.0000E+00	0.0000E+00	0.0000E+00
68	0.0000E+00	0.0000E+00	0.0000E+00
69	0.0000E+00	0.0000E+00	0.0000E+00
70	0.0000E+00	0.0000E+00	0.0000E+00
71	0.0000E+00	0.0000E+00	0.0000E+00
72	0.0000E+00	0.0000E+00	0.0000E+00
73	0.0000E+00	0.0000E+00	0.0000E+00
74	0.0000E+00	0.0000E+00	0.0000E+00
75	0.0000E+00	0.0000E+00	0.0000E+00
76	0.0000E+00	0.0000E+00	0.0000E+00
77	0.0000E+00	0.0000E+00	0.0000E+00
78	0.0000E+00	0.0000E+00	0.0000E+00
79	0.0000E+00	0.0000E+00	0.0000E+00
80	0.0000E+00	0.0000E+00	0.0000E+00
81	0.0000E+00	0.0000E+00	0.0000E+00
82	0.0000E+00	0.0000E+00	0.0000E+00
83	0.0000E+00	0.0000E+00	0.0000E+00
84	0.0000E+00	0.0000E+00	0.0000E+00
85	0.0000E+00	0.0000E+00	0.0000E+00
86	0.0000E+00	0.0000E+00	0.0000E+00
87	0.0000E+00	0.0000E+00	0.0000E+00
88	0.0000E+00	0.0000E+00	0.0000E+00
89	0.0000E+00	0.0000E+00	0.0000E+00
90	0.0000E+00	0.0000E+00	0.0000E+00
91	0.0000E+00	0.0000E+00	0.0000E+00
92	0.0000E+00	0.0000E+00	0.0000E+00
93	0.0000E+00	0.0000E+00	0.0000E+00

94	0.0000E+00	0.0000E+00	0.0000E+00
95	0.0000E+00	0.0000E+00	0.0000E+00
96	0.0000E+00	0.0000E+00	0.0000E+00
97	0.0000E+00	0.0000E+00	0.0000E+00
98	0.0000E+00	0.0000E+00	0.0000E+00
99	0.0000E+00	0.0000E+00	0.0000E+00
100	0.0000E+00	0.0000E+00	0.0000E+00

1

# nodal point velocities

np	x-vel	y-vel	z-vel
101	0.0000E+00	0.0000E+00	0.0000E+00
102	0.0000E+00	0.0000E+00	0.0000E+00
103	0.0000E+00	0.0000E+00	0.0000E+00
104	0.0000E+00	0.0000E+00	0.0000E+00
105	0.0000E+00	0.0000E+00	0.0000E+00
106	0.0000E+00	0.0000E+00	0.0000E+00
107	0.0000E+00	0.0000E+00	0.0000E+00
108	0.0000E+00	0.0000E+00	0.0000E+00
109	0.0000E+00	0.0000E+00	0.0000E+00
110	0.0000E+00	0.0000E+00	0.0000E+00
111	0.0000E+00	0.0000E+00	0.0000E+00
112	0.0000E+00	0.0000E+00	0.0000E+00
113	0.0000E+00	0.0000E+00	0.0000E+00
114	0.0000E+00	0.0000E+00	0.0000E+00
115	0.0000E+00	0.0000E+00	0.0000E+00
116	0.0000E+00	0.0000E+00	0.0000E+00
117	0.0000E+00	0.0000E+00	0.0000E+00
118	0.0000E+00	0.0000E+00	0.0000E+00
119	0.0000E+00	0.0000E+00	0.0000E+00
120	0.0000E+00	0.0000E+00	0.0000E+00
121	0.0000E+00	0.0000E+00	0.0000E+00
122	0.0000E+00	0.0000E+00	0.0000E+00
123	0.0000E+00	0.0000E+00	0.0000E+00
124	0.0000E+00	0.0000E+00	0.0000E+00
125	0.0000E+00	0.0000E+00	0.0000E+00
126	0.0000E+00	0.0000E+00	0.0000E+00
127	0.0000E+00	0.0000E+00	0.0000E+00
128	0.0000E+00	0.0000E+00	0.0000E+00
129	0.0000E+00	0.0000E+00	0.0000E+00
130	0.0000E+00	0.0000E+00	0.0000E+00
131	0.0000E+00	0.0000E+00	0.0000E+00
132	0.0000E+00	0.0000E+00	0.0000E+00
133	0.0000E+00	0.0000E+00	0.0000E+00
134	0.0000E+00	0.0000E+00	0.0000E+00
135	0.0000E+00	0.0000E+00	0.0000E+00
136	0.0000E+00	0.0000E+00	0.0000E+00
137	0.0000E+00	0.0000E+00	0.0000E+00
138	0.0000E+00	0.0000E+00	0.0000E+00
139	0.0000E+00	0.0000E+00	0.0000E+00
140	0.0000E+00	0.0000E+00	0.0000E+00
141	0.0000E+00	0.0000E+00	0.0000E+00
142	0.0000E+00	0.0000E+00	0.0000E+00
143	0.0000E+00	0.0000E+00	0.0000E+00
144	0.0000E+00	0.0000E+00	0.0000E+00
145	0.0000E+00	0.0000E+00	0.0000E+00
146	0.0000E+00	0.0000E+00	0.0000E+00
147	0.0000E+00	0.0000E+00	0.0000E+00
148	0.0000E+00	0.0000E+00	0.0000E+00
149	0.0000E+00	0.0000E+00	0.0000E+00
150	0.0000E+00	0.0000E+00	0.0000E+00

1

nodal point velocities

np	x-vel	y-vel	z-vel
151	0.0000E+00	0.0000E+00	0.0000E+00
152	0.0000E+00	0.0000E+00	0.0000E+00
153	0.0000E+00	0.0000E+00	0.0000E+00
154	0.0000E+00	0.0000E+00	0.0000E+00
155	0.0000E+00	0.0000E+00	0.0000E+00
156	0.0000E+00	0.0000E+00	0.0000E+00
157	0.0000E+00	0.0000E+00	0.0000E+00
158	0.0000E+00	0.0000E+00	0.0000E+00
159	0.0000E+00	0.0000E+00	0.0000E+00
160	0.0000E+00	0.0000E+00	0.0000E+00
161	0.0000E+00	0.0000E+00	0.0000E+00
162	0.0000E+00	0.0000E+00	0.0000E+00
163	0.0000E+00	0.0000E+00	0.0000E+00
164	0.0000E+00	0.0000E+00	0.0000E+00
165	0.0000E+00	0.0000E+00	0.0000E+00
166	0.0000E+00	0.0000E+00	0.0000E+00
167	0.0000E+00	0.0000E+00	0.0000E+00
168	0.0000E+00	0.0000E+00	0.0000E+00
169	0.0000E+00	0.0000E+00	0.0000E+00
170	0.0000E+00	0.0000E+00	0.0000E+00
171	0.0000E+00	0.0000E+00	0.0000E+00
172	0.0000E+00	0.0000E+00	0.0000E+00
173	0.0000E+00	0.0000E+00	0.0000E+00
174	0.0000E+00	0.0000E+00	0.0000E+00
175	0.0000E+00	0.0000E+00	0.0000E+00
176	0.0000E+00	0.0000E+00	0.0000E+00
177	0.0000E+00	0.0000E+00	0.0000E+00
178	0.0000E+00	0.0000E+00	0.0000E+00
179	0.0000E+00	0.0000E+00	0.0000E+00
180	0.0000E+00	0.0000E+00	0.0000E+00
181	0.0000E+00	0.0000E+00	0.0000E+00
182	0.0000E+00	0.0000E+00	0.0000E+00
183	0.0000E+00	0.0000E+00	0.0000E+00
184	0.0000E+00	0.0000E+00	0.0000E+00
185	0.0000E+00	0.0000E+00	0.0000E+00
186	0.0000E+00	0.0000E+00	0.0000E+00
187	0.0000E+00	0.0000E+00	0.0000E+00
188	0.0000E+00	0.0000E+00	0.0000E+00
189	0.0000E+00	0.0000E+00	0.0000E+00
190	0.0000E+00	0.0000E+00	0.0000E+00
191	0.0000E+00	0.0000E+00	0.0000E+00
192	0.0000E+00	0.0000E+00	0.0000E+00
193	0.0000E+00	0.0000E+00	0.0000E+00
194	0.0000E+00	0.0000E+00	0.0000E+00
195	0.0000E+00	0.0000E+00	0.0000E+00
196	0.0000E+00	0.0000E+00	0.0000E+00
197	0.0000E+00	0.0000E+00	0.0000E+00
198	0.0000E+00	0.0000E+00	0.0000E+00
199	0.0000E+00	0.0000E+00	0.0000E+00
200	0.0000E+00	0.0000E+00	0.0000E+00

1

nodal point velocities

np	x-vel	y-vel	z-vel
----	-------	-------	-------

201	0.0000E+00	0.0000E+00	0.0000E+00
202	0.0000E+00	0.0000E+00	0.0000E+00
203	0.0000E+00	0.0000E+00	0.0000E+00
204	0.0000E+00	0.0000E+00	0.0000E+00
205	0.0000E+00	0.0000E+00	0.0000E+00
206	0.0000E+00	0.0000E+00	0.0000E+00
207	0.0000E+00	0.0000E+00	0.0000E+00
208	0.0000E+00	0.0000E+00	0.0000E+00
209	0.0000E+00	0.0000E+00	0.0000E+00
210	0.0000E+00	0.0000E+00	0.0000E+00
211	0.0000E+00	0.0000E+00	0.0000E+00
212	0.0000E+00	0.0000E+00	0.0000E+00
213	0.0000E+00	0.0000E+00	0.0000E+00
214	0.0000E+00	0.0000E+00	0.0000E+00
215	0.0000E+00	0.0000E+00	0.0000E+00
216	0.0000E+00	0.0000E+00	0.0000E+00
217	0.0000E+00	0.0000E+00	0.0000E+00
218	0.0000E+00	0.0000E+00	0.0000E+00
219	0.0000E+00	0.0000E+00	0.0000E+00
220	0.0000E+00	0.0000E+00	0.0000E+00
221	0.0000E+00	0.0000E+00	0.0000E+00
222	0.0000E+00	0.0000E+00	0.0000E+00
223	0.0000E+00	0.0000E+00	0.0000E+00
224	0.0000E+00	0.0000E+00	0.0000E+00
225	0.0000E+00	0.0000E+00	0.0000E+00
226	0.0000E+00	0.0000E+00	0.0000E+00
227	0.0000E+00	0.0000E+00	0.0000E+00
228	0.0000E+00	0.0000E+00	0.0000E+00
229	0.0000E+00	0.0000E+00	0.0000E+00
230	0.0000E+00	0.0000E+00	0.0000E+00
231	0.0000E+00	0.0000E+00	0.0000E+00
232	0.0000E+00	0.0000E+00	0.0000E+00
233	0.0000E+00	0.0000E+00	0.0000E+00
234	0.0000E+00	0.0000E+00	0.0000E+00
235	0.0000E+00	0.0000E+00	0.0000E+00
236	0.0000E+00	0.0000E+00	0.0000E+00
237	0.0000E+00	0.0000E+00	0.0000E+00
238	0.0000E+00	0.0000E+00	0.0000E+00
239	0.0000E+00	0.0000E+00	0.0000E+00
240	0.0000E+00	0.0000E+00	0.0000E+00
241	0.0000E+00	0.0000E+00	0.0000E+00
242	0.0000E+00	0.0000E+00	0.0000E+00
243	0.0000E+00	0.0000E+00	0.0000E+00
244	0.0000E+00	0.0000E+00	0.0000E+00
245	0.0000E+00	0.0000E+00	0.0000E+00
246	0.0000E+00	0.0000E+00	0.0000E+00
247	0.0000E+00	0.0000E+00	0.0000E+00
248	0.0000E+00	0.0000E+00	0.0000E+00
249	0.0000E+00	0.0000E+00	0.0000E+00
250	0.0000E+00	0.0000E+00	0.0000E+00

1

# nodal point velocities

np	x-vel	y-vel	z-vel
251	0.0000E+00	0.0000E+00	0.0000E+00
252	0.0000E+00	0.0000E+00	0.0000E+00
253	0.0000E+00	0.0000E+00	0.0000E+00
254	0.0000E+00	0.0000E+00	0.0000E+00
255	0.0000E+00	0.0000E+00	0.0000E+00
256	0.0000E+00	0.0000E+00	0.0000E+00
257	0.0000E+00	0.0000E+00	0.0000E+00



258	0.0000E+00	0.0000E+00	0.0000E+00
259	0.0000E+00	0.0000E+00	0.0000E+00
260	0.0000E+00	0.0000E+00	0.0000E+00
261	0.0000E+00	0.0000E+00	0.0000E+00
262	0.0000E+00	0.0000E+00	0.0000E+00
263	0.0000E+00	0.0000E+00	0.0000E+00
264	0.0000E+00	0.0000E+00	0.0000E+00
265	0.0000E+00	0.0000E+00	0.0000E+00
266	0.0000E+00	0.0000E+00	0.0000E+00
267	0.0000E+00	0.0000E+00	0.0000E+00
268	0.0000E+00	0.0000E+00	0.0000E+00
269	0.0000E+00	0.0000E+00	0.0000E+00
270	0.0000E+00	0.0000E+00	0.0000E+00
271	0.0000E+00	0.0000E+00	0.0000E+00
272	0.0000E+00	0.0000E+00	0.0000E+00
273	0.0000E+00	0.0000E+00	0.0000E+00
274	0.0000E+00	0.0000E+00	0.0000E+00
275	0.0000E+00	0.0000E+00	0.0000E+00
276	0.0000E+00	0.0000E+00	0.0000E+00
277	0.0000E+00	0.0000E+00	0.0000E+00
278	0.0000E+00	0.0000E+00	0.0000E+00
279	0.0000E+00	0.0000E+00	0.0000E+00
280	0.0000E+00	0.0000E+00	0.0000E+00
281	0.0000E+00	0.0000E+00	0.0000E+00
282	0.0000E+00	0.0000E+00	0.0000E+00
283	0.0000E+00	0.0000E+00	0.0000E+00
284	0.0000E+00	0.0000E+00	0.0000E+00
285	0.0000E+00	0.0000E+00	0.0000E+00
286	0.0000E+00	0.0000E+00	0.0000E+00
287	0.0000E+00	0.0000E+00	0.0000E+00
288	0.0000E+00	0.0000E+00	0.0000E+00
289	0.0000E+00	0.0000E+00	0.0000E+00
290	0.0000E+00	0.0000E+00	0.0000E+00
291	0.0000E+00	0.0000E+00	0.0000E+00
292	0.0000E+00	0.0000E+00	0.0000E+00
293	0.0000E+00	0.0000E+00	0.0000E+00
294	0.0000E+00	0.0000E+00	0.0000E+00
295	0.0000E+00	0.0000E+00	0.0000E+00
296	0.0000E+00	0.0000E+00	0.0000E+00
297	0.0000E+00	0.0000E+00	0.0000E+00
298	0.0000E+00	0.0000E+00	0.0000E+00
299	0.0000E+00	0.0000E+00	0.0000E+00
300	0.0000E+00	0.0000E+00	0.0000E+00

1

nodal point velocities

np	x-vel	y-vel	z-vel
301	0.0000E+00	0.0000E+00	0.0000E+00
302	0.0000E+00	0.0000E+00	0.0000E+00
303	0.0000E+00	0.0000E+00	0.0000E+00
304	0.0000E+00	0.0000E+00	0.0000E+00
305	0.0000E+00	0.0000E+00	0.0000E+00
306	0.0000E+00	0.0000E+00	0.0000E+00
307	0.0000E+00	0.0000E+00	0.0000E+00
308	0.0000E+00	0.0000E+00	0.0000E+00
309	0.0000E+00	0.0000E+00	0.0000E+00
310	0.0000E+00	0.0000E+00	0.0000E+00
311	0.0000E+00	0.0000E+00	0.0000E+00
312	0.0000E+00	0.0000E+00	0.0000E+00
313	0.0000E+00	0.0000E+00	0.0000E+00
314	0.0000E+00	0.0000E+00	0.0000E+00

315	0.0000E+00	0.0000E+00	0.0000E+00
316	0.0000E+00	0.0000E+00	0.0000E+00
317	0.0000E+00	0.0000E+00	0.0000E+00
318	0.0000E+00	0.0000E+00	0.0000E+00
319	0.0000E+00	0.0000E+00	0.0000E+00
320	0.0000E+00	0.0000E+00	0.0000E+00
321	0.0000E+00	0.0000E+00	0.0000E+00
322	0.0000E+00	0.0000E+00	0.0000E+00
323	0.0000E+00	0.0000E+00	0.0000E+00
324	0.0000E+00	0.0000E+00	0.0000E+00
325	0.0000E+00	0.0000E+00	0.0000E+00
326	0.0000E+00	0.0000E+00	0.0000E+00
327	0.0000E+00	0.0000E+00	0.0000E+00
328	0.0000E+00	0.0000E+00	0.0000E+00
329	0.0000E+00	0.0000E+00	0.0000E+00
330	0.0000E+00	0.0000E+00	0.0000E+00
331	0.0000E+00	0.0000E+00	0.0000E+00
332	0.0000E+00	0.0000E+00	0.0000E+00
333	0.0000E+00	0.0000E+00	0.0000E+00
334	0.0000E+00	0.0000E+00	0.0000E+00
335	0.0000E+00	0.0000E+00	0.0000E+00
336	0.0000E+00	0.0000E+00	0.0000E+00
337	0.0000E+00	0.0000E+00	0.0000E+00
338	0.0000E+00	0.0000E+00	0.0000E+00
339	0.0000E+00	0.0000E+00	0.0000E+00
340	0.0000E+00	0.0000E+00	0.0000E+00
341	0.0000E+00	0.0000E+00	0.0000E+00
342	0.0000E+00	0.0000E+00	0.0000E+00
343	0.0000E+00	0.0000E+00	0.0000E+00
344	0.0000E+00	0.0000E+00	0.0000E+00
345	0.0000E+00	0.0000E+00	0.0000E+00
346	0.0000E+00	0.0000E+00	0.0000E+00
347	0.0000E+00	0.0000E+00	0.0000E+00
348	0.0000E+00	0.0000E+00	0.0000E+00
349	0.0000E+00	0.0000E+00	0.0000E+00
350	0.0000E+00	0.0000E+00	0.0000E+00

1

# nodal point velocities

np	x-vel	y-vel	z-vel
351	0.0000E+00	0.0000E+00	0.0000E+00
352	0.0000E+00	0.0000E+00	0.0000E+00
353	0.0000E+00	0.0000E+00	0.0000E+00
354	0.0000E+00	0.0000E+00	0.0000E+00
355	0.0000E+00	0.0000E+00	0.0000E+00
356	0.0000E+00	0.0000E+00	0.0000E+00
357	0.0000E+00	0.0000E+00	0.0000E+00
358	0.0000E+00	0.0000E+00	0.0000E+00
359	0.0000E+00	0.0000E+00	0.0000E+00
360	0.0000E+00	0.0000E+00	0.0000E+00
361	0.0000E+00	0.0000E+00	0.0000E+00
362	0.0000E+00	0.0000E+00	0.0000E+00
363	0.0000E+00	0.0000E+00	0.0000E+00
364	0.0000E+00	0.0000E+00	0.0000E+00
365	0.0000E+00	0.0000E+00	0.0000E+00
366	0.0000E+00	0.0000E+00	0.0000E+00
367	0.0000E+00	0.0000E+00	0.0000E+00
368	0.0000E+00	0.0000E+00	0.0000E+00
369	0.0000E+00	0.0000E+00	0.0000E+00
370	0.0000E+00	0.0000E+00	0.0000E+00
371	0.0000E+00	0.0000E+00	0.0000E+00

372	0.0000E+00	0.0000E+00	0.0000E+00
373	0.0000E+00	0.0000E+00	0.0000E+00
374	0.0000E+00	0.0000E+00	0.0000E+00
375	0.0000E+00	0.0000E+00	0.0000E+00
376	0.0000E+00	0.0000E+00	0.0000E+00
377	0.0000E+00	0.0000E+00	0.0000E+00
378	0.0000E+00	0.0000E+00	0.0000E+00
379	0.0000E+00	0.0000E+00	0.0000E+00
380	0.0000E+00	0.0000E+00	0.0000E+00
381	0.0000E+00	0.0000E+00	0.0000E+00
382	0.0000E+00	0.0000E+00	0.0000E+00
383	0.0000E+00	0.0000E+00	0.0000E+00
384	0.0000E+00	0.0000E+00	0.0000E+00
385	0.0000E+00	0.0000E+00	0.0000E+00
386	0.0000E+00	0.0000E+00	0.0000E+00
387	0.0000E+00	0.0000E+00	0.0000E+00
388	0.0000E+00	0.0000E+00	0.0000E+00
389	0.0000E+00	0.0000E+00	0.0000E+00
390	0.0000E+00	0.0000E+00	0.0000E+00
391	0.0000E+00	0.0000E+00	0.0000E+00
392	0.0000E+00	0.0000E+00	0.0000E+00
393	0.0000E+00	0.0000E+00	0.0000E+00
394	0.0000E+00	0.0000E+00	0.0000E+00
395	0.0000E+00	0.0000E+00	0.0000E+00
396	0.0000E+00	0.0000E+00	0.0000E+00
397	0.0000E+00	0.0000E+00	0.0000E+00
398	0.0000E+00	0.0000E+00	0.0000E+00
399	0.0000E+00	0.0000E+00	0.0000E+00
400	0.0000E+00	0.0000E+00	0.0000E+00

1

# n o d a l   p o i n t   v e l o c i t i e s

np	x-vel	y-vel	z-vel
401	0.0000E+00	0.0000E+00	0.0000E+00
402	0.0000E+00	0.0000E+00	0.0000E+00
403	0.0000E+00	0.0000E+00	0.0000E+00
404	0.0000E+00	0.0000E+00	0.0000E+00
405	0.0000E+00	0.0000E+00	0.0000E+00
406	0.0000E+00	0.0000E+00	0.0000E+00
407	0.0000E+00	0.0000E+00	0.0000E+00
408	0.0000E+00	0.0000E+00	0.0000E+00
409	0.0000E+00	0.0000E+00	0.0000E+00
410	0.0000E+00	0.0000E+00	0.0000E+00
411	0.0000E+00	0.0000E+00	0.0000E+00
412	0.0000E+00	0.0000E+00	0.0000E+00
413	0.0000E+00	0.0000E+00	0.0000E+00
414	0.0000E+00	0.0000E+00	0.0000E+00
415	0.0000E+00	0.0000E+00	0.0000E+00
416	0.0000E+00	0.0000E+00	0.0000E+00
417	0.0000E+00	0.0000E+00	0.0000E+00
418	0.0000E+00	0.0000E+00	0.0000E+00
419	0.0000E+00	0.0000E+00	0.0000E+00
420	0.0000E+00	0.0000E+00	0.0000E+00
421	0.0000E+00	0.0000E+00	0.0000E+00
422	0.0000E+00	0.0000E+00	0.0000E+00
423	0.0000E+00	0.0000E+00	0.0000E+00
424	0.0000E+00	0.0000E+00	0.0000E+00
425	0.0000E+00	0.0000E+00	0.0000E+00
426	0.0000E+00	0.0000E+00	0.0000E+00
427	0.0000E+00	0.0000E+00	0.0000E+00
428	0.0000E+00	0.0000E+00	0.0000E+00

429	0.0000E+00	0.0000E+00	0.0000E+00
430	0.0000E+00	0.0000E+00	0.0000E+00
431	0.0000E+00	0.0000E+00	0.0000E+00
432	0.0000E+00	0.0000E+00	0.0000E+00
433	0.0000E+00	0.0000E+00	0.0000E+00
434	0.0000E+00	0.0000E+00	0.0000E+00
435	0.0000E+00	0.0000E+00	0.0000E+00
436	0.0000E+00	0.0000E+00	0.0000E+00
437	0.0000E+00	0.0000E+00	0.0000E+00
438	0.0000E+00	0.0000E+00	0.0000E+00
439	0.0000E+00	0.0000E+00	0.0000E+00
440	0.0000E+00	0.0000E+00	0.0000E+00
441	0.0000E+00	0.0000E+00	0.0000E+00
442	0.0000E+00	0.0000E+00	0.0000E+00
443	0.0000E+00	0.0000E+00	0.0000E+00
444	0.0000E+00	0.0000E+00	0.0000E+00
445	0.0000E+00	0.0000E+00	0.0000E+00
446	0.0000E+00	0.0000E+00	0.0000E+00
447	0.0000E+00	0.0000E+00	0.0000E+00
448	0.0000E+00	0.0000E+00	0.0000E+00
449	0.0000E+00	0.0000E+00	0.0000E+00
450	0.0000E+00	0.0000E+00	0.0000E+00

1

# nodal point velocities

np	x-vel	y-vel	z-vel
451	0.0000E+00	0.0000E+00	0.0000E+00
452	0.0000E+00	0.0000E+00	0.0000E+00
453	0.0000E+00	0.0000E+00	0.0000E+00
454	0.0000E+00	0.0000E+00	0.0000E+00
455	0.0000E+00	0.0000E+00	0.0000E+00
456	0.0000E+00	0.0000E+00	0.0000E+00
457	0.0000E+00	0.0000E+00	0.0000E+00
458	0.0000E+00	0.0000E+00	0.0000E+00
459	0.0000E+00	0.0000E+00	0.0000E+00
460	0.0000E+00	0.0000E+00	0.0000E+00
461	0.0000E+00	0.0000E+00	0.0000E+00
462	0.0000E+00	0.0000E+00	0.0000E+00
463	0.0000E+00	0.0000E+00	0.0000E+00
464	0.0000E+00	0.0000E+00	0.0000E+00
465	0.0000E+00	0.0000E+00	0.0000E+00
466	0.0000E+00	0.0000E+00	0.0000E+00
467	0.0000E+00	0.0000E+00	0.0000E+00
468	0.0000E+00	0.0000E+00	0.0000E+00
469	0.0000E+00	0.0000E+00	0.0000E+00
470	0.0000E+00	0.0000E+00	0.0000E+00
471	0.0000E+00	0.0000E+00	0.0000E+00
472	0.0000E+00	0.0000E+00	0.0000E+00
473	0.0000E+00	0.0000E+00	0.0000E+00
474	0.0000E+00	0.0000E+00	0.0000E+00
475	0.0000E+00	0.0000E+00	0.0000E+00
476	0.0000E+00	0.0000E+00	0.0000E+00
477	0.0000E+00	0.0000E+00	0.0000E+00
478	0.0000E+00	0.0000E+00	0.0000E+00
479	0.0000E+00	0.0000E+00	0.0000E+00
480	0.0000E+00	0.0000E+00	0.0000E+00
481	0.0000E+00	0.0000E+00	0.0000E+00
482	0.0000E+00	0.0000E+00	0.0000E+00
483	0.0000E+00	0.0000E+00	0.0000E+00
484	0.0000E+00	0.0000E+00	0.0000E+00
485	0.0000E+00	0.0000E+00	0.0000E+00

486	0.0000E+00	0.0000E+00	0.0000E+00
487	0.0000E+00	0.0000E+00	0.0000E+00
488	0.0000E+00	0.0000E+00	0.0000E+00
489	0.0000E+00	0.0000E+00	0.0000E+00
490	0.0000E+00	0.0000E+00	0.0000E+00
491	0.0000E+00	0.0000E+00	0.0000E+00
492	0.0000E+00	0.0000E+00	0.0000E+00
493	0.0000E+00	0.0000E+00	0.0000E+00
494	0.0000E+00	0.0000E+00	0.0000E+00
495	0.0000E+00	0.0000E+00	0.0000E+00
496	0.0000E+00	0.0000E+00	0.0000E+00
497	0.0000E+00	0.0000E+00	0.0000E+00
498	0.0000E+00	0.0000E+00	0.0000E+00
499	0.0000E+00	0.0000E+00	0.0000E+00
500	0.0000E+00	0.0000E+00	0.0000E+00

1

nodal point velocities

np	x-vel	y-vel	z-vel
501	0.0000E+00	0.0000E+00	0.0000E+00
502	0.0000E+00	0.0000E+00	0.0000E+00
503	0.0000E+00	0.0000E+00	0.0000E+00
504	0.0000E+00	0.0000E+00	0.0000E+00
505	0.0000E+00	0.0000E+00	0.0000E+00
506	0.0000E+00	0.0000E+00	0.0000E+00
507	0.0000E+00	0.0000E+00	0.0000E+00
508	0.0000E+00	0.0000E+00	0.0000E+00
509	0.0000E+00	0.0000E+00	0.0000E+00
510	0.0000E+00	0.0000E+00	0.0000E+00
511	0.0000E+00	0.0000E+00	0.0000E+00
512	0.0000E+00	0.0000E+00	0.0000E+00
513	0.0000E+00	0.0000E+00	0.1000E+04
514	0.0000E+00	0.0000E+00	0.1000E+04
515	0.0000E+00	0.0000E+00	0.1000E+04
516	0.0000E+00	0.0000E+00	0.1000E+04
517	0.0000E+00	0.0000E+00	0.1000E+04
518	0.0000E+00	0.0000E+00	0.1000E+04
519	0.0000E+00	0.0000E+00	0.1000E+04
520	0.0000E+00	0.0000E+00	0.1000E+04
521	0.0000E+00	0.0000E+00	0.1000E+04
522	0.0000E+00	0.0000E+00	0.1000E+04
523	0.0000E+00	0.0000E+00	0.1000E+04
524	0.0000E+00	0.0000E+00	0.1000E+04
525	0.0000E+00	0.0000E+00	0.1000E+04
526	0.0000E+00	0.0000E+00	0.1000E+04
527	0.0000E+00	0.0000E+00	0.1000E+04
528	0.0000E+00	0.0000E+00	0.1000E+04
529	0.0000E+00	0.0000E+00	0.1000E+04
530	0.0000E+00	0.0000E+00	0.1000E+04
531	0.0000E+00	0.0000E+00	0.1000E+04
532	0.0000E+00	0.0000E+00	0.1000E+04
533	0.0000E+00	0.0000E+00	0.1000E+04
534	0.0000E+00	0.0000E+00	0.1000E+04
535	0.0000E+00	0.0000E+00	0.1000E+04
536	0.0000E+00	0.0000E+00	0.1000E+04
537	0.0000E+00	0.0000E+00	0.1000E+04
538	0.0000E+00	0.0000E+00	0.1000E+04
539	0.0000E+00	0.0000E+00	0.1000E+04
540	0.0000E+00	0.0000E+00	0.1000E+04
541	0.0000E+00	0.0000E+00	0.1000E+04
542	0.0000E+00	0.0000E+00	0.1000E+04

543	0.0000E+00	0.0000E+00	0.1000E+04
544	0.0000E+00	0.0000E+00	0.1000E+04
545	0.0000E+00	0.0000E+00	0.1000E+04
546	0.0000E+00	0.0000E+00	0.1000E+04
547	0.0000E+00	0.0000E+00	0.1000E+04
548	0.0000E+00	0.0000E+00	0.1000E+04
549	0.0000E+00	0.0000E+00	0.1000E+04
550	0.0000E+00	0.0000E+00	0.1000E+04

1

# nodal point velocities

np	x-vel	y-vel	z-vel
551	0.0000E+00	0.0000E+00	0.1000E+04
552	0.0000E+00	0.0000E+00	0.1000E+04
553	0.0000E+00	0.0000E+00	0.1000E+04
554	0.0000E+00	0.0000E+00	0.1000E+04
555	0.0000E+00	0.0000E+00	0.1000E+04
556	0.0000E+00	0.0000E+00	0.1000E+04
557	0.0000E+00	0.0000E+00	0.1000E+04
558	0.0000E+00	0.0000E+00	0.1000E+04
559	0.0000E+00	0.0000E+00	0.1000E+04
560	0.0000E+00	0.0000E+00	0.1000E+04
561	0.0000E+00	0.0000E+00	0.1000E+04
562	0.0000E+00	0.0000E+00	0.1000E+04
563	0.0000E+00	0.0000E+00	0.1000E+04
564	0.0000E+00	0.0000E+00	0.1000E+04
565	0.0000E+00	0.0000E+00	0.1000E+04
566	0.0000E+00	0.0000E+00	0.1000E+04
567	0.0000E+00	0.0000E+00	0.1000E+04
568	0.0000E+00	0.0000E+00	0.1000E+04
569	0.0000E+00	0.0000E+00	0.1000E+04
570	0.0000E+00	0.0000E+00	0.1000E+04
571	0.0000E+00	0.0000E+00	0.1000E+04
572	0.0000E+00	0.0000E+00	0.1000E+04
573	0.0000E+00	0.0000E+00	0.1000E+04
574	0.0000E+00	0.0000E+00	0.1000E+04
575	0.0000E+00	0.0000E+00	0.1000E+04
576	0.0000E+00	0.0000E+00	0.1000E+04
577	0.0000E+00	0.0000E+00	0.1000E+04
578	0.0000E+00	0.0000E+00	0.1000E+04
579	0.0000E+00	0.0000E+00	0.1000E+04
580	0.0000E+00	0.0000E+00	0.1000E+04
581	0.0000E+00	0.0000E+00	0.1000E+04
582	0.0000E+00	0.0000E+00	0.1000E+04
583	0.0000E+00	0.0000E+00	0.1000E+04
584	0.0000E+00	0.0000E+00	0.1000E+04
585	0.0000E+00	0.0000E+00	0.1000E+04
586	0.0000E+00	0.0000E+00	0.1000E+04
587	0.0000E+00	0.0000E+00	0.1000E+04
588	0.0000E+00	0.0000E+00	0.1000E+04
589	0.0000E+00	0.0000E+00	0.1000E+04
590	0.0000E+00	0.0000E+00	0.1000E+04
591	0.0000E+00	0.0000E+00	0.1000E+04
592	0.0000E+00	0.0000E+00	0.1000E+04
593	0.0000E+00	0.0000E+00	0.1000E+04
594	0.0000E+00	0.0000E+00	0.1000E+04
595	0.0000E+00	0.0000E+00	0.1000E+04
596	0.0000E+00	0.0000E+00	0.1000E+04
597	0.0000E+00	0.0000E+00	0.1000E+04
598	0.0000E+00	0.0000E+00	0.1000E+04
599	0.0000E+00	0.0000E+00	0.1000E+04

```

1      600      0.0000E+00      0.0000E+00      0.1000E+04

```

```

n o d a l   p o i n t   v e l o c i t i e s

```

np	x-vel	y-vel	z-vel
601	0.0000E+00	0.0000E+00	0.1000E+04
602	0.0000E+00	0.0000E+00	0.1000E+04
603	0.0000E+00	0.0000E+00	0.1000E+04
604	0.0000E+00	0.0000E+00	0.1000E+04
605	0.0000E+00	0.0000E+00	0.1000E+04
606	0.0000E+00	0.0000E+00	0.1000E+04
607	0.0000E+00	0.0000E+00	0.1000E+04
608	0.0000E+00	0.0000E+00	0.1000E+04
609	0.0000E+00	0.0000E+00	0.1000E+04
610	0.0000E+00	0.0000E+00	0.1000E+04
611	0.0000E+00	0.0000E+00	0.1000E+04
612	0.0000E+00	0.0000E+00	0.1000E+04
613	0.0000E+00	0.0000E+00	0.1000E+04
614	0.0000E+00	0.0000E+00	0.1000E+04
615	0.0000E+00	0.0000E+00	0.1000E+04
616	0.0000E+00	0.0000E+00	0.1000E+04
617	0.0000E+00	0.0000E+00	0.1000E+04
618	0.0000E+00	0.0000E+00	0.1000E+04
619	0.0000E+00	0.0000E+00	0.1000E+04
620	0.0000E+00	0.0000E+00	0.1000E+04
621	0.0000E+00	0.0000E+00	0.1000E+04
622	0.0000E+00	0.0000E+00	0.1000E+04
623	0.0000E+00	0.0000E+00	0.1000E+04
624	0.0000E+00	0.0000E+00	0.1000E+04
625	0.0000E+00	0.0000E+00	0.1000E+04
626	0.0000E+00	0.0000E+00	0.1000E+04
627	0.0000E+00	0.0000E+00	0.1000E+04
628	0.0000E+00	0.0000E+00	0.1000E+04
629	0.0000E+00	0.0000E+00	0.1000E+04
630	0.0000E+00	0.0000E+00	0.1000E+04
631	0.0000E+00	0.0000E+00	0.1000E+04
632	0.0000E+00	0.0000E+00	0.1000E+04
633	0.0000E+00	0.0000E+00	0.1000E+04
634	0.0000E+00	0.0000E+00	0.1000E+04
635	0.0000E+00	0.0000E+00	0.1000E+04
636	0.0000E+00	0.0000E+00	0.1000E+04
637	0.0000E+00	0.0000E+00	0.1000E+04
638	0.0000E+00	0.0000E+00	0.1000E+04
639	0.0000E+00	0.0000E+00	0.1000E+04
640	0.0000E+00	0.0000E+00	0.1000E+04
641	0.0000E+00	0.0000E+00	0.1000E+04
642	0.0000E+00	0.0000E+00	0.1000E+04
643	0.0000E+00	0.0000E+00	0.1000E+04
644	0.0000E+00	0.0000E+00	0.1000E+04
645	0.0000E+00	0.0000E+00	0.1000E+04
646	0.0000E+00	0.0000E+00	0.1000E+04
647	0.0000E+00	0.0000E+00	0.1000E+04
648	0.0000E+00	0.0000E+00	0.1000E+04
649	0.0000E+00	0.0000E+00	0.1000E+04
650	0.0000E+00	0.0000E+00	0.1000E+04

```

1

```

```

n o d a l   p o i n t   v e l o c i t i e s

```

np	x-vel	y-vel	z-vel
----	-------	-------	-------

651	0.0000E+00	0.0000E+00	0.1000E+04
652	0.0000E+00	0.0000E+00	0.1000E+04
653	0.0000E+00	0.0000E+00	0.1000E+04
654	0.0000E+00	0.0000E+00	0.1000E+04
655	0.0000E+00	0.0000E+00	0.1000E+04
656	0.0000E+00	0.0000E+00	0.1000E+04
657	0.0000E+00	0.0000E+00	0.1000E+04
658	0.0000E+00	0.0000E+00	0.1000E+04
659	0.0000E+00	0.0000E+00	0.1000E+04
660	0.0000E+00	0.0000E+00	0.1000E+04
661	0.0000E+00	0.0000E+00	0.1000E+04
662	0.0000E+00	0.0000E+00	0.1000E+04
663	0.0000E+00	0.0000E+00	0.1000E+04
664	0.0000E+00	0.0000E+00	0.1000E+04
665	0.0000E+00	0.0000E+00	0.1000E+04
666	0.0000E+00	0.0000E+00	0.1000E+04
667	0.0000E+00	0.0000E+00	0.1000E+04
668	0.0000E+00	0.0000E+00	0.1000E+04
669	0.0000E+00	0.0000E+00	0.1000E+04
670	0.0000E+00	0.0000E+00	0.1000E+04
671	0.0000E+00	0.0000E+00	0.1000E+04
672	0.0000E+00	0.0000E+00	0.1000E+04
673	0.0000E+00	0.0000E+00	0.1000E+04
674	0.0000E+00	0.0000E+00	0.1000E+04
675	0.0000E+00	0.0000E+00	0.1000E+04
676	0.0000E+00	0.0000E+00	0.1000E+04
677	0.0000E+00	0.0000E+00	0.1000E+04
678	0.0000E+00	0.0000E+00	0.1000E+04
679	0.0000E+00	0.0000E+00	0.1000E+04
680	0.0000E+00	0.0000E+00	0.1000E+04
681	0.0000E+00	0.0000E+00	0.1000E+04
682	0.0000E+00	0.0000E+00	0.1000E+04
683	0.0000E+00	0.0000E+00	0.1000E+04
684	0.0000E+00	0.0000E+00	0.1000E+04
685	0.0000E+00	0.0000E+00	0.1000E+04
686	0.0000E+00	0.0000E+00	0.1000E+04
687	0.0000E+00	0.0000E+00	0.1000E+04
688	0.0000E+00	0.0000E+00	0.1000E+04
689	0.0000E+00	0.0000E+00	0.1000E+04
690	0.0000E+00	0.0000E+00	0.1000E+04
691	0.0000E+00	0.0000E+00	0.1000E+04
692	0.0000E+00	0.0000E+00	0.1000E+04
693	0.0000E+00	0.0000E+00	0.1000E+04
694	0.0000E+00	0.0000E+00	0.1000E+04
695	0.0000E+00	0.0000E+00	0.1000E+04
696	0.0000E+00	0.0000E+00	0.1000E+04
697	0.0000E+00	0.0000E+00	0.1000E+04
698	0.0000E+00	0.0000E+00	0.1000E+04
699	0.0000E+00	0.0000E+00	0.1000E+04
700	0.0000E+00	0.0000E+00	0.1000E+04

1

# nodal point velocities

np	x-vel	y-vel	z-vel
701	0.0000E+00	0.0000E+00	0.1000E+04
702	0.0000E+00	0.0000E+00	0.1000E+04
703	0.0000E+00	0.0000E+00	0.1000E+04
704	0.0000E+00	0.0000E+00	0.1000E+04
705	0.0000E+00	0.0000E+00	0.1000E+04
706	0.0000E+00	0.0000E+00	0.1000E+04



707	0.0000E+00	0.0000E+00	0.1000E+04
708	0.0000E+00	0.0000E+00	0.1000E+04
709	0.0000E+00	0.0000E+00	0.1000E+04
710	0.0000E+00	0.0000E+00	0.1000E+04
711	0.0000E+00	0.0000E+00	0.1000E+04
712	0.0000E+00	0.0000E+00	0.1000E+04
713	0.0000E+00	0.0000E+00	0.1000E+04
714	0.0000E+00	0.0000E+00	0.1000E+04
715	0.0000E+00	0.0000E+00	0.1000E+04
716	0.0000E+00	0.0000E+00	0.1000E+04
717	0.0000E+00	0.0000E+00	0.1000E+04
718	0.0000E+00	0.0000E+00	0.1000E+04
719	0.0000E+00	0.0000E+00	0.1000E+04
720	0.0000E+00	0.0000E+00	0.1000E+04
721	0.0000E+00	0.0000E+00	0.1000E+04
722	0.0000E+00	0.0000E+00	0.1000E+04
723	0.0000E+00	0.0000E+00	0.1000E+04
724	0.0000E+00	0.0000E+00	0.1000E+04
725	0.0000E+00	0.0000E+00	0.1000E+04
726	0.0000E+00	0.0000E+00	0.1000E+04
727	0.0000E+00	0.0000E+00	0.1000E+04
728	0.0000E+00	0.0000E+00	0.1000E+04
729	0.0000E+00	0.0000E+00	0.1000E+04
730	0.0000E+00	0.0000E+00	0.1000E+04
731	0.0000E+00	0.0000E+00	0.1000E+04
732	0.0000E+00	0.0000E+00	0.1000E+04
733	0.0000E+00	0.0000E+00	0.1000E+04
734	0.0000E+00	0.0000E+00	0.1000E+04
735	0.0000E+00	0.0000E+00	0.1000E+04
736	0.0000E+00	0.0000E+00	0.1000E+04
737	0.0000E+00	0.0000E+00	0.1000E+04
738	0.0000E+00	0.0000E+00	0.1000E+04
739	0.0000E+00	0.0000E+00	0.1000E+04
740	0.0000E+00	0.0000E+00	0.1000E+04
741	0.0000E+00	0.0000E+00	0.1000E+04
742	0.0000E+00	0.0000E+00	0.1000E+04
743	0.0000E+00	0.0000E+00	0.1000E+04
744	0.0000E+00	0.0000E+00	0.1000E+04
745	0.0000E+00	0.0000E+00	0.1000E+04
746	0.0000E+00	0.0000E+00	0.1000E+04
747	0.0000E+00	0.0000E+00	0.1000E+04
748	0.0000E+00	0.0000E+00	0.1000E+04
749	0.0000E+00	0.0000E+00	0.1000E+04
750	0.0000E+00	0.0000E+00	0.1000E+04

1

# nodal point velocities

np	x-vel	y-vel	z-vel
751	0.0000E+00	0.0000E+00	0.1000E+04
752	0.0000E+00	0.0000E+00	0.1000E+04
753	0.0000E+00	0.0000E+00	0.1000E+04
754	0.0000E+00	0.0000E+00	0.1000E+04
755	0.0000E+00	0.0000E+00	0.1000E+04
756	0.0000E+00	0.0000E+00	0.1000E+04
757	0.0000E+00	0.0000E+00	0.1000E+04
758	0.0000E+00	0.0000E+00	0.1000E+04
759	0.0000E+00	0.0000E+00	0.1000E+04
760	0.0000E+00	0.0000E+00	0.1000E+04
761	0.0000E+00	0.0000E+00	0.1000E+04
762	0.0000E+00	0.0000E+00	0.1000E+04
763	0.0000E+00	0.0000E+00	0.1000E+04

764	0.0000E+00	0.0000E+00	0.1000E+04
765	0.0000E+00	0.0000E+00	0.1000E+04
766	0.0000E+00	0.0000E+00	0.1000E+04
767	0.0000E+00	0.0000E+00	0.1000E+04
768	0.0000E+00	0.0000E+00	0.1000E+04
769	0.0000E+00	0.0000E+00	0.1000E+04
770	0.0000E+00	0.0000E+00	0.1000E+04
771	0.0000E+00	0.0000E+00	0.1000E+04
772	0.0000E+00	0.0000E+00	0.1000E+04
773	0.0000E+00	0.0000E+00	0.1000E+04
774	0.0000E+00	0.0000E+00	0.1000E+04
775	0.0000E+00	0.0000E+00	0.1000E+04
776	0.0000E+00	0.0000E+00	0.1000E+04
777	0.0000E+00	0.0000E+00	0.1000E+04
778	0.0000E+00	0.0000E+00	0.1000E+04
779	0.0000E+00	0.0000E+00	0.1000E+04
780	0.0000E+00	0.0000E+00	0.1000E+04
781	0.0000E+00	0.0000E+00	0.1000E+04
782	0.0000E+00	0.0000E+00	0.1000E+04
783	0.0000E+00	0.0000E+00	0.1000E+04
784	0.0000E+00	0.0000E+00	0.1000E+04
785	0.0000E+00	0.0000E+00	0.1000E+04
786	0.0000E+00	0.0000E+00	0.1000E+04
787	0.0000E+00	0.0000E+00	0.1000E+04
788	0.0000E+00	0.0000E+00	0.1000E+04
789	0.0000E+00	0.0000E+00	0.1000E+04
790	0.0000E+00	0.0000E+00	0.1000E+04
791	0.0000E+00	0.0000E+00	0.1000E+04
792	0.0000E+00	0.0000E+00	0.1000E+04
793	0.0000E+00	0.0000E+00	0.1000E+04
794	0.0000E+00	0.0000E+00	0.1000E+04
795	0.0000E+00	0.0000E+00	0.1000E+04
796	0.0000E+00	0.0000E+00	0.1000E+04
797	0.0000E+00	0.0000E+00	0.1000E+04
798	0.0000E+00	0.0000E+00	0.1000E+04
799	0.0000E+00	0.0000E+00	0.1000E+04
800	0.0000E+00	0.0000E+00	0.1000E+04

1

nodal point velocities

np	x-vel	y-vel	z-vel
801	0.0000E+00	0.0000E+00	0.1000E+04
802	0.0000E+00	0.0000E+00	0.1000E+04
803	0.0000E+00	0.0000E+00	0.1000E+04
804	0.0000E+00	0.0000E+00	0.1000E+04
805	0.0000E+00	0.0000E+00	0.1000E+04
806	0.0000E+00	0.0000E+00	0.1000E+04
807	0.0000E+00	0.0000E+00	0.1000E+04
808	0.0000E+00	0.0000E+00	0.1000E+04
809	0.0000E+00	0.0000E+00	0.1000E+04
810	0.0000E+00	0.0000E+00	0.1000E+04
811	0.0000E+00	0.0000E+00	0.1000E+04
812	0.0000E+00	0.0000E+00	0.1000E+04
813	0.0000E+00	0.0000E+00	0.1000E+04
814	0.0000E+00	0.0000E+00	0.1000E+04
815	0.0000E+00	0.0000E+00	0.1000E+04
816	0.0000E+00	0.0000E+00	0.1000E+04
817	0.0000E+00	0.0000E+00	0.1000E+04
818	0.0000E+00	0.0000E+00	0.1000E+04
819	0.0000E+00	0.0000E+00	0.1000E+04
820	0.0000E+00	0.0000E+00	0.1000E+04

821	0.0000E+00	0.0000E+00	0.1000E+04
822	0.0000E+00	0.0000E+00	0.1000E+04
823	0.0000E+00	0.0000E+00	0.1000E+04
824	0.0000E+00	0.0000E+00	0.1000E+04
825	0.0000E+00	0.0000E+00	0.1000E+04
826	0.0000E+00	0.0000E+00	0.1000E+04
827	0.0000E+00	0.0000E+00	0.1000E+04
828	0.0000E+00	0.0000E+00	0.1000E+04
829	0.0000E+00	0.0000E+00	0.1000E+04
830	0.0000E+00	0.0000E+00	0.1000E+04
831	0.0000E+00	0.0000E+00	0.1000E+04
832	0.0000E+00	0.0000E+00	0.1000E+04
833	0.0000E+00	0.0000E+00	0.1000E+04
834	0.0000E+00	0.0000E+00	0.1000E+04
835	0.0000E+00	0.0000E+00	0.1000E+04
836	0.0000E+00	0.0000E+00	0.1000E+04
837	0.0000E+00	0.0000E+00	0.1000E+04
838	0.0000E+00	0.0000E+00	0.1000E+04
839	0.0000E+00	0.0000E+00	0.1000E+04
840	0.0000E+00	0.0000E+00	0.1000E+04
841	0.0000E+00	0.0000E+00	0.1000E+04
842	0.0000E+00	0.0000E+00	0.1000E+04
843	0.0000E+00	0.0000E+00	0.1000E+04
844	0.0000E+00	0.0000E+00	0.1000E+04
845	0.0000E+00	0.0000E+00	0.1000E+04
846	0.0000E+00	0.0000E+00	0.1000E+04
847	0.0000E+00	0.0000E+00	0.1000E+04
848	0.0000E+00	0.0000E+00	0.1000E+04
849	0.0000E+00	0.0000E+00	0.1000E+04
850	0.0000E+00	0.0000E+00	0.1000E+04

1

# nodal point velocities

np	x-vel	y-vel	z-vel
851	0.0000E+00	0.0000E+00	0.1000E+04
852	0.0000E+00	0.0000E+00	0.1000E+04
853	0.0000E+00	0.0000E+00	0.1000E+04
854	0.0000E+00	0.0000E+00	0.1000E+04
855	0.0000E+00	0.0000E+00	0.1000E+04
856	0.0000E+00	0.0000E+00	0.1000E+04
857	0.0000E+00	0.0000E+00	0.1000E+04
858	0.0000E+00	0.0000E+00	0.1000E+04
859	0.0000E+00	0.0000E+00	0.1000E+04
860	0.0000E+00	0.0000E+00	0.1000E+04
861	0.0000E+00	0.0000E+00	0.1000E+04
862	0.0000E+00	0.0000E+00	0.1000E+04
863	0.0000E+00	0.0000E+00	0.1000E+04
864	0.0000E+00	0.0000E+00	0.1000E+04
865	0.0000E+00	0.0000E+00	0.1000E+04
866	0.0000E+00	0.0000E+00	0.1000E+04
867	0.0000E+00	0.0000E+00	0.1000E+04
868	0.0000E+00	0.0000E+00	0.1000E+04
869	0.0000E+00	0.0000E+00	0.1000E+04
870	0.0000E+00	0.0000E+00	0.1000E+04
871	0.0000E+00	0.0000E+00	0.1000E+04
872	0.0000E+00	0.0000E+00	0.1000E+04
873	0.0000E+00	0.0000E+00	0.1000E+04
874	0.0000E+00	0.0000E+00	0.1000E+04
875	0.0000E+00	0.0000E+00	0.1000E+04
876	0.0000E+00	0.0000E+00	0.1000E+04
877	0.0000E+00	0.0000E+00	0.1000E+04

878	0.0000E+00	0.0000E+00	0.1000E+04
879	0.0000E+00	0.0000E+00	0.1000E+04
880	0.0000E+00	0.0000E+00	0.1000E+04
881	0.0000E+00	0.0000E+00	0.1000E+04
882	0.0000E+00	0.0000E+00	0.1000E+04
883	0.0000E+00	0.0000E+00	0.1000E+04
884	0.0000E+00	0.0000E+00	0.1000E+04
885	0.0000E+00	0.0000E+00	0.1000E+04
886	0.0000E+00	0.0000E+00	0.1000E+04
887	0.0000E+00	0.0000E+00	0.1000E+04
888	0.0000E+00	0.0000E+00	0.1000E+04
889	0.0000E+00	0.0000E+00	0.1000E+04
890	0.0000E+00	0.0000E+00	0.1000E+04
891	0.0000E+00	0.0000E+00	0.1000E+04
892	0.0000E+00	0.0000E+00	0.1000E+04
893	0.0000E+00	0.0000E+00	0.1000E+04
894	0.0000E+00	0.0000E+00	0.1000E+04
895	0.0000E+00	0.0000E+00	0.1000E+04
896	0.0000E+00	0.0000E+00	0.1000E+04
897	0.0000E+00	0.0000E+00	0.1000E+04
898	0.0000E+00	0.0000E+00	0.1000E+04
899	0.0000E+00	0.0000E+00	0.1000E+04
900	0.0000E+00	0.0000E+00	0.1000E+04

1

# nodal point velocities

np	x-vel	y-vel	z-vel
901	0.0000E+00	0.0000E+00	0.1000E+04
902	0.0000E+00	0.0000E+00	0.1000E+04
903	0.0000E+00	0.0000E+00	0.1000E+04
904	0.0000E+00	0.0000E+00	0.1000E+04
905	0.0000E+00	0.0000E+00	0.1000E+04
906	0.0000E+00	0.0000E+00	0.1000E+04
907	0.0000E+00	0.0000E+00	0.1000E+04
908	0.0000E+00	0.0000E+00	0.1000E+04
909	0.0000E+00	0.0000E+00	0.1000E+04
910	0.0000E+00	0.0000E+00	0.1000E+04
911	0.0000E+00	0.0000E+00	0.1000E+04
912	0.0000E+00	0.0000E+00	0.1000E+04
913	0.0000E+00	0.0000E+00	0.1000E+04
914	0.0000E+00	0.0000E+00	0.1000E+04
915	0.0000E+00	0.0000E+00	0.1000E+04
916	0.0000E+00	0.0000E+00	0.1000E+04
917	0.0000E+00	0.0000E+00	0.1000E+04
918	0.0000E+00	0.0000E+00	0.1000E+04
919	0.0000E+00	0.0000E+00	0.1000E+04
920	0.0000E+00	0.0000E+00	0.1000E+04
921	0.0000E+00	0.0000E+00	0.1000E+04
922	0.0000E+00	0.0000E+00	0.1000E+04
923	0.0000E+00	0.0000E+00	0.1000E+04
924	0.0000E+00	0.0000E+00	0.1000E+04
925	0.0000E+00	0.0000E+00	0.1000E+04
926	0.0000E+00	0.0000E+00	0.1000E+04
927	0.0000E+00	0.0000E+00	0.1000E+04
928	0.0000E+00	0.0000E+00	0.1000E+04
929	0.0000E+00	0.0000E+00	0.1000E+04
930	0.0000E+00	0.0000E+00	0.1000E+04
931	0.0000E+00	0.0000E+00	0.1000E+04
932	0.0000E+00	0.0000E+00	0.1000E+04
933	0.0000E+00	0.0000E+00	0.1000E+04
934	0.0000E+00	0.0000E+00	0.1000E+04

935	0.0000E+00	0.0000E+00	0.1000E+04
936	0.0000E+00	0.0000E+00	0.1000E+04
937	0.0000E+00	0.0000E+00	0.1000E+04

1

s l i d i n g   s u r f a c e s   &   v o i d s

d e f i n i t i o n   n o.   1

slide line type..... 3

type.eq.1	sliding
type.eq.2	tied sliding
type.eq.3	sliding and voids
type.eq.4	single surface
type.eq.5	discrete nodes on surface
type.eq.6	discrete nodes tied to surface
type.eq.7	shell edge tied to shell surface
type.eq.8	spot welded nodes to surface
type.eq.9	tie break interfaces
type.eq.10	one-way sliding and voids

no. of slave segments.....	48
no. of master segments.....	225
static coefficient of friction .....	0.00000E+00
kinetic coefficient of friction.....	0.00000E+00
exponential decay coefficient .....	0.00000E+00
small penetration in contact search .....	0
= 0 default	
= 1 penetration.gt..1*thic of element ignored	

include slave side in printed interface file . 0

include master side in printed interface file 0

scale factor on default slave stiffness ..... 0.10000E+01

scale factor on default master stiffness .... 0.10000E+01

s l a v e   s u r f a c e   s e g m e n t s

segment node1 node2 node3 node4

1	515	540	542	518
2	540	541	543	542
3	518	542	544	521
4	542	543	545	544
5	521	544	576	560
6	544	545	577	576
7	560	576	578	563
8	576	577	579	578
9	899	902	914	912
10	912	914	915	913
11	902	905	916	914
12	914	916	917	915
13	905	926	934	916
14	916	934	935	917

15	926	929	936	934
16	934	936	937	935
17	590	596	616	612
18	612	616	617	613
19	596	605	622	616
20	616	622	623	617
21	605	760	776	622
22	622	776	777	623
23	760	769	782	776
24	776	782	783	777
25	733	748	752	739
26	748	749	753	752
27	739	752	756	745
28	752	753	757	756
29	745	756	882	873
30	756	757	883	882
31	873	882	886	879
32	882	883	887	886
33	667	673	675	669
34	669	675	677	671
35	671	677	721	717
36	717	721	723	719
37	673	679	681	675
38	675	681	683	677
39	677	683	725	721
40	721	725	727	723
41	679	821	823	681
42	681	823	825	683
43	683	825	861	725
44	725	861	863	727
45	821	827	829	823
46	823	829	831	825
47	825	831	865	861
48	861	865	867	863

master surface segments

segment	node1	node2	node3	node4
1	1	3	35	33
2	3	5	37	35
3	5	7	39	37
4	7	9	41	39
5	9	11	43	41
6	11	13	45	43
7	13	15	47	45
8	15	17	49	47
9	17	19	51	49
10	19	21	53	51
11	21	23	55	53
12	23	25	57	55
13	25	27	59	57
14	27	29	61	59
15	29	31	63	61
16	33	35	67	65
17	35	37	69	67
18	37	39	71	69
19	39	41	73	71
20	41	43	75	73
21	43	45	77	75
22	45	47	79	77
23	47	49	81	79

24	49	51	83	81
25	51	53	85	83
26	53	55	87	85
27	55	57	89	87
28	57	59	91	89
29	59	61	93	91
30	61	63	95	93
31	65	67	99	97
32	67	69	101	99
33	69	71	103	101
34	71	73	105	103
35	73	75	107	105
36	75	77	109	107
37	77	79	111	109
38	79	81	113	111
39	81	83	115	113
40	83	85	117	115
41	85	87	119	117
42	87	89	121	119
43	89	91	123	121
44	91	93	125	123
45	93	95	127	125
46	97	99	131	129
47	99	101	133	131
48	101	103	135	133
49	103	105	137	135
50	105	107	139	137
51	107	109	141	139
52	109	111	143	141
53	111	113	145	143
54	113	115	147	145
55	115	117	149	147
56	117	119	151	149
57	119	121	153	151
58	121	123	155	153
59	123	125	157	155
60	125	127	159	157
61	129	131	163	161
62	131	133	165	163
63	133	135	167	165
64	135	137	169	167
65	137	139	171	169
66	139	141	173	171
67	141	143	175	173
68	143	145	177	175
69	145	147	179	177
70	147	149	181	179
71	149	151	183	181
72	151	153	185	183
73	153	155	187	185
74	155	157	189	187
75	157	159	191	189
76	161	163	195	193
77	163	165	197	195
78	165	167	199	197
79	167	169	201	199
80	169	171	203	201
81	171	173	205	203
82	173	175	207	205
83	175	177	209	207
84	177	179	211	209
85	179	181	213	211
86	181	183	215	213
87	183	185	217	215

88	185	187	219	217
89	187	189	221	219
90	189	191	223	221
91	193	195	227	225
92	195	197	229	227
93	197	199	231	229
94	199	201	233	231
95	201	203	235	233
96	203	205	237	235
97	205	207	239	237
98	207	209	241	239
99	209	211	243	241
100	211	213	245	243
101	213	215	247	245
102	215	217	249	247
103	217	219	251	249
104	219	221	253	251
105	221	223	255	253
106	225	227	259	257
107	227	229	261	259
108	229	231	263	261
109	231	233	265	263
110	233	235	267	265
111	235	237	269	267
112	237	239	271	269
113	239	241	273	271
114	241	243	275	273
115	243	245	277	275
116	245	247	279	277
117	247	249	281	279
118	249	251	283	281
119	251	253	285	283
120	253	255	287	285
121	257	259	291	289
122	259	261	293	291
123	261	263	295	293
124	263	265	297	295
125	265	267	299	297
126	267	269	301	299
127	269	271	303	301
128	271	273	305	303
129	273	275	307	305
130	275	277	309	307
131	277	279	311	309
132	279	281	313	311
133	281	283	315	313
134	283	285	317	315
135	285	287	319	317
136	289	291	323	321
137	291	293	325	323
138	293	295	327	325
139	295	297	329	327
140	297	299	331	329
141	299	301	333	331
142	301	303	335	333
143	303	305	337	335
144	305	307	339	337
145	307	309	341	339
146	309	311	343	341
147	311	313	345	343
148	313	315	347	345
149	315	317	349	347
150	317	319	351	349
151	321	323	355	353



152	323	325	357	355
153	325	327	359	357
154	327	329	361	359
155	329	331	363	361
156	331	333	365	363
157	333	335	367	365
158	335	337	369	367
159	337	339	371	369
160	339	341	373	371
161	341	343	375	373
162	343	345	377	375
163	345	347	379	377
164	347	349	381	379
165	349	351	383	381
166	353	355	387	385
167	355	357	389	387
168	357	359	391	389
169	359	361	393	391
170	361	363	395	393
171	363	365	397	395
172	365	367	399	397
173	367	369	401	399
174	369	371	403	401
175	371	373	405	403
176	373	375	407	405
177	375	377	409	407
178	377	379	411	409
179	379	381	413	411
180	381	383	415	413
181	385	387	419	417
182	387	389	421	419
183	389	391	423	421
184	391	393	425	423
185	393	395	427	425
186	395	397	429	427
187	397	399	431	429
188	399	401	433	431
189	401	403	435	433
190	403	405	437	435
191	405	407	439	437
192	407	409	441	439
193	409	411	443	441
194	411	413	445	443
195	413	415	447	445
196	417	419	451	449
197	419	421	453	451
198	421	423	455	453
199	423	425	457	455
200	425	427	459	457
201	427	429	461	459
202	429	431	463	461
203	431	433	465	463
204	433	435	467	465
205	435	437	469	467
206	437	439	471	469
207	439	441	473	471
208	441	443	475	473
209	443	445	477	475
210	445	447	479	477
211	449	451	483	481
212	451	453	485	483
213	453	455	487	485
214	455	457	489	487
215	457	459	491	489

216	459	461	493	491
217	461	463	495	493
218	463	465	497	495
219	465	467	499	497
220	467	469	501	499
221	469	471	503	501
222	471	473	505	503
223	473	475	507	505
224	475	477	509	507
225	477	479	511	509

1

# storage allocation

storage needed for solution..... 39976

## mass properties of material # 1

total mass of material = 0.3250E+10  
x-coordinate of mass center = -0.8172E-06  
y-coordinate of mass center = 0.6528E-05  
z-coordinate of mass center = 0.1500E+03

### inertia tensor of material

row1=	0.7644E+14	0.9953E+06	0.2734E+06
row2=	0.9953E+06	0.7644E+14	0.2199E+07
row3=	0.2734E+06	0.2199E+07	0.1366E+15

## mass properties of material # 2

total mass of material = 0.3115E+11  
x-coordinate of mass center = 0.2780E-05  
y-coordinate of mass center = 0.3719E-06  
z-coordinate of mass center = 0.2272E-05

### inertia tensor of material

row1=	0.1258E+15	-0.1660E+07	-0.4137E+06
row2=	-0.1660E+07	0.1258E+15	0.3318E+06
row3=	-0.4137E+06	0.3318E+06	0.1258E+15

## mass properties of body

total mass of body = 0.3440E+11  
x-coordinate of mass center = 0.2517E-05  
y-coordinate of mass center = 0.8130E-06  
z-coordinate of mass center = 0.1417E+02

### inertia tensor of body

row1=	0.2685E+15	-0.6113E+06	0.1600E+07
row2=	-0.6113E+06	0.2685E+15	-0.1894E+06
row3=	0.1600E+07	-0.1894E+06	0.2624E+15

1

total mass = 0.343996E+11

material number	mass
1	0.325E+10
2	0.311E+11

restart file d3dump written, 43091 words

normal termination  
1

timing information

	cpu(sec)	io(sec)
initialization .....	0.3360E+01	0.7100E+00
solution (excl. slidelines).....	0.1371E+02	0.3500E+00
write binary database for plotting .....	0.8000E-01	0.3000E-01
write high speed printer file.....	0.1000E-01	0.2000E-01
slideline algorithm .....	0.6000E-01	0.6000E-01
t o t a l s	0.1722E+02	0.1170E+01

problem time = 0.1007E+00  
number of time steps= 80 cpu= 0.1722E+02 io= 0.1170E+01